

Portland State University

**PDXScholar**

---

Civil and Environmental Engineering Faculty  
Publications and Presentations

Civil and Environmental Engineering

---

May 1984

# Circulatory Processes in the Columbia River Estuary

David A. Jay  
*Portland State University*

Follow this and additional works at: [https://pdxscholar.library.pdx.edu/cengin\\_fac](https://pdxscholar.library.pdx.edu/cengin_fac)



Part of the [Civil and Environmental Engineering Commons](#)

**Let us know how access to this document benefits you.**

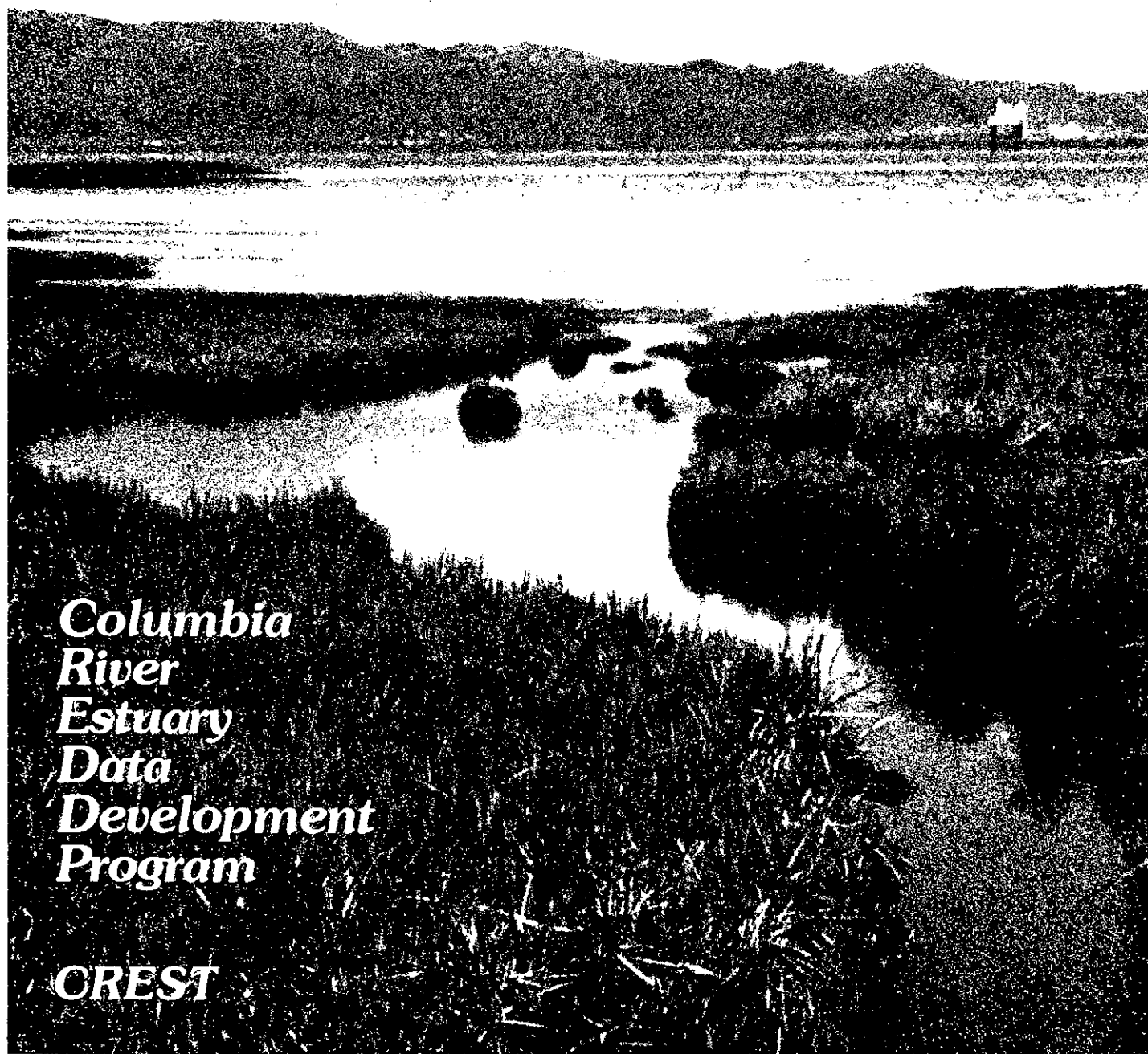
---

## Citation Details

Jay, D. A., 1984, Circulatory processes in the Columbia River Estuary, CREST, Astoria, Oregon, 169 pp. plus appendices.

This Article is brought to you for free and open access. It has been accepted for inclusion in Civil and Environmental Engineering Faculty Publications and Presentations by an authorized administrator of PDXScholar. Please contact us if we can make this document more accessible: [pdxscholar@pdx.edu](mailto:pdxscholar@pdx.edu).

# CIRCULATORY PROCESSES IN THE COLUMBIA RIVER ESTUARY



*Columbia  
River  
Estuary  
Data  
Development  
Program*

**CREST**

Final Report on the Circulation Work Unit  
of the Columbia River Estuary Data Development Program

CIRCULATORY PROCESSES IN THE  
COLUMBIA RIVER ESTUARY

Contractor:

Geophysics Program  
University of Washington  
Seattle, WA 98195

Principal Investigator:

David Jay  
Geophysics Program  
University of Washington  
Seattle, WA 98195

May 1984

Geophysics Program  
University of Washington  
Seattle, WA 98195

REPORT PREPARED BY  
David Jay

PRINCIPAL INVESTIGATOR  
David Jay

## PREFACE

### The Columbia River Estuary Data Development Program

This document is one of a set of publications and other materials produced by the Columbia River Estuary Data Development Program (CREDDP). CREDDP has two purposes: to increase understanding of the ecology of the Columbia River Estuary and to provide information useful in making land and water use decisions. The program was initiated by local governments and citizens who saw a need for a better information base for use in managing natural resources and in planning for development. In response to these concerns, the Governors of the states of Oregon and Washington requested in 1974 that the Pacific Northwest River Basins Commission (PNRBC) undertake an interdisciplinary ecological study of the estuary. At approximately the same time, local governments and port districts formed the Columbia River Estuary Study Taskforce (CREST) to develop a regional management plan for the estuary.

PNRBC produced a Plan of Study for a six-year, \$6.2 million program which was authorized by the U.S. Congress in October 1978. For the next three years PNRBC administered CREDDP and \$3.3 million was appropriated for the program. However, PNRBC was abolished as of October 1981, leaving CREDDP in abeyance. At that point, much of the field work had been carried out, but most of the data were not yet analyzed and few of the planned publications had been completed. To avoid wasting the effort that had already been expended, in December 1981 Congress included \$1.5 million in the U.S. Water Resources Council (WRC) budget for the orderly completion of CREDDP. The WRC contracted with CREST to evaluate the status of the program and prepare a revised Plan of Study, which was submitted to the WRC in July 1982. In September, after a hiatus of almost one year, CREDDP work was resumed when a cooperative agreement was signed by CREST and the WRC to administer the restructured program and oversee its completion by June 1984. With the dissolution of the WRC in October 1982, the National Oceanic and Atmospheric Administration (NOAA) assumed the role of the WRC as the federal representative in this cooperative agreement.

CREDDP was designed to meet the needs of those groups who were expected to be the principal users of the information being developed. One such group consists of local government officials, planning commissions, CREST, state and federal agencies, permit applicants, and others involved in planning and permitting activities. The other major anticipated user group includes research scientists and educational institutions. For planning purposes, an understanding of the ecology of the estuary is particularly important, and CREDDP has been designed with this in mind. Ecological research focuses on the linkages among different elements in the food web and the influence on the food web of such physical processes as currents, sediment transport and salinity intrusion. Such an ecosystem view of the estuary is necessary to

predict the effects of estuarine alterations on natural resources.

Research was divided into thirteen projects, called work units. Three work units, Emergent Plant Primary Production, Benthic Primary Production, and Water Column Primary Production, dealt with the plant life which, through photosynthesis and uptake of chemical nutrients, forms the base of the estuarine food web. The goals of these work units were to describe and map the productivity and biomass patterns of the estuary's primary producers and to describe the relationship of physical factors to primary producers and their productivity levels.

The higher trophic levels in the estuarine food web were the focus of seven CREDDP work units: Zooplankton and Larval Fish, Benthic Infauna, Epibenthic Organisms, Fish, Avifauna, Wildlife, and Marine Mammals. The goals of these work units were to describe and map the abundance patterns of the invertebrate and vertebrate species and to describe these species' relationships to relevant physical factors.

The other three work units, Sedimentation and Shoaling, Currents, and Simulation, dealt with physical processes. The work unit goals were to characterize and map bottom sediment distribution, to characterize sediment transport, to determine the causes of bathymetric change, and to determine and model circulation patterns, vertical mixing and salinity patterns.

Final reports on all of these thirteen work units have been published. In addition, these results are integrated in a comprehensive synthesis entitled The Dynamics of the Columbia River Estuarine Ecosystem, the purpose of which is to develop a description of the estuary at the ecosystem level of organization. In this document, the physical setting and processes of the estuary are described first. Next, a conceptual model of biological processes is presented, with particular attention to the connections among the components represented by the work unit categories. This model provides the basis for a discussion of relationships between physical and biological processes and among the functional groups of organisms in the estuary. Finally, the estuary is divided into regions according to physical criteria, and selected biological and physical characteristics of the habitat types within each region are described. Historical changes in physical processes are also discussed, as are the ecological consequences of such changes.

Much of the raw data developed by the work unit researchers is collected in a magnetic tape archive established by CREDDP at the U.S. Army Corps of Engineers North Pacific Division Data Processing Center in Portland, Oregon. These data files, which are structured for convenient user access, are described in an Index to CREDDP Data. The index also describes and locates several data sets which were not adaptable to computer storage.

The work unit reports, the synthesis, and the data archive are intended primarily for scientists and for resource managers with a scientific background. However, to fulfill its purposes, CREDDP has developed a set of related materials designed to be useful to a wide

range of people.

Guide to the Use of CREDDP Information highlights the principal findings of the program and demonstrates how this information can be used to assess the consequences of alterations in the estuary. It is intended for citizens, local government officials, and those planners and other professionals whose training is in fields other than the estuary-related sciences. Its purpose is to help nonspecialists use CREDDP information in the planning and permitting processes.

A detailed portrait of the estuary, but one still oriented toward a general readership, is presented in The Columbia River Estuary: Atlas of Physical and Biological Characteristics, about half of which consists of text and illustrations. The other half contains color maps of the estuary interpreting the results of the work units and the ecological synthesis. A separate Bathymetric Atlas of the Columbia River Estuary contains color bathymetric contour maps of three surveys dating from 1935 to 1982 and includes differencing maps illustrating the changes between surveys. CREDDP has also produced unbound maps of the estuary designed to be useful to resource managers, planners and citizens. These black-and-white maps illustrate the most recent (1982) bathymetric data as contours and show intertidal vegetation types as well as important cultural features. They are available in two segments at a scale of 1:50,000 and in nine segments at 1:12,000.

Two historical analyses have been produced. Changes in Columbia River Estuary Habitat Types over the Past Century compares information on the extent and distribution of swamps, marshes, flats, and various water depth regimes a hundred years ago with corresponding recent information and discusses the causes and significance of the changes measured. Columbia's Gateway is a two-volume set of which the first volume is a cultural history of the estuary to 1920 in narrative form with accompanying photographs. The second volume is an unbound, boxed set of maps including 39 reproductions of maps originally published between 1792 and 1915 and six original maps illustrating aspects of the estuary's cultural history.

A two-volume Literature Survey of the Columbia River Estuary (1980) is also available. Organized according to the same categories as the work units, Volume I provides a summary overview of the literature available before CREDDP while Volume II is a complete annotated bibliography.

All of these materials are described more completely in Abstracts of Major CREDDP Publications. This document serves as a quick reference for determining whether and where any particular kind of information can be located among the program's publications and archives. In addition to the abstracts, it includes an annotated bibliography of all annual and interim CREDDP reports, certain CREST documents and maps, and other related materials.

To order any of the above documents or to obtain further information about CREDDP, its publications or its archives, write to CREST, P.O. Box 175, Astoria, Oregon 97103, or call (503) 325-0435.

## FOREWORD

The research reported here was funded primarily by the Columbia River Estuary Data Development Program (CREDDP). Particular thanks are due to Jim Good, Dr. Jack Damron, David Fox, all past or present CREST/CREDDP staff, and Ann Saari, citizen volunteer, all of whom worked to obtain the funds for completion of the program. Parts of the theoretical work, tidal modeling, salt transport, energy budget, and residual flow calculations were funded by National Science Foundation (NSF) Grant OCE 8208856. The US Army Engineers, Portland District funded part of the salinity distribution work.

The CREDDP work was begun at Mathematical Sciences Northwest of Bellevue, Washington, and finished at the University of Washington, Geophysics Program. Field work for (CREDDP) was carried out by Dobrocky Seatech, Ltd. of Victoria, B. C. The author has benefited greatly from numerous discussions with Dr. J. Dungan Smith of the University of Washington. Others who have contributed ideas to the program include Ian Webster, then of Dobrocky Seatech, Ltd, and W. R. Geyer and Chris Sherwood, both of the University of Washington.

Dr. Gary Minton, Dr. Sig Hoverson and Chris Boerner all of MSNW, contributed to the early stages of the project. Tom Juhasz and other Dobrocky Seatech field personnel, an enthusiastic group of students recruited by Gary Muehlberg of Clatsop College, and Chris Sherwood, Guy Gelfenbaum and Ed Roy of the University of Washington, Oceanography Department all helped make the CREDDP field program a success. Dr. Savithri Narayanan of Dobrocky Seatech, Ltd, and David Askren and Steve Chesser of the Portland District Corps of Engineers were responsible for the preliminary processing of the 1980 CREDDP profile data.

Benjamin Giese did the tidal inundation time calculations, the tidal modeling and the energy budget work; Jean Newman wrote data processing programs and processed and edited the many NOS current meter files; and Bill Fredericks wrote several plotting programs. Drafting was done by Lin Sylvester and report preparation by Kathryn Sharpe, Madelyn Troxclair, Sam Blair, and Lisa Peterson.

Data have been received from the National Ocean Survey (NOS) Tidal Datums and Information, and Circulatory Surveys Branchs, both of Rockeville; Oregon State University; the US Army Engineers, Waterways Experiment Station, Portland District and North Pacific Division; US Geological Survey, Portland and Tacoma Offices; the National Data Buoy Office of Bay St. Louis; and the National Marine Fisheries Service, Pacific Environmental Group of Monterey. Richard Morse of NOAA, Seattle was instrumental in the obtaining the 1981 NOS data.

This document was prepared under contract with the Columbia River Estuary Study Taskforce (CREST). The views are solely those of the author and do not necessarily reflect the viewpoint of CREST member agencies.



## TABLE OF CONTENTS

	<u>Page</u>
LIST OF FIGURES	xv
LIST OF TABLES	xix
1. INTRODUCTION AND BACKGROUND	1
1.1 MODES OF CIRCULATION	1
1.1.1 The Primary Tidal Circulation	7
1.1.2 The Secondary Circulation	8
1.2 THE SALINITY DISTRIBUTION EQUATION	8
1.3 RESIDUAL FLOW PROCESSES	9
1.3.1 Tidal Effects on Residual Circulation	10
1.3.2 River Flow and Density Effects on Residual Circulation	11
1.3.3 Atmospheric Effects on Residual Flow	12
1.4 VERTICAL MIXING, STRATIFICATION AND CIRCULATION	15
1.4.1 Types of Vertical Exchange Processes	16
1.4.2 Formulations of Vertical Mixing and the Effects of Stratification	16
1.5 STRUCTURE OF THE REPORT	18
2. METHODS	21
2.1 FIELD PROGRAM AND INSTRUMENTATION	21
2.2 PRELIMINARY DATA PROCESSING	29
2.3 DETERMINATION OF TIDAL PROPERTIES	30
2.3.1 Harmonic Analysis Methods	30
2.3.2 Harmonic Constant Reduction	31
2.3.3 Tidal Inundation Time Calculations	31
2.4 THE ONE-DIMENSIONAL, HARMONIC MODEL OF THE M2 TIDE	33
2.4.1 Model Formulation	33
2.4.2 Formulation of the Energy Budget	36
2.5 STATISTICAL METHODS	40
2.6 SALT TRANSPORT CALCULATIONS	43
2.7 MISCELLANEOUS CALCULATIONS	44

	<u>Page</u>
3. RESULTS AND DISCUSSION	45
3.1 TIDAL PROCESSES	45
3.1.1 Tidal Heights	45
3.1.2 Factors Influencing the Tidal Range and the Times of High and Low Water	53
3.1.3 Tidal Inundation Time	57
3.2 CURRENTS	57
3.2.1 Observed Spatial Distribution	57
3.2.2 Vertical Structure of the Tidal Flow -- Boun- dary Layer and Density Effects	63
3.2.3 Tidal Effects on the Mean Flow	71
3.3 TIDAL-FLUVIAL INTERACTIONS	77
3.3.1 Observations	77
3.3.2 Model Results	81
3.4 THE ENERGY BUDGET	89
3.4.1 Interpretation of Energy Budget Terms	89
3.4.2 Neap-Spring Effects	89
3.4.3 Energy Budget Calculations	91
3.5 THE SALINITY DISTRIBUTION	97
3.5.1 Water Masses and Mixing	97
3.5.2 Seasonal-Average Salinity Distributions	100
3.5.3 The Low-Flow Salinity Distribution	114
3.5.4 The High-Flow Salinity Distribution	117
3.5.5 Neap-to-Spring Transitions, Riverflow and Tidal Range	133
3.6 TRANSPORT PROCESSES	133
3.6.1 Transport at Clatsop Spit: the Seasonal Pat- tern	135
3.6.2 Salt Transport at Other Transects	141
3.7 RESIDUAL FLOW PROCESSES	147
3.7.1 Seasonal cycles	147
3.7.2 Tests of Hypotheses	153
4. SUMMARY AND RECOMMENDATIONS	161
4.1 SUMMARY OF PRESENT KNOWLEDGE	161
4.2 AREAS OF INADEQUATE KNOWLEDGE	163

LITERATURE CITED

APPENDIX A. Field sampling locations, 1977 to 1981

APPENDIX B. Tidal height and tidal current harmonic analysis results

APPENDIX C. Tidal constants (Table 25) and tidal height observation stations (Table 26), compiled from NOS records

APPENDIX D. Tidal inundation time for the 1940-61 period, as calculated by National Ocean Survey

APPENDIX E. Salinity intrusion plots

APPENDIX F. Daily estimated riverflow at Astoria, 1979-81

## LIST OF FIGURES

	<u>Page</u>
1. The Columbia River Estuary	3
2. Columbia River Estuary bathymetry	5
3. Mean longitudinal salinity distribution in	
a. A typical partially mixed estuary	
b. The Columbia River Estuary	13
4. Columbia River riverflow at Astoria and sampling periods	20
5. Time-series stations for 1980	22
6. Density and velocity profile stations for 1980	24
7. Time-series stations for 1981	26
8. Density profile stations for 1981	28
9. Definition of tidal model parameters	32
10. Definition of tidal model geometry	37
11. Current meter locations Clatsop Spit-Sand Is. Section	
a. High-flow season	
b. Low-flow Season	42
12. Power spectrum of tidal height	
a. At Tongue Pt., 1981	
b. At Wauna, 1981	46
13. Tidal model results for a riverflow of 146 kcfs	48
14. Tidal model results for a riverflow of 433 kcfs	49
15. Tidal model results for a riverflow of 1,000 kcfs	50
16. M2 tidal heights characteristics vs. river mile	
a. Phase	
b. Amplitude	51
17. Tidal model results	
a. For M2 + S2 + N2 and 146 kcfs riverflow	
b. For M2 - S2 - N2 and 146 kcfs riverflow	54
18. Greenwich intervals vs. river mile	58
19. Tidal inundation time curve for Tongue Pt. reference	59

	<u>Page</u>
station, 1940-1961.	59
20. M2 tidal current phase and amplitude in the South and North Channels	60
21. M2 tidal current vs. depth and river mile	62
22. Clatsop Spit-Sand Is. Section M2 current phase and amplitude	64
23. October 1980 ebb T, S, and velocity profiles at station 5NB	66
24. October 1980 Flood T, S, and velocity profiles at station 4NA	67
25. October 1980 ebb T, S, and velocity profiles at station 2N	68
26. Time-series of along-channel velocity at station CM-2S	69
27. Typical salinity and velocity profiles for the lower and upper estuary	70
28. Two-dimensional model results -- mean salinity and velocity	
a. Low flow, neap tide	
b. Low flow, spring tide	75
29. Tidal heights at Tongue Pt., Wauna and Columbia City during the 1981 spring freshet	76
30. Tidal and tidal-fluvial characteristics, March 1980 - December 1981	78
31. The effect of riverflow on river stage -- historical freshets	79
32. Tidal model results	
a. Predicted tidal transport as a function of river mile for selected riverflows	
b. Predicted stage as a function of river mile for selected riverflows	80
33. Energy budget results	
a. Tidal energy flux	
b. Fluvial energy flux	88
34. Energy budget results -- dissipation as a function of river mile	92
35. The mixing of RW with SOW, and SOW with SSOW	99

	<u>Page</u>
36. Seasonal mean and maximum salinity -- high-flow season, South Channel	101
37. Seasonal mean and maximum salinity -- high-flow season, North Channel	102
38. Seasonal mean salinities at MLLW and 12 m; low-flow season and high-flow season	103
39. Seasonal extreme salinity intrusion low-flow season and high-flow season	104
40. Seasonal minimum, maximum and mean salinity -- low-flow season, South and North Channels	105
41. October 1980 (neap tide) -- minimum, maximum and mean salinity, and salinity range, South Channel	112
42. October 1980 flood T, S and velocity profiles at station 6SA	115
43. October 1980 flood and ebb T and S profiles at station 6SD	116
44. October 1980 (spring tide) -- minimum, maximum and mean salinity, and salinity range, South Channel	118
45. October 1980 flood T, S and velocity profiles at station 4SB	120
46. Extreme salinity intrusion october 1980	121
47. Mean salinities at MLLW and 12 m, October 1980,	122
48. June 1959 freshet -- mean and maximum salinity, South Channel minimum salinity intrusion	123
49. Accoustic profiles of the Fraser River salt wedge a. Early ebb b. Late ebb	124
50. S and velocity profiles from the Fraser River salt wedge	125
51. June 1981 freshet -- minimum, mean and maximum salinity, and salinity range South Channel	128
52. Time-Series of speed, direction, salinity and temperature at station CM-1, during the June 1981 freshet	130
53. June 1959 and 1981 freshet mean salinities at MLLW and 12 m	131

	<u>Page</u>
54. The neap-spring transition as a function of riverflow	132
55. Mean flow through Clatsop Spit-Sand Is. Section	
a. High-flow season	
b. Low-flow season	134
56. Mean salinity Clatsop Spit-Sand Is. Section	
a. High-flow season	
b. Low-flow season	136
57. Tidal advective salt transport Clatsop Spit-Sand Is. Section	
a. High-flow season	
b. Low-flow season	137
58. Mean flow salt transport Clatsop Spit-Sand Is. Section	
a. High-flow season	
b. Low-flow season	138
59. Total salt transport Clatsop Spit-Sand Is. Section	
a. High-flow season	
b. Low-flow season	139
60. Time-series of salt and water transport parameters at mid-depth at station CM-1, spring 1981	142
61. June 1981 T, S and density profiles at station TS-12	143
62. Time-series of salt and water transport parameters at mid-depth at CM-9, spring 1981	145
63. Power spectra	
a. Low-passed, Wauna-Tongue Pt. slope	
b. Tongue Pt. tidal range	157
64. June 1980 (neap tide) minimum, maximum and mean salinity, and salinity range, South Channel	E-1
65. June 1980 (spring tide) minimum, maximum and mean salinity, and salinity range, South Channel	E-5
66. June 1980 (neap tide) minimum, maximum and mean salinity, and salinity range, North Channel	E-9
67. June 1980 (spring tide) minimum, maximum and mean salinity, and salinity range, North Channel	E-13
68. June 1981 freshet minimum, mean and maximum salinity, North Channel	E-17

## LIST OF TABLES

	<u>Page</u>
1. Tidal constituent ratios - Columbia River and Estuary	47
2. Tidal properties as a function of river mile	56
3. Mean flows, Columbia River Estuary, October 1980	73
4. Tidal properties as a function of riverflow and tidal range - model predictions	82
5. Tidal model predictions --	
a. Tidal prism and ratio of tidal prism to riverflow volume	
b. Stokes drift volume and ratio of stokes drift volume to riverflow volume	86
6. Total tidal and mean flow potential energy fluxes and total dissipations	90
7. Defining properties of surface ocean water (SOW) and sub- surface ocean water (SSOW), near mouth of Columbia River	98
8. Salinity characteristics, Astoria-Megler Bridge, selected spring and neap tides, March - October 1980	108
9. Seasonal cycle of mean water level (MWL) Tongue Point	146
10. Seasonal cycle of riverflow 1969-82 and 1980-81	148
11. Seasonal cycles of atmospheric parameters	
a. Geostrophic winds, 1980-81	
b. Newport, OR winds, 1980-81	150
12. Maximum correlations and lags between wind data from various sources	152
13. Maximum correlation and lags between height and various forcing functions	
a. Heights	
b. Slopes	154
14. Percent of variance in low-passed heights and slopes accounted for by forcing functions, as determined by regression analysis	156



	<u>Page</u>
15. CREDDP time-series data 1980	A-1
16. CREDDP velocity and density profile data 1980	A-3
17. NOS and USGS tidal-height data 1980-81	A-5
18. NOS current meter and anemometer data 1981	A-6
19. NOS density profile data 1981	A-8
20. Corps of Engineers current meter data 1977	A-9
21. Corps of Engineers current meter data 1978	A-10
22. Current meter harmonic analysis results CM-1	B-1
23. Tidal height harmonic analysis results Tongue Pt. TG-21	B-2
24. Tidal Height harmonic constant reduction Tongue Pt. TG-21	B-3
25. Tidal constants for Columbia River and Estuary stations, from USCGS historical data	C-1
26. USCGS historical observations Columbia River and Estuary 1852-1959	C-5
27. Tidal inundation time at Tongue Pt. 1940-61	D-2
28. Columbia riverflow at the mouth 1979-81	F-1

## EXECUTIVE SUMMARY

This report summarizes results from a four-year study of the physical oceanography of the Columbia River Estuary. Work was carried out in six areas: theory of estuarine circulation, tidal processes, system energetics, salinity distribution, salt transport, and low-frequency flow processes.

The major theoretical results are the definition of modes of estuarine circulation and an analysis of the forces maintaining the salinity distribution. The circulation modes are defined by application of a scaling analysis and a perturbation expansion. This mathematical procedure separates the primary tidal circulatory processes from secondary, modifying features. The primary tidal circulation occurs at diurnal (daily) and semidiurnal (twice-daily) frequencies. It is driven both by the surface slope and the time-varying salinity distribution. The secondary circulation modifies the primary tidal circulation. It can be divided into three modes that occur at different frequencies: the tidal overtones (that occur at frequencies higher than semidiurnal and are produced by the distortion of the tidal wave as it moves upriver), the secondary tidal circulation (at diurnal and semidiurnal frequencies), and the residual (or time-averaged) circulation, which varies during the tidal month and seasonally. The residual circulation is driven by the riverflow, the salinity distribution, tidal energy transferred from the primary tidal circulation, and, to a lesser extent, atmospheric effects.

Although a model encompassing the tidal circulation and all residual flow processes was beyond the scope of work, a one-dimensional (in the along-channel direction), numerical, harmonic water transport model was constructed that reproduced many important features of the tidal and tidal residual circulations in the presence of riverflow. This model avoids the complexities of salinity intrusion effects by treating only the transport (vertical integral of the flow). The purpose of the model was to investigate the interaction between geometric, frictional, tidal and fluvial (riverflow) effects. Data analysis and the model show that:

- tidal range decreases rapidly in the upriver direction on the tides of higher range; that is, an increase in tidal range at the mouth results in a less than proportional increase upriver. Conversely, tidal range drops off slowly with river mile on tides of lesser range. This occurs because friction increases with the cube of the tidal range, but the energy supplied from the ocean by the tides varies only with approximately the square of the tidal range.
- There is more energy available for mixing on the ebb than on the flood, because of the strength of the riverflow. The greater mixing on the ebb and the effects of salinity intrusion combine to make the vertical structure of the ebb currents very different than that of flood currents; this is the ebb-flood asymmetry. The vertical distribution of the mean flow is determined by the differences between the ebb and flood flows. The large shear (vertical differences in velocity) on ebb, the greater vertical uniformity of the flood flow and the salinity intrusion combine to generate net upstream bottom currents in the lower estuary.
- The vertical structure of the currents is also strongly influenced by along-channel changes in depth and width. Mean upstream bottom flow associated with strong horizontal salinity gradients is not continuous from the entrance to the upstream limits of salinity intrusion. Its continuity is often interrupted by pockets of mean downstream bottom flow caused by topographic features. This suggests that the estuarine turbidity maximum, which is dependent upon the upstream bottom flow, may form preferentially in certain parts of the estuary and may be spatially discontinuous.

- o Tidal transports and tidal velocities are greater in the North Channel than in the South Channel. Most of the tidal prism of the lower estuary is filled by the flow in the North Channel.
- o Freshets reduce the tidal range and greatly increase the river stage (mean water surface level) above RM (river mile)-20, because the riverflow increases the friction. Tides and stage below Tongue Pt. are much less affected by such changes in riverflow.
- o Energy budget calculations based on the tidal model show that the tidal energy entering the mouth of the estuary from the ocean is the dominant source of energy for circulatory processes in the estuary proper (below about RM-18). The dominant source of energy in the river is the potential energy released as the river water runs downhill; most of this energy is lost to friction above RM-30. Energy from the riverflow is much less important than tidal energy below RM-18, but both tidal and fluvial energy inputs must be considered in the area of minimum energy between about RM-18 and RM-30 that coincides with the islands and other depositional features of Cathlamet Bay.

The same perturbation expansion used to define modes of estuarine circulation has also been used to investigate the factors that govern salinity intrusion into the estuary. This analysis indicates that salt is maintained in the estuary primarily by the tidal currents acting on the salinity gradient (the horizontal salinity differences), not by the mean upstream bottom flow. Salt must also be transported vertically, as well horizontally, if the salinity distribution is to be maintained. It appears that mixing and tidal transport, rather than the vertical mean flow are primarily responsible for this vertical transport, but details of salt transport processes remain unclear.

During periods of low riverflow, there is a neap-to-spring transition that changes the salinity structure from partially-mixed or well-mixed (spring tide) to stratified (neap tide). Neap-to-spring changes in salinity structure becomes less important as the riverflow increases. The transition may occur abruptly, because of the interaction of vertical mixing and stratification; increased stratification during the period of decreasing tidal range before the neap tide inhibits mixing which, in turn, allows a further increase in stratification. The process is reversed as the tidal range increases after the neap tide. Salinity intrusion length is greatest under low-flow, neap-tide conditions, when salinity intrusion may reach to about RM-30 in the navigation channel, because the stratification allows upstream movement of salt without significant mixing with the overlying river water. Under the highest flow conditions, salt may be absent upriver of RM-2 for several hours at the end of ebb. Salinity intrusion into the shallower bays, and particularly into Grays and Cathlamet Bays which are at the upstream limits of salinity intrusion, is highly variable.

The high riverflow (~310 kcfs) and low riverflow (~155 kcfs) seasonal mean, minimum and maximum salinity distributions have been defined for North and South Channels. These seasonal distributions should be useful in understanding biological processes having seasonal time scales, but averaging obscures physical processes which are better understood in terms of the actual states of the system. The seasonal averages suggest that salinity intrusion into the North Channel is somewhat greater than that into the South Channel under high-flow conditions, because of the stronger riverflow in the South Channel. The difference is less pronounced under low-flow conditions.

Salt and water transport calculations show that most of the net outflow of water is near the surface in the South Channel. Upstream bottom flow is

strongest in the North Channel. Salt is brought into the estuary primarily by tidal mechanisms in a near-surface jet in the North Channel, at the same lateral position as the strongest tidal currents. Unlike the currents, the maximum salt transport is below the surface, because the salinity is lower at the surface. The mean upstream bottom flow appears to be important in inward salt transport only on neap tides, in those parts of the estuary where horizontal salinity gradients are strong. Salt transports near the bottom are otherwise small. The large, near-surface, mean outflow (primarily riverflow) in the South Channel transports salt out of the estuary.

The response to changes in riverflow, atmospheric effects (wind and pressure) and tidal range of that part of the residual or mean flow which is driven by the slope of the water's surface (the barotropic residual flow) was investigated by use of the statistical properties of the atmospheric data, tidal heights and surface slopes in the estuary and river. Record lengths of up to two years were used. The primary conclusions of the residual flow work were:

- atmospheric pressure fluctuations, wind-driven changes in elevation of the coastal ocean, and winds over the estuary all influence tidal heights in the estuary, but this atmospheric forcing is too weak to dominate the residual currents in the estuary.
- The dominant factors controlling the residual circulation (slopes, currents and salinity) in the estuary proper (below Tongue Pt.) are the tidal range and river inflow. Tidal processes and riverflow are about equally dominant in controlling residual flows in the Wauna-Tongue Pt. reach. Riverflow is dominant above Wauna.

*I do not know much about gods; but I think that the river  
Is a strong brown god - sullen, untamed and intractable  
Patient to some degree, at first recognized as a frontier;  
Useful, untrustworthy, as a conveyer of commerce;  
then only a problem confronting the builder of bridges.  
The problem once solved, the brown god is almost forgotten  
By the dwellers in cities - ever, however, implacable,  
Keeping his seasons and rages, destroyer, reminder  
Of what men choose to forget. Unhonored, unpropitiated  
by worshipers of the machine, but waiting, watching and waiting*

T. S. Eliot  
"The Four Quartets"

## 1 INTRODUCTION AND BACKGROUND

The Columbia River Estuary (Figure 1) has been the subject of intensive study from a number of points of view during the 1979-83 period, through the Columbia River Estuary Data Development Program (CREDDP). This report summarizes the work of the Circulation Work Unit. The purposes of this work unit were to describe the flow and density fields and analyze the complex and numerous interactions between these fields. This report should be read in conjunction with that of the Simulation Work Unit (Hamilton 1984); the modeling results presented there further illustrate many of the phenomena discussed here.

The dominant factors in the circulation of the Columbia River Estuary are the high energy level, the strong horizontal salinity gradient and the high temporal variability provided by the strong tides and large riverflow, and the complex topography that consists of narrow (~0.5 to 3 km), well-defined channels separated by broad sand banks (Figure 2). The resulting flow is three-dimensional, moderately non-linear with respect to the tidal processes (e.g. ebb to flood asymmetry in friction and distortion of the tidal wave by topography) and strongly non-linear with regard to the influence of stratification.

Despite the breadth of the lower estuary (5 to 12 km; Figure 2), most of the flow is confined to the channels. Processes occurring on flats are essential to biological and sedimentological processes, but our analysis has focused on the channels, where most of the flow is conveyed. This allows us to make a vital simplification: that the flow at many locations is essentially two-dimensional in depth and along-channel distance. This pragmatic assumption was necessary in light of the very limited data available from previous studies and the difficulties in collecting new data. Having made this assumption, we are able to venture outside the channels to only a limited extent.

### 1.1 MODES OF CIRCULATION

The ultimate aim of most physical oceanographic investigations is to explain the observed phenomena in terms of the governing equations, in this case: the equations of motion (conservation of momentum), continuity (conservation of mass), and salt continuity or salinity distribution (conservation of salt). The most direct procedure is to solve these equations with the applicable boundary conditions and parameters. For a shallow, partially-mixed system with strong tides and complex topography, no analytical solutions are known. Only a full three-dimensional, numerical model would resolve all the important phenomena; this was beyond the resources of the program.

A more productive procedure for the purposes of this report is to simplify the governing equations through the assumption of two-dimensionality and the use of a scaling analysis and a perturbation expansion. This method is often used by oceanographers faced with complex, non-linear phenomena, for which no exact mathematical solutions are available. We use the method, not to produce solutions, but to determine the importance of the various driving forces and to define modes of circulation. These circulation modes will be used to interpret the observed flow and salinity distributions.

It is necessary here to introduce the idea of non-linearity of a differential equation because the equations which describe the circulation of our system are non-linear in important respects. A differential equation is linear, if the unknown function  $f(x,y)$  (and all derivations thereof) appear in the equation in individual terms which are linear. Terms such as  $f$ ,  $\frac{\partial f}{\partial x}$ ,  $\frac{\partial^2 f}{\partial x^2}$  and  $\frac{\partial^2 f}{\partial x \partial y}$  are all linear, while  $f^2$ ,  $(\frac{\partial f}{\partial x})^2$ ,  $\frac{\partial f}{\partial x} \frac{\partial f}{\partial y}$  and  $e^{-f}$  are all non-linear. Because estuarine circulation is non-linear, we can expect that it will behave in complex, non-intuitive ways (e.g.

transfer of energy between different frequencies and abrupt transitions between states). This richness of behavior is not characteristic of linear systems.

We need also to state the assumption of two-dimensionality in more precise form: we have assumed that the estuary is narrow and uniform enough that the effects of channel curvature and the earth's rotation (Coriolis effect) do not enter into the along-channel equation of motion, and that changes in channel cross-section are gradual enough to prevent the convective accelerations from making circulation strongly non-linear. The analysis described below allows, by an extension of the method of Ianniello (1979), determination of criteria for curvative and channel non-uniformity (in terms of other scale parameters) that are allowable. Many parts of the estuary meet these criteria and are effectively two-dimensional in  $x$  and  $z$  (the along-channel and vertical coordinates). Finally, since the semidiurnal tide provides most of the tidal energy, we have used the frequency of the semidiurnal tide in the analysis.

The scaling analysis and perturbation expansion is a means to determine the most important terms in the hydrodynamic equations and to separate each governing equation into a series of equations which may then be solved sequentially. The method is based on the assumption that not all the phenomena involved are of the same importance. Thus, a large term in a governing equation can only be balanced by some other large term, and not a series of smaller terms. The perturbation expansion groups together the largest terms in the original governing equation in a single equation that represents a simple approximation to the observed flow. This equation is the  $O(1)$  (for which read: "order 1") equation; the terms in it represent the most important features of the flow. The next most important processes are represented in the  $O(\epsilon)$  (for which read "order epsilon") equation, the processes of which are driven by terms determined in the  $O(1)$  equation, and so on through the  $O(\epsilon^2)$  and higher order equations. Each of these higher-order equations represents a finer modification to the  $O(1)$  flow, and contains non-linear driving terms stemming from lower orders. These driving terms illustrate how energy is transferred from one frequency or process to another by non-linearities in the equations of motion.

To carry out the perturbation expansion, it is necessary that all the major variables (height, velocity, etc.) be non-dimensional (without units) and  $O(1)$  (varying from 0 to about 1). This is accomplished by what is known as "scaling" and "non-dimensionalizing" the variables. We write, for example, the along-estuary velocity  $U$  and depth  $Z$  as:

$$U = U_0 u \quad (1)$$

$$Z = H_0 z$$

$$X = L_x x$$

where:

$U$  = velocity in m/sec,

$Z$  = height in m,

$U_0$  = the characteristic speed of the tidal currents ( $\sim 1$  m/sec),

$H_0$  = the mean depth of the flow,

$X$  = horizontal distance in m,

$L_x$  = horizontal length scale ( $\sim 5 \times 10^3$  m),

$u$  = the non-dimensional,  $O(1)$  velocity,

$z$  = the non-dimensional,  $O(1)$  depth, and

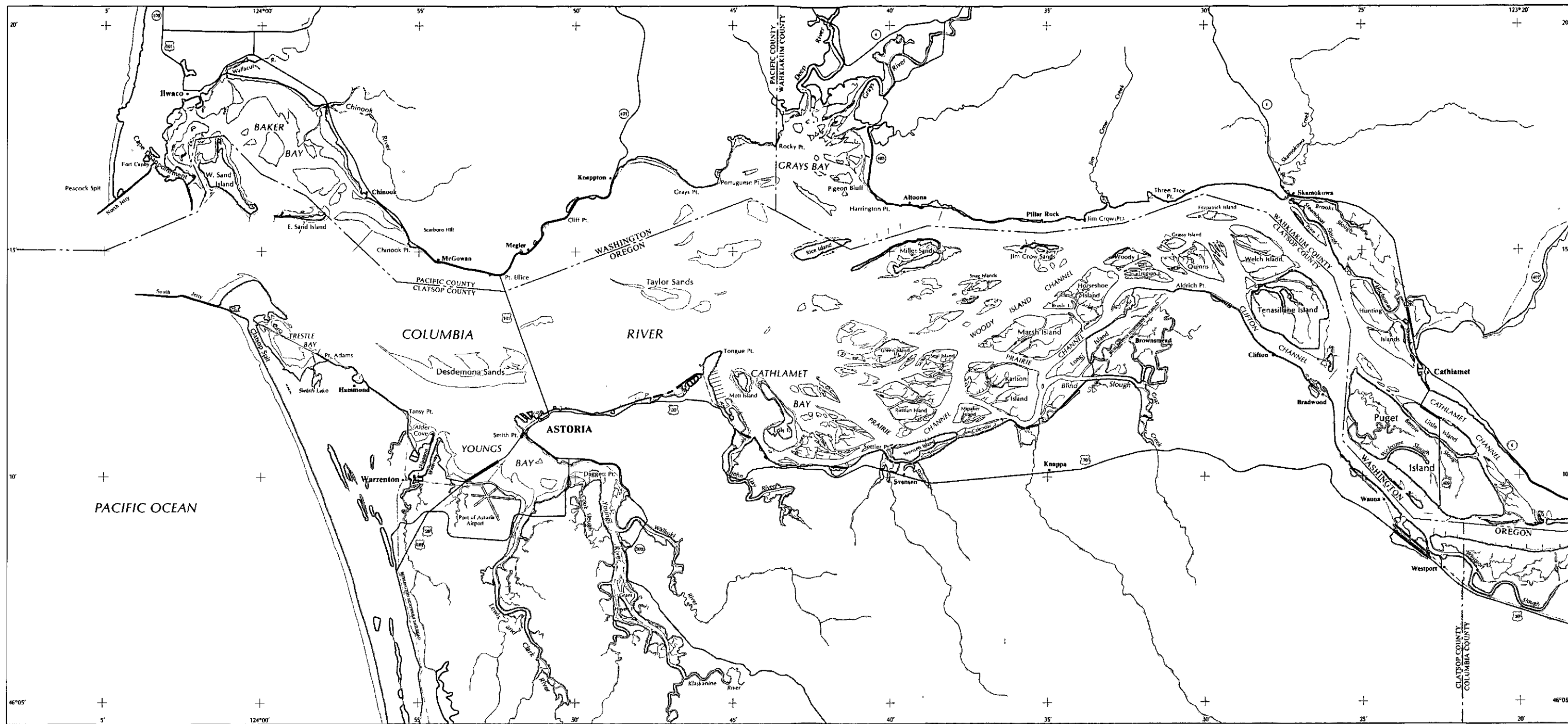
$x$  = the non-dimensional,  $O(1)$  horizontal distance.

The non-dimensional velocity  $u$  might vary during a tidal cycle from 0 to  $\sim 2$ ;

---

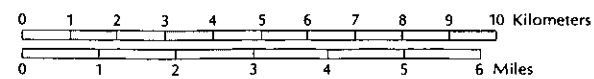
Figure 1. Columbia River Estuary





# Columbia River Estuary

Scale 1:160,000



Map produced in 1983 by Northwest Cartography, Inc.  
 for the Columbia River Estuary Data Development Program


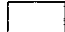





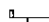
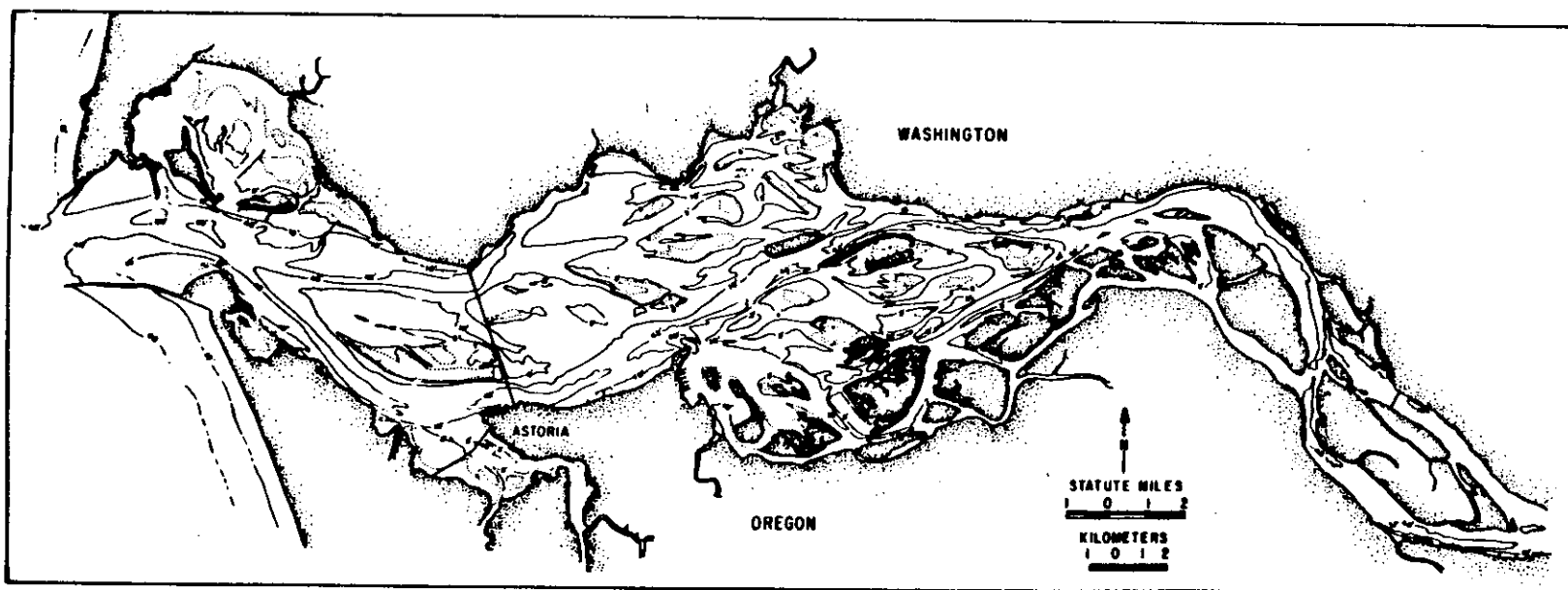
-  Shoreline (limit of non-aquatic vegetation)
-  Major highways
-  Intertidal vegetation
-  Cities, towns
-  Shoals and flats
-  Railroads
-  Lakes, rivers, other non-tidal water features
-  Other cultural features

Figure 2. Columbia River Estuary bathymetry -- narrow channels are separated by broad sand bars. The principal channels seaward of Tongue Pt. are the North Channel, along the north shore, and the South Channel, off Astoria. The South Channel is connected much more directly to the Navigation Channel above Altoona.



independent of the units (m/sec or cm/sec) in which the problem was originally posed. The vertical coordinate  $z$  can vary only from 0 to  $\sim 1$ , since we have used the mean depth of the flow as the vertical scale length. Were the non-dimensional velocity (or any other non-dimensional quantity) to reach a much larger value (e.g. 10) or never to exceed  $\sim 0.1$ , then the scale velocity (or other scaling quantity) would have been incorrectly chosen.

Use of non-dimensional variables accomplishes several things. First, it eliminates the units in which the problem is posed; a term is large, because it is important, not because we have measured it in a particular set of units. Second, we have found the characteristic velocities, length scales, etc. associated with the flow. For example, the length scale  $L_x$  is determined by changes in channel curvature and channel cross-section. All variables that are functions of  $x$  may vary significantly (but not radically) over this distance.

Third, we learn whether all the terms we have included in the equation of motion are of equal importance. After scaling and non-dimensionalizing, each term in the equation will be a collection of non-dimensional variables, multiplied by groups of dimensional variables that indicate the importance of the term. These groups of dimensional variables will appear only in combinations that are also non-dimensional. Thus, for example, the convective non-linear term  $u(\frac{\partial u}{\partial x})$  in the non-dimensional equation of motion is multiplied by:

$$\left(\frac{U_0}{L_x \sigma}\right) \left(\frac{\delta A}{A_0}\right) \quad (2)$$

where:

$\sigma$  = the frequency of the semidiurnal tides  
 $\delta A$  = the change in cross-sectional area over length  $L_x$   
 $A_0$  = average cross-sectional area

The units chosen for the individual terms are irrelevant because the units cancel. The size of this non-dimensional number that multiplies the non-linear term varies with  $\frac{\delta A}{A_0}$ . In this case, if  $\frac{\delta A}{A_0}$  is  $O(\epsilon)$ , so are the non-dimensional number and the convective acceleration term that is multiplied by this number. Thus, the convective non-linear term is only  $O(\epsilon)$  relative to other terms in the equation of motion in many parts of the estuary, and the system is only moderately non-linear with respect to this effect at these locations. This means that the convective term will first appear in the  $O(\epsilon)$  equation, not in the  $O(1)$  equation. We expect that parts of the estuary where the convective accelerations are  $O(1)$  will be more complex.

The relationship between terms in the  $O(1)$  and higher order equations can be seen, using the (non-dimensional) velocity in the  $x$  (along-channel) direction as an example:

$$u(x,z,t) = u^0(x,z,t) + \epsilon u^1(x,z,t) + \epsilon^2 u^2(x,z,t) + \dots \quad (3)$$

where:

$u$  is the non-dimensionalized along-channel velocity,  
 $\epsilon$  = perturbation parameter, defined below, and  
the superscripts on  $u$  are not powers, but indicate terms of different orders, and the superscripts on  $\epsilon$  are powers.

The variable  $u^0$  appears in the  $O(1)$  equation (and again as a driving term in the  $O(\epsilon)$  equation, but only in terms that are multiplied by constants that are  $O(\epsilon)$ ).

The term  $\varepsilon u^1$  is only  $\varepsilon$  times as large as  $u^0$ ; it appears, accordingly, only in the  $O(\varepsilon)$  and higher order equations, that indicate progressively smaller effects. The time average horizontal velocity  $\bar{u}(x,z)$  is (on the basis of data and scaling arguments):

$$\bar{u}(x,z) = \varepsilon \bar{u}^1(x,z) + \varepsilon^2 \bar{u}^2(x,z) + \dots \quad (4)$$

where the overbar indicates a time average. There is no  $\bar{u}^0$  (i.e. no  $O(1)$  time average velocity), because the time average circulation is only small relative to the tidal circulation;  $\bar{u}^0$  must therefore vanish. That the convective non-linear term  $\frac{U_0}{L_x \sigma} \frac{\delta A}{A_0} u^0 \frac{\partial u^0}{\partial x}$  appears in the  $O(\varepsilon)$  equation and that its time average appears in the time-averaged equation illustrates how non-linear terms transfer energy between processes occurring at different frequencies.

The perturbation parameter  $\varepsilon$  is not merely a housekeeping device to separate the different orders of equations. The choice of  $\varepsilon$  is critical. If  $\varepsilon$  is too large (only slightly smaller than 1), then all terms are of comparable importance and no separation of orders is possible. If  $\varepsilon$  is too small (e.g.  $\sim \frac{1}{100}$ ), then nothing useful has been accomplished, because all the important phenomena are still in the  $O(1)$  equation. We seek, therefore, an  $\varepsilon$  of  $O(\frac{1}{10})$ . This is equivalent to saying that the problem is moderately non-linear. The perturbation parameter used in this work is that suggested by Ianniello (1977a,b); it is  $\frac{\xi}{H}$ , the ratio of tidal range  $\xi$  to mean depth  $H$  and is a measure of the importance of non-linear processes associated with the tides. Its value in the Columbia River Estuary is between 0.05 and 0.2. The estuary is therefore moderately non-linear in this respect, and the perturbation expansion is appropriate. In contrast, Chesapeake Bay is weakly non-linear with respect to the tides, because it is much deeper; and the estuaries of the Atlantic Coast of France are strongly non-linear, because they are shallower and have larger tidal ranges (Allen et al. 1980).

We do not attempt here to solve the equations resulting from the perturbation expansion, so we omit the mathematical apparatus. We merely discuss the circulation modes that arise out of the  $O(1)$  and  $O(\varepsilon)$  equations. The higher order equations are of lesser importance and greater complexity.

### 1.1.1 The Primary Tidal Circulation

The primary or  $O(1)$  circulation in the estuary consists of the tidal circulation, which is governed by a force balance between acceleration of the flow, vertical stress divergence and pressure gradient. This force balance is equivalent to Newton's Second Law: force = mass  $\times$  acceleration. The pressure gradient consists of two parts, barotropic and baroclinic or internal, which may be of equal magnitude. The barotropic part of the pressure gradient is that caused by the surface slope; it is independent of depth. The baroclinic pressure gradient at any depth  $-h$  contains an integral from the surface to that depth of the horizontal salinity gradient. It is proportional to  $\int_{-h}^{\xi} \frac{\partial s}{\partial x} dz$ , and it increases with depth.

The sign of the total pressure gradient may change with depth when  $\frac{\partial s}{\partial x}$  is large and opposes the surface slope. The tidal circulation is the most important circulation mode and dominates the energy balance for the estuary. The differential equation describing this mode is linear only in a system with constant density. The horizontal and vertical density (i.e. salinity) structure of real estuaries causes the circulation and stratification to interact in a complex manner, which is manifested in the stress divergence term, which represents

the vertical exchange of momentum in the flow. No analytical solutions are known for the variable salinity case.

The inter-dependence of the circulation, density stratification (i.e. vertical difference in density) and vertical mixing processes that is expressed in the vertical stress divergence term in the equation of motion is fundamental to the problem of estuarine circulation and can not, at least in this analysis, be removed from the primary tidal circulation. Fluids have a very strong tendency to move, under the influence of gravity, along level surfaces. Vertical turbulent mixing and other processes such as breaking internal waves transfer both momentum and mass (i.e. salt) between layers. The effect of momentum loss to the sea bed (bottom friction) is felt in the interior, as turbulence diffuses momentum toward the bed. Stratification inhibits this vertical transfer in major way (Section 1.4)

In the presense of this stratification, the momentum equation is coupled to the  $O(1)$  salt continuity equation because the circulation changes the density structure and the density structure affects the circulation. This coupling arises through the stress divergence and the baroclinic pressure gradient terms in the momentum equation, and the vertical salt flux term and non-linear tidal transport terms in the  $O(1)$  salt continuity equation. That the circulation, stratification and the salinity distribution are linked in so complex a manner and that this interaction is so fundamental as to play a major role in the  $O(1)$  circulation, means that the flow is fundamentally complex; no simple model will explain the behavior of the system.

#### 1.1.2 The Secondary Circulation

The secondary or  $O(\epsilon)$  circulation can be resolved into three modes that occur at different frequencies. These are the  $O(\epsilon)$  secondary tidal circulation that occurs at the same frequencies as the tidal forcing (semidiurnal and diurnal), the  $O(\epsilon)$  tidal higher harmonics or tidal overtones (at frequencies that are multiples of the basis tidal frequencies), and the residual circulation or mean flow. All the  $O(\epsilon)$  modes embody more than one non-linear process. Vertical mixing processes are important in all three. The secondary tidal circulation is driven by the salinity distribution, irregularities of channel cross-section, and frictional non-linearities in the primary tidal circulation. The tidal higher harmonics are the result of distortion and friction in the tidal wave in shallow water; this distortion transfers energy from tidal frequencies to higher frequencies. Tidal higher harmonics are often observed in shallow tidal channels, and have been treated by Kreiss (1957) and others. The quasi-steady residual circulation (Section 1.3) is influenced by the tidal range (with variations on tidal monthly time scales), the riverflow (with variations on scales from a few days to seasonal), and the density distribution (which varies with the tides, river inflow and changes in salinity at the mouth). Atmospheric processes (which varies on time scales from a few days to seasonal) are relatively less important in this estuary than in many other systems.

A somewhat different separation of flow modes is appropriate upriver of the limits of salinity intrusion. Salinity is absent, and the flow is simpler. The ratio of riverflow to tidal flow increases in the upriver direction. In the tidal-fluvial portions of system, there are two primary flow modes: the tidal flow and the quasi-steady riverflow. They interact non-linearly, through bottom friction. The  $O(\epsilon)$  tidal modes are still present. Under the highest flow conditions, the tidal flow in the tidal-fluvial reach becomes only an  $O(\epsilon)$  perturbation on the  $O(1)$  riverflow.

### 1.2 THE SALINITY DISTRIBUTION EQUATION

Perhaps the best place to begin in understanding the salinity distribution and salt transport is to consider how salt can be maintained in the estuary, in the presence of a substantial outward transport of salt by the mean flow. The salt transport calculations presented in Section 3.6 show that salt is brought into the estuary primarily by the  $O(1)$  tidal circulation acting on the salinity gradient, and secondarily, by inward mean flow near the bottom. Inward transport by the Stokes drift (associated with the  $O(\epsilon)$  tidal residual circulation, Section 1.3.) is important near the entrance, and perhaps elsewhere.

The salinity distribution and the circulation modes defined in Section 1.1 are linked to each other in a complex, feedback system. We have attempted to simplify this problem by application of the perturbation expansion used in Section 1.1 to the salt conservation equation, again using the perturbation parameter  $\frac{\epsilon}{H}$  as a measure of the importance of the tidal non-linearities. The data and scaling arguments suggest that the non-dimensional salinity should appear in the perturbation expansion in the following manner:

$$s(x,y,t) = s^0(x,z,t) + \epsilon s^1(x,z,t) + \epsilon^2 s^2(x,z,t) + \dots \quad (5)$$

$$\bar{s}(x,z) = \bar{s}^0(z) + \epsilon \bar{s}^1(x,z) + \epsilon^2 \bar{s}^2(x,z) + \dots$$

Unlike the time average of the velocity, where  $\bar{u}^0 = 0$ , there is a  $O(1)$  time average salinity  $\bar{s}^0$ , but  $\bar{s}^0$  is a function only of  $z$ . That is,  $\frac{\partial s}{\partial x}$ ,  $\frac{\partial s}{\partial z}$  and  $\frac{\partial \bar{s}}{\partial z}$  are  $O(1)$ , but  $\frac{\partial \bar{s}}{\partial x}$  is only  $O(\epsilon)$ . This follows from the fact that there is no  $O(1)$  residual flow; were  $\frac{\partial \bar{s}}{\partial x}$   $O(1)$ , it would drive an  $O(1)$  residual flow. We shall see in Section 3.5 that  $\frac{\partial \bar{s}}{\partial x}$  is substantially smaller than the maximum values of  $\frac{\partial s}{\partial x}$ . The assumed form for  $\bar{s}$  is, therefore, reasonable.

The resulting  $O(1)$  salinity distribution is a balance of time change of salinity, advection of the salinity pattern by the  $O(1)$  tidal currents (including the baroclinic part of these currents), and vertical salt flux divergence (vertical mixing and transfer of salt). The lowest-order, time-averaged salinity distribution is a balance between the time average of the tidal salt advection and the time average of the vertical flux divergence. Thus, the primary or  $O(1)$  tidal circulation is in the present theory the only circulation mode involved directly in determining the  $O(1)$  salinity distribution. Neither the  $O(\epsilon)$  mean flow nor any form of vertical advection (entrainment) appear in this equation.

We must determine the salinity distribution to  $O(\epsilon)$ , just as we did with the circulation, because the time-averaged horizontal salinity gradient and the vertical advection of salt are both  $O(\epsilon)$  features; they are not accounted for by the  $O(1)$  circulation. The traditional picture of this problem is that the time-averaged salinity distribution maintains and is maintained by the density-driven part of the residual flow, as explained in Section 1.3. But in our analysis, the residual circulation does not appear in the  $O(1)$  or  $O(\epsilon)$  expressions. The physical reasons why it does not appear is that it is not a large enough feature to control the salinity distribution. This does not mean that the interaction between the flow and the density structure is eliminated, because the tidal flow, which does control the salinity distribution, is strongly influenced by the salinity distribution.

### 1.3 RESIDUAL FLOW PROCESSES

The term "residual flow" includes several processes that are often considered individually, because they are not all of the same importance. These include the classical, two-layer, gravitational circulation of Hansen and Rattray

(1965), in which a density-driven, inward flow of sea water along the bottom is coupled with a net outflow of river water at the surface, the tidal residual circulation (a non-linear tidal process important in shallow estuaries), and the atmospherically-driven circulation (driven by winds over the estuary and wind- and pressure-induced changes in coastal sea level).

For many purposes it is a useful simplification to consider the response of the tidal residual or density-driven circulations individually (as we do in the rest of the section), or to think of the time-averaged properties of the system as responding directly to low-frequency forcing (e.g., to a change in riverflow). However, the perturbation expansion shows that system response to low-frequency external forcing does not occur directly through the residual flow or any part thereof, in isolation. The response occurs through complex adjustments to the tidal circulation and salinity distribution, which then alter the residual flow as a whole. Thus, although it is convenient to separate the residual flow processes from the tidal circulation, this simplification is not always applicable, because the  $O(1)$  circulation drives the  $O(\epsilon)$  residual flow.

### 1.3.1 Tidal Effects on Residual Circulation

The tidal part of the  $O(\epsilon)$  residual circulation is the result of the non-linear transfer of energy from the  $O(1)$  semidiurnal and diurnal tidal circulation to lower frequencies, and of differences in the intensity of vertical mixing processes during the tidal month. There are two aspects of the tidal residual circulation that are of concern here: its origin, and its time variation.

Let us first try to understand how tidal energy is transferred to lower and higher frequencies, that is how the tidal flow can give rise to the tidal overtones and to steady (or nearly steady) flow. The residual flow resulting from the presence of any single tidal constituent (e.g. the lunar semidiurnal component M2 discussed in detail in Section 3.1) would be steady and proportional to the ratio of tidal range to depth times and the tidal current amplitude. It arises as follows. Consider a tidal wave entering one end of an idealized, narrow, shallow channel of simple form and infinite length, without riverflow. Even though the ebb and flood tidal currents at any level of the flow in this channel are by definition equal, the upstream transport of water by the flood tide exceeds the downstream transport on ebb tide, because the depth of the flood current is greater than that of the ebb current. This occurs, because peak flood occurs near the time of high water and peak ebb near the time of low water. That is, the tidal height and the current are correlated and the product  $U\xi$  has a positive time average  $[U\xi]$  that corresponds to a shoreward transport. This product is called the Stokes drift (Longuet-Higgins 1969). (In a wide channel or one of complex form, the expression for the Stokes drift is more complicated than this.)

The correlation of tidal heights and currents has still another effect: distortion of the tidal wave, which produces the tidal overtones. The peak of the tidal waves is in deeper water than the trough of the tidal wave. Since the propagation speed of the wave in shallow water is  $(gd)^{\frac{1}{2}}$ , where  $g$  is the gravitational acceleration and  $d$  is the water depth, the peak of the wave propagates more rapidly than the trough, distorting the wave. This distortion causes the tide (as observed at any tide gauge) to rise rapidly and fall slowly, with strong, brief flood tides, and long, weak ebb tides. Mathematically, this corresponds to reducing the M2 amplitude and adding overtones (e.g., M4 and M6), that occur at multiples of the basic M2 frequency.

There is a close connection between the net energy transported into an estuary by the tide and the Stokes drift, as discussed in Section 3.4. In a shallow system like the Columbia River Estuary, much of the energy of the incoming tidal wave is lost to bottom friction. The outgoing (reflected) tidal wave is much

smaller and carries less energy out of the estuary. The tide is partially or totally progressive, and the Stokes drift, which is proportional to the energy transport, is significant. In contrast, in a system with little friction (or with strong, direct tidal forcing by the moon), the incoming and reflected tidal waves will be of similar amplitude (a standing wave tide). In such a system, high water will occur at slack water,  $U$  and  $\xi$  will be weakly correlated, and there will be little Stokes drift and little net tidal energy transport into the estuary.

The Stokes drift is a property of the vertically integrated flow in the sense that a current meter at any point in the flow in the above, idealized channel measures only the perfectly reversing tidal currents. Nonetheless, a particle in the fluid will, as it is moved back and forth by the tidal currents, experience a net inward transport, because of the greater channel cross-section on flood tide and frictional non-linearities of the flow. This is a case where the Lagrangian motion (that following a particle) is different from the Eulerian motion (that observed at a fixed point in the flow field). Even if the Stokes drift is not directly measurable with a current meter, its consequences are usually measurable. The shoreward transport of water by the Stokes drift in a real channel of finite length causes a surface slope sufficient to drive a steady return flow, that carries an identical amount of water seaward. This Eulerian compensation current may, during low flow periods, be a substantial fraction of the total discharge (riverflow plus Stokes drift compensation flow; Section 3.3). This return flow is distributed differently in the vertical than the Stokes drift itself. Thus, while the effect of the Stokes drift for the water column as a whole is compensated by the Stokes drift return flow, the net effect at any given level may be substantial (Ianniello 1977a,b, 1979, 1981).

A second major feature of the tidal residual circulation is its variation with tidal range. As discussed in Section 3.2 and 3.3, tidal constituents interact with one another, because of frictional and other non-linearities in the equations of motion. The result is both the tidal harmonics at frequencies greater than twice daily, and low-frequency variations at  $\sim 15$  and  $\sim 28$  days. The low-frequency variations correspond to major tidal constituents being in phase (e.g. M2 and S2 at the spring tide) and 180 deg out of phase (e.g. M2 and S2 at a neap tide). The Stokes drift and Stokes drift compensation current driven by a pair of constituents that are close in frequency (e.g. M2 and N2, or M2 and S2; Section 3.1) vary with the same  $\sim 15$  and  $\sim 28$  day periodicities as the tidal range (Ianniello 1977a, b).

Just as important as the variation in Stokes drift during the tidal month is the variation in time-averaged surface slope. There are several reasons for this variation; one is the change in the Stokes drift compensation current; a larger Stokes drift on a spring tide requires a larger slope to drive a larger compensation current. Another reason has been discovered during the course of CREDDP investigations and related work. As discussed in Section 3.4, the dissipation of tidal energy varies with the cube of the tidal range. Although the energy used to increase the potential energy of the water column by vertical mixing of salt is a very small part of the total energy dissipated, much more energy is available for mixing on spring tides and stratification is reduced. The greater vertical mixing and lesser stratification, in turn, mean enhanced vertical momentum transfer in the water column; a greater part of the total flow "feels" the effects of bottom friction. Because of the enhanced friction, a greater surface slope is needed to drive the same mean flow seaward. Thus, river slope increases on a spring tide, not only because Stokes drift compensation current increases, but also because of enhanced friction.

### 1.3.2 River Flow and Density Effects on Residual Circulation



The riverflow enters the system from the upstream end and increases the surface slope of the system so that more water may be transported through the estuary. Increased river flow effects, in a complex way, the stratification, mixing, friction and salinity distribution. Fluvial effects increase in the upriver direction, because the ratio of riverflow to tidal transport increases upriver. The tidal-fluvial interaction is examined in detail in sections 3.3 and 3.4.

Most previous works on estuarine circulation have assumed that the time-averaged, horizontal salinity gradient ( the baroclinic pressure gradient) and riverflow were the primary factors maintaining the salinity distribution. Theory (Section 1.2) and observations (Sections 3.6) show that tidal processes must also be considered in the Columbia River Estuary. Nonetheless, available theoretical studies of gravitational circulation yield important insights. The primary treatments of steady, density-driven estuarine flow are those of Hansen and Rattray (1965) and Hamilton and Rattray (1978); Officer (1976) treats the same material in a simpler fashion. The starting point for Hansen and Rattray (1965) theory is the commonly observed form of the time-averaged salinity distribution (Figure 3a). Theories were developed for the central, inner and outer regimes, but it is the central regime theory that is most relevant here. In this region of many estuaries, the salinity gradient  $\frac{\partial S}{\partial x}$  is nearly constant in time and space. It is possible to use conservation of momentum, mass and salt to obtain time-averaged salinity and horizontal velocity as a function of depth. Since  $\frac{\partial S}{\partial x}$  is assumed constant, the solutions have the same form throughout the central regime.

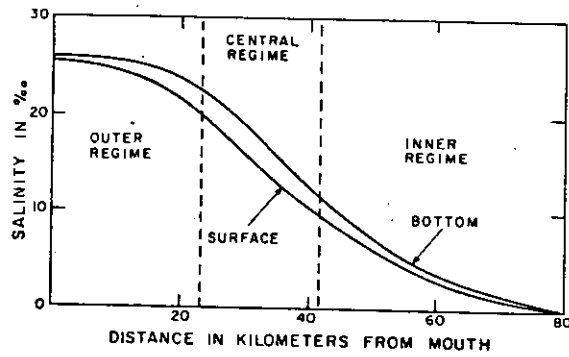
The time-averaged force balance of the Hansen and Rattray theory is pressure gradient versus vertical stress divergence (a subset of the steady,  $O(\epsilon)$  force balance suggested in Section 1.1). The salt conservation equation distribution contains salt flux by the mean flow and entrainment, vertical mixing and horizontal mixing. The horizontal mixing term is a representation of the tidal transport that we find to be the dominant term. To obtain solutions, the horizontal mixing is constrained to vary in an arbitrary manner, and the vertical eddy diffusion coefficient in the vertical mixing term is assumed to be constant. The Hansen and Rattray (1965) theory does not include several processes known to be important in governing the salinity distribution in the Columbia River Estuary. For example, the salinity gradient in the Columbia River Estuary is highly variable in space and time (Figure 3b) and sometimes looks quite different from that in Figure 3a. This theory, nonetheless, makes certain predictions which are qualitatively correct.

The Hansen and Rattray (1965) theory suggests that the top-to-bottom salinity stratification is dependent on the wind stress, the square of the riverflow and the inverse of the vertical mixing (eddy diffusion) coefficient. Neap-to-spring variability can be incorporated into the model by assuming that an increased tidal range results in greater vertical mixing coefficient; this decreases the stratification, in accordance with observations (McConnell et al. 1981; Haas 1977 and Section 3.5). The 1965 theory also predicts a steady gravitational circulation that is increasingly inward, toward the bottom. This is caused by the baroclinic pressure gradient (i.e., the salinity distribution). When this gravitational circulation is combined with a steady, outward riverflow of proper magnitude, the result is surface outflow and bottom inflow. This is the classical paradigm of estuarine circulation.

### 1.3.3 Atmospheric Effects on Residual Flow

With regard to the atmospherically-driven circulation, we need to distinguish at least three effects: the flow driven by winds over the estuary, the flow driven by the set down or set up of the continental shelf, and the inverse

(a)



(b)

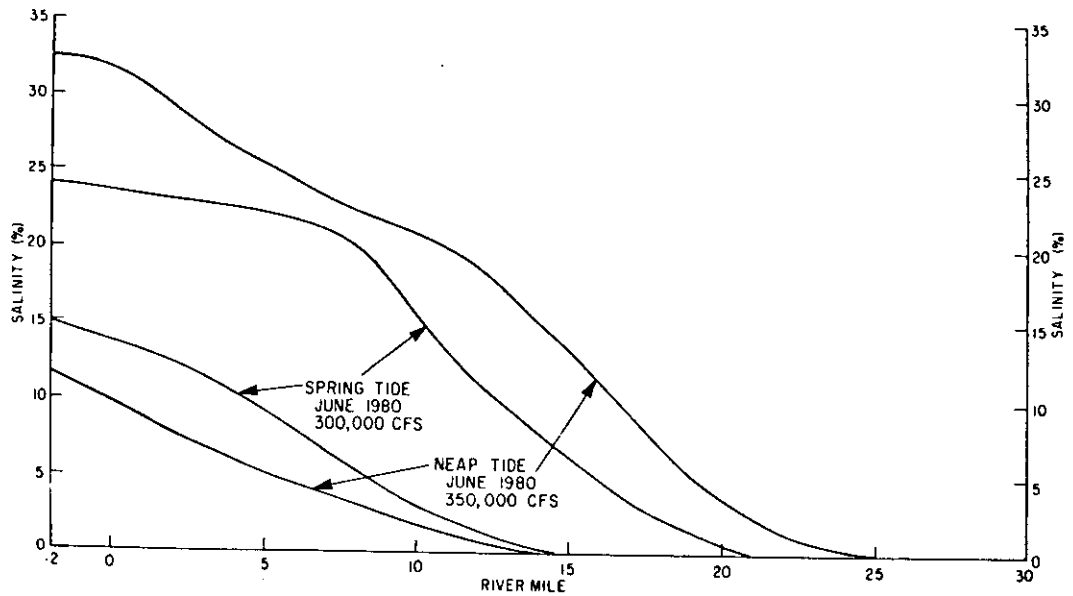


Figure 3. Tidal cycle average surface and bottom salinity in (a) a typical East Coast estuary (from Hamilton and Rattray, 1978), and (b) for spring and neap tide and moderate river flow in the Columbia River Estuary. The horizontal salinity gradient is much stronger and more variable in the Columbia River Estuary.

barometer effect.

The CREDDP two-dimensional, vertically integrated model has been used to estimate the effects of local wind stress on the system, in the absence of tidal flow; the following discussion of model results follows that in Hamilton (1984); reference to Figures 20 to 22 of that report is useful. The model was run using steady winds of 7 m/s, directed 0, 90, 180, 270 and 45 degrees true (deg true) and a steady freshwater flow of 7350 cubic meters/second ( $m^3/s$ ) or 260 thousand cubic feet/second (kcfs). In the absence of wind, the height difference between Tongue Pt. and Jetty A was found to be  $\sim 1$  cm, with the surface level somewhat higher along the north shore; this is presumably a result of the Coriolis effect. A wind directed to the south causes an upwelling type coastal circulation that decreases coastal sea levels by  $\sim 2$  cm; the Jetty A to Tongue Pt. surface slope is nearly unchanged. Substantial cross-estuary height differences ( $\sim 6$  to  $\sim 8$  cm) are introduced, with the largest anomalies in Baker, Grays and Cathlamet Bays. Downstream flow is intensified in the South Channel because of the water piled up along the south shore. A wind directed to the north causes a  $\sim 3$  cm setup at the entrance and somewhat greater cross-estuary height differences between Hammond and Altoona ( $\sim 10$  cm). The strongest downstream flow is shifted to the North Channel, because of the water piled up along the north shore.

The results for onshore and offshore (east and west) winds show minimal effects on sea level at the entrance, small cross-channel slopes and much larger effects on long-channel surface slopes and currents in the estuary. In the case of an east wind, substantial upstream transport across the mid-estuary flats is compensated by enhanced downstream currents in the channel and a height difference between Tongue Pt. and the entrance of  $> 8$  cm. Sea level increases at Beaver (RM-53) by  $\sim 20$  cm. An offshore wind causes sea level to drop nearly 20 cm below the no-wind case at Beaver, and the height difference between Tongue Pt. and Jetty A is  $\sim -5$  cm. A wind directed 45 deg true (northeast) causes effects similar to both the north and east wind cases, except that the large setup in Baker Bay does not occur.

The model changes in surface slope seem qualitatively correct; the absolute values are not. This occurs for two primary reasons. First, in the absence of tides, the friction in the model is much too small, because the tides are the dominant source of the frictional energy loss. NOS tidal height records suggest that mean water level (MWL) at Tongue Pt. is  $\sim 30$  to  $35$  cm above mean sea level (MSL); this is a mean surface slope of  $\sim 10^{-5}$ . The model results show a surface slope (in the absence of the tides) of only  $\sim 3 \times 10^{-7}$ . This comparison between model and observed tidal heights provides one estimate of the effect of tidal range on estuary surface slope. Second, the model is intended to model only local effects, and, therefore, includes only a small part of the continental shelf. We shall see that one major effect of an alongshore wind is to bring about changes in sea level at the entrance of 10 cm to 1 m. To correctly model this effect would require that a much larger part of the continental shelf be included in the model.

The atmosphere affects the continental shelf circulation (and thus sea level at the entrance) on a variety of time scales, from a few days to inter-annual. Effects on two time scales (event, and seasonal to inter-annual) are of primary interest to us.

Seasonal fluctuations in coastal sea level are associated with local and ocean-basin scale, seasonal changes in pressure, wind stress and wind stress gradients (Chelton and Davis 1982; Hickey 1979; Hickey and Pola 1983). In summer, the North Pacific (atmospheric pressure) High strengthens and moves north; winds directed to the south predominate off the Oregon-Washington coast, atmospheric pressure is high, sea levels are low and upwelling occurs. Shelf

circulation in the winter is driven by north-directed winds, associated with the Aleutian Low. Downwelling occurs, atmospheric pressure is low, and sea level is elevated. The variability of all atmospheric parameters is much higher during the winter, and intense storms may be interspersed with periods of relatively good weather.

Seasonal atmospheric pressure and winds affect sea-level at the coast in two ways. First, atmospheric pressure acts directly on coastal sea level through the inverse barometer effect (IBE). IBE refers to the fact that sea level (or a water barometer) will rise about 1 cm for every 1 millibar (mb) fall in sea level atmospheric pressure (Gill 1982). We shall see that removal of the IBE from Tongue Pt. low-passed (daily tides removed) sea level data reduces the variance by ~35%. Second, continental shelf currents are, in large part, driven by the alongshore component of the wind stress (Hickey 1979; Allen 1980). Because of the Coriolis effect, wind-driven ocean currents move to the right (in the northern hemisphere) of the wind. Predominantly south-directed winds during the summer push water off-shore, lowering sea level at the coast; the reverse is true during the winter. Thus, the coastal sea level cycle is closely related to upwelling and downwelling.

With regard to the ocean-basin scale fluctuations, Hickey and Pola (1983) and Werner and Hickey (1983) have demonstrated that the alongshore pressure gradient of the North Pacific Gyre strongly modifies the seasonal and inter-annual fluctuations in currents caused by the wind stress off the west coast of North America. Further, the seasonal cycle of coastal sea levels was predicted very successfully by combining the effect of deep ocean currents with a model that utilized the alongshore gradient in wind stress. Remote contributions from winds in regions to the south were found to be important in the Pacific Northwest. The combined seasonal sea level cycle predicted by the model at 46 deg north latitude is ~20 cm, on the average (Hickey and Pola 1983). Contributions to this cycle from seasonal heating and cooling were estimated to be less than 1 cm.

The Columbia River effluent has a substantial effect on the density of sea water in the adjacent coastal ocean, by changing the salinity of surface layers (Barnes et al. 1972). The seasonal runoff cycle may have, therefore, a steric effect on regional sea level in addition to causing sea levels in the estuary to rise above the level of the adjacent coastal ocean so that more water may be discharged. Hickey and Pola (1983) found steric fluctuations of about 8 dyn cm (dynamic centimeters) during a one month period in March. Substantially larger seasonal effects are possible (Barnes et al. 1972). Evaluation of the seasonal cycle of sea level caused by steric effects of the plume is complicated by seasonal changes in the position of the plume; this questions has not yet been resolved.

Event scale fluctuations (lasting a few days to a week) in currents and sea level may be associated with storms of a longshore spatial scales of between a few hundred to a 1000 km. Storm surges may be as large as two to three times the amplitude of the seasonal cycle of sea level changes (up to ~1 m). Coastal sea level and currents may also be altered by energy from distant events transmitted along the coast by coastally trapped waves (Gill 1982). Various authors have argued that these waves drive fluctuations off the Oregon-Washington coast of between 0.15 and 0.44 cycles per day (cpd) (Hickey 1979).

#### 1.4 VERTICAL MIXING, STRATIFICATION AND CIRCULATION

The essential role played in the  $O(1)$  circulation and salinity distribution by vertical mixing requires that we examine this process further. We wish to know both the dependence of vertical turbulent mixing on stratification, and under what circumstances other processes may be responsible for vertical momentum

exchange.

#### 1.4.1 Types of Vertical Exchange Processes

We must distinguish (Dyer 1973) between situations where the vertical salt balance is satisfied primarily by vertical mixing and vertical tidal salt transport, and those where it is satisfied by entrainment. Entrainment occurs when a turbulent fluid flows over a relatively less turbulent layer; net vertical movements of momentum, water and salt occur as the upper layer erodes the lower. In contrast, vertical mixing and vertical tidal salt transport transfer momentum and salt without a net movement of water. There is, furthermore, a necessary connection between the horizontal and vertical salt transport modes in an estuary. Conservation of mass ensures that significant upward entrainment can occur only in an estuary with a two-layer flow. Water enters the estuary along the bottom (because of the baroclinic pressure gradient and tidal flow; Section 3.2), is entrained into the surface layer, and is carried out of the estuary in the surface layer, diluted by river runoff. There will be a substantial, net upstream salt transport, driven by the gravitational circulation.

We have argued that the upstream salt transport in the Columbia River Estuary is dominated by tidal transport terms, rather than the steady, density-driven circulation. We will show in Section 3.2 that net upstream bottom flow is quite variable in time and space and is not continuous over the entire salinity intrusion length into the estuary. Finally, the scaling and perturbation analysis of the salinity equation discussed in Section 1.2 does not place a time average, vertical velocity term in either  $O(1)$  or  $O(\epsilon)$ . All this strongly suggests that vertical tidal salt transport and vertical mixing processes, rather than entrainment dominate the vertical salt transport in the Columbia River Estuary, at least in the average picture.

We can further distinguish between the turbulent, bottom boundary layer dynamics that govern partially to well-mixed locations in the flow, and the more complex pycnocline processes that govern salt transfer in highly stratified situations (Gardner et al. 1980). In the first case, energy for turbulent mixing arises primarily from the frictional interaction of the flow with the bottom. The bottom layer of such a flow is fully turbulent, and we should expect vertical mixing to outweigh entrainment. This would correspond to maintenance of a horizontal salt balance by primarily tidal oscillatory mechanisms. Vertical salt fluxes can occur both with and without net vertical movement of water at the pycnocline of a shallow, highly stratified flow. In this case, turbulence is suppressed to such a degree that it is not the principal agent of vertical salt transport there. The processes bringing about vertical salt transport under these conditions are episodic, diverse and poorly understood (Gardner et al. 1980).

The difficulty with a system such as the Columbia River Estuary is that the variability of stratification and mixing processes; processes as diverse as vertical turbulent mixing and the breaking of internal waves are responsible for vertical momentum and salt transfer. We can deduce from the profiles presented in Section 3.2 and 3.5 that the more complex interfacial processes associated with highly stratified systems occur under certain conditions in the Columbia River Estuary. We can not, on the basis of the large scale studies carried out to date, quantitatively describe such processes. Nor can we definitely state how important they are, on the average, to the dynamics of the system, because the profile data from the high flow season is very limited.

#### 1.4.2 Formulations of Vertical Mixing and the Effects of Stratification

Terms representing the vertical gradients of turbulent stress or momentum flux and salt flux occur in the  $O(1)$  equations of motion and salt continuity, respectively. The importance of these vertical fluxes suggests that we need to

know more about their representation, and the effect of stratification on them. The relevant turbulent stress in the along-channel momentum equation may be written:  $\tau_z = -\rho[u'w']$ , where the brackets represent a time average over a suitable interval (perhaps a few minutes), and the primes denote instantaneous deviations from the time average. The stress results from the correlation between fluctuations ( $u'$  and  $w'$ ) in velocities  $U$  and  $W$ ; it can be thought of as a vertical transfer of momentum from a more energetic part of the flow to a less energetic part.

In the case of turbulent flow over a boundary (the seabed), energy is lost from the mean flow as a result of the interaction of the flow with the bottom. The energy lost from the tidal flow appears as turbulence. The velocity  $U$  in the vicinity of the seabed for a steady, unstratified, turbulent boundary layer can be given by:

$$U = \frac{u_*}{k} \ln\left(\frac{Z}{z_0}\right) \quad (6)$$

where (in dimensional variables):

$$u_* \text{ is a scale velocity given by } u_* = \left(\frac{\tau_b}{\rho}\right)^{\frac{1}{2}}$$

$\tau_b$  is the shear stress at the bottom,

$k$  is a von Karman constant  $\approx 0.41$ ,

$\ln$  is the natural logarithm,

$Z$  is the depth of the flow, measured upward from the seabed, and

$z_0$  is a roughness scale length specified by the grain size of the bottom (or the bedforms, if any are present)

This velocity increases very rapidly close to the seabed, and more slowly higher in the flow; the shear is given by  $\frac{\partial U}{\partial Z} = \frac{u_*}{kz}$ . As soon as stratification appears in the flow, the turbulence is inhibited and the logarithmic profile is modified. Time dependence of the flow also alters the flow (Lavelle and Mojfield 1983), but to a lesser degree. The energy loss to turbulence (the turbulent production) is closely related to the shear; the turbulent energy production is given by:  $[u'w'] \frac{\partial U}{\partial Z}$ .

The turbulent salt flux  $[w'S']$  that appears in the salt continuity equation arises from correlations between fluctuation ( $s'$  and  $w'$ ) in salinity  $S$  and vertical velocity  $W$ . In a stably-stratified system, this flux will normally move salt toward the surface. Since this raises the center of gravity of the fluid, it changes turbulent energy into potential energy.

We may express the vertical turbulent salt flux  $[w'S']$  more generally as a buoyancy flux  $\frac{g}{\rho} [w'\rho']$  since the density is essentially determined by the salinity. When the energy lost to the buoyancy flux exceeds the turbulent production at any point, then the turbulence is losing energy faster than it is gaining energy. In the absence of diffusion of turbulence from some other part of the flow, the flow will cease to be turbulent at this point. The condition for the cessation of turbulence is expressed in terms of the flux Richardson number:

$$Ri_f = \frac{\frac{g}{\rho} [\rho'w']}{\frac{\partial u}{\partial z} [u'w']} > 1 \quad (7)$$

which is the ratio of buoyancy flux to turbulent production.

It is generally impossible in synoptic-scale oceanographic studies to measure either the buoyancy flux or production; both must be represented in terms of the mean properties of the flow that can be measured. It is customary to represent the turbulent momentum flux  $[u'w']$  in terms of the mean momentum gradient  $\frac{\partial U}{\partial Z}$  and a proportionality constant or parameter  $K_m$ , and the turbulent buoyancy flux  $\frac{g}{\rho} [\rho'w']$  in terms of the mean density gradient  $\frac{g}{\rho} \left(\frac{\partial \rho}{\partial Z}\right)$  and a parameter  $K_p$ . The turbulent salt flux  $[S'w']$  can then be expressed as  $K_p \left(\frac{\partial S}{\partial Z}\right)$ . The above condition for the cessation of turbulence can then be rewritten in terms of the gradient Richardson number, which contains measurable quantities (the mean velocity and density gradients):

$$Ri_g = \frac{\frac{g}{\rho} \frac{\partial \rho}{\partial Z}}{\left(\frac{\partial U}{\partial Z}\right)^2} \geq .25 \quad (8)$$

Specification of the turbulent fluxes still requires determination of the form of the parameters  $K_m$  and  $K_p$ . This has been done in many ways; the method used here was derived for boundary layer flows by Bosinger and Arya (1974) and Long (1981):

$$K_m = ku_* z e^{\frac{-z}{h}} \quad (9)$$

where:

$h$  is a length scale, which we take as  $\frac{1}{3}$  of the depth.

$K_m$  increases nearly linearly from the bottom, reaches a maximum at the height  $h$ , and then decreases more slowly toward the surface. This reflects the vertical change in size of the turbulent eddies responsible for the turbulent fluxes. This value for unstratified flow can be corrected for the effects of stratification, for which (Long 1981):

$$K_m = \frac{ku_* z e^{\frac{-z}{h}}}{\left[1 + \beta f(Ri_g, \tau_z, u_*)\right]} \quad (10)$$

$$K_p = \frac{ku_* z e^{\frac{-z}{h}}}{\left[\gamma + \beta f(Ri, \tau_z, u_*)\right]}$$

where:

$f(Ri_g, \tau_z, u_*)$  is a known function, and  $\gamma$  and  $\beta$  are constants.

$Ri_g$  enters here, because it is a measure of energy lost by the turbulence to the potential energy field. As is clear from the form of the expression, vertical mixing is reduced in the presence of stratification.

## 1.5 STRUCTURE OF THE REPORT

Section 2 presents the methods used by the circulation work unit. The results presented in Section 3 include analyses of tidal processes and tidal-fluvial interactions, the energy budget, the salinity distribution and the factors maintaining it, vertical mixing processes, salt transport mechanisms, and the forcing of the low-frequency or residual circulation. Appendix A presents sampling stations; Appendix B, selected harmonic analysis results; Appendix C, historical tidal data; Appendix D, inundation time data; Appendix E, salinity distribution plots; and Appendix F, 1979-81 riverflow.



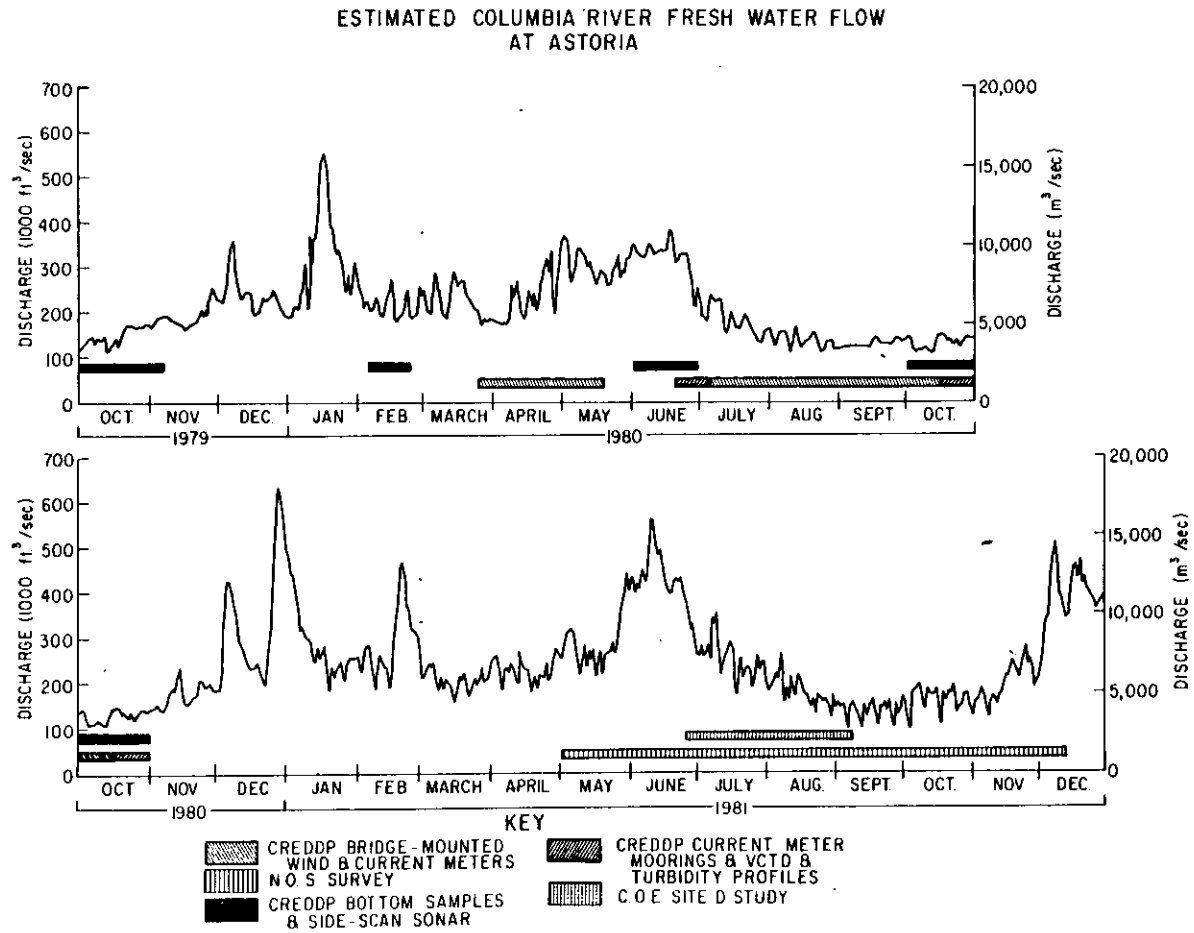


Figure 4. Discharge of the Columbia River Estuary and study periods.

## 2. METHODS

### 2.1 FIELD PROGRAM AND INSTRUMENTATION

The 1980 CREDDP field program, instrument calibration, and preliminary data processing have been described in detail in an earlier report (Webster and Juhasz 1980). The field program consisted of a continuous monitoring program (March to November 1980) and two intensive cruises (high-flow, June 1980, and low-flow, October 1980). The sampling periods and riverflow are shown in Figure 4. The purpose of the continuous monitoring program was to assess seasonal and tidal monthly variability at important locations. The intensive cruises were designed to provide detailed information over half a tidal month, under high and low-flow conditions. Station locations are shown in Figures 5 and 6. More detailed information regarding sampling stations is given in Appendix A.

The continuous monitoring program consisted of repeated deployments of five Aanderaa current meters on the Astoria-Megler Bridge (two North and three South Channel) and two pressure gauges near Beaver at River Mile 53 (RM-53; Figure 5). The Astoria-Megler Bridge location was selected because of its position in the critical middle reach of the estuary, and because the bridge pilings offered a secure location for the instruments. The pressure sensors were located at Beaver because of the need for upriver tidal height data. The Aanderaa current meters were equipped with conductivity, temperature and pressure (or in some cases, transmissivity) sensors, in addition to the usual speed and direction sensors. Additional tidal height data were available at Tongue Pt. (RM-18) from the National Ocean Service (NOS); and at Jetty A (RM-3), Wauna (RM-42), and Columbia City (RM-83) from the US Geological Survey (USGS). The continuous monitoring program was interrupted by the eruption of Mt. St. Helens; all instruments were removed May 19, 1980, and were not replaced until the June cruise.

The two intensive cruises each consisted of two-week deployments of 17 Aanderaa current meters, 30-day deployments of seven or eight Aanderaa pressure gauges, and a 15 to 30-day deployment of an Aanderaa anemometer (Figure 5). Extensive profiling was carried out during the October cruise with two velocity-conductivity-temperature-depth (VCTD) profilers (Figure 6). The characteristics and calibration of, and data processing from these instruments are described in Narayanan, et al. (1982). The velocity (two orthogonal components) was measured using an electromagnetic sensor. Probe orientation was determined by use of two tilt sensors and a compass. This allowed for correction of the velocity record for the lowering velocity, which enters the velocity record under high current conditions (when the instrument is not vertical). The other sensors and the data transmission were provided by a Guildline CTD. All data were recorded on tape cassettes. Preliminary plots were made on shipboard to check instrument function. Data were transferred to nine-track tape after despiking and calibration. Because of the extensive current meter and profile data available, the CREDDP data for October 1980 constitute the best available realization of a low-flow period. Station locations for all time-series (current, anemometer, and pressure gauge) and profiles for 1980 are given in Appendix A.

NOS staged a very extensive field program in the estuary in 1981 (Figures 7 and 8 and Appendix A). These data provide (for some time periods) far more extensive time-series data than were available through CREDDP. Moreover, the spring freshet in 1981 was the largest in the 1975 to 1982 period. Some CTD profile data are available, but no velocity profiles were collected. The NOS field program, instrumentation and data processing is described in more detail in the project instructions (Townsend and Hull 1981). These data were received too late to be completely analyzed during the program.

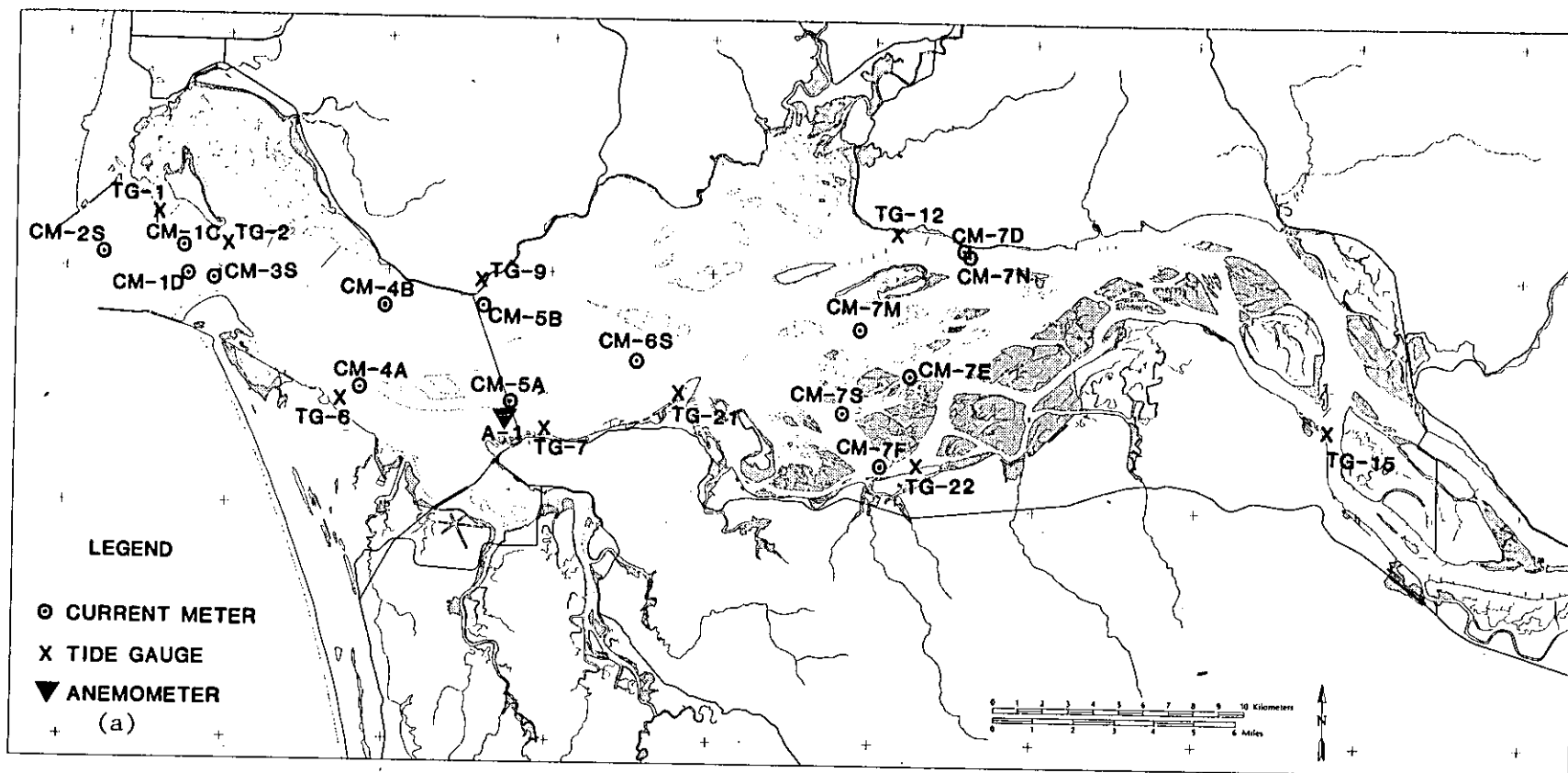


Figure 5. CREDDP 1980 sampling stations, (a) mouth to RM-47, and (b) above RM-47. Stations CM-5A, CM-5B, TG-1, TG-21, TG-19, and TG-20 were included in the continuous monitoring program. These and all other stations were used in one or both intensive cruises. Two additional tide gauge stations - TG-21 (NOS) and TG-1 (Geological Survey) - are also shown. Additional deployment information is included in Appendix A.

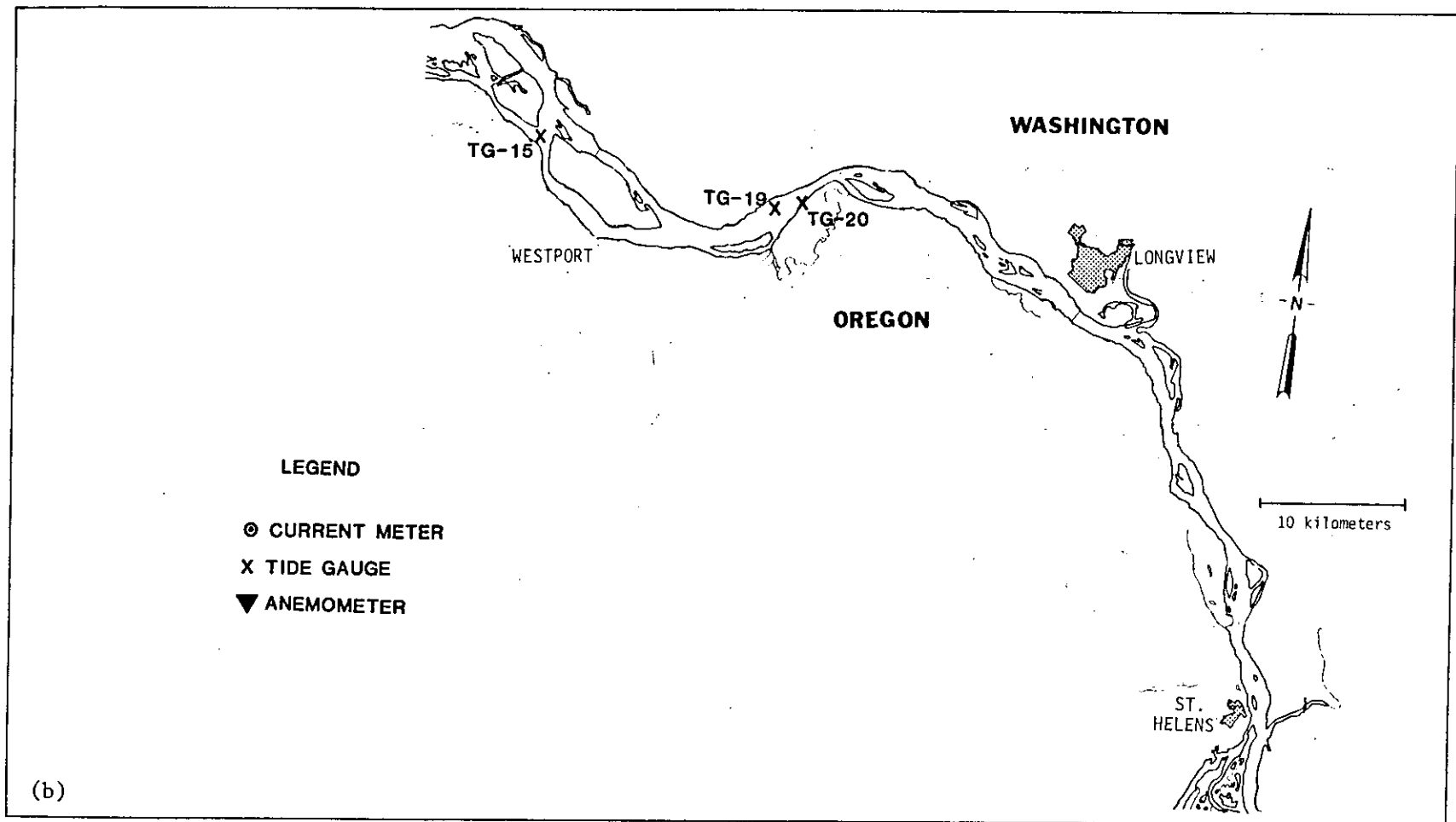


Figure 5. (continued).

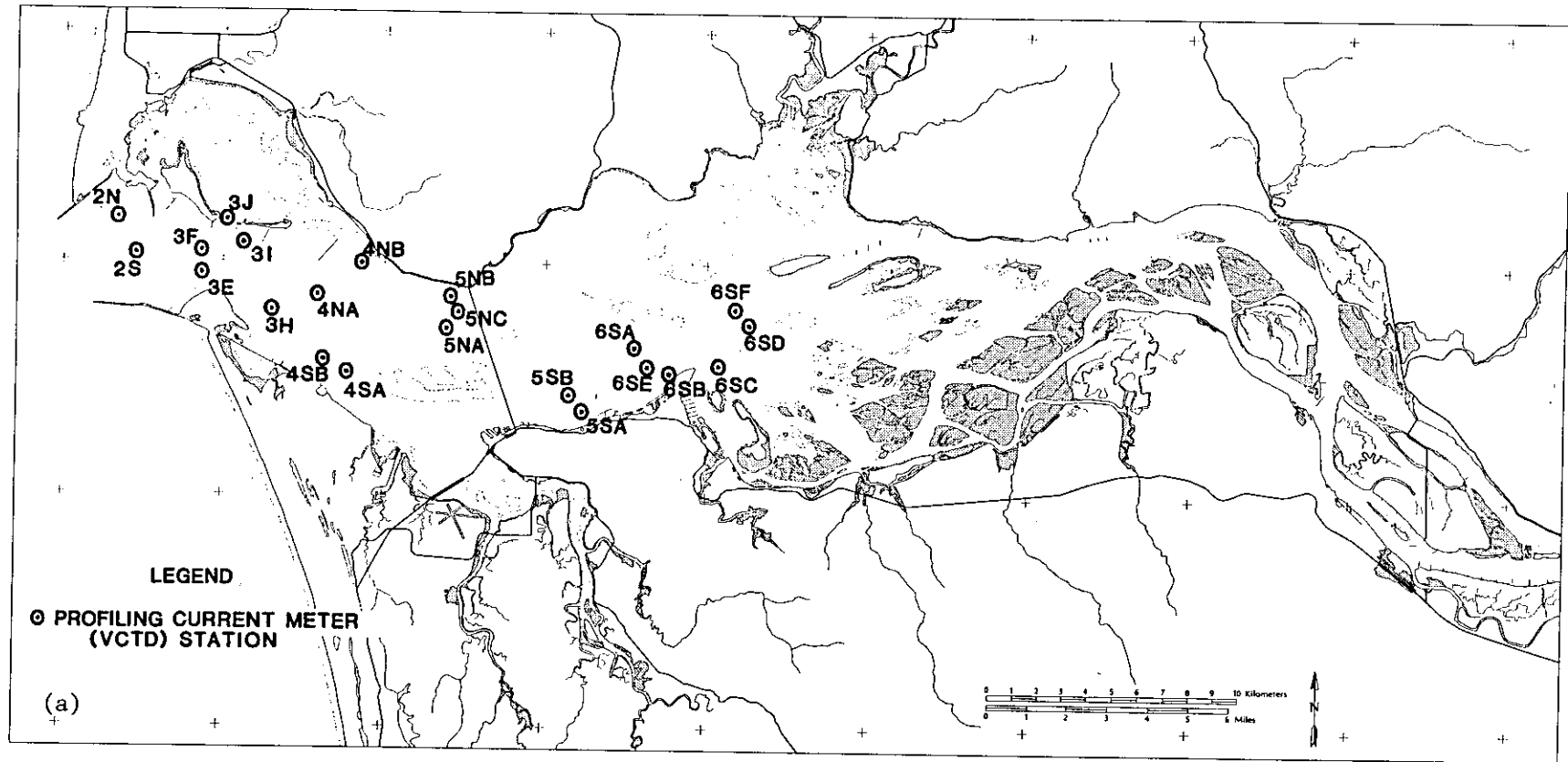


Figure 6. CREDDP October 1980 VCTD profile stations, (a) mouth to RM-47, and (b) above RM-47. Further information concerning stations is included in Appendix A.

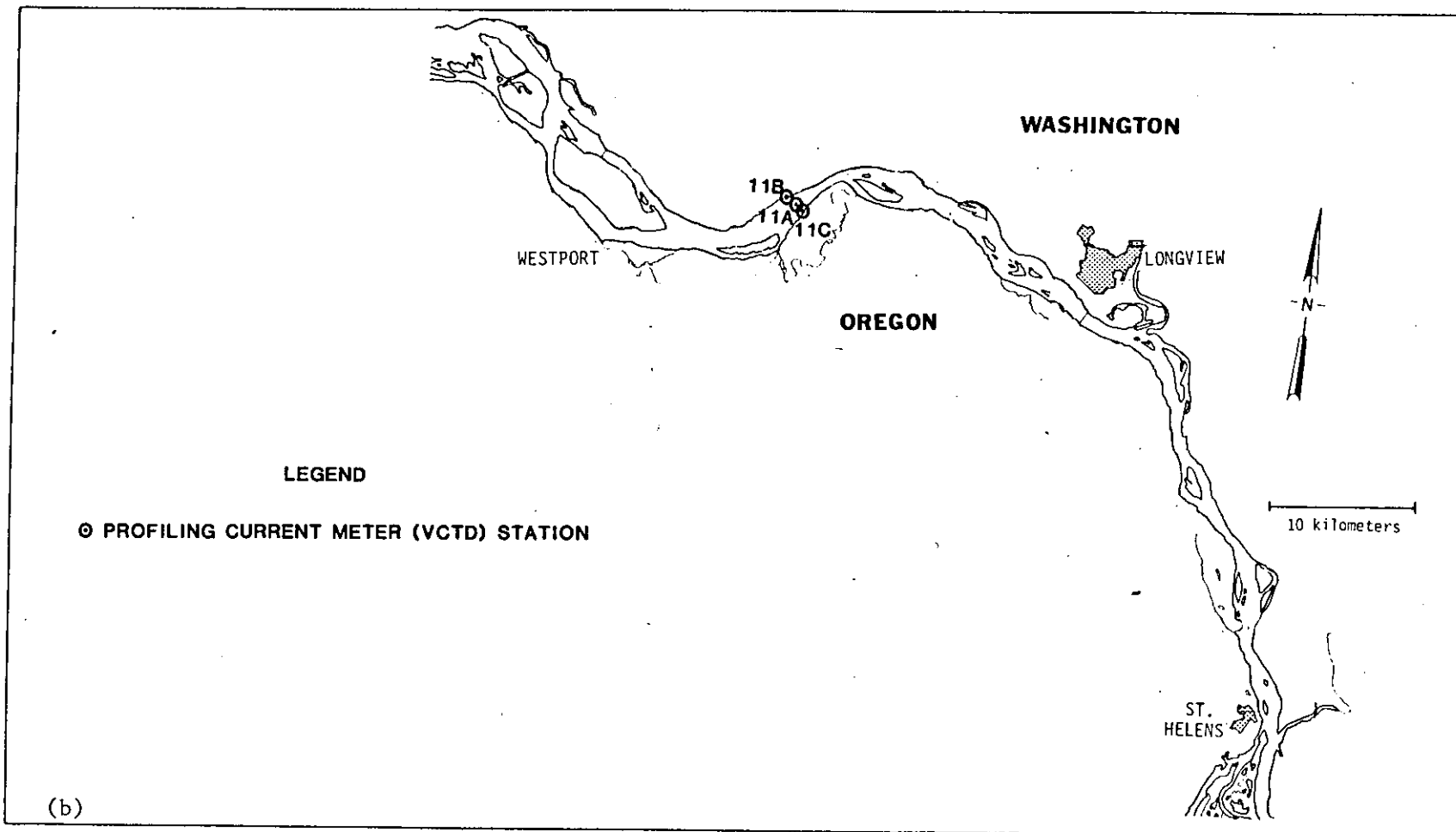


Figure 6. (continued).

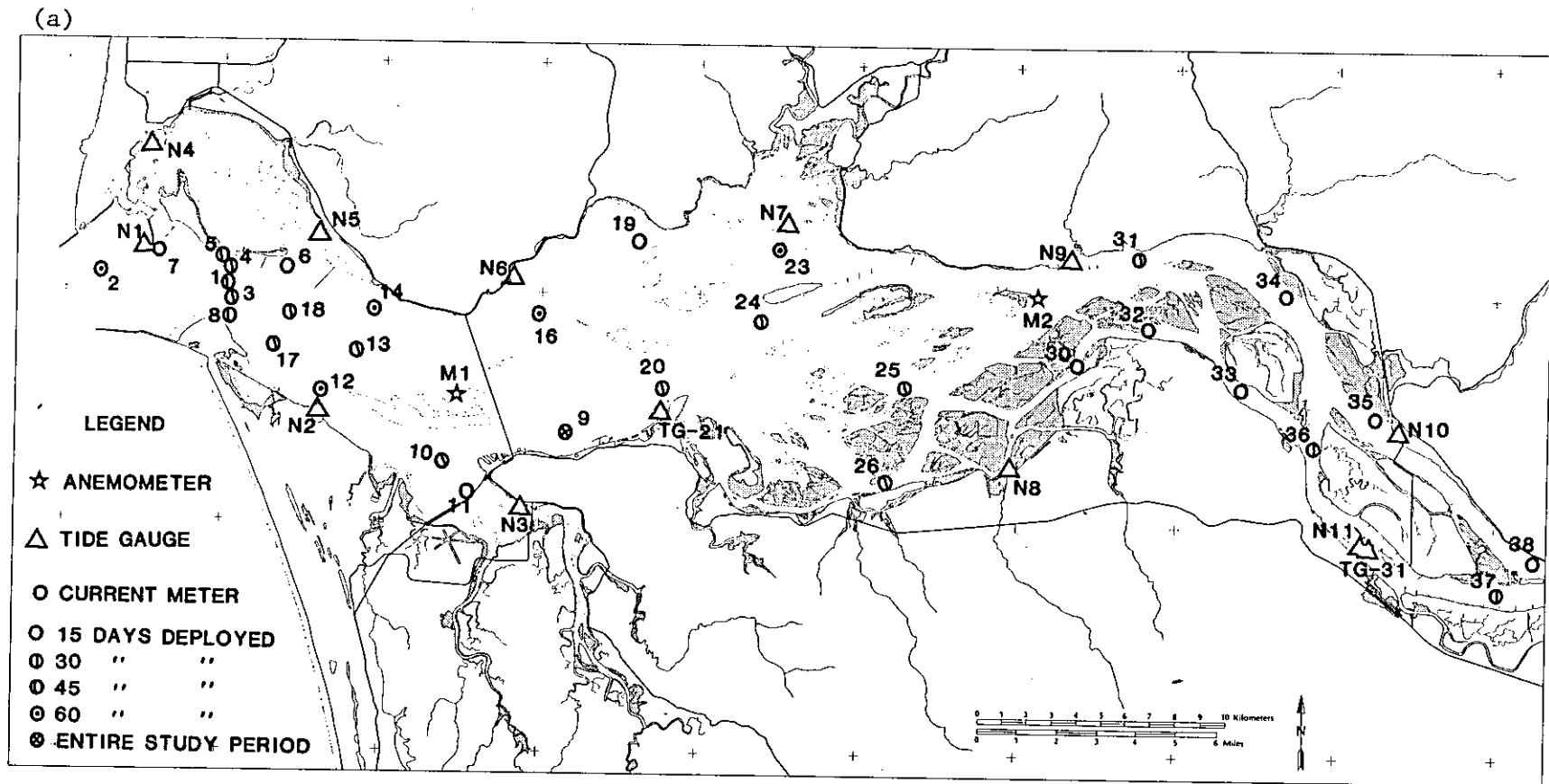


Figure 7. NOS 1981 current meter, tide and anemometer stations (a) mouth to RM-47, and (b) upriver of RM-47. Two additional Geological Survey tide gauge stations are shown: TG-31 and TG-41. Additional deployment information is provided in Appendix A.

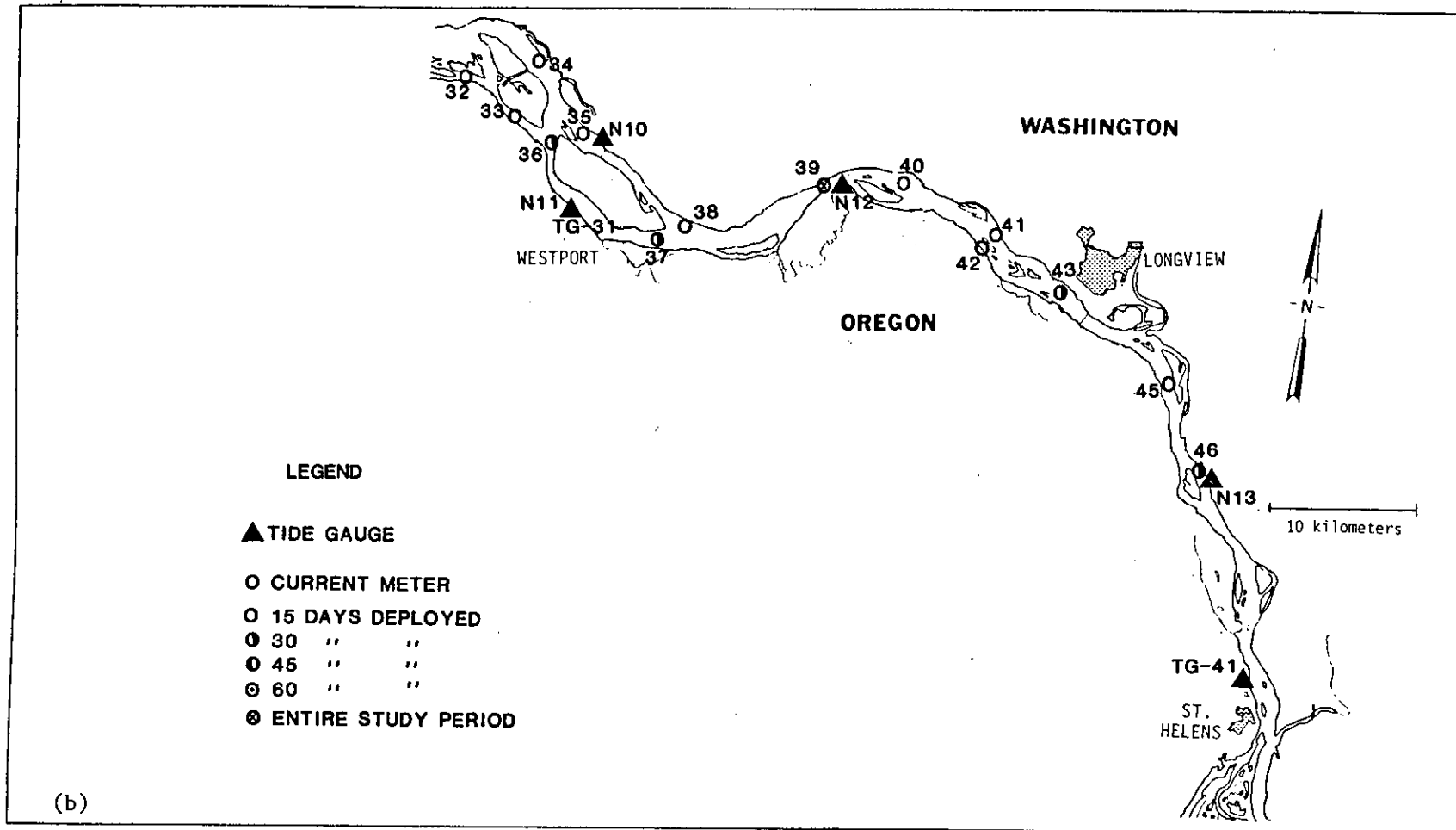
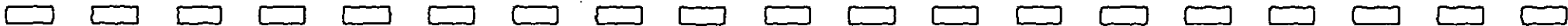
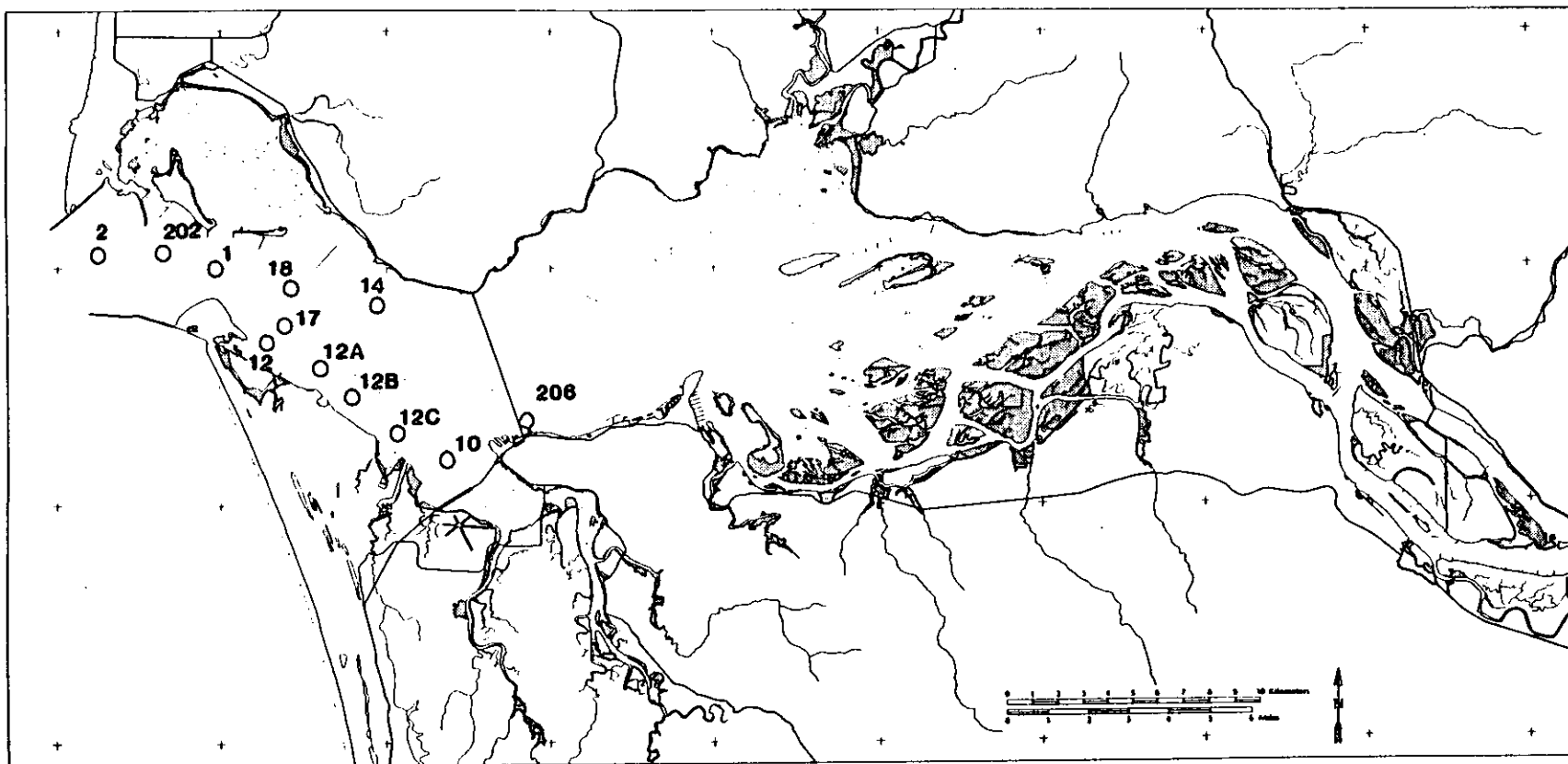


Figure 7. (continued).



Figure 8. NOS 1981 CTD profile stations. Further sampling information is included in Appendix A



Additional data sets are available from Corps of Engineers work in 1975, 1977 and 1978. These data have also been analyzed and incorporated into the CREDDP data base, and 1977 - 1978 Station locations are given in Appendix A.

## 2.2 PRELIMINARY DATA PROCESSING

The handling of time-series data (anemometer, current meter, and tide/pressure gauge) follows a process designed to detect and eliminate errors. This process consists of file creation, plotting, filtering, harmonic analysis (not used for anemometer files) and calculation of statistics for each measured parameter (current meter data only). Calibration procedures for CREDDP data are described in Webster and Juhasz (1981); NOS procedures are described in Townsend and Hull (1981) and Kalvaitis (1981).

Errors in tidal height records are relatively easily detected through plotting and harmonic analysis (Section 2.3). Some errors in current velocity records (e.g. lost or jammed rotors) are very easily detected in plots or by comparison with other records. The harmonic analyses are sufficient to detect major errors in timing or direction. Wave-pumping can often be detected because of roughness in the direction record. Uncorrected errors due to fouling, mooring motion, wave action, etc. are still almost certainly larger, when they occur, than the calibration errors. During periods of strong tidal flow ( $>100$  cm/s), these errors will be only a few percent of the measured flow; during periods of weak tidal flow, wave action may introduce major errors. This occurs because the Aanderaa current meters measure direction only once every sampling interval, while the speed is averaged over the entire sampling interval.

Halpern et al. (1974) nonetheless found that an Aanderaa current meter moored at 20m on the continental shelf gave the same (at the 95% confidence level) spectral estimates as a nearby vector-averaging current meter, at all frequencies less than 2 cycles/hour. The vector-averaging current meter is nearly immune to the wave-pumping and mooring motion problems that affect the Aanderaa current meters. Differences in the mean flow and time-series record between the two meters were smallest during the periods of strongest flow. While our meters were generally closer than 20 meters (m) from the surface, the tidal flows in the Columbia River Estuary are much larger than, and the mean flows comparable to, those on the continental shelf. Wave action is much less severe. We may therefore expect that our measurements of the tidal and lower frequency circulation are not seriously influenced by mooring motion problems. Fouling is believed to be unimportant for short deployments ( $<15$  days). It may result in errors in records from longer deployments; however, few velocity records exceed one month, because of rotor loss or jamming.

Detection of invalid temperature and salinity data is largely a matter of internal consistency -- comparison with other data collected at the same time at adjacent meters. This is done through temperature-salinity (T-S) plots and a T-S statistics program. The riverine end-member water type can be established from records taken upstream of all salinity intrusion. Oceanic water types are defined in Conomos et al. (1972) and discussed in Section 3.5.1. Extensive inter-comparison of records suggests that the accuracy of Aanderaa records is limited by systematic errors to about  $\sim 0.5$  parts per thousand (ppt) in salinity and  $\sim 0.2$  degrees Celsius (deg C) in temperature. Larger errors occur sporadically. These accuracies are quite sufficient for the work at hand.

No tests beyond visual inspection and comparison of records have been employed with the anemometer data. Winds are notoriously difficult to measure in coastal regions because of the spatial variability induced by topography, sea breeze circulations, etc. For many time periods, only one anemometer record is available, and the only comparisons that can be made are with the geostrophic wind data calculated by NOAA by the method of Bakun (1975) or with Newport,

OR winds provided by Oregon State University. The geostrophic winds are representative of winds off the coast, averaged over spatial scales of three deg of latitude and longitude. They are consistently stronger than measured coastal winds. The Newport winds have been used in numerous studies of circulation off the coasts of Oregon and Washington, because they seem to be more closely related to continental shelf processes than data from most other coastal stations (Allen 1980). Nonetheless, longshore gradients in the winds between Newport and Astoria are significant (Barnes et al. 1972). The statistical relationships between Newport winds, local winds, and geostrophic winds are explored in Section 3.7.

All current meter and most tidal height and anemometer data were received on magnetic tape. In those instances where it was necessary to enter data by hand, the data were punched on data cards twice. Errors were detected by computer comparison of the two copies of the data. Isolated errors in time-series records and gaps of a few hours between current meter deployments were corrected by interpolation. Gaps of more than a few hours usually can not be interpolated. In two instances where a T-S curve that was both linear and stable in time could be defined from an adjacent meter, the T-S curve was used to interpolate missing salinity data (Jay 1982).

No analyses have been undertaken to determine the validity of the VCTD and NOS profile data. Calibration and preliminary processing of these data are described in Narayanan et al. (1982), Townsend and Hull (1981) and Kalvaitis (1981).

## 2.3 DETERMINATION OF TIDAL PROPERTIES

### 2.3.1 Harmonic Analysis Methods

The programs used for harmonic analysis of tides and currents were those developed by the Canadian government for their tidal height and current prediction work (Foreman 1977 and 1978). They have been modified and extended for application to the Columbia River Estuary. The harmonic analysis routines have been tested by comparison of results at Tongue Pt. with historical analyses conducted by NOS (obtained through personal communications with the NOS Tidal Datums Branch).

Errors in the harmonic analyses result primarily from inadequate record length, which limits the number of tidal constituents that can be calculated, and shallow water tidal effects not accounted for by the harmonic analysis (tidal currents); and from inadequate resolution of the low-frequency flow (both tidal heights and currents). For short records, failure to calculate some constituents may introduce significant errors into the calculation of nearby larger constituents. This problem is dealt with by use of longer records, or by inference of the missing constituent from its magnitude at a nearby station. The method is explained in Foreman (1977 and 1978).

A calculation of the root mean square (rms) residual error (difference between observed and predicted values) is part of each analysis. This residual error consists of a contribution from the time-dependent, non-tidal circulation and the actual error; these two are difficult to separate. The rms errors normally range from  $\pm 4$  to  $\pm 20$  cm for tidal heights, and  $\pm 4$  to  $\pm 20$  cm/s for tidal currents (for deployments of 15 days or longer). Larger rms differences are sometimes found in the tidal-fluvial part of the system, because of freshwater effects. The rms error will, in the absence of errors in the data or of a strong, unsteady, non-tidal circulation, decrease as the record length increases, because of the inclusion of more constituents in the longer analysis.

Numerical experiments described in Foreman and Henry (1979) and further experiments with CREDDP data suggest that a record length of six months

suffices to define the values of the major tidal height constituents to within  $\sim 2$  cm and  $\sim 5$  minutes in time. Inference of one diurnal constituent allows a resolution nearly as good with a one month record. Comparison of pressure gauge records (which have an additional low-frequency component, due to shifting of bottom sediment) with nearby tide gauge records suggests that the poor resolution of the low-frequency flow has very little effect on the calculated tidal height harmonic constituents. In conclusion, our knowledge of tidal height harmonic constants is quite adequate for most oceanographic purposes.

Despite the analyses carried out on more than 220 current meter files, the resolution of the current harmonic constituents remains less than totally satisfactory. This occurs, because most of the files are shorter than one month, and because currents are inherently more complex, variable and difficult to measure than the tidal heights.

### 2.3.2 Harmonic Constant Reduction

Most methods of analysis of time series data require that the data be spaced evenly in time. Tidal heights are routinely tabulated in the form of hourly observations, from which harmonic constants can be determined. The mariner and marine manager are commonly more interested in the traditional tidal parameters such as tidal range (distance between tidal extremes) and high and low water intervals (time of high or low water at a station) that appear in tide tables. Since tidal extremes only occasionally coincide with evenly spaced observations, NOS has developed methods (known as harmonic constant reduction) of calculating the traditional tidal parameters from harmonic constants (US Coast and Geodetic Survey (USCGS) 1952). Our computer program, based on this publication, was tested using the known tidal properties at Tongue Pt., obtained by personal communication with the NOS Tidal Datums Branch.

Errors occur in the quantities calculated by harmonic constant reduction if the harmonic constants are not known with sufficient accuracy. Additional errors result if the calculated datum level is not reduced to a long term value. The magnitude of these errors may be estimated by comparison of Mean Lower Low Water (MLLW) calculated by harmonic constant reduction with the values provided by NOS. Comparison of calculations based on five  $\sim 6$  to  $\sim 9$ -month and three 12-month records with accepted datum levels suggests that an error of  $\pm 3$  to  $\pm 10$  cm results from use of records of this length. Use of shorter records may produce substantially greater errors. No attempt has been made to reduce calculated datum levels to 18.6 year epoch values. The calculated MLLW in tidal-fluvial part of the system (above Altoona) may also differ substantially from the accepted Columbia River Datum (CRD), because of riverflow effects, and the tidal range varies substantially with riverflow at upriver stations.

### 2.3.3 Tidal Inundation Time Calculations

The tidal inundation times were calculated for 11 stations between Jetty A (RM-3) and Columbia City (RM-83). The tidal data used for these calculations were provided by NOS and USGS. These inundation time calculations are discussed in Jay (1983). Subsequently, NOS provided a calculation of tidal inundation time based on 21 years of data, 1940 to 1969. Only these results are presented here. The data used by NOS are from the time period 1940 to 1961. The secular sea level trend at Astoria for the period 1940 to 1978 is  $\sim -0.2$  to  $-0.3$  cm/yr (Chelton and Davis 1982). Sea level has, therefore, declined  $\sim 4$  to  $\sim 6$  cm between 1951 (mid point of data used for the tidal inundation plot) and 1981. The results for the 1940 to 1961 period have, accordingly, been referred to MLLW for the 1941-59 epoch, which is  $\sim 5$  cm lower than the datum for the 1960-78 epoch used for the 1978 to 1981 data.

suffices to define the values of the major tidal height constituents to within ~2 cm and ~5 minutes in time. Inference of one diurnal constituent allows a resolution nearly as good with a one month record. Comparison of pressure gauge records (which have an additional low-frequency component, due to shifting of bottom sediment) with nearby tide gauge records suggests that the poor resolution of the low-frequency flow has very little effect on the calculated tidal height harmonic constituents. In conclusion, our knowledge of tidal height harmonic constants is quite adequate for most oceanographic purposes.

Despite the analyses carried out on more than 220 current meter files, the resolution of the current harmonic constituents remains less than totally satisfactory. This occurs, because most of the files are shorter than one month, and because currents are inherently more complex, variable and difficult to measure than the tidal heights.

### 2.3.2 Harmonic Constant Reduction

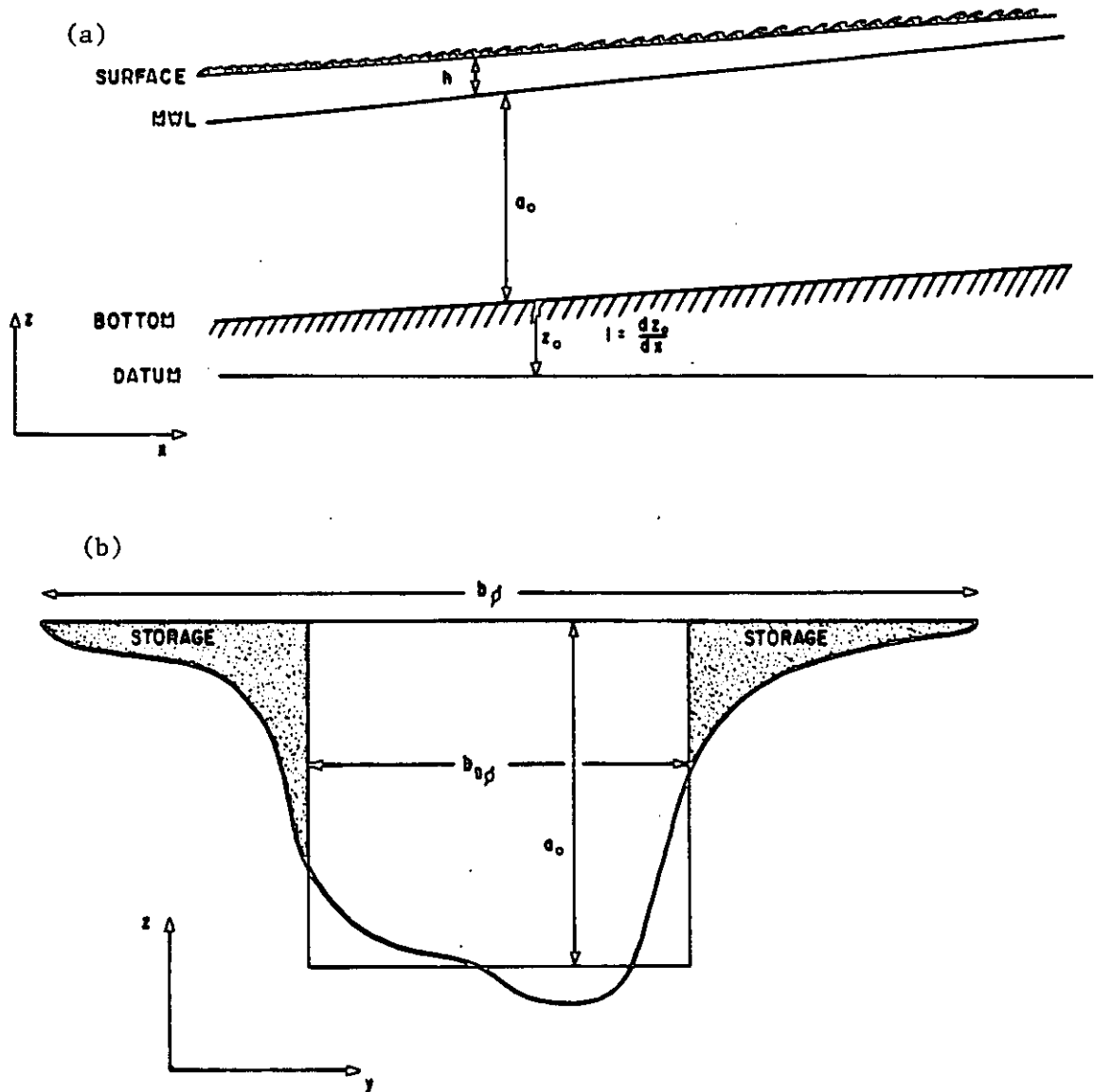
Most methods of analysis of time series data require that the data be spaced evenly in time. Tidal heights are routinely tabulated in the form of hourly observations, from which harmonic constants can be determined. The mariner and marine manager are commonly more interested in the traditional tidal parameters such as tidal range (distance between tidal extremes) and high and low water intervals (time of high or low water at a station) that appear in tide tables. Since tidal extremes only occasionally coincide with evenly spaced observations, NOS has developed methods (known as harmonic constant reduction) of calculating the traditional tidal parameters from harmonic constants (US Coast and Geodetic Survey (USCGS) 1952). Our computer program, based on this publication, was tested using the known tidal properties at Tongue Pt., obtained by personal communication with the NOS Tidal Datums Branch.

Errors occur in the quantities calculated by harmonic constant reduction if the harmonic constants are not known with sufficient accuracy. Additional errors result if the calculated datum level is not reduced to a long term value. The magnitude of these errors may be estimated by comparison of Mean Lower Low Water (MLLW) calculated by harmonic constant reduction with the values provided by NOS. Comparison of calculations based on five ~6 to ~9-month and three 12-month records with accepted datum levels suggests that an error of  $\pm 3$  to  $\pm 10$  cm results from use of records of this length. Use of shorter records may produce substantially greater errors. No attempt has been made to reduce calculated datum levels to 18.6 year epoch values. The calculated MLLW in tidal-fluvial part of the system (above Altoona) may also differ substantially from the accepted Columbia River Datum (CRD), because of riverflow effects, and the tidal range varies substantially with riverflow at upriver stations.

### 2.3.3 Tidal Inundation Time Calculations

The tidal inundation times were calculated for 11 stations between Jetty A (RM-3) and Columbia City (RM-83). The tidal data used for these calculations were provided by NOS and USGS. These inundation time calculations are discussed in Jay (1983). Subsequently, NOS provided a calculation of tidal inundation time based on 21 years of data, 1940 to 1969. Only these results are presented here. The data used by NOS are from the time period 1940 to 1961. The secular sea level trend at Astoria for the period 1940 to 1978 is ~-0.2 to -0.3 cm/yr (Chelton and Davis 1982). Sea level has, therefore, declined ~4 to ~6 cm between 1951 (mid point of data used for the tidal inundation plot) and 1981. The results for the 1940 to 1961 period have, accordingly, been referred to MLLW for the 1941-59 epoch, which is ~5 cm lower than the datum for the 1960-78 epoch used for the 1978 to 1981 data.

Figure 9. Tidal model geometry: (a) definitions of mean depth  $a_0$ , tidal height  $h$ , and bed elevation  $z_0$ ; and (b) stream width  $b_{s0}$  and total width  $b_0$ .



## 2.4 THE ONE-DIMENSIONAL HARMONIC MODEL OF THE M2 TIDE

### 2.4.1 Model Formulation

The model chosen was the simplest available model that incorporated all the essential features of the M2 tide (the lunar semidiurnal tidal constituent, which accounts for most of the tidal energy in the system; Section 3.4): variable-width, friction, river inflow and storage of water over the sand flats. The model may be characterized as a one dimensional, quasi-analytical, harmonic model. Its formulation and use are described in great detail in Dronkers (1964). The equations of motion and continuity are:

$$\frac{\partial h}{\partial x} + \frac{\partial a_0}{\partial x} + l + \frac{1}{gA} \frac{\partial Q}{\partial t} - \frac{\alpha_2 b + b_s}{gA^2} Q \frac{\partial h}{\partial t} + \frac{1}{C^2(a_0 + h)A^2} |Q|Q = 0 \quad (11)$$

$$\frac{\partial Q}{\partial x} + b \frac{\partial h}{\partial t} = 0 \quad (12)$$

where:

- Q = transport in m<sup>3</sup>/s
- h = tidal height in m
- x = horizontal distance (positive upriver, with the origin at the mouth), in m
- a<sub>0</sub> = mean water level, in m
- l = slope of the bed
- b and b<sub>s</sub> describe channel geometry (Figures 9a and b)
- A = a<sub>0</sub>b<sub>s0</sub>
- t = time in s
- α<sub>2</sub> =  $\frac{1}{U^3 A} \int U A^3 dA$
- g = the acceleration due to gravity in m/s<sup>2</sup>
- C = DeChezy's coefficient in s/m<sup>1/2</sup>

Height h and transport Q, and all the coefficients of the equations are functions of x and t. The time-dependence of h, Q and the equation coefficients can be eliminated by the assumption of sinusoidal time-dependence and expansion in Fourier series; complex notation is introduced to simplify the algebra. The expansions for h and Q are:

$$h(x,t) = \sum_{n=1}^{\infty} h_n(x) \cos(n\omega t + \alpha_n) \quad (13)$$

where:

$$h_n(x) \cos(n\omega t + \alpha_n) = H_n(x) e^{in\omega t} + H_{-n}(x) e^{-in\omega t}$$

$$h_n(x) = 2 |H_n(x)|$$

$$H_n(x) = \frac{1}{2} h_n(x) e^{i\alpha_n(x)}$$

$$H_{-n}(x) = \frac{1}{2} h_n(x) e^{-i\alpha_n(x)}$$

b<sub>n</sub> and α<sub>n</sub> are the amplitude and phase of the nth tidal component, and H<sub>n</sub>(x) and H<sub>-n</sub>(x) are complex functions.

$$Q(x,t) = q_0(x) + \sum_{n=1}^{\infty} q_n(x) \cos(n\omega t + \beta_n(x)) \quad (14)$$

where:

$\beta_n$  = the phase of the nth current component in deg  
 $\omega$  = the frequency of the lowest order tidal component (in our case, M2) in cycles/s,  
 $q_0(x)$  is the riverflow transport and  
 $q_n(x)$  is the transport due to the nth tidal constituent and may be expressed in complex form in the same way as  $h_n(x)$ .

The expansion for the various coefficients in Eqs. (11) and (12) is done in an analogous manner.

The assumption of sinusoidal time-dependence and the Fourier expansion to account for the various tidal constituents allows separation of the time and space parts of governing differential equations. Only the riverflow and the M2 constituent (corresponding to the first term in the expansion for  $h$  and the first two terms in the expansion for  $Q$ ) have been so far modeled. Higher harmonics (e.g. M4, M6, etc.) may be added to the model, but addition of the diurnal tide will require reformulation of the model. Addition of the diurnal tide is difficult because the model assumes that the lowest frequency tidal component (in this case, the diurnal tide) is the largest in amplitude, whereas the semidiurnal M2 component is in fact larger.

The non-linear advection and friction terms in Eq. (11) prevent direct analytical solution of the problem. The non-linearity of the friction term is overcome by expanding the friction term as a Fourier series:

$$|Q|Q = C_0 + \sum_1^{\infty} (C_n Q_n e^{in\omega t} + C_{-n} Q_{-n} e^{-in\omega t}) \quad (15)$$

The coefficients ( $C_0$ , the  $C_n$  and the  $C_{-n}$ ) are then evaluated from the corresponding Fourier integrals; evaluation beyond  $n=1$  is too cumbersome to be practical. The coefficients for the first order terms depend on whether  $Q_0(x)$  (the riverflow) is greater than  $Q_1(x)$  (the transport for the M2 tide) for each section. The details are given in Dronkers (1964). Expansion of the friction term in a Fourier series linearizes it; however, the terms of the expansion are recalculated during each iteration, as successively better estimates of  $Q$  become available.

Evaluation of all Fourier integrals leads to the following equations of motion and continuity:

$$\frac{dH_1}{dx} + (r_0 k_{10} |Q_1| + i(\omega m_0) Q_1) + \left[ r_1 k_{00} |Q_1|^2 - \frac{i\omega(\alpha_2 b_0 + b_{s0}) Q_0}{gA^2} + r_2 k_{10} |Q_1| |H_1 Q_{-1}| \right] H_1 = 0 \quad (16)$$

The expression for evaluation of the surface slope  $\frac{da_0}{dx}$  is:

$$\frac{da_0}{dx} + I + r_0 k_{00} |Q_1|^2 + 2r_1 k_{10} |Q_1|^2 |H_1| \cos(\arg H_1 - \arg Q_1) \quad (17)$$

$$+ 2\omega \left[ m_1 + \frac{\alpha_2 b_0 + b_{s0}}{gA^2} \right] |H_1| |Q_1| \sin(\arg H_1 - \arg Q_1) = 0 \quad (18)$$



The equation of continuity becomes

$$\frac{dQ_1}{dx} + i\omega b_0 H_1 = 0 \quad (19)$$

where:

$r_0, k_{00}, r_1,$  and  $k_{10}$  are all coefficients resulting from the Fourier decomposition of the friction term,

$$\arg(H_1) = \arctan \left( \frac{\text{Im}(H_1)}{\text{Re}(H_1)} \right),$$

$\text{Im}(H_1)$  = imaginary part of  $H_1$ ,

$\text{Re}(H_1)$  = real part of  $H_1$ ,

$b_0, b_{s0},$  are geometrical factors defined in Figure 9b,

$A = a_0 b_{s0}$ ,

$m_0$  and  $m_1$  are coefficients arising from the Fourier expansion of the cross-sectional area

all of the above geometrical factors and coefficients are functions of  $x$ , and  $\alpha_2$  has been set to zero, which neglects the convective acceleration associated with water stored over the tidal flats.

The resulting equations remain non-linear, and all the coefficients are functions of  $x$ . The exact solution to the non-linear problem is not known, but an approximate solution can be derived iteratively, using an assumption of the form of  $Q_1$  as derived from the analytical solution to the linear-friction case, where the boundary shear stress is taken to be proportional to  $Q$ , instead of to  $|Q|Q$  (Officer 1976). The estuary must be divided into segments, each of which has (approximately) constant coefficients. The segments must be short enough that the average values employed for the friction and geometric expansions are realistic for the entire segment.

The solution for each section is assumed to be of the form (including the sinusoidal, time-dependent part):

$$H_1 = C_1 e^{i\omega t - \mu_1 x - i\nu_1 x} + C_2 e^{i\omega t + \mu_2 x + i\nu_2 x} \quad (20)$$

and:

$$Q_1 = -i\omega b_0 \left[ \frac{C_1}{k_1} e^{i\omega t - \mu_1 x - i\nu_1 x} + \frac{C_2}{k_2} e^{i\omega t + \mu_2 x + i\nu_2 x} \right] \quad (21)$$

where:

$C_1$  and  $C_2$  are complex constants,

$$k_1 = -(\mu_1 + i\nu_1)$$

$$k_2 = (\mu_2 + i\nu_2)$$

The solution consists of two waves propagating in opposite directions. The  $\nu_i$  are the wave numbers ( $\frac{2\pi}{\lambda}$ , where  $\lambda$  is the wave length) for the wave going upriver ( $i=1$ ) and downriver ( $i=2$ ). The  $\mu_i$  are damping coefficients; note that the inbound wave dies out exponentially, whereas the outbound wave grows exponentially. For the no riverflow case,  $\mu_1 \approx \mu_2$ , otherwise, the additional friction associated with the riverflow causes  $\mu_1$  to be greater than  $\mu_2$ .

Determination of the values of the wave numbers, damping coefficients and other factors for each section completes the solution. This is carried out iteratively by use of the complex function:  $Z(x) = \frac{H_1(x)}{Q_1(x)}$ , where  $Q_1$  is assumed to be

constant with  $x$  on the first iteration. The matching of  $Z(x)$  at boundaries between sections is carried out using a linear relationship between  $Z(x)$  at the beginning of the section and  $Z(x)$  at the end. This linear relationship is derived under the assumption:  $e^{k_1 x} \cong 1 + k_1 x$ . This assumption requires that the segments used be a small fraction of the wavelength of the tidal wave; this is not a severe limitation. Segment lengths of one mile were used below RM-20, to resolve in detail the response of the system to changing geometry and friction in this reach. Segment lengths of two to five river miles were used between RM-20 and RM-100. The tidal wavelength is of the order of 200 miles.

The boundary conditions are:  $H_1(x)$  at  $x=0$  specified (i.e. amplitude and phase of the tide at the mouth) and  $H_1(x)=Q_1(x)=0$  as  $x$  approaches infinity. The later condition leads to:  $Z(x) = \frac{k_1 i}{\omega b_0}$ . In practical application, the boundary condition for  $x$  approaching infinity is applied at River Mile 150. Since the form of the tide only in the lower  $\sim 85$  river miles (to Columbia City) was of interest, the complexities of Willamette River/Portland Harbor were not included in the model. The model normally converges after about six iterations.

The study of the tidal-fluvial interactions and the evaluation of the importance of friction and geometry to the tide were the primary purposes of constructing the model. The specification of friction and geometry is, accordingly, of some importance. The geometry used in the model is shown in Figure 10a and b. The division between storage areas and stream areas (areas which transmit flow) is somewhat arbitrary. All peripheral bays and selected other areas were excluded from the stream area, the largest such area was the bight north of the navigation channel and between Jetty A and North Jetty. Eddy like currents are known to occur there (US Army Engineers 1960), and the exclusion of this area does not lead to unreasonably large currents near the entrance.

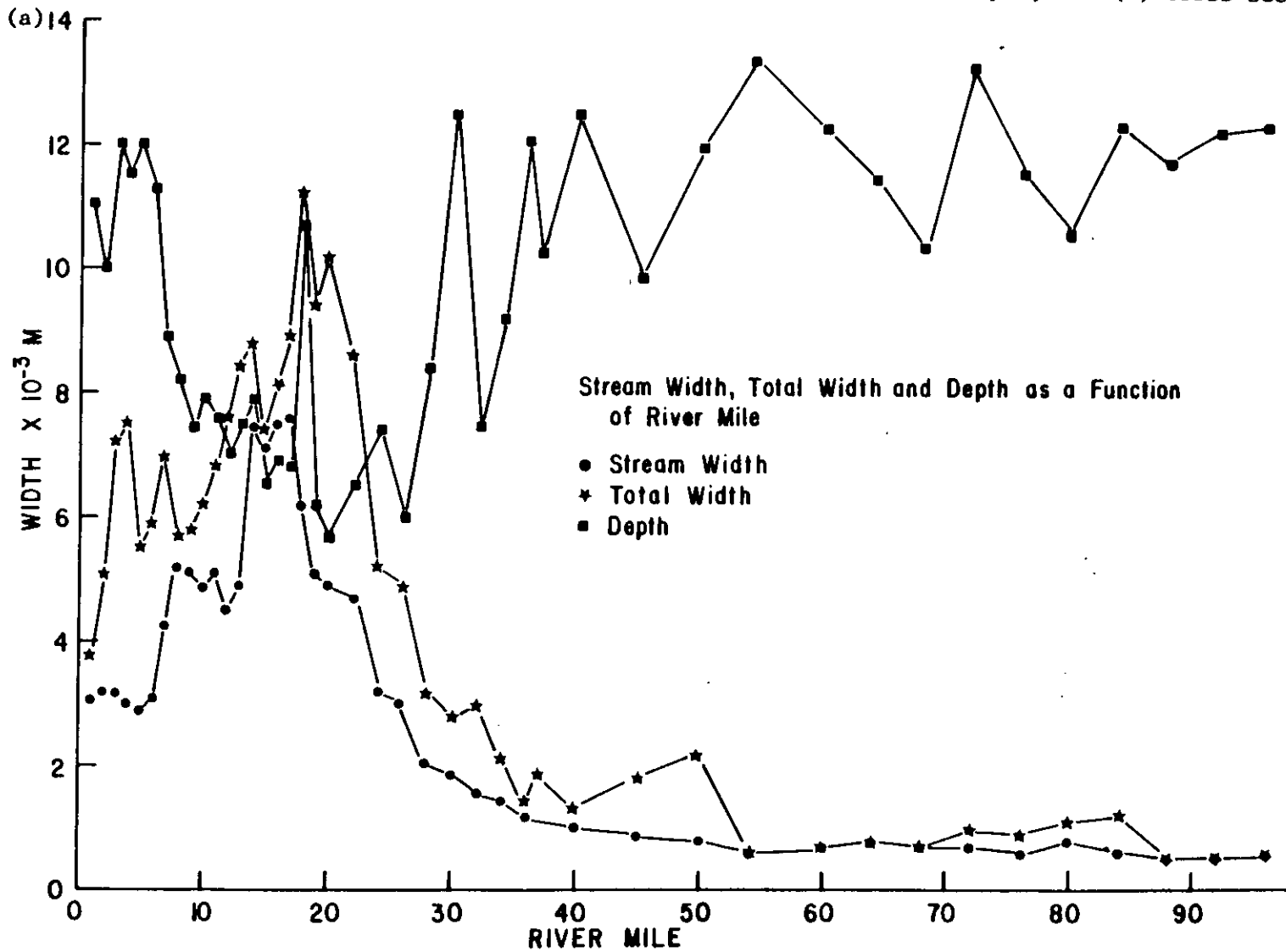
Specification of the friction was found to be dependent on riverflow and channel position but not tidal range. The drag coefficient (which is related to DeChezy's coefficient  $C$  as  $C_D = \frac{g}{C^2}$ ) was taken as .0011 for RM-1 to RM-12 for all runs. Its value was increased linearly with river mile to .0051 between RM-16 to RM-28. The value above RM-28 was found to be dependent on riverflow; higher riverflows required lower drag coefficients. The range of drag coefficient for this part of the system was 0.0039 to 0.068. The decrease in friction coefficient with increasing river flow reflects the increase (by as much as a factor of two) in flow depth associated with higher riverflows. The spatial variation of the drag coefficient in part reflects spatial variations in form drag due to bedforms and channel configuration; the area of low friction near the entrance coincides roughly with the area of small, tidally-reversing bedforms (Sherwood et al. 1984). But form drag is only part of the problem; the area of low friction is also the part of the estuary where stratification alters the velocity profile and reduces boundary shear stress (Section 3.2).

The model was verified for the M2 tide for three different river flows (146, 277 and 433 kcfs; or 4139, 12,261 and 28,320  $m^3/s$ ) using tidal height harmonic analysis results for months having this average flow. For the 146 kcfs case, two additional tidal ranges were run, corresponding to  $M2 + S2 + N2$  and  $M2 - S2 - N2$  tides. These represent tidal ranges of  $\sim 2.7$  and  $\sim 1.06$  m at Tongue Pt.; the M2 tide alone corresponds to a tidal range of a  $\sim 1.9$  m at Tongue Pt. The agreement between the model and the data was generally excellent; results are given in Section 3.1.

#### 2.4.2 Formulation of the Energy Budget

The M2 tide accounts for most ( $>70\%$ ) of the total tidal energy that enters the system from the ocean, and the major semidiurnal constituents ( $M2+N2+S2$ )

Figure 10. Tidal model geometry: (a) stream width, total width and depth, and (b) cross sectional area



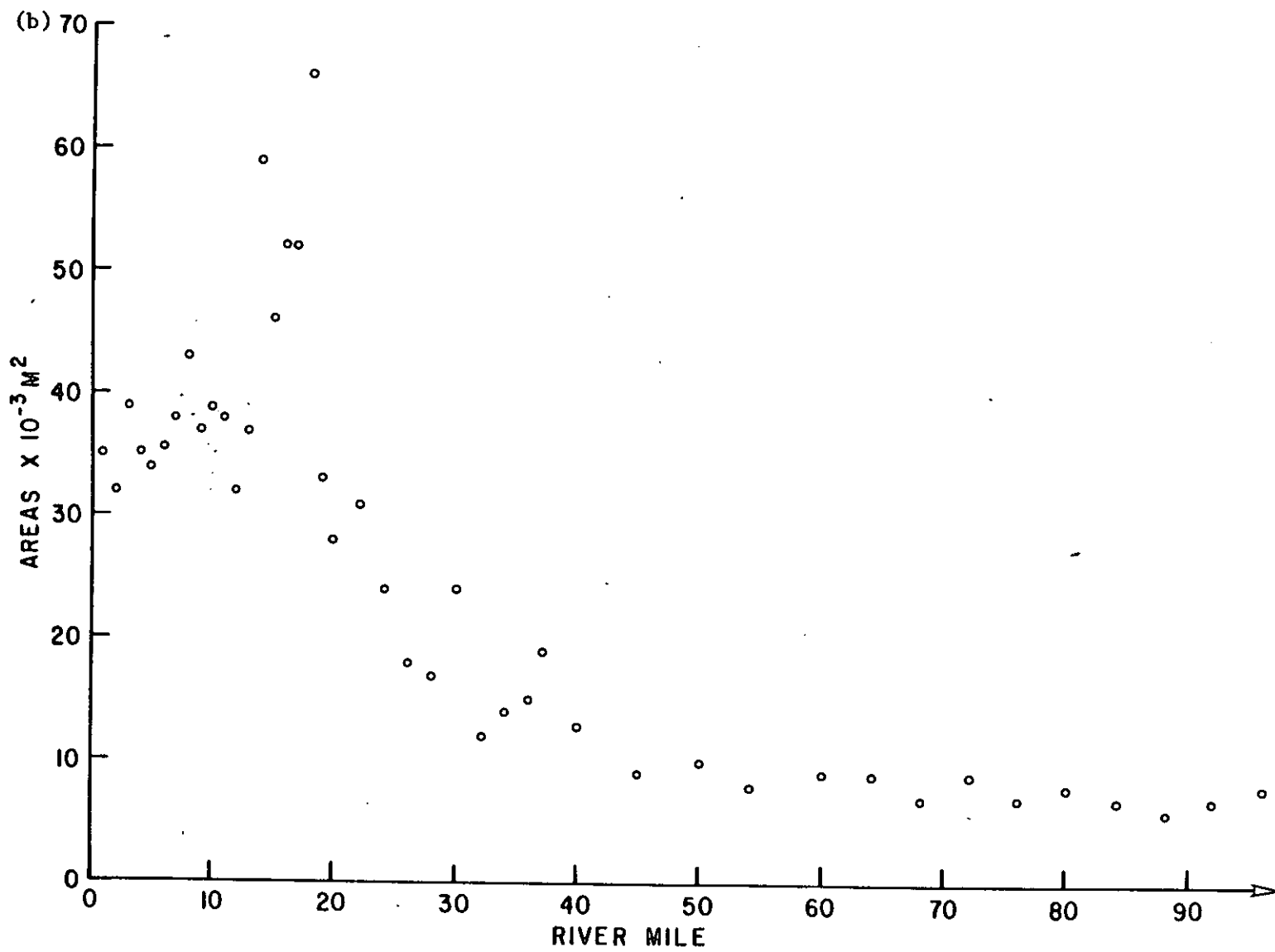
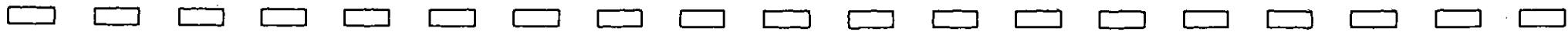


Figure 10. (continued).



account for more than 80% of the total tidal energy input. We can, therefore, account for most of the energy available for circulation by considering only the semidiurnal tide and the river inflow. Although the oceanic and direct tidal forcing at the frequency of M4 (the lunar quarterdiurnal) is insignificant, we know from sections 1.1 and 1.3 that energy from the M2 tide is transferred to overtides (M4, etc.) and the tidal residual (quasi-steady flow). We should therefore consider the M4 energy in the tidal terms and the Stokes drift compensation flow in the mean flow.

The riverflow in the system is sufficiently large that it dominates the energy budget in the tidal-fluvial part of the system. We have been unable to find in the oceanographic literature on energy budget for any estuary that included riverflow. We therefore begin by defining the energy budget for a system where the riverflow (assumed steady) plays an important role.\* Consider a longitudinal section of estuary (e.g. from the mouth to some arbitrary river mile). The energy budget for this section of the system is found by multiplying the vertically and laterally integrated along-estuary equation of motion by the along-estuary velocity and the density. Integration with respect to longitudinal distance over some finite length of the estuary then yields:

Tidal terms:

(22)

- tidal energy flux in at downstream end (M2 + M4)
- tidal energy flux out at upstream end (M2 + M4)
- ± direct work by moon on water's surface in section

Mean flow terms:

- + mean flow kinetic energy flux in at downstream end
- mean flow kinetic energy flux out at upstream end
- + mean flow potential energy flux in at downstream end
- mean flow kinetic energy flux out at upstream end

Interaction term:

- + tidal/mean flow kinetic energy flux in at downstream end
- tidal/mean flow kinetic energy flux out at upstream end

Sink terms:

- = tidal dissipation + mean flow dissipation
- + tidal/mean flow interaction dissipation
- + buoyancy flux ± temporal change of energy stored in tidal oscillation, within the section

This general formulation is too complex for present purposes and contains terms that can be dismissed as unimportant. Scaling arguments and calculations for other estuaries (Uncles and Jordan 1980; Heath 1981) suggest that dissipation is the only important sink term. Direct work by the moon is unimportant for a body as small as the Columbia River Estuary. We neglect the transfer of M2 energy to other frequencies and write the resulting energy balance in terms of model parameters  $Q_0(x)$  (the riverflow transport) and  $Q_1(x)$  (the tidal transport amplitude):

$$\Delta\left(\frac{1}{2}\rho gh_1 q_1 \cos\delta_1\right) + \Delta(\rho gh_0 q_0) \quad (23)$$

$$\Delta(M_2 \text{ energy flux}) \quad \Delta(\text{potential energy flux of mean flow})$$

\* Personal communication with B. Giese, Seattle: University of Washington.

$$\begin{aligned}
& + \Delta \left[ \frac{\rho q_0^3}{2A^2} \right] & + \Delta \left[ \frac{3\rho q_0 q_1^2}{4A^2} \right] \\
\Delta(\text{mean flow kinetic energy flux}) & \quad \Delta(\text{tidal/mean flow interaction kinetic energy}) \\
= & \frac{4\rho C_D q_1^3 \cos\gamma (\sin^2\gamma + 2)}{3\omega A^2} & + \frac{4\rho C_D q_0^3 \gamma}{\omega A^3} \\
& \text{tidal dissipation} & \quad \text{mean flow dissipation} \\
& + \frac{3\rho C_D q_0 q_1}{\omega A^3} (4q_0 \cos\gamma - q_1(2\gamma - \sin(2\gamma))) \\
& \text{tidal/mean flow interaction dissipation}
\end{aligned}$$

where:

$\delta = \alpha_1 - \beta_1$ , the phase difference between the tidal height and the tidal transport,

the  $\Delta$  indicates the difference between the downstream and upstream ends of a section of the estuary,

$h_0$  and  $q_0$  are stage and mean flow at the midpoint of the estuary section,

$h_1$  and  $q_1$  are the tidal height and tidal transport amplitudes at the midpoint of the section,

$A$  = flow cross-sectional area for the section, and

$\gamma = \arccos\left(\frac{-q_0}{2|q_1|}\right)$ , for  $q_0 \leq 2|q_1|$

$\gamma = \pi$  for  $q_0 \geq 2|q_1|$

Expression of the energy budget in terms of the model parameters is straightforward except for the phase angle  $\gamma$ . The phase  $\gamma$  represents the difference in duration of flood and ebb tides, caused by the mean flow (Dronkers 1964). Thus, if the duration of one tidal cycle is  $2\pi$  radians, flood tide lasts from  $+\gamma$  to  $2\pi-\gamma$ , radians and ebb tide lasts from  $-\gamma$  to  $+\gamma$  radians. At the entrance,  $\gamma$  is close to  $\frac{\pi}{2}$ ; (ebb and flood have nearly equal durations). Upriver, where ebb tide prevails at all times,  $\gamma = \pi$ .

## 2.5 STATISTICAL METHODS

The analysis of residual flow processes relies heavily on statistical methods. To use statistical models to investigate dynamical processes, it is generally necessary to remove the tidal signal (and higher frequency signals) by use of the digital filter described in Section 2.7. and then to remove the seasonal signal. The seasonal signal is removed because the seasonal cycles of flow and forcing variables are often strongly correlated for reasons that are either not causal or not of interest in the present study (Chelton and Davis 1982). This correlation may result in erroneous conclusions concerning cause and effect. All atmospheric variables (wind velocity components and pressure) are, for example, correlated at low frequencies. Elimination of the seasonal part of the inter-correlation between forcing variables also improves the statistical results, because inter-correlation between variables used in a statistical model badly degrades the reliability of the model (Chelton and Davis 1982). The time-series data used in the statistical models remain somewhat noisy and inter-correlated, and the dynamical relationships that we wish to examine may show significant seasonal variation. Long records must, therefore, be used if statistical

conclusions are to be valid.

The need for long records has dictated an approach based primarily on atmospheric and tidal height data, for which long records are available. Current and salinity records have been used to a much lesser extent because the record lengths are generally too short to draw definite conclusions. Geostrophic winds and Newport, OR winds have been used instead of local winds because local wind observations were incomplete. Seasonal signals in riverflow and Tongue Pt. tidal height were removed using long-term records of monthly mean riverflow (obtained from the USGS) and monthly mean tidal height (obtained from NOS). In all other cases, the seasonal signal was that internal to the data actually used for the correlations. Records were three or more years in length for atmospheric variables and tidal range, and varied from six to 18 months for other tidal heights (other than Tongue Pt.) and the slope data calculated from tidal heights at adjacent stations.

All statistical calculations were carried out using the Minitab statistical computing package, which is described in Ryan et al. (1976, 1980).

Daily riverflows for the Mouth of the Columbia River were calculated from Bonneville Dam flow data (obtained from the Corps of Engineers, Portland District) and Willamette River at the Mouth flow data (obtained from the USGS). A relationship was obtained between flow at Bonneville, Willamette River data and flow at the mouth by means of regression analysis on monthly averages of the three parameters. Best results were obtained when high-flow months were treated separately from low-flow months; this probably indicates that Willamette River flow is not a good indicator of flow for other west-side rivers.

The relationships used to calculate flow at the mouth were:

For Bonneville Dam flow <200,000 cfs and Willamette River flow <90,000 cfs:

$$\begin{aligned} \text{Flow at mouth (t+6 hours)} &= 4139 \text{ cfs} && (24) \\ &+ 1.003 (\text{Bonneville Dam flow in cfs}(t)) \\ &+ 1.632 (\text{Willamette River at Portland in cfs}(t)) \end{aligned}$$

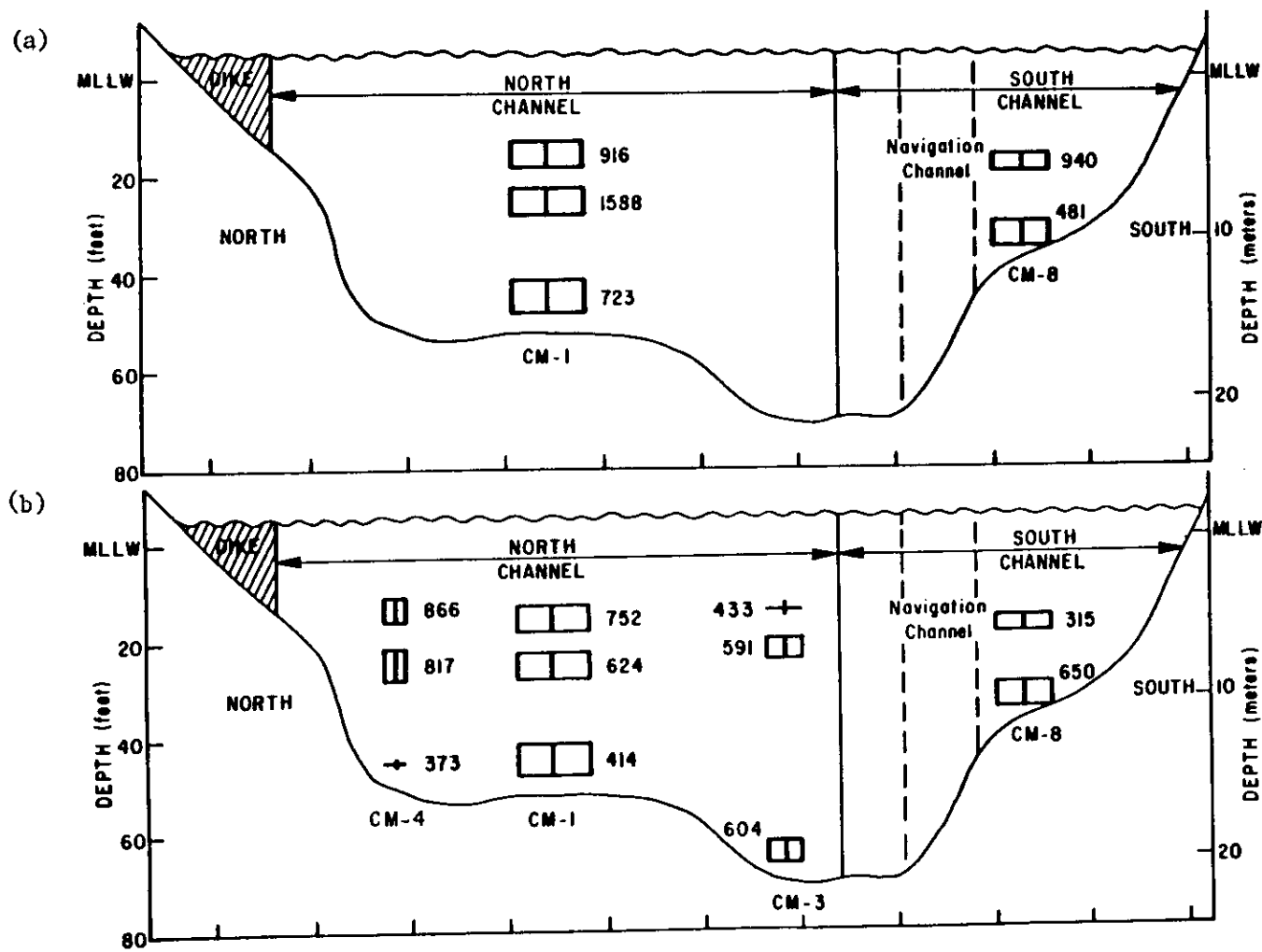
For Bonneville Dam flow >200,000 cfs or Willamette River flow >90,000 cfs:

$$\begin{aligned} \text{Flow at mouth (t+6 hrs)} &= 10300 \text{ cfs} && (25) \\ &+ 1.084 (\text{Bonneville Dam flow in cfs}(t)) \\ &+ 1.757 (\text{Willamette River at Portland in cfs}(t)) \end{aligned}$$

The freshwater flow is highly variable and runoff may be distributed unevenly in west-side drainage basins, particularly during winter storms. Thus, the above method provides, on a day to day basis, an indication of the trend in riverflow, not an exact runoff calculation. On a monthly average basis, the low-flow model accounted for ~97% of the variation in USGS calculated monthly average flow at the mouth for 44 'low-flow' months; the high-flow model accounted for ~92% of the variance for 12 'high-flow' months. The high-flow model is less accurate both because there were fewer high-flow months on which to base the model, and because high-flow periods are inherently less predictable.

The lag used in the model (six hours) was determined after consideration of continuity and wave speed constraints. Orem (1968) suggested that changes in flow at the Dalles Dam and the mouth of the Willamette River were followed by

Figure 11. Length of record (in hours) and meter positions for current meters on the Clatsop Spit-Sand Island Section for (a), 1981 high-flow season and (b), 1981 low-flow season. Boxes indicate range of depth and horizontal position for successive current meter deployments.





changes in flow at the mouth several days later, the delay depending on the runoff. Such lags would result in flooding at Portland during freshet periods. The six-hour lag used here is based on the assumption that changes in flow move downstream at the barotropic wave speed ( $c=(gd)^{\frac{1}{2}}$ ), the travel time of which is less than nine hours from Bonneville Dam to the mouth.

## 2.6 SALT TRANSPORT CALCULATIONS

The salt transport was calculated using the expansion of Robe (1968) adapted to a per unit area basis. The expansion is:

$$\begin{aligned} \text{transport per unit area in } \frac{\text{kg}}{\text{m}^2\text{s}} = & U_0 S_0 + [U_1 S_1] \\ & + [U_1 \frac{h_1}{H}] S_0 + [S_1 \frac{h_1}{H}] U_0 + [S_1 U_1 \frac{h_1}{H}] + \text{turbulent transport} \end{aligned} \quad (26)$$

where:

the brackets indicate an average over a 24.84 hour tidal cycle,  
the subscript "0" indicates a tidal cycle average,  
the subscript "1" indicates a tidal cycle deviation from the tidal cycle average,  
U is the velocity, S is the salinity, h is the tidal height, and  $\bar{H}$  is the mean depth.

The terms of the expansion represent (from left to right) advection by the mean flow (mean flow transport), tidal advective (or tidal oscillatory) transport, transport by the Stokes drift, the salinity-height correlation transport, the triple-product transport, and transport by turbulent processes. The first term is associated with the  $O(\epsilon)$  mean flow. The remaining terms are all in some way associated with tidal processes. The second term is important when the salinity is, on the average, larger on flood than on ebb. The Stokes drift term is analogous to transport by the net flow, but is always inward. The mean-flow transport and the tidal transport usually are the dominant terms in the salt transport balance, but the Stokes drift transport is sometimes important. Previous studies in the Columbia River Estuary have found the last three terms on the right hand side to be unimportant (Robe 1968; Hughes and Rattray 1980).

More detailed expansions have been used in the Columbia River Estuary (Hughes and Rattray 1980) and other estuaries. Dyer (1973) has reviewed these salt transport calculations. These methods were originally used with detailed (in the vertical) salinity and velocity data and incorporate additional terms representing lateral or vertical deviations from lateral or vertical means. These vertical and lateral deviation terms have been associated with the steady, density-driven and lateral circulations. The current meter data used here are very sparse in the vertical (only two or three data points on a profile); this renders the more detailed expansions impractical. The great strength of the use of current meter data is the ability (unprecedented in any previous study or salt transport) to assess temporal variability.

There are also reasons to distrust the interpretations made on the basis of the detailed expansions. Rattray and Dworski (1980) have shown the sensitivity of the results to the details of the methods used. Moreover, association of the vertical deviation terms with the steady, density-driven circulation requires an assumption as to what vertical salinity and velocity profiles would be in the absence of a baroclinic pressure gradient. The customary assumption of a uniform velocity profile as a standard would be very nearly correct for a constant-density flow. We will see, however, that the tidal velocity profile in a stratified

system is very different from a that for the constant-density case, and that only part of this difference is due to the baroclinic pressure gradient (Section 3.2). It is not particularly reasonable then to assume the constant-density form for the mean flow. The form of the reference salinity profile is even more problematic.

The salt transport integration was carried out using hourly Aanderaa velocity and salinity data and hourly tidal height data for successive 24.84-hour periods and a Simpson's rule integration, modified to account for the last 0.84 hours. The terms in Eq.(26) are specific to the position in the vertical of the meter (first two terms) and a vertical average for water column below the meter (next three terms). The three vertical average terms are generally insignificant, although the Stokes drift is occasionally important near the surface. While salt transport results were routinely calculated for all current meter files, the most extensive results were for the Clatsop Spit-Sand Is. Section, which crosses the estuary at ~RM-5, between Clatsop Spit and the dike at the downstream end of Little Sand Is. The locations of stations on this transect (CM-1, CM-3, CM-4 and CM-8) are shown in Figure 7. Meter locations are shown in Figures 11a and b, for this cross-section. The numbers adjacent to the boxes in Figures 11a and b indicate the number of hours of data available for the season at each meter location. The size of the box indicates variations in position of the meter in successive deployments.

The most likely source of error in the calculated salt transport is errors in the Aanderaa current meter salinity and velocity data. Aanderaa salinity data are (above) accurate to ~0.5 ppt, which is small relative to salinity changes of 10 to 30 ppt during a tidal cycle. Harmonic analysis results demonstrate the general correctness of the Aanderaa velocity observations. Filtering of the data to hourly (Section 2.7) helps to eliminate random errors. The internal consistency of the salt transport results suggests that they are reliable, but no error estimates have been derived.

## 2.7 MISCELLANEOUS CALCULATIONS

Time series data are filtered using the routines described in Irish et al. (1976). The Lanczos filter used to produce hourly data for harmonic analysis from data sampled at smaller sampling intervals has a half-power point at  $(150 \text{ min})^{-1}$ , passes >98% of the signal at the frequency of M8 (the lunar eighth-diurnal constituent), and eliminates 98% of the signal at frequencies above  $(\sim 128 \text{ min})^{-1}$ . The Lanczos filter used to remove tidal signals has a half power point at  $(32 \text{ hours})^{-1}$  and removes 98% of the energy at  $(25 \text{ hrs})^{-1}$ . The fast-Fourier transform (fft) and associated calculational routines used in spectral analysis are those described in Irish et al. (1976).

### 3. RESULTS AND DISCUSSION

#### 3.1 TIDAL PROCESSES

The tidal wave entering the mouth of the estuary and the potential energy of the riverflow are the major sources of energy for circulatory processes in the estuary and river; the tides are the major source of energy for estuary proper. The strength of the tidal forcing and the well-defined frequencies involved can be seen in the power spectrum of the tidal heights at Tongue Pt. (RM-18; Figure 12a). The largest peaks in Figure 12b are the semidiurnal (twice-daily; frequency  $\sim 0.08$  cycles/hr) and diurnal (daily; frequency  $\sim 0.04$  cycles/hr) tidal peaks which make up the  $O(1)$  tidal circulation. Numerous different effects, each represented in a harmonic analysis by a tidal constituent and each having a different frequency and magnitude, contribute to both of these peaks; the principal tidal constituents are identified in Section 3.1.1. The evenly spaced peaks to the right (at higher frequencies) are the tidal overtones that are generated by the interactions of the incoming diurnal and semidiurnal waves with the shallow water of the estuary (the  $O(\epsilon)$  higher harmonic tidal circulation). To the left of the diurnal and semidiurnal peaks are poorly resolved, low-frequency peaks caused by tidal effects and riverflow fluctuations, which dominate the  $O(\epsilon)$  residual circulation.

Tidal energy enters the estuary almost exclusively at diurnal and semidiurnal frequencies; it is effectively transferred by the non-linear processes described in Section 1.1 to higher and lower frequencies as the wave travels up the river. The power spectrum of the tidal heights at Wauna, RM-42 (Figure 12b), shows that the main tidal peaks have diminished, and the peaks corresponding to the  $O(\epsilon)$  higher harmonics and the residual flow have grown, relative to Figure 12a. Peaks at  $\sim 15$  days ( $\sim 0.0028$  cycles/hr) and  $\sim 28$  days ( $\sim 0.0014$  cycles/hr) are now resolved; these are caused by the tidal monthly variations in residual circulation.

##### 3.1.1 Tidal Heights

Tidal height is perhaps the single most useful and most accurately known estuarine circulation parameter. Harmonic analysis results for selected estuary stations are shown in Table 1 and Appendix B. Historical tidal observations are compiled in Appendix C. Virtually all of the tidal energy coming into the estuary is contained in the three largest semidiurnal constituents (Section 3.4): M2 (the lunar semidiurnal component), S2 (the solar semidiurnal component), and N2 (the larger lunar elliptic component) and two largest diurnal constituents: K1 (the lunar-solar diurnal component) and O1 (the lunar diurnal component). The energy flux for M2 is nearly eight times as large as the next most important constituent, K1; S2, N2, and O1 are still weaker. The effect of each of these constituents on the range of the tide is discussed in Section 3.1.2. Columbia River Estuary tidal height harmonic constants are similar to those of other nearby coastal systems; the tidal range and relative amplitudes of major constituents at Tongue Pt. differ from those of other stations between Waldport, OR, and Aberdeen, WA, by less than 20% (Callaway 1971; Hopkins 1971). Because the M2 tide accounts for such a large fraction of the total tidal energy in the system, it is useful to examine the propagation of the M2 tidal wave through the system, using both data and model results. The behavior of the other semidiurnal constituents, the diurnal constituents, and higher harmonics is considered below.

##### Behavior of the M2 Tide - The Balance Between Topography and Friction

Figures 13 to 15 show model results for the amplitude and phase of the M2 tidal heights as a function of river mile for several different riverflows. The model used is the one-dimensional, harmonic model of the M2 tide in the presence of riverflow, described in Section 2.4. Figures 16a and b show the phase and

Figure 12. Power spectra of tidal height at (a), Tongue Pt. and (b), Wauna. Dots indicate 95% confidence limits.

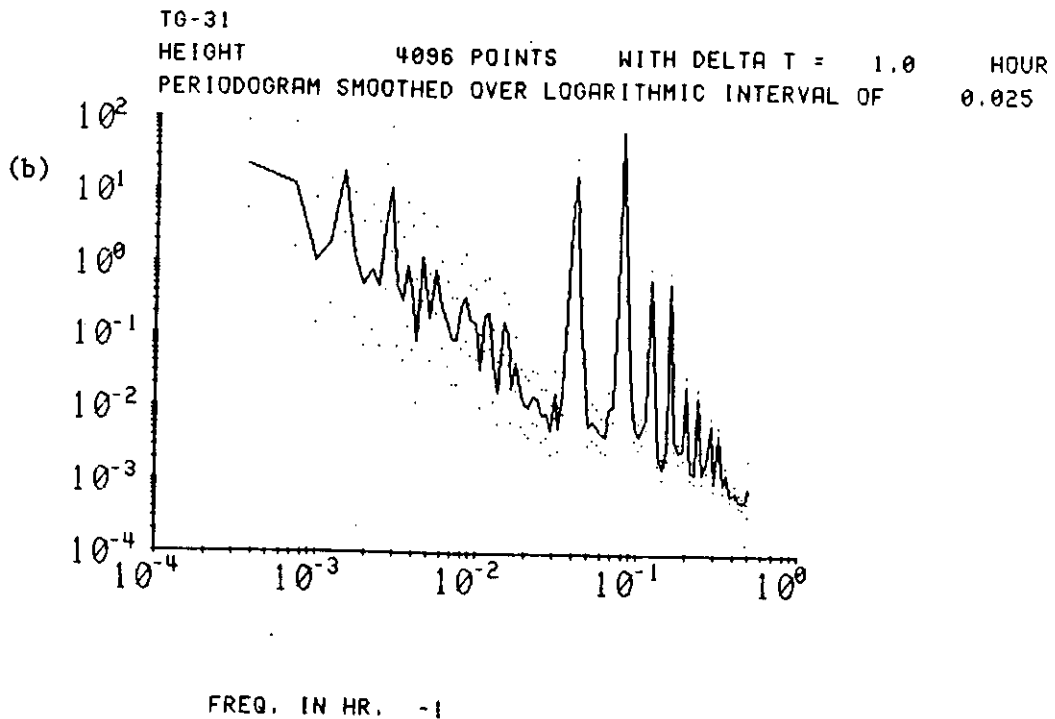
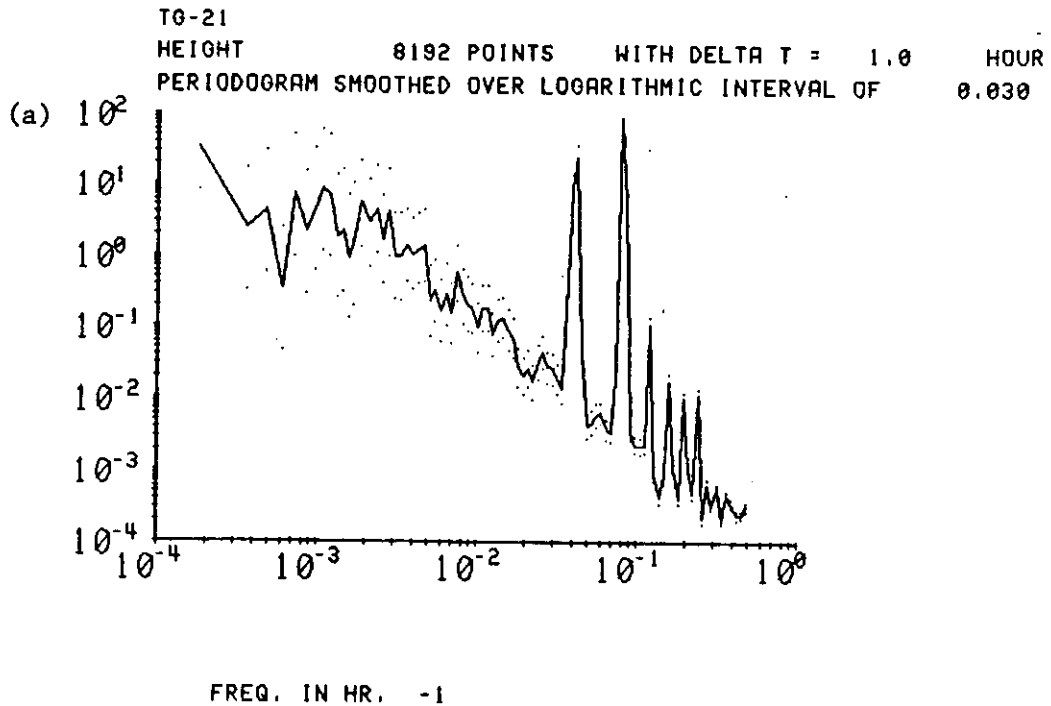


Table 1. Tidal constituent ratios - Columbia River and Estuary

<u>Length of Record</u>	<u>Station</u>	<u>RM</u>	$M_2$	$\frac{S_2}{M_2}$	$\frac{N_2}{M_2}$	$\frac{M_4}{M_2}$	$\frac{MK_3}{M_2}$	$\frac{K_1}{M_2}$	$\frac{O_1}{M_2}$	$\frac{O_1}{K_1}$	$\frac{M_2+S_2+N_2}{O_1+K_1+P_1}$
7 mos.	Jetty A	3	.833	.255	.207	.026	.015	.487	.328	.674	1.51
7 mos.	Ft. Stevens	8.3	.935	.256	.202	.027	.011	.441	.276	.625	1.72
1 yr.	Tongue Pt.	17.6	.947	.247	.189	.012	.025	.423	.252	.596	1.81
7 mos.	Altoona	24.4	.897	.238	.185	.042	.036	.400	.238	.595	1.91
1 yr.	Wauna	42.0	.736	.234	.188	.110	.089	.384	.205	.533	2.05
7 mos.	Beaver	53.3	.578	.236	.176	.155	.122	.385	.200	.519	2.10
1 yr.	Columbia City	83.0	.231	.236	.195	.208	.145	.478	.241	.504	1.78

Figure 13. Model results for river flow of 146 kcfs (4139 m<sup>3</sup>/s)

- \* Model tidal height amplitude
- + Model tidal height phase
- l Model tidal current phase
- H Observed tidal height amplitude
- A Observed tidal height phase

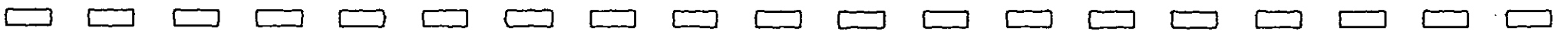
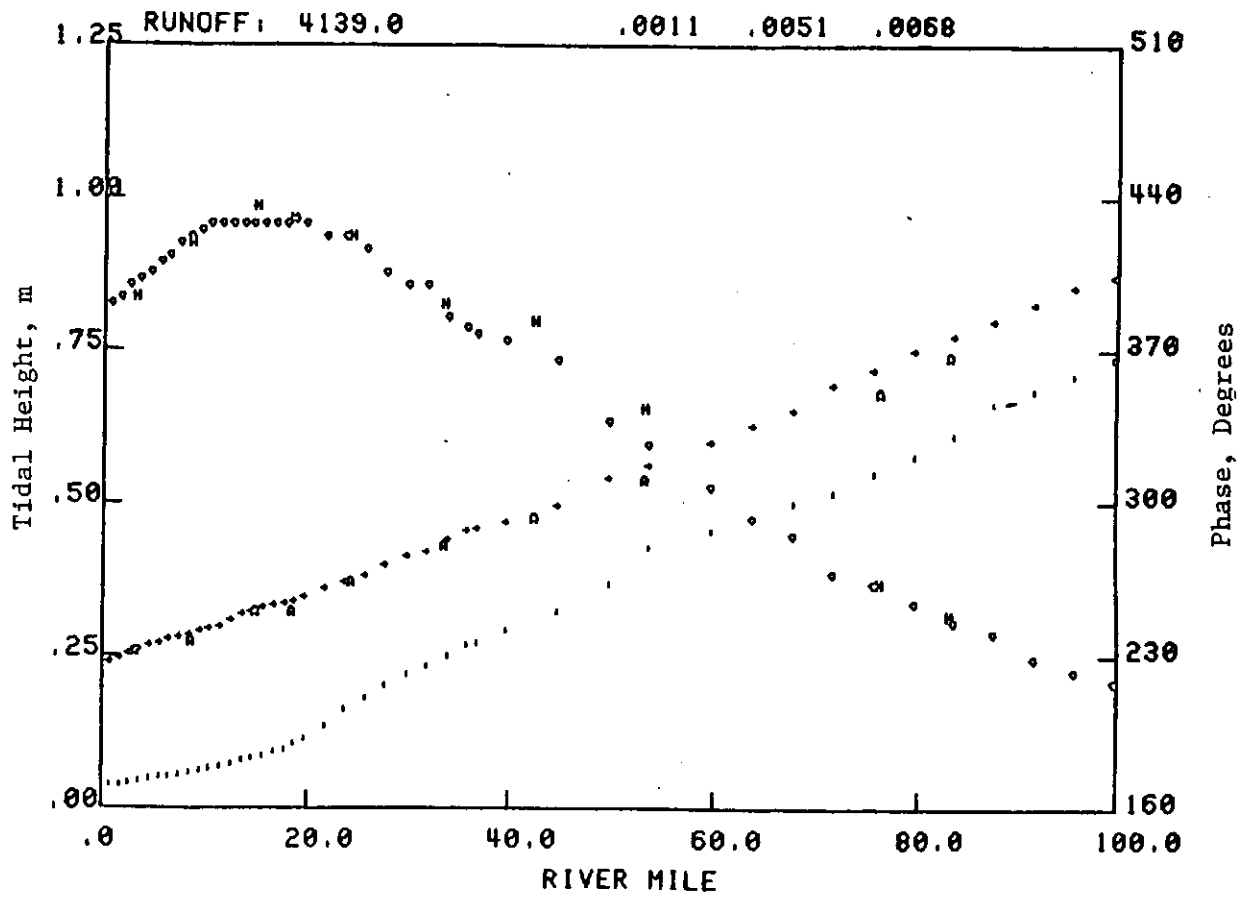


Figure 14. Model results for river flow of 433 kcfs (12,261 m<sup>3</sup>/s)  
symbols as in Figure 13.

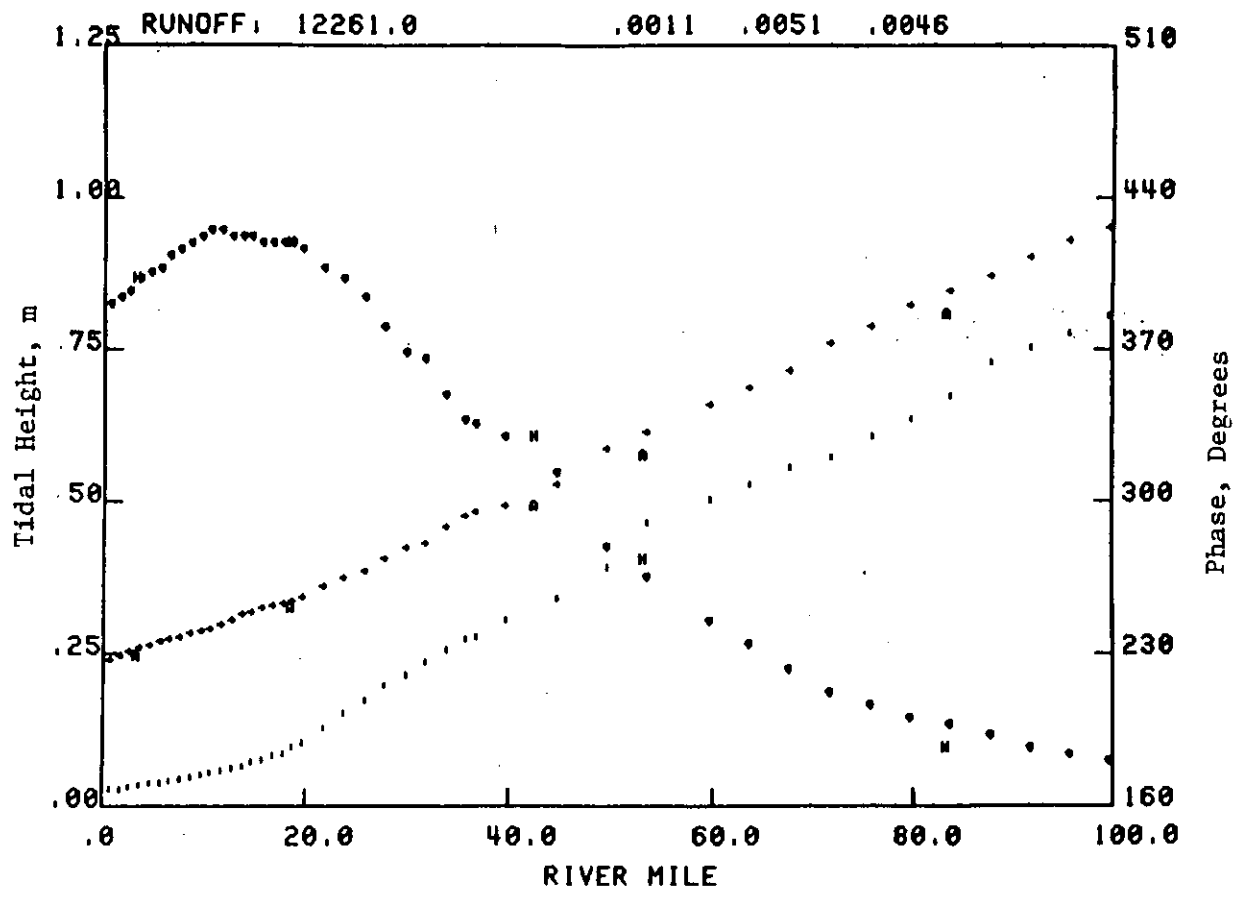


Figure 15. Model results for river flow of 1,000 kcfs (28,320 m<sup>3</sup>/s) symbols as in Figure 13.

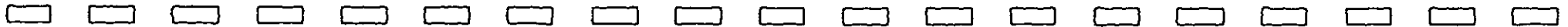
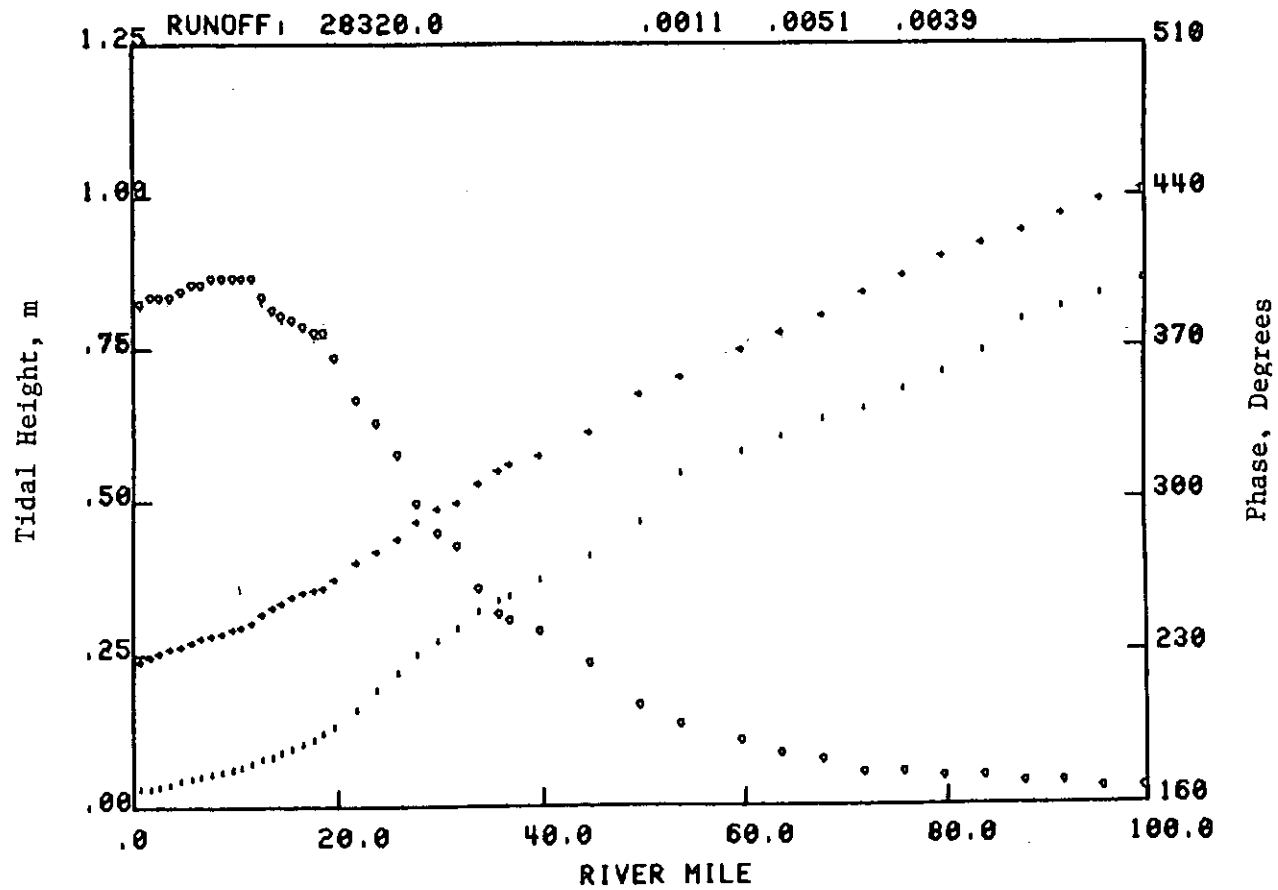
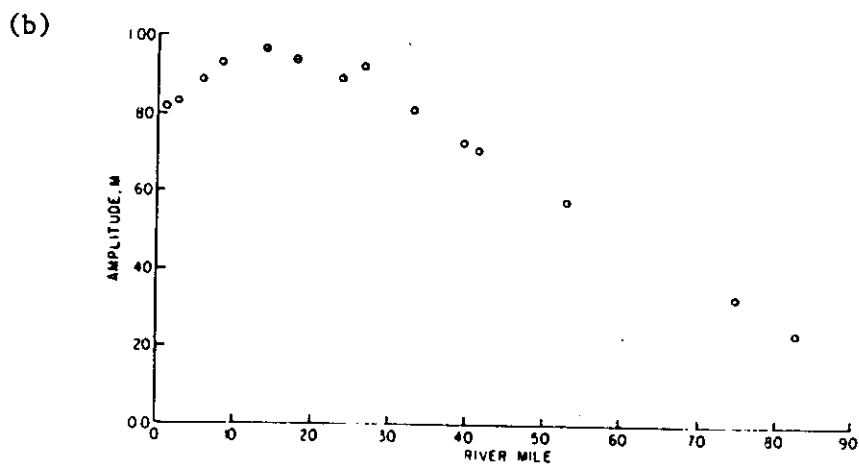
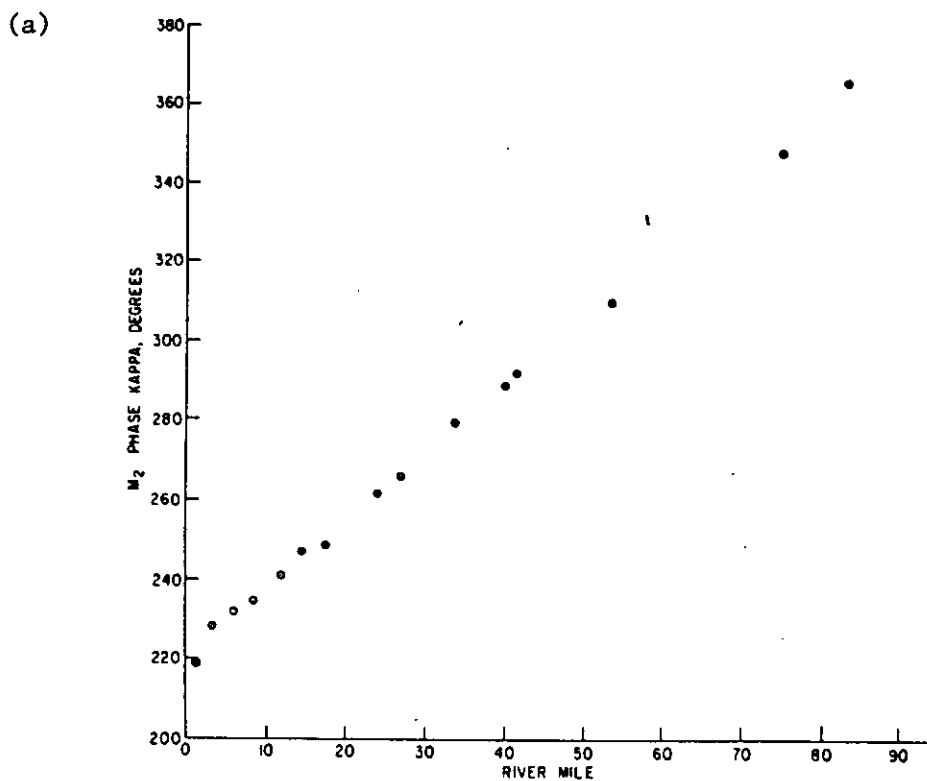




Figure 16.  $M_2$  tidal height (a) phase and (b) amplitude vs. river mile in the Columbia River and Estuary.



amplitude of the M2 tidal heights, as determined from observations. Record lengths used in Figures 16a and b range from several months to a year; these results approximate a yearly average. The agreement between the model results and prototype tidal height data is generally excellent; the differences between model and prototype in the upriver areas is believed to be caused by omission of the tidal overtones from the model. The phase of the M2 tidal height increases nearly linearly with river mile (Figure 16a). The M2 tidal height amplitude (Figure 16b) first increases from the mouth to Astoria and then decreases almost linearly upriver. Figures 13 to 15 show that tidal heights upriver of Tongue Pt. (RM-19) are strongly affected by riverflow changes, as discussed in Section 3.3.

Experimentation with the harmonic tidal model suggests that these patterns result from the balance between topography and friction. The M2 tide is essentially a heavily damped wave in a channel with a constricted entrance, attached to a funnel that decreases in area almost linearly in the upstream direction (Figure 10b). The tidal amplitude increases, because of the partial standing wave character of the tide in the lower estuary and the funnel shaped geometry; the highest amplitude occurs as the estuary narrows between RM-13 and 20, because of the partial reflection of the wave by the funnel-like topography above Astoria. The increasing friction in this reach, the shallowest part of the system, is also critical in determining the shape of the wave. As the tidal wave's energy is more strongly dissipated, friction eventually outweighs the funnel effect, and tidal range decreases and the tide becomes more progressive upriver (Figures 13 to 15).

The harmonic analysis results for Ilwaco, Chinook, Youngs Bay, Knappton, and Knappa show that the tides in the peripheral bays are similar to the tides in the rest of the estuary. There is a slight damping of the M2 wave in Baker Bay and slight amplification in Youngs Bay, Cathlamet Bay, and Grays Bay; the greatest M2 amplitudes in the entire estuary are found at Knappton and Youngs Bay (~2 cm greater than at Tongue Pt.), and the M2 amplitude at Knappa is about 2 cm greater than that at Altoona. Information concerning tidal processes in the peripheral bays is found in the Integration Report.

#### Non-Linear Effects

The non-linearity of tides in shallow estuaries manifests itself in at least three other ways, in addition to the transfer of energy from the  $O(1)$  tidal circulation to the various  $O(\epsilon)$  circulation modes (Section 1.1). First, the increase in riverflow during a freshet has a dramatic effect on the damping of the tidal wave in the tidal-fluvial portion of the system above Altoona (Figures 13 to 15). Second, the residual flow due to river inflow causes a marked flood-ebb asymmetry in the currents and the degree of mixing. Much more energy is dissipated by bottom friction and much more mixing occurs during the ebb; this difference is reflected in the velocity and salinity profiles and vertical mixing processes (Section 3.2). Third, we can hypothesize that the tendency for the tides to be amplified slightly in most of the peripheral bays may be the result of the lesser freshwater flow velocities, which would reduce the bottom friction there.

#### The Diurnal Constituents

The behavior of the diurnal constituents is different from that of M2. The ratio of semidiurnal constituents to diurnal constituents  $\frac{(M2+S2+N2)}{(O1+K1+P1)}$  decreases sharply from the entrance to Ft. Stevens and more slowly from Ft. Stevens to Beaver (Table 1); it then increases again at Columbia City. The only diurnal constituent that increases in amplitude in the lower estuary is the largest, K1. The K1 and O1 phases do not vary linearly with river mile; the waves propagate much more quickly below Tongue Pt. than above, and K1 propagates more quickly than O1. The much faster propagation of the diurnal wave in the

estuary proper suggests a partial reflection of the diurnal wave, associated with the funnel shape of the channel upriver of Astoria. We do not presently understand in detail why the diurnal wave behaves differently than the semidiurnal wave.

### The Tidal Overtones

The behavior of the tidal overtones also differs from that of the the semidiurnal constituents. The amplitudes of M4 (the first overtide of M2) and MK3 (an overtide of M2 and K1) are both small and variable in the lower estuary below Tongue Pt. (Table 1). Both strongly increase relative to M2 upriver from Tongue Pt. The irregular phase progression of the overtones below Tongue Pt. suggests that they are too small in this reach for their characteristics to be reliably determined by harmonic analysis. From Tongue Pt. upriver, the phase progression of M4 is quite uniform. These observations are consistent with the idea that the higher harmonics as measured below Tongue Pt. are in part those produced in the ocean. The higher harmonics observed in the tidal-fluvial part of the system are those of the non-linearly driven  $O(\epsilon)$  circulation.

### 3.1.2 Factors Influencing the Tidal Range and the Times of High and Low Water

The harmonic analysis results discussed in Section 3.1.1 are based on evenly-spaced-in-time (hourly) observations. The mariner and marine manager are commonly more interested in the traditional tidal parameters such as tidal range (distance between tidal extremes) and high and low-water intervals (time of high or low water at a station) that appear in tide tables. Since tidal extremes only occasionally coincide with evenly spaced observations, NOS has developed harmonic constant reduction methods to calculate the traditional tidal parameters from harmonic constants (USCGS 1952). A computer program based on this publication was developed to calculate the traditional tidal properties (Section 2.3).

Selected tidal parameters are shown as a function of river mile in Table 2. The mean tidal range (Mean High Water-Mean Low Water (MHW-MLW)) at Tongue Pt. is about 2.03 m, the diurnal range (Mean Higher High Water- Mean Lower Low Water (MHHW-MLLW)) is about 2.62 m, and the spring range is about 2.44 m. There are three principal factors that influence the tidal range in a system with tides like those in the Columbia River Estuary (Marmer 1951). They are the phase of the moon (neap-spring effect), the declination of the moon above the equator as it passes over the longitude of the tide station (equatorial-versus-tropic tides; the diurnal inequality), and the distance of the moon from the earth (the apogee-perigee effect). A spring tide occurs when M2 and S2 are in phase, and a lunar apogean tide occurs when M2 and N2 are in phase. The spring-neap effect is  $\sim 1.3$  times as important in the Columbia River Estuary as the apogee-perigee effect. The more extreme tides occur when several of these effects reinforce one another; for example, the higher of the two tides on the day of the spring tide each month will have a range larger than the spring range of 2.44 m, because of the effect of the diurnal tide or diurnal inequality. A really large higher high water occurs on those spring tides when the diurnal inequality is at its maximum, that is, when the moon is at its greatest distance from the equator; M2, S2, K1 and O1 are then in phase. The most extreme tide would occur when all the major constituents affecting the range of the tide were all in phase. The tidal range at Tongue Pt. would then be  $2x(M2+S2+N2+K1+O1) = \sim 4.0$  m. Such a tide is a rare occurrence. Model results and data (Figures 17a and b) show that the ratios of spring and apogean tidal ranges to mean tidal range decrease with river mile (Table 2), because the ratios of N2 and S2 to M2 decrease with river mile (Table 1). This is a function of system energetics (Section 3.4). We will henceforth refer to tides of large range as "spring tides" and those of small range as "neap tides", regardless of the factors acting to produce

Figure 17. Model results for (a) M2 + S2 + N2, and (b) M2 + S2 + N2 and 146 kcfs (4139 m<sup>3</sup>/s) riverflow symbols as in Figure 13. Note difference in vertical scale

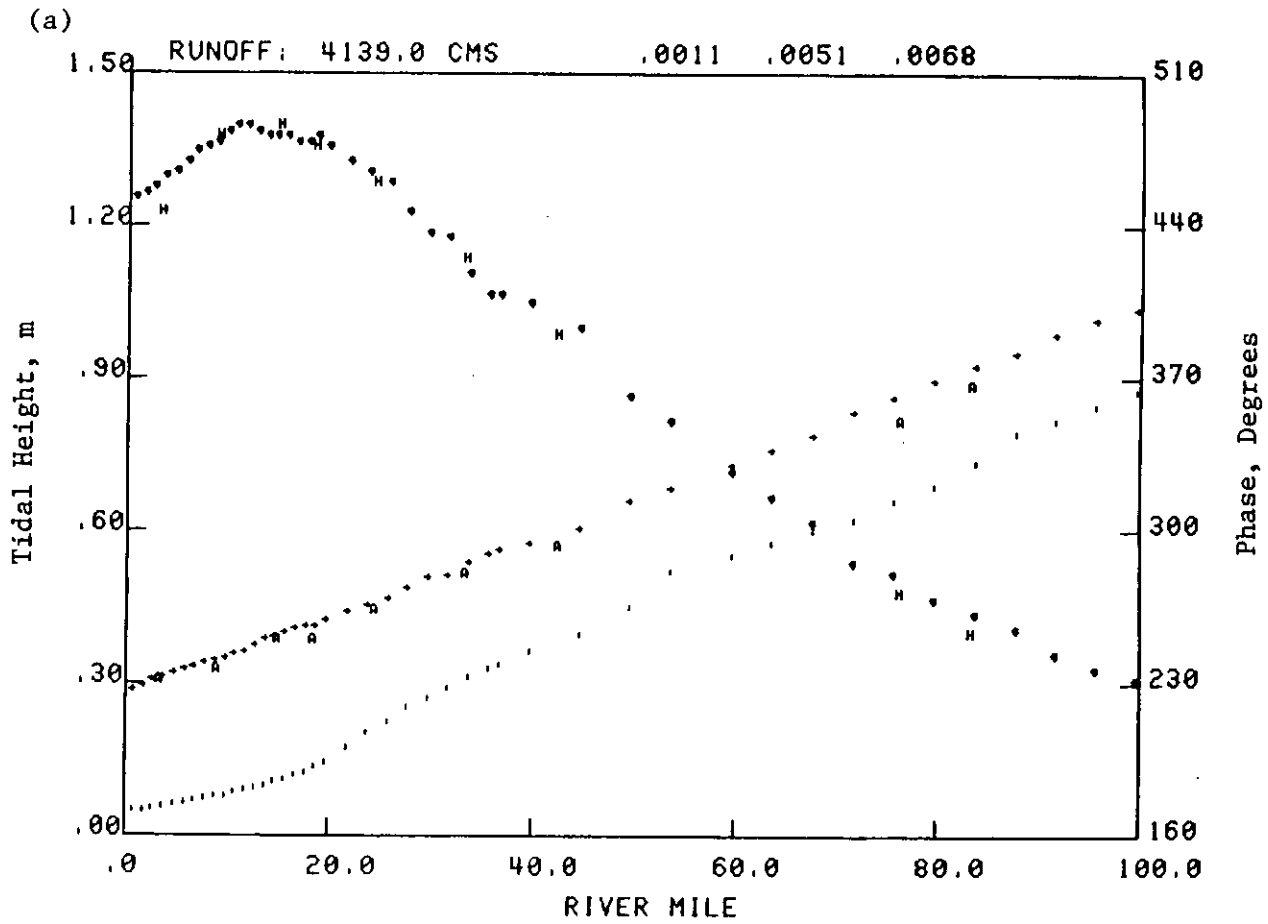


Figure 17. (continued).

(b)

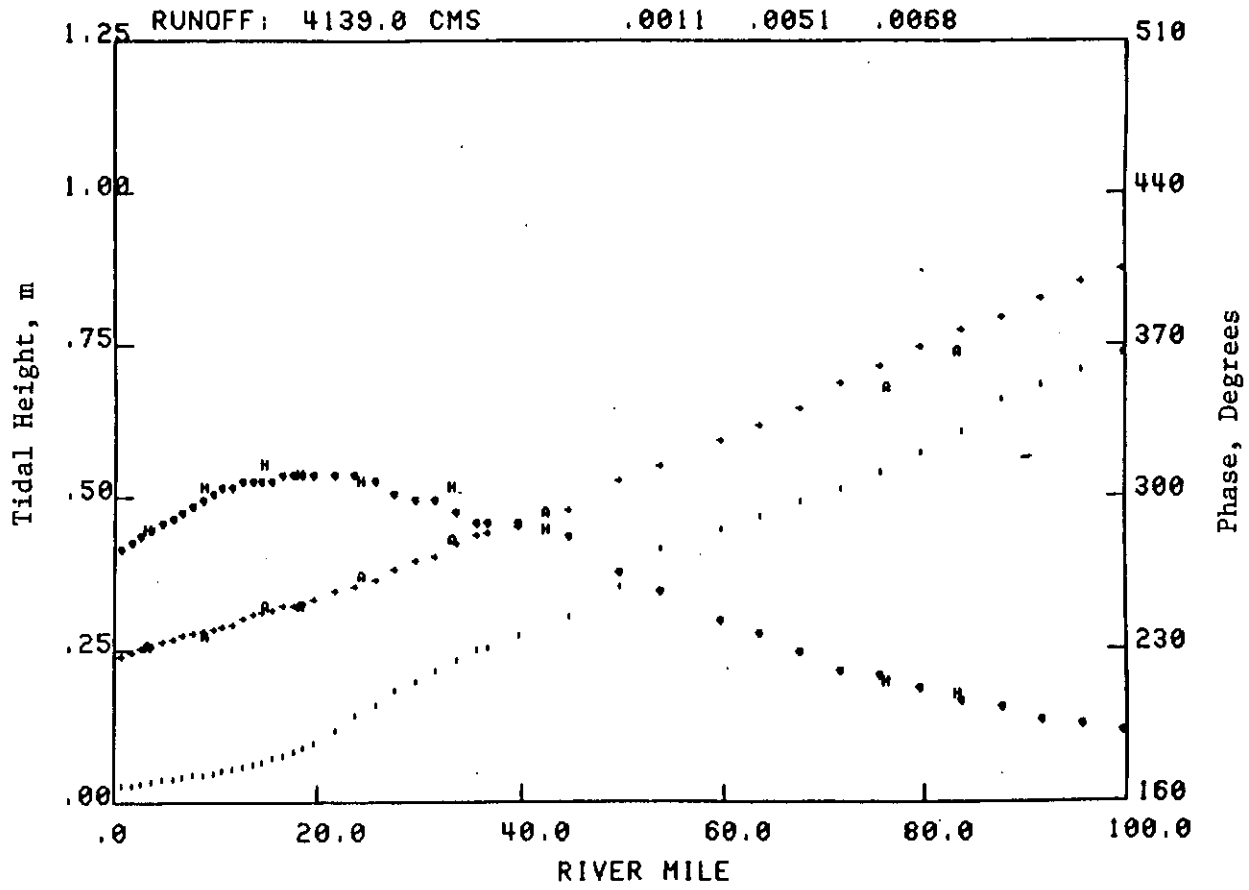


Table 2. Tidal properties as a function of river mile

Length of Record	Station	RM	<u>Ranges, m</u>								<u>Greenwich</u>		<u>Inequalities, m</u>	
			mean/ greater diurnal	spring/ neap	perigean/ apogean	greater tropic/ lesser tropic	HW Interval	LW Interval	Diurnal HW Inequality	Diurnal LW Inequality				
7 mos.	Jetty A	3.0	1.81	2.40	2.23	1.32	2.18	1.52	2.65	0.88	7.94	1.57	.21	.39
7 mos.	Ft. Stevens	8.3	2.01	2.62	2.47	1.49	2.42	1.71	2.85	1.07	8.22	1.81	.22	.39
1 yr.	Tongue Pt.	17.6	2.03	2.62	2.44	1.57	2.42	1.74	2.81	1.11	8.58	2.46	.21	.37
7 mos.	Altoona	24.4	1.93	2.46	2.28	1.52	2.28	1.66	.62	1.06	8.96	3.05	.20	.33
1 yr.	Wauna	42.0	1.59	2.01	1.86	1.27	1.89	1.38	2.07	0.86	9.72	4.38	.17	.24
7 mos.	Beaver	53.3	1.26	1.60	1.49	1.01	1.49	1.10	1.60	0.63	10.24	5.28	.15	.18
1 yr.	Columbia City	83.0	.51	.66	.59	.41	.61	.43	.74	.36	11.46	7.53	.11	.04

the observed range.

The high and low water intervals in Table 2 and Figure 18 give the number of hours after the passage of the moon over Greenwich that high and low waters occur at each station. The observed times of high and low water differ from those values that could be determined solely from the phase of the M2 tide, principally because of the distorting effect of the  $O(\epsilon)$  tidal overtones. A wave is considered to be in shallow water when the depth is less than half the wavelength ( $\sim 300$  km for the tidal wave). The wave speed for shallow water waves is dependent on the depth of the water (Section 1.3.1). The average depth of the estuary is only  $\sim 6$  to 12 m, and the change in depth of the estuary between high water and low water ( $\sim 2$  m) is a significant fraction of the average depth. Thus, the wave is in very shallow water and the peak of the wave travels somewhat faster than the trough of the wave. It can be seen in Figure 18 that considerable distortion of the wave occurs as it moves upstream. The time of low water approaches the time of high water, and the rise of the tide is much more rapid than the subsequent fall. In extreme situations the result is a tidal bore (e.g. on the Amazon River). This distortion appears in the harmonic analysis as the presence of the tidal overtones, as shown in Figures 12a and b.

### 3.1.3 Tidal Inundation Time

The tidal inundation time curve for Tongue Pt. (based on 21 years of data, as tabulated in Appendix D by NOS; personal communication, Tidal Datums Branch) is shown in Figure 19. This curve may be compared to those for other west coast tide stations (NOAA 1980). The three basic factors governing inundation time curves are the tidal characteristics, the freshwater inflow, and atmospheric effects (both local and over the continental shelf). As discussed in Section 3.1.1, the tides are somewhat more diurnal near the mouth than elsewhere in the estuary, and the amplitude of the M2 tide drops almost linearly with river mile, above Tongue Pt. The change in surface level associated with changes in riverflow are relatively minor in the estuary but increase rapidly upriver (Section 3.3).

Chelton and Davis (1982) have estimated that about 3.4 cm of the total 9.2 cm standard deviation in the monthly MWL (Mean Water Level) at Tongue Pt. is due to riverflow; the rest is due to the inverse barometer effect and seasonal shifts in coastal circulation patterns (Section 1.3). Changes in riverflow totally dominate the inundation time curve at upriver stations during high flow periods; changes in stage of more than 3 m occur during freshets of even moderate size.

It should also be noted that non-linear effects increase in shallow water, and inundation time curves over tidal flats may differ substantially from those in deeper water. Chinook is the only tidal station situated in shallow water, and its inundation time curve is somewhat anomalous. This may be due to ebb-flood asymmetries associated with the multiple mouths of Baker Bay, or it may be the result of shallow water effects.

## 3.2 CURRENTS

### 3.2.1 Observed Spatial Distribution

The M2 current phase and amplitude are shown as a function of river mile in Figures 20 and 21. These results may be compared to the model results in Figures 13 to 15. Systematic variations in phase and amplitude occur both with river mile and depth. The systematic vertical variations are a result of topography and stratified boundary layer effects, as discussed in Section 3.2.2. The strong effect of the sills between RM-6 and RM-10 in both channels is also evident in the salinity distribution (Section 3.5).

Figure 18. Greenwich intervals (times of high and low water) vs. river mile.

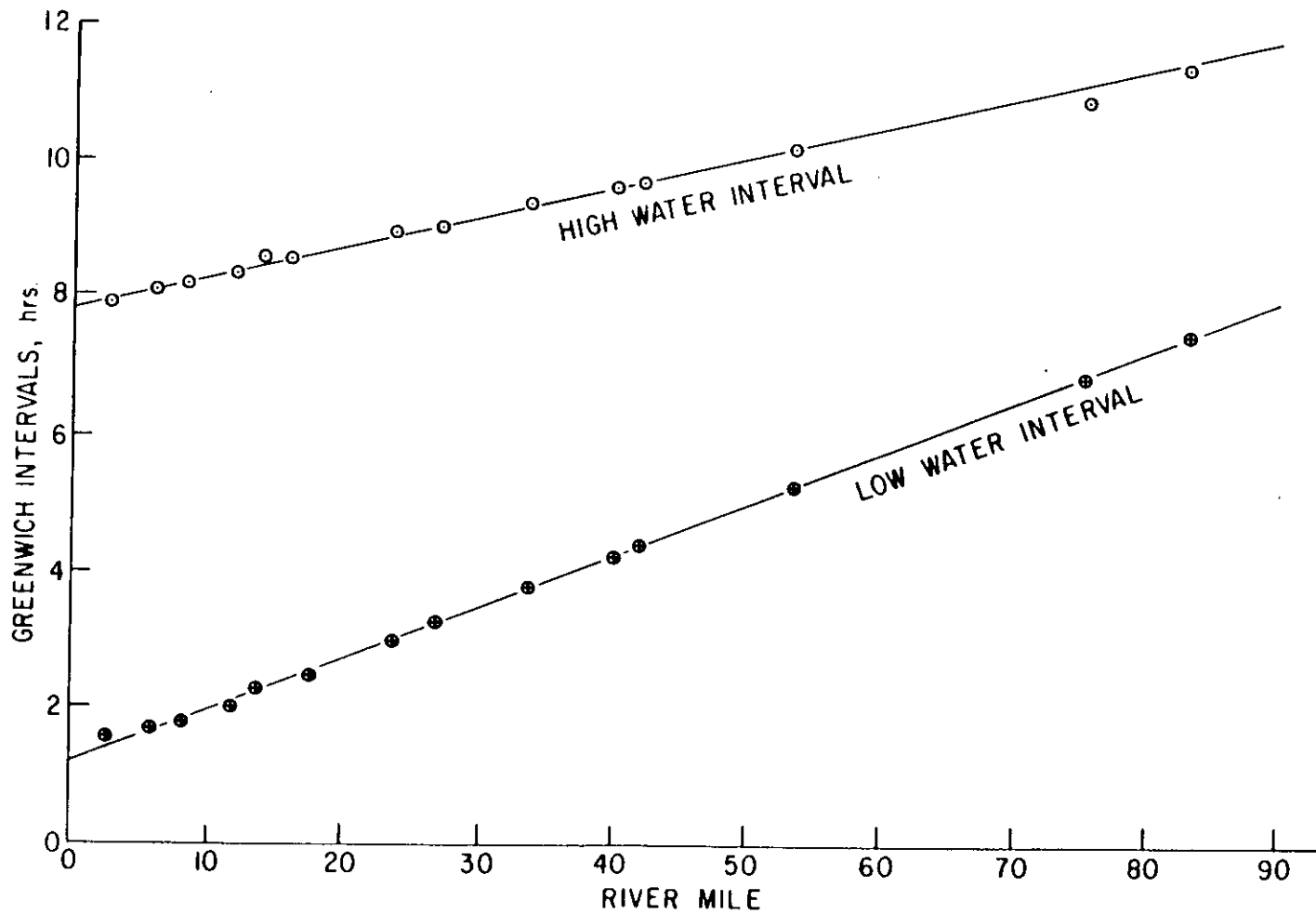




Figure 19. Tidal inundation time versus depth for NOS Tongue Pt. reference station, 1940-1961, referred to MLLW for the 1949-1959 epoch. An inundation time of 20% indicates that the inter-tidal land of the indicated level is inundated 20% of the time.

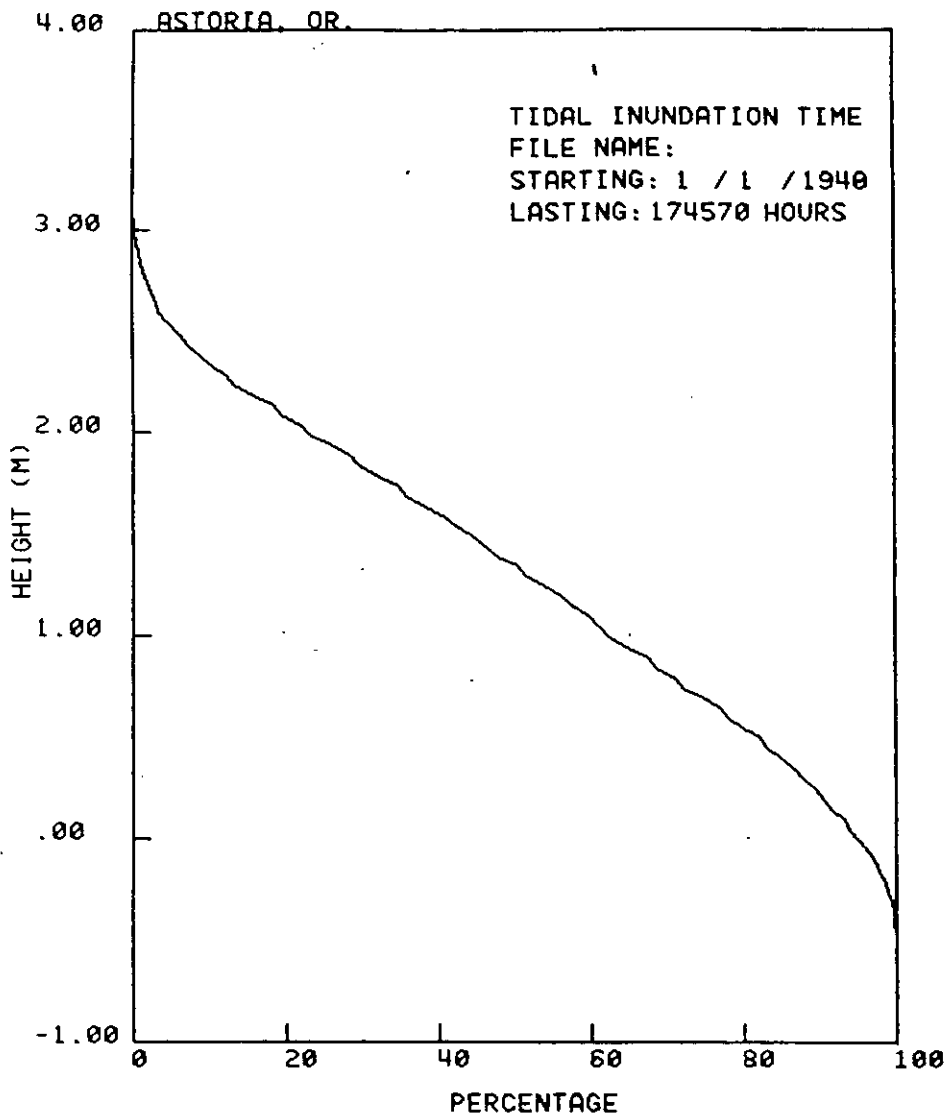


Figure 20. Phase in degrees (a) and amplitude in cm/s (b) of M2 tidal currents in the South Channel, and (c) and (d) in the North Channel, based on all available current meter data. Vertical variations in phase and amplitude are greatest in deeper water, near the entrance, where stratification effects are most important. The shallow bars in both channels at Desdemona Sands greatly reduce these vertical variations

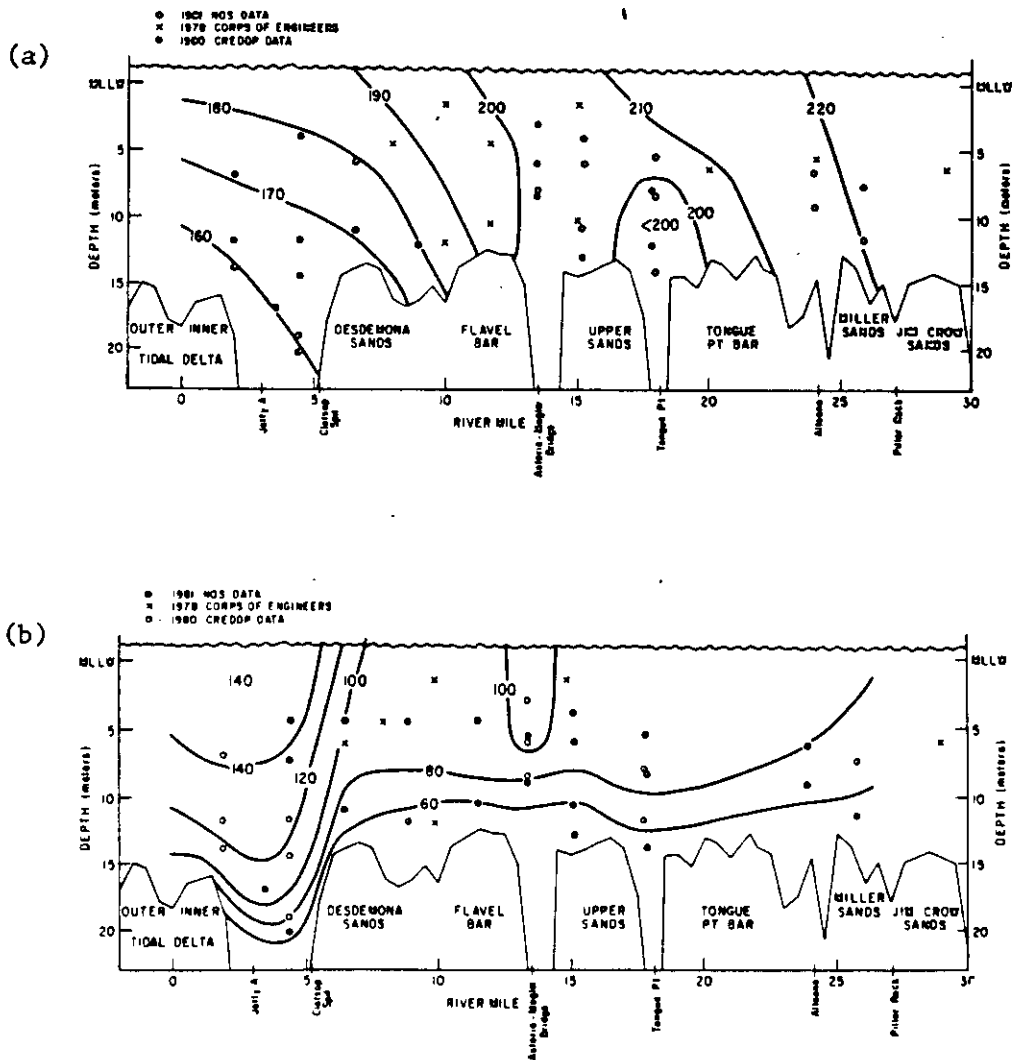


Figure 20. (continued).

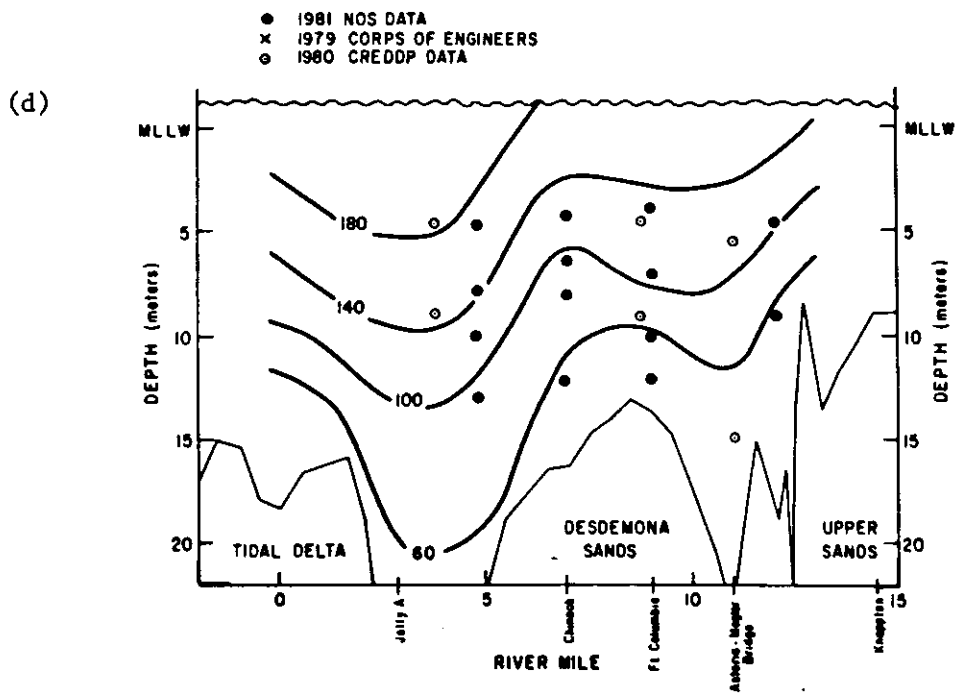
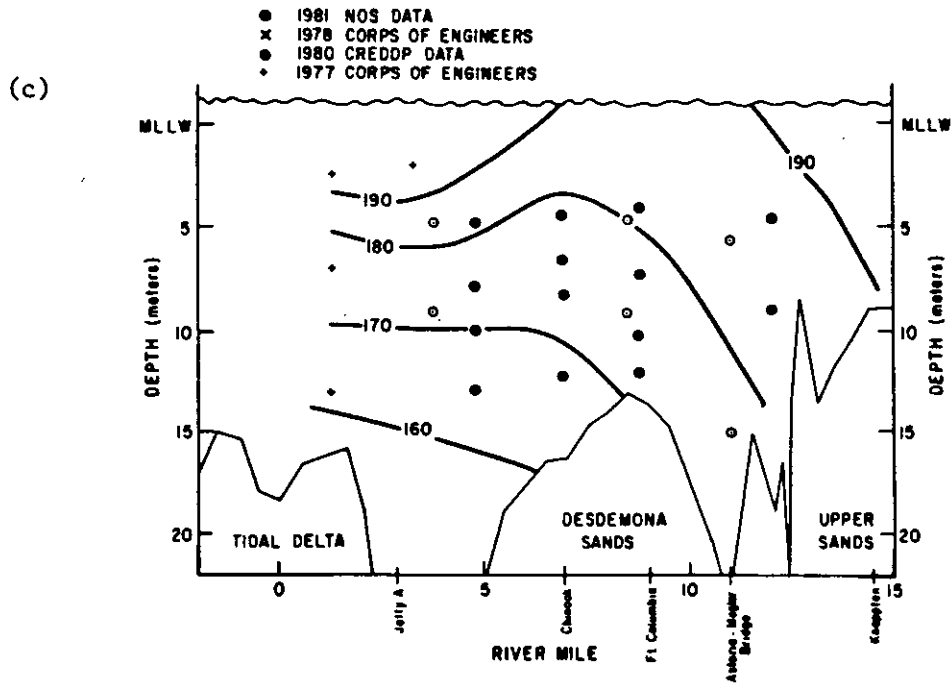
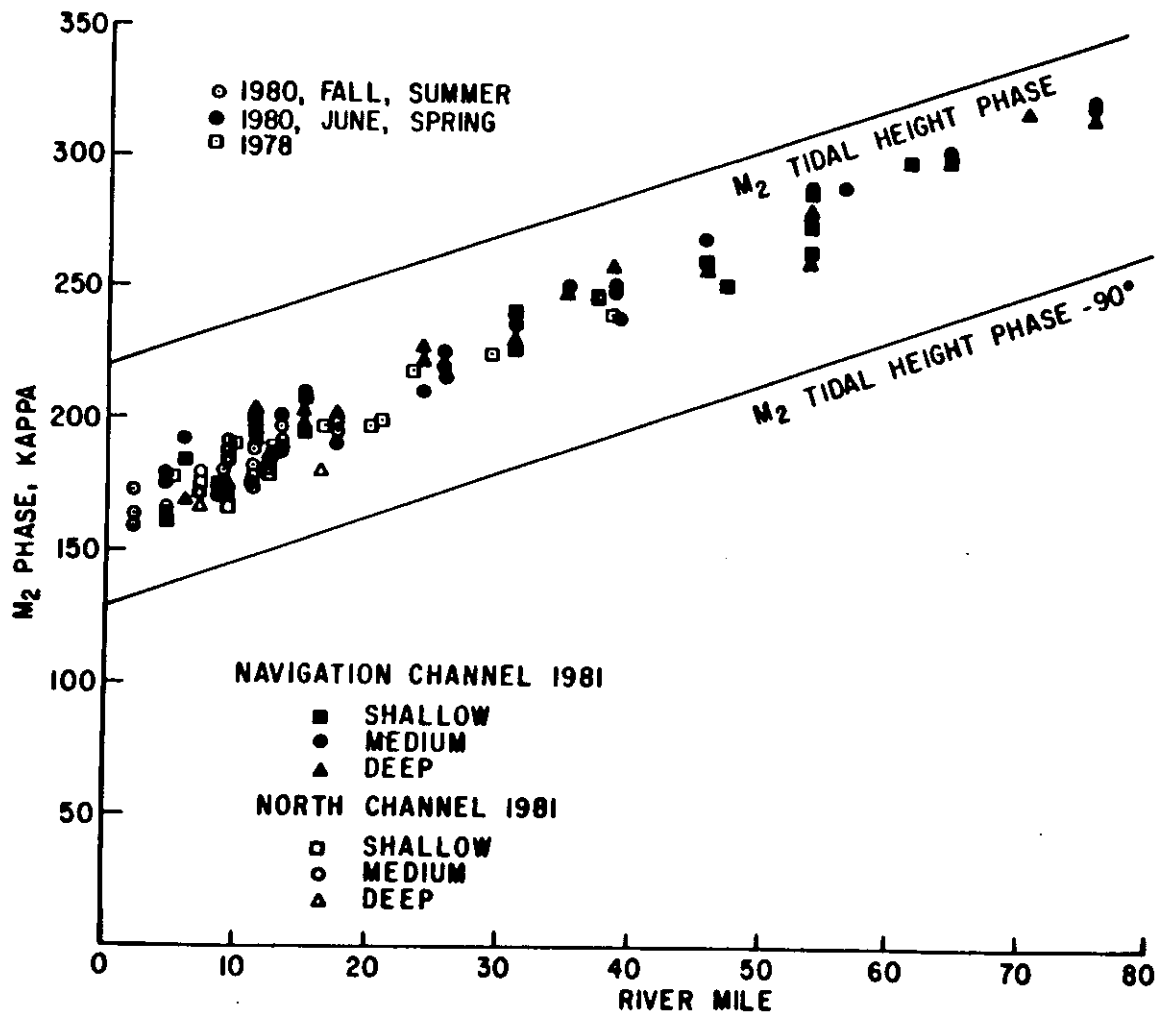


Figure 21. Phase of the  $M_2$  tidal currents as a function of river mile in the North and South (navigation) channels, based on all available current meter data. Systematic variations of phase with depth occur, which are related to stratification and topographic effects.



The M2 current phase lags the tidal height phase by about 50 to 60 deg at the mouth and by about 45 to 50 deg upriver (Figures 20a and 21). The current phase is intermediate between that for a progressive wave (tides and flow in phase) and a standing wave (tides and flow 90 deg out of phase). These phase differences can be converted to time differences by use of the conversion factor 29 deg/hour for the M2 tide. The currents become more closely in phase with the heights (more progressive) above Tongue Pt.; this is a result of the strong friction in the system. The distribution of flow in the vertical is influenced by local topographic effects. The tidal transport, as predicted by the one-dimensional, tidal model, is far more regular (Section 3.3). A strong decrease in currents (and tidal transport) upriver occurs, because most of the tidal prism is below Tongue Pt., where both the tidal range and surface area are large. Changes in riverflow strongly affect tidal current amplitude above Tongue Pt. For that reason, results are not shown for upriver areas in Figure 20b. Tidal currents are much stronger in the North Channel (Figure 20d) than in the South Channel (Figure 20b); most of the tidal flow below the Astoria-Megler Bridge is in the North Channel, and most of the riverflow is in the South Channel.

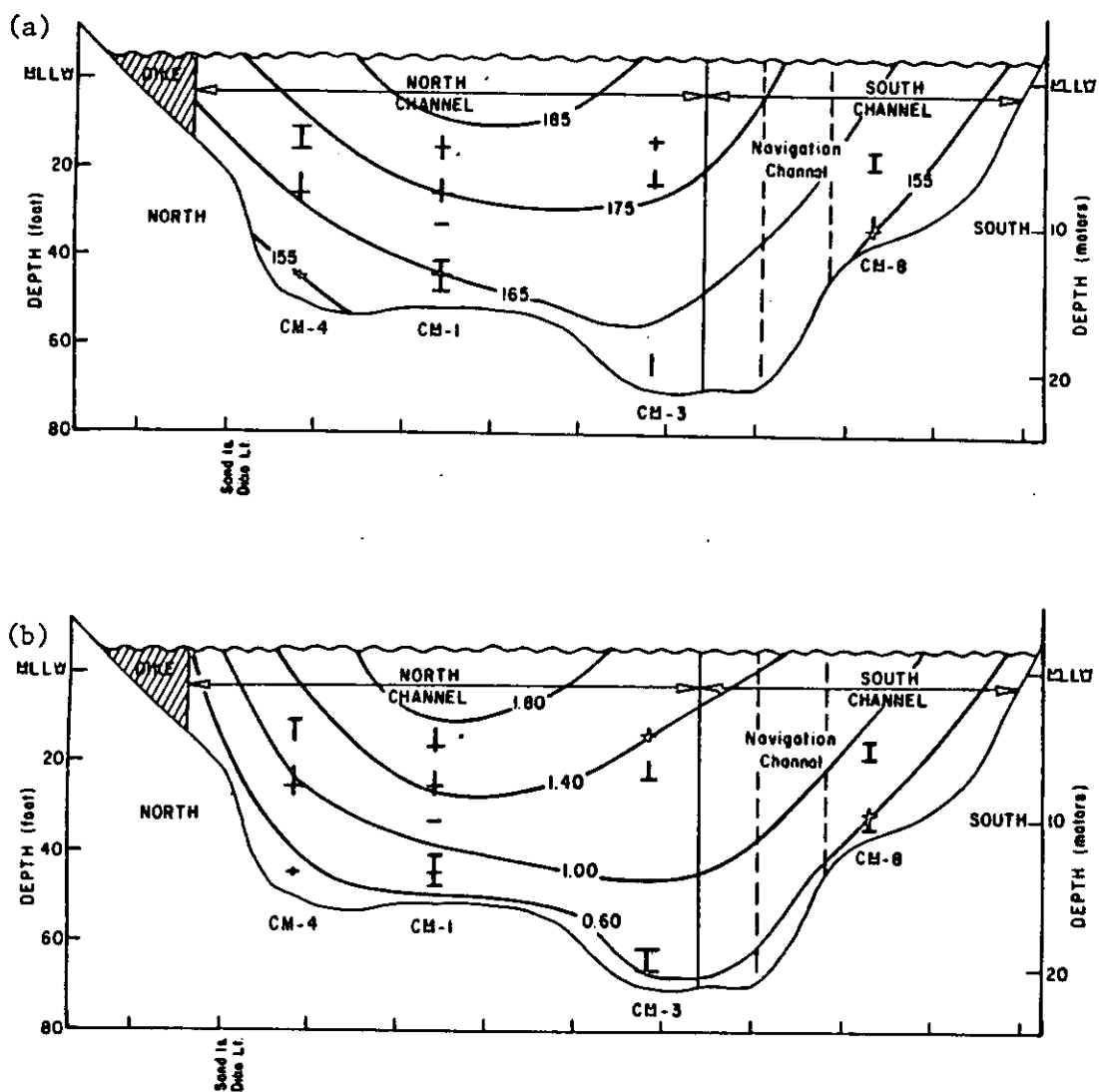
Figures 20 and 21 show that vertical variations in the phase and amplitude of the current are substantial, and that this vertical structure varies in the along-channel direction. Examination of tidal currents at the Clatsop Spit-Sand Island cross-section show that cross-channel variations are also important (Figures 22a and 22b). The M2 amplitude is strongest and the phase latest at the surface in the North Channel. The top to bottom phase difference is greater than 30 deg (~1 hour) and the top to bottom shear in the tidal currents is more than 1.2 m/s. The vertical shear and phase difference in the  $O(1)$  tidal circulation that is under consideration here should not be confused with the vertical variation in the  $O(\epsilon)$  steady flow.

### 3.2.2 Vertical Structure of the Tidal Flow -- Boundary Layer and Density Effects

We investigate in this subsection the factors that maintain the vertical structure of the tidal flow, and that cause the variations of this vertical structure along and across the channel (Figures 20 to 22). Let us assume that the entire flow is a stratified boundary layer; that is, that the effects of bottom friction are felt throughout the flow (high stratification sometimes isolates the surface layer from the effects of bottom friction, but this highly-stratified case is more complex than the boundary layer case, so we neglect it for the present). The vertical structure of a boundary layer flow is determined by the stratification, the surface slope, the baroclinic pressure gradient, bottom friction (boundary shear stress), and channel topography. Most of these factors vary in time as well as space, so ebb-flood differences must be considered. Since the mean flow is essentially the difference between the  $O(1)$  ebb and flood tidal flows, we will find that the ebb-to-flood asymmetry determines the vertical structure of the  $O(\epsilon)$  mean flow.

Let us first consider the structure of a neutral boundary layer flow (i.e. in the absence of stratification and baroclinic pressure gradient). Since the velocity profile in a neutral (unstratified) bottom boundary layer is nearly logarithmic even in a time-dependent flow (Section 1.4 and Lavelle and Mojfield 1983), most of the vertical shear and phase differences in a neutral boundary layer occur very close to the seabed (i.e. in the bottom meter). This shear is the result of deceleration of flow near the bed by bottom friction. The phase differences arise in the time-dependent flow, because of the shear. For example, at the end of flood or ebb tide, the surface slope reverses some time before the flow changes direction, because the flow must first be decelerated before it can change direction. The parts of the flow with greater inertia (greater velocity) take longer to decelerate. Reversal, therefore, occurs last in the parts of the flow with the greatest velocity (normally near the surface). The neutral

Figure 22. Phase in degrees (a) and amplitude in m/s (b) of M2 tidal currents at Clatsop spit at ~RM-5. Tidal currents are strongest in the North Channel.



boundary layer is an adequate model of the structure of the tidal flow in the tidal-fluvial areas, where salinity intrusion is not found, but this model can not explain the magnitude and location of the shear and phase differences seen at the Clatsop Spit-Sand Island Section (Figures 22a and b) and elsewhere in the estuary.

To explain the magnitude of the shear and phase differences seen in the lower estuary, stratification, the baroclinic pressure gradient and the mean flow must all be considered. An ebb velocity profile in the lower estuary (Figures 23a and b) shows more shear high in the water column than the flood profile (Figures 24a and b), because the vertical structure of the total pressure gradient and the stratification effect on vertical mixing act together to allow large velocities to develop near the surface and, thus, to allow a large shear in the velocity structure. That is, on ebb (at least until after the time of peak ebb), the barotropic pressure gradient caused by the surface slope (independent of depth) accelerates the entire flow seaward, but is counteracted at depth by the baroclinic pressure gradient caused by the horizontal salinity gradient. Near-bottom velocities tend to be small and, late in the ebb, the total pressure gradient may actually change sign with depth; this pushes the top and bottom of the water column in opposite directions. Furthermore, the stratification allows layers of fluid to slide over each other more easily, because it inhibits vertical momentum transfer, as was discussed in Section 1.4. Thus, stratification also favors the development of large velocities near the surface.

An extreme example of shear in the tidal flow can occur at the end of ebb near the entrance, after flood has begun at the bottom. A thin, near-surface jet of low salinity water continues to flow rapidly outward over the incoming sea water (Figures 25a and b). The stratification isolates the surface jet from loss of momentum downward, and the stratification is strengthened by the shear and the strong horizontal salinity gradient. Surface reversal of the flow may be delayed as much as 2 hours after onset of flood at the bottom and can only occur after the adverse pressure gradient has decelerated the near-surface flow (Figure 26). Shears of up to 2 m/s can occur during the neap tide, when stratification is greatest, and the phenomenon is most strongly-developed.

On the flood in the lower estuary (at least until after peak flood), the surface slope and the baroclinic pressure gradient induced by the horizontal salinity gradient act in the same direction, and since the baroclinic pressure gradient increases with depth, the total, inward pressure gradient is largest near the bottom. Because vertical mixing is less, stratification is usually greater on flood than on ebb (except in the extreme ebb-flow case mentioned above). The stratification effect favors large flood velocities near the surface, but the pressure gradient favors large velocities near the bottom. The result is that shear is minimized and the velocity profile is typically much more uniform with depth than on the ebb. At the end of flood, vertical differences in inertia are small and the reversal in flow occurs nearly simultaneously at all depths (Figure 24b).

This discussion of boundary layer processes allows us to further interpret the spatial variations in the tidal flow in Figures 20 to 22. The shear and phase differences are largest in the lower estuary. This is the area where salinity intrusion is present on both flood and ebb and where tidal flows are strongest; the potential for developing large shears is greatest there. The largest shear and phase differences on the Clatsop Spit-Sand Island Section (Figures 22a and b) are found at the surface in the center of the section, where the inertia of the flow is greatest. It appears, however, that some of the spatial variations in structure of the tidal flow may be due to other causes. Bottom topography causes along-channel changes in the density structure (e.g. between RM-8 and RM-9 in both channels) that probably cause along-channel changes in velocity

Figure 23. (a) Salinity, temperature and sigma - t, and (b) speed and direction at station 5NB on ebb tide. The shear between 3.5m and the bottom is typical for ebb tide; note velocities in excess of 200cm/s near the surface

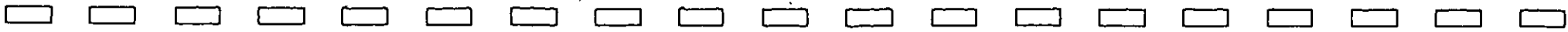
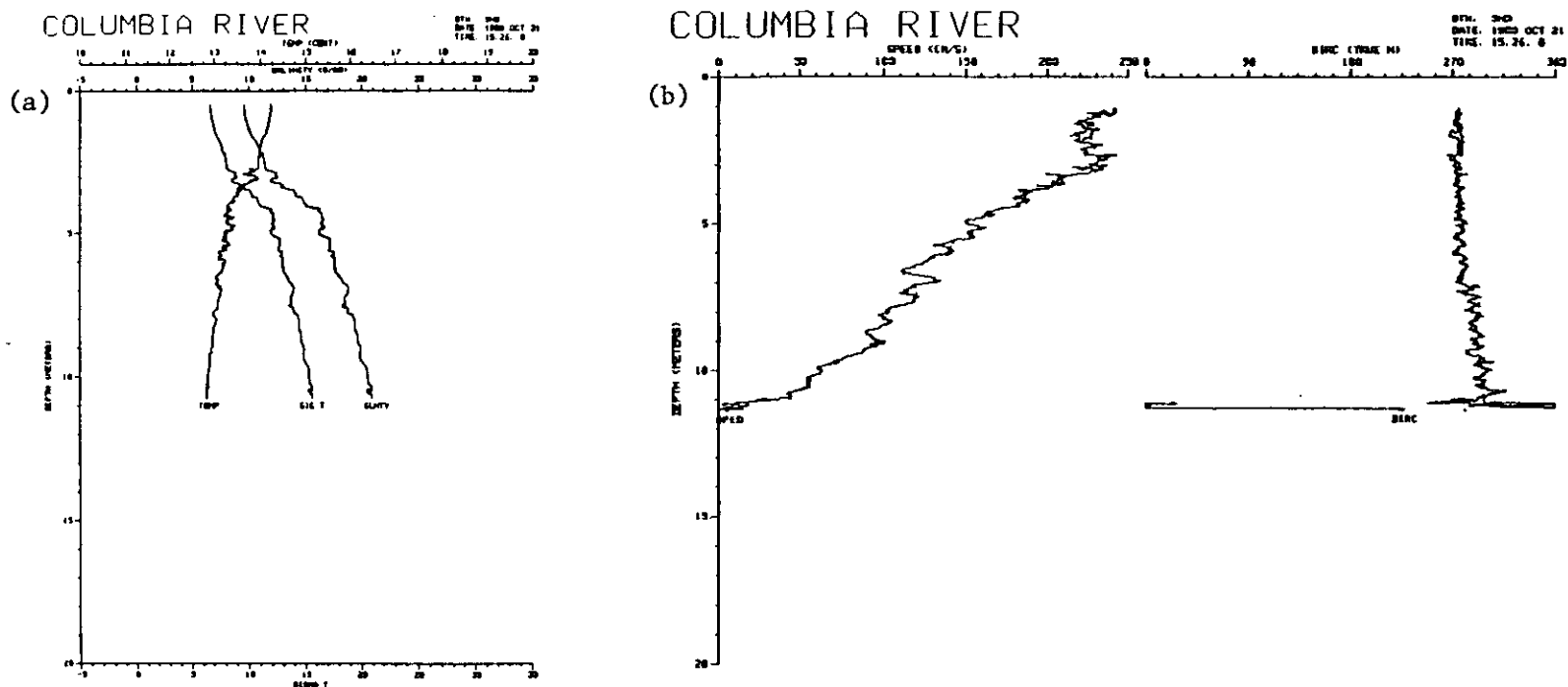




Figure 24. (a) Salinity, temperature and  $\sigma_{\theta}$  - t and (b) speed and direction at station 4NA on flood tide. The velocity profile is very uniform, and stratification is sharper than on ebb tide

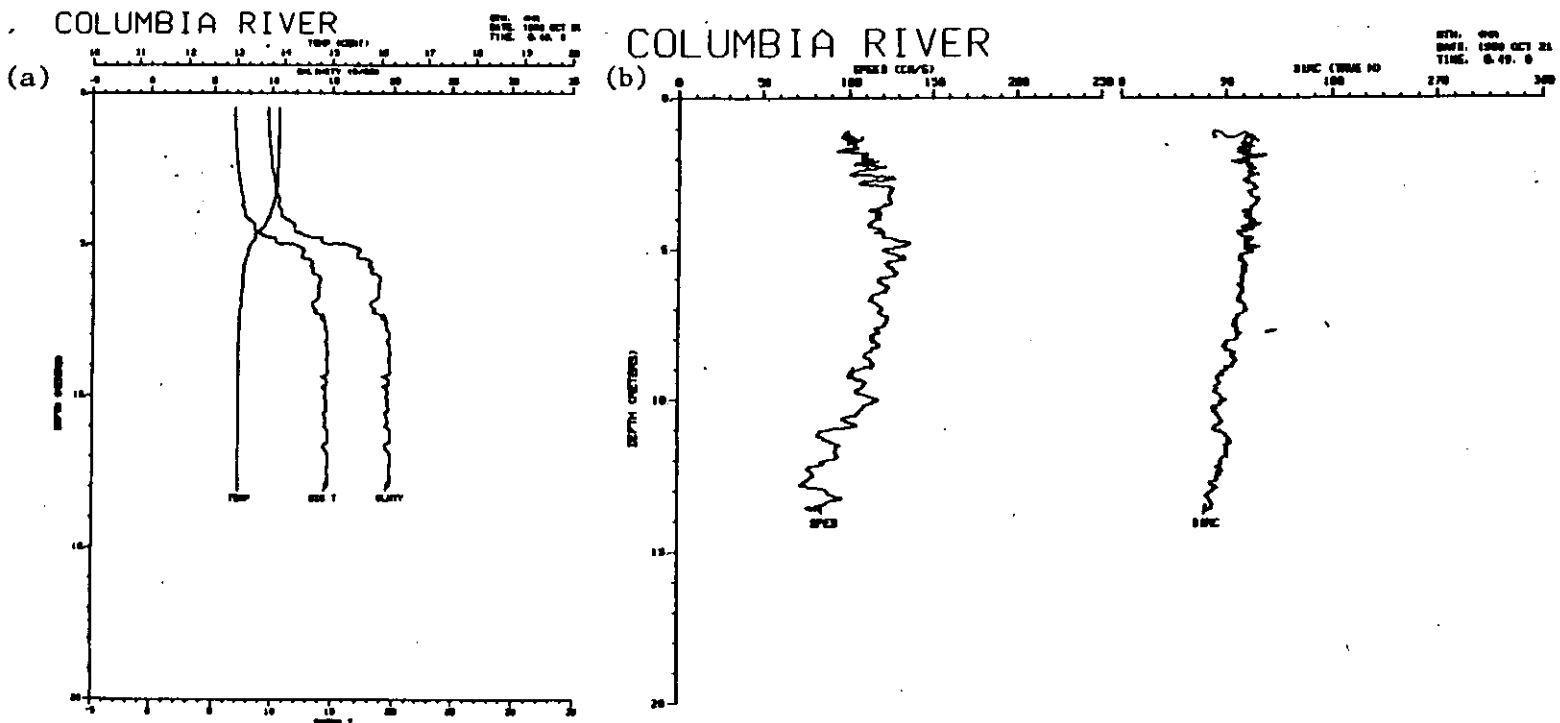


Figure 25. (a) Temperature, salinity and sigma - t, and (b) speed and direction at station 2N(RM-2) at the end of greater ebb. There is strong shear in the water column at mid-depth, but the the high energy level has destroyed the sharp layering evident at this station on flood. Speeds near the bottom are low, because the ebb has only just begun at this level. Note large speeds (~250 cm/s) above 3m. Near-surface velocities are noisy because of interference from boat hull.

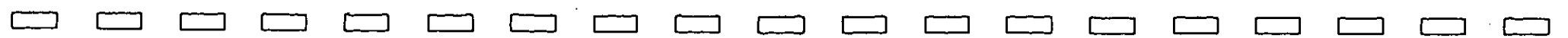
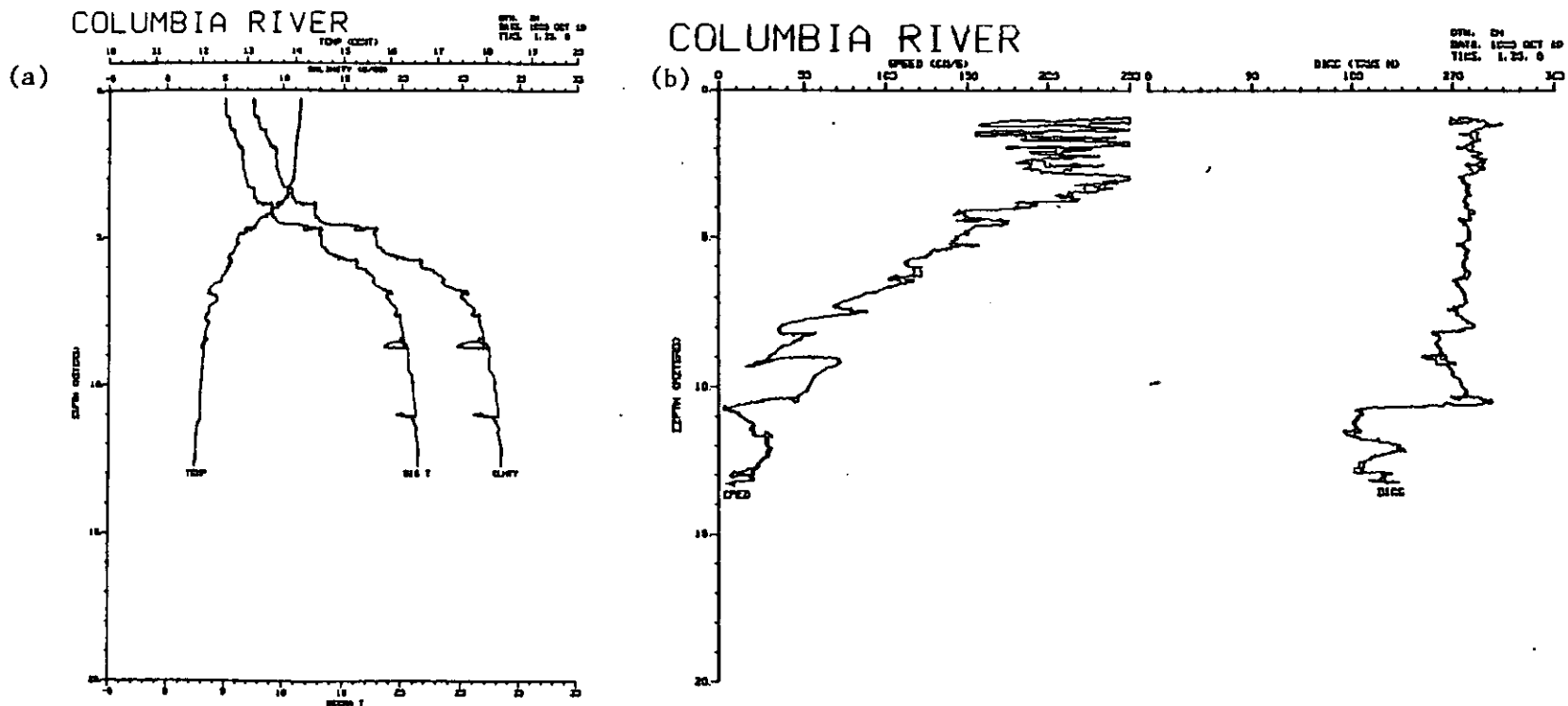
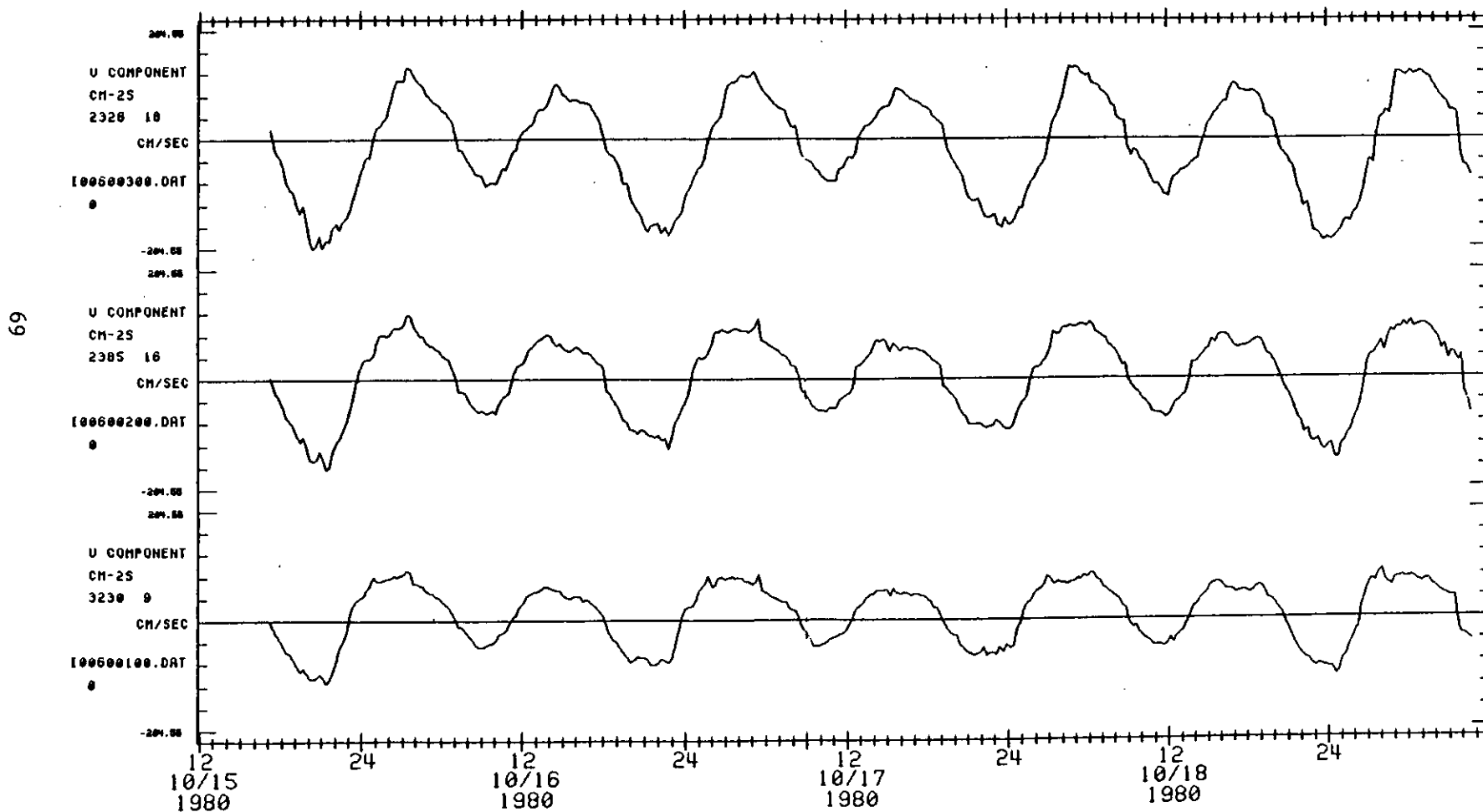


Figure 26. The joint effects of stratification and the horizontal density gradient at Station CM-25 (RM-2) on boundary layer flow; the reversal of flow at the end of ebb occurs several hours earlier at the bottom than at the surface (particularly at the end of the greater ebb), while the reversal of flow is almost simultaneous at all depths at the end of flood. Positive flows are inward (flood tide). The meters are located (bottom to top) at 14, 11 and 7m below MLLW.



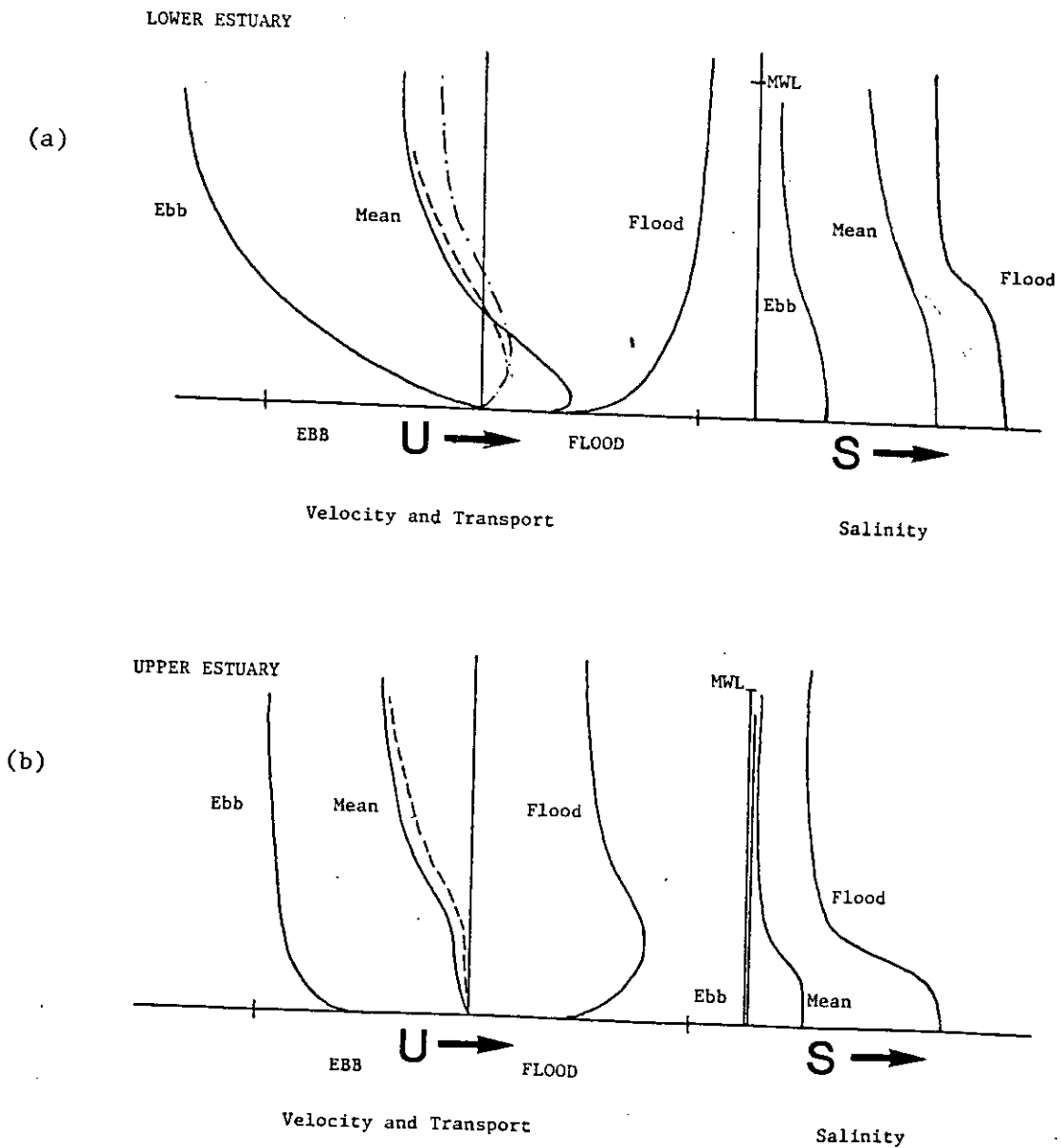


Figure 27. Typical profiles of flood, ebb and mean flows, and flood, ebb and mean salinities for (a) the lower estuary, and (b) the upper estuary. The dotted lines show the width-weighted flow and the effect of the Stokes drift. The Stokes drift is negligible in (b), and is not shown

profiles in this reach. Changes in channel cross-section also cause non-linear convective acceleration terms in the equation of motion to be locally large. We have argued in Section 1.1 that these non-linear effects are in general only an  $O(\epsilon)$  perturbation to the  $O(1)$  tidal flow. These non-linear terms are, however, almost certainly important in the vicinity of large changes in channel cross-section. It is probable, then, that changes in channel cross-section have an important influence in some areas, that can only be resolved by modeling studies, as discussed in Hamilton (1984).

### 3.2.3 Tidal Effects on The Mean Flow

#### Vertical Structure of the Mean Flow

The vertical structure of the mean flow can be understood most easily in terms of conservation of mass and the typical velocity and salinity profiles for the lower and upper estuary shown in Figure 27 a and b. These profiles are not observed data; they are intended, however, to be typical of profiles during periods of low to moderate riverflow and tidal range. Conservation of mass requires that the total ebb flow through any cross-section of the estuary be greater than the total flood flow by an amount that is equal to the riverflow plus the Stokes drift compensation flow. Thus in Figure 27a for the lower estuary, the vertical distribution of the  $O(\epsilon)$  mean flow is simply the difference between the flood and ebb flows. Because of the strongly-sheared ebb and the more uniform flood, the net flow near the bottom is inward. The dotted lines in Figure 27a show Eulerian transport per unit depth (i.e. velocity times channel width) and the sum of Eulerian and Lagrangian transport per unit depth and remind us that very little inward transport is associated with the inward mean flow at the bottom, because the channel is narrow there. The effect of the Stokes drift is felt mainly at the surface, where it is a substantial fraction of the total mean flow.

The situation in the upper estuary is somewhat different (Figure 27b). Salt is absent during much of the ebb, so the ebb velocity profile is that of a neutral boundary layer, and current reversal at the end of ebb is nearly simultaneous at all depths. The flood flow frequently exhibits a velocity maximum in the pycnocline, as the adverse surface slope (after peak flood) decelerates the flow, and the baroclinic pressure gradient continues to push the bottom flow upriver. The baroclinic pressure gradient and the sub-surface velocity maximum greatly delay current reversal at the end of flood near the bottom. The mean flow is outward at all depths, despite the intrusion of salinity on flood tide, because the shear on the ebb is not large enough to allow net upstream bottom flow. The dotted line again shows the Eulerian net transport per unit depth; since the Stokes drift is small, the Lagrangian transport is not noticeably different from the Eulerian transport.

#### Tidal Monthly Variations in the Mean Flow

We have already argued that the vertical distribution of the mean flow is determined by the tidal circulation; let us now consider neap-to-spring variations in the mean flow. During periods of low riverflow and large tidal range, a significant fraction of the total mean flow is Stokes drift compensation flow (Section 3.3.2). It should not be surprising, then, that neap-to-spring changes in mean flow are significant. The neap-to-spring changes in structure of the mean flow occur primarily as a result of the neap-to-spring changes in vertical mixing that change the vertical profile of the tidal flow; the neap-to-spring changes in Stokes drift compensation change only the size of the mean flow.

The increase in vertical mixing that accompanies the increase in tidal range on a spring tide decreases the stratification. Decreasing tidal ranges decrease vertical mixing and increase stratification. The relationship between vertical turbulent mixing and stratification is expressed in the Richardson number  $Ri_g$

(the ratio of density gradient to the square of the shear; Section 1.4). Whenever this ratio becomes large enough, vertical turbulent mixing effectively ceases. Reduction of turbulent mixing during periods of weaker tides allows large shears and increased baroclinic circulation to develop, which tend to further increase the stratification. On neap tides, particularly during the low-flow season, the system goes through a transition from relatively well-mixed to a highly stratified, two-layered state. The salinity intrusion length also increases greatly (Section 3.5). The increasing energy level in the estuary as the tidal range increases (after the neap) reverses this process: mixing increases and salinity intrusion length decreases.

The October 1980 period provides an excellent example of these tidal monthly changes. In a period of only 8 days, the tidal range increased from less than 2 m to more than 3.4 m. The density structure and vertical mixing processes were greatly altered as a result of the increased mixing (Section 3.5); the change in density structure, in turn, changed the structure of the mean flow. Observations (Table 3) show strong shear and upstream bottom flow on neap tide in two areas where strong horizontal salinity gradients occurred, near RM-2 (at CM-2S) and near Tongue Pt. (RM-18, CM-6S; Section 3.5). Upstream bottom flow was not continuous in the South Channel at all points between CM-2S and CM-6S; it was absent even at ~20m depth at CM-3S (at ~RM-5). The situation on spring tide was different (Table 3); top to bottom shear was greatly reduced at CM-6S, and the flow was outward at all depths. This was not the result of an increase in riverflow, which was nearly constant during the period, as shown by the data for CM-7N (Table 3). CM-7N was near the upstream limits of salinity intrusion on neap tide and well upstream of all salinity intrusion on spring tide; shear and mean flow were nearly constant there during the entire period.

Results from the two-dimensional, time-dependent, laterally averaged circulation model (described in detail in Hamilton 1984) support this picture. Figure 28a shows model results (mean salinity and velocity) for the Main Channel for the same neap tide period in October 1980. There is substantial upstream bottom flow at sections 2 and 3 in the Main Channel, but upstream bottom flow is totally absent at section 4 (~RM-6.2). The model then shows another zone of upstream bottom flow between sections 5 and 8 (~RM-8 to 15.5). The maximum horizontal salinity gradient is somewhat farther downstream than observed in the prototype (Section 3.5), so the upstream bottom flow does not quite extend to Tongue Pt. Spring tide model results show much less stratification and a shorter intrusion length of the 5 ppt salinity contour, particularly in the South Channel (Figures 28b), but the neap-spring differences in salinity intrusion are weaker than in the prototype (Section 3.5). Net upstream bottom flow on spring tide in both channels is discontinuous; it appears in three isolated cells in the Main Channel. This suggests the possibility that several turbidity maxima may occur in the estuary, each associated with an area of net upstream bottom flow that traps particulate matter.

There are two possible causes of this pattern of isolated pockets of net upstream bottom flow. The first is pockets of unusually saline, near-bottom water (Figures 28 a and b) which, in the model, are associated with the junction between the North and South Channels and which cause changes in sign of the salinity gradient (normally negative, since salinity usually decreases in the upstream direction). These pockets may, however, be artifacts of the modeling process. The second is redistribution of the mean flow in the vertical, due to changes in mixing resulting from along-channel changes in channel cross-section (as suggested in Ianniello 1977a, 1979, 1981; Simmons 1966). The effects seem to be interdependent; use of a uniform bottom topography in the circulation model for the Main Channel above ~RM-8 eliminates both the topographic effect and the reversed salinity gradient (Hamilton 1983). Ianniello (1979), has, on the basis of theoretical calculations for the constant density case, argued

Table 3. Mean flows, Columbia River Estuary, October 1980

<u>River Mile</u>	<u>Station</u>	<u>Depths, M on MLLW</u>	<u>Speed* cm/s</u>	<u>Direction</u>	<u>Comments</u>
(10/16 - 10/18 Neap Tide Period)					
2	CM-2S Bouy 10	7	8.2	Ebb	Minimum tidal range; greatest ebb runoff: 2.0m; strong inflow at bottom
		11	7.6	Flood	
		14	11.6	Flood	
18	CM-6S Tongue Pt.	8	25.1	Ebb	Salt-wedge effect at upper end of estuary
		12	6.7	Flood	
25.5	CM-7N Altoona	6.5	29.0	Ebb	Strong outflow, slight salinity intrusion on flood
		10.5	25.0	Ebb	
(10/21 - 10/23 Minimum Salinity Intrusion)					
2	CM-2S	7	5.8	Ebb	Large tidal range; greatest ebb runoff: 3.2m
		11	4.8	Flood	
		14	6.4	Flood	
18	CM-6S	8	29.0	Ebb	Upstream bottom flow absent, stratification reduced
		12	13.0	Ebb	
25.5	CM-7N	6.5	31.0	Ebb	No salinity
		10.5	20.0	Ebb	
(10/24 - 10/28 Spring Tide Period)					
2	CM-2S	7	11.0	Ebb	Maximum tidal range; greatest ebb runoff: 3.4 m; minimal upstream flow at the bottom
		11.0	5.0	Ebb	
		14.0	1.0	Flood	
18	CM-6S	8.0	30.0	Ebb	No upstream bottom flow; stratification reduced
		12.0	13.0	Ebb	
25.5	CM-7N	6.5	31.0	Ebb	Very slight salinity; intrusion
		10.5	28.0	Ebb	

Table 3. (continued)

<u>River Mile</u>	<u>Station</u>	<u>Depths, M on MLLW</u>	<u>Speed* cm/s</u>	<u>Direction</u>	<u>Comments</u>
(Means for 10-15 day deployment)					
2	CM-2S	7.0	10.0	Ebb	~11 days for all meters
		11.0	4.5	Flood	
		14.0	5.8	Flood	
18	CM-6S	8.0	29.0	Ebb	~10 days for both meters
		12.0	3.0	Ebb	
25.5	CM-7N	6.5	30.0	Ebb	~10 days for both meters
		10.5	26.0	Ebb	

\*Speeds have been calculated along the direction of the major axis of the  $M_2$  current.



Figure 28. Two-dimensional (laterally averaged) model predictions from Hamilton (1984) of mean salinity and currents in South Channel for (a), neap tide and (b), spring tide, October 1980, low-flow period.

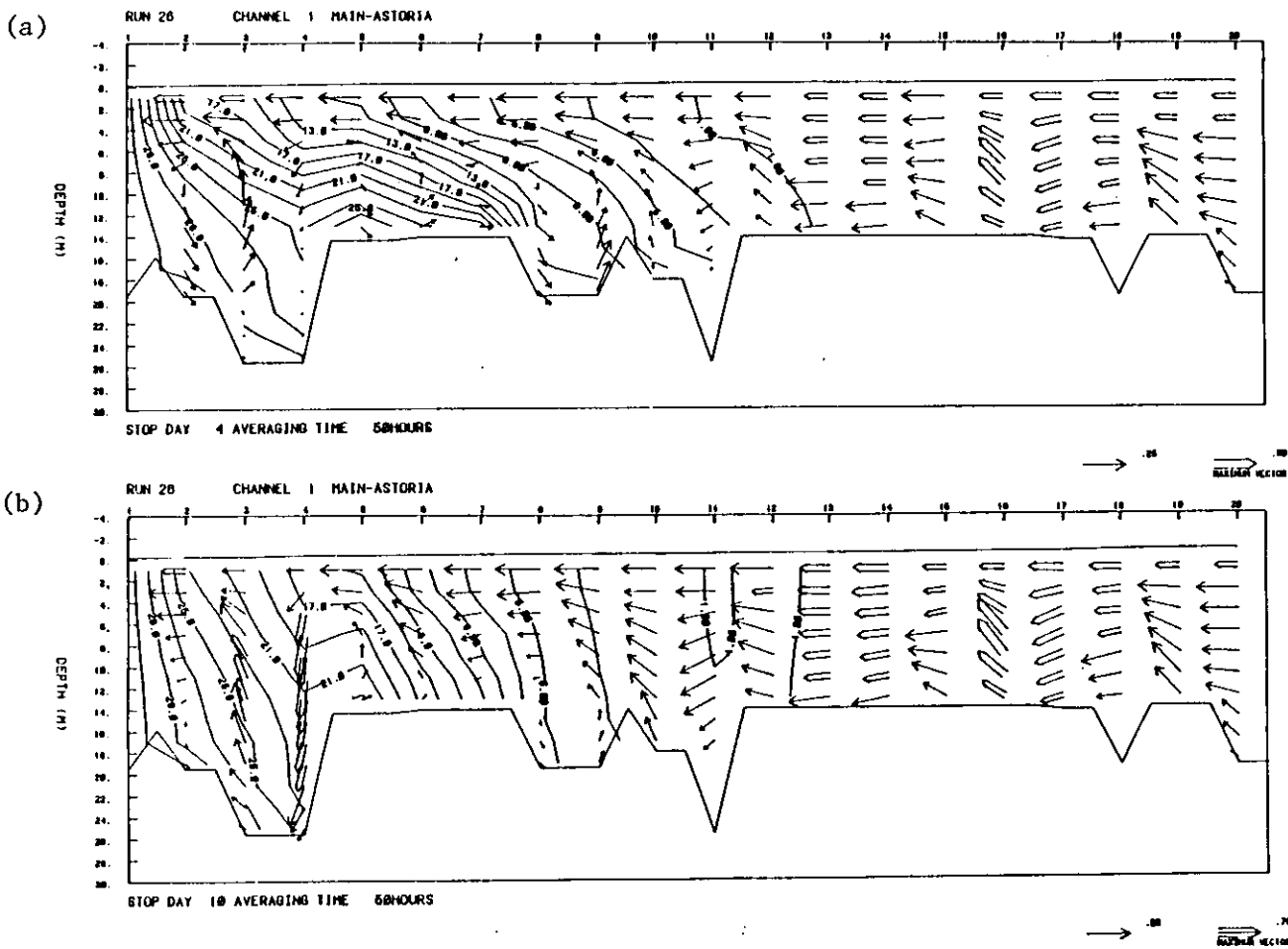
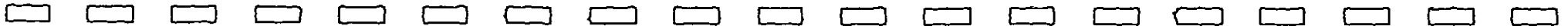
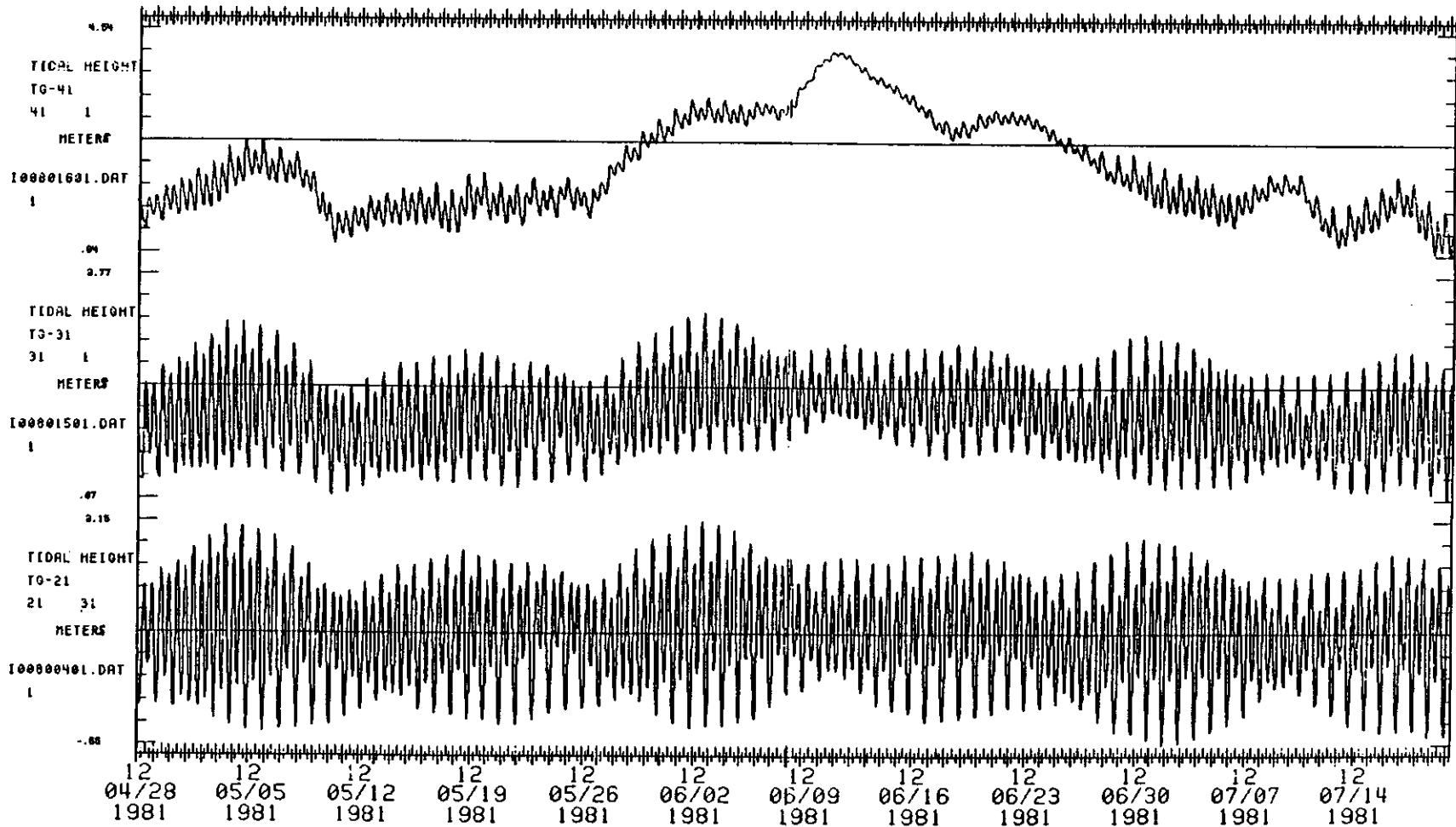


Figure 29. Tidal heights in m at (from bottom to top) Tongue Pt. (RM-18), Wauna (RM-42) and Columbia City (RM-83) during the June 1981 spring freshet. The highest flows occurred on June 10 and 11. Tides at upriver stations were suppressed by the high runoff for most of May and June.



that a topographic hole is accompanied by a divergence in bottom currents that will tend to deepen the hole on its upstream side and shoal it on its downstream side (just as at sections 2 to 5 in the model; Figures 28a and b). The reversed salinity gradient of Figures 28a and b tends to further increase the mean flow divergence. The theoretical calculations and the circulation model predict convergence in the bottom flow near a sill, that would tend to maintain the sill (e.g., at the Upper Sands Shoal at ~RM-16, model grid sections 9 and 10). Ianniello (1979, 1981) has also shown that similar effects should occur as a result of constrictions in breadth.

The profound effect of the sills at ~RM-6 to 9 in both channels on the mean flow raises the question of whether critical conditions for propagation of internal waves may not occur at certain stages of the tide over the sills (or over the entrance bar). Such internal hydraulic controls have been found (Gardner et al. 1980) in strongly stratified systems to exert a major influence on the density distribution. They provide a mechanism for transfer of tidal energy into mixing that is often localized in time and space, but repeatable from tidal cycle to tidal cycle (Gardner et al. 1980). Neap-to-spring variations could be expected, because stratification and shear both vary during the tidal month. The existence of such internal hydraulic controls might strongly affect the vertical structure of both the tidal and the mean flow. This is another possible explanation of the along-channel variations in the tidal and the mean flows

### 3.3 TIDAL-FLUVIAL INTERACTIONS

#### 3.3.1 Observations

There is a gradual change in the relative importance of riverine and tidal effects with distance upriver. The river stage (mean water level) and tidal properties at Tongue Pt. are dominated by the tides and atmospheric effects, and the riverflow plays a minor role. In contrast, the stage and tidal properties at Columbia City (RM-83) are dominated by the riverflow. This can be readily demonstrated by examining the system response to the freshet of June 1981. Flow was high for all of June 1981, and there was a sharp freshet between June 9 and 13, 1981, with peak flows of 560 kcfs ( $\sim 15,900 \text{ m}^3/\text{s}$ ; Figure 4 and Appendix F). Figure 29 shows (from bottom to top) the response of the tidal heights at Tongue Pt. (RM-17.6), Wauna (RM 42), and Columbia City (RM-83) to this freshet. Larger freshets even more strongly affect the tidal properties in the tidal-fluvial part of the system; this is clear from Figures 13 to 15.

The seasonal cycle of tidal-fluvial interactions is shown in Figure 30, which shows monthly-mean tidal and fluvial properties over a 20-month period. The mean water level at Columbia City closely follows the riverflow; it was 86 cm higher in June 1981 than in June 1980. The M2 amplitude at Columbia City in June 1980 was 14 cm, but only 9 cm in 1981. These are, respectively,  $\sim 45$  and  $\sim 29\%$  of the low-flow amplitude of 31 cm. The tide is also delayed about 25 to 30 minutes in reaching Columbia City under high-flow conditions. The tidal properties at Tongue Pt. show a different pattern. Mean water levels are highest in December of both years. While mean water level at Tongue Pt. is influenced by the riverflow, continental shelf and atmospheric forcing predominates (Chelton and Davis 1982). The M2 phase and amplitude at Tongue Pt. and Columbia City are scarcely affected by the riverflow. The factors governing sea level at Tongue Pt. and Columbia City are quantitatively analyzed in Sections 3.7.

The increase in riverflow has at least four important effects on the dynamics of the system. First, the surface slope is increased, so that more water can be discharged. That is, surface elevations are much more strongly affected upriver than in the estuary (Figure 31). The flood of 1894 (1,250 kcfs;  $35,400 \text{ m}^3/\text{s}$ ), for example, caused water levels of  $\sim 10$  m above CRD at RM-100.

Figure 30. Tidal-fluvial effects:  $M_2$  phase and amplitude at Columbia City (RM-83) (a), and Monthly mean flow and MWL at Tongue Pt. (RM-18) and Columbia City (b) from March 1980 to December 1981.

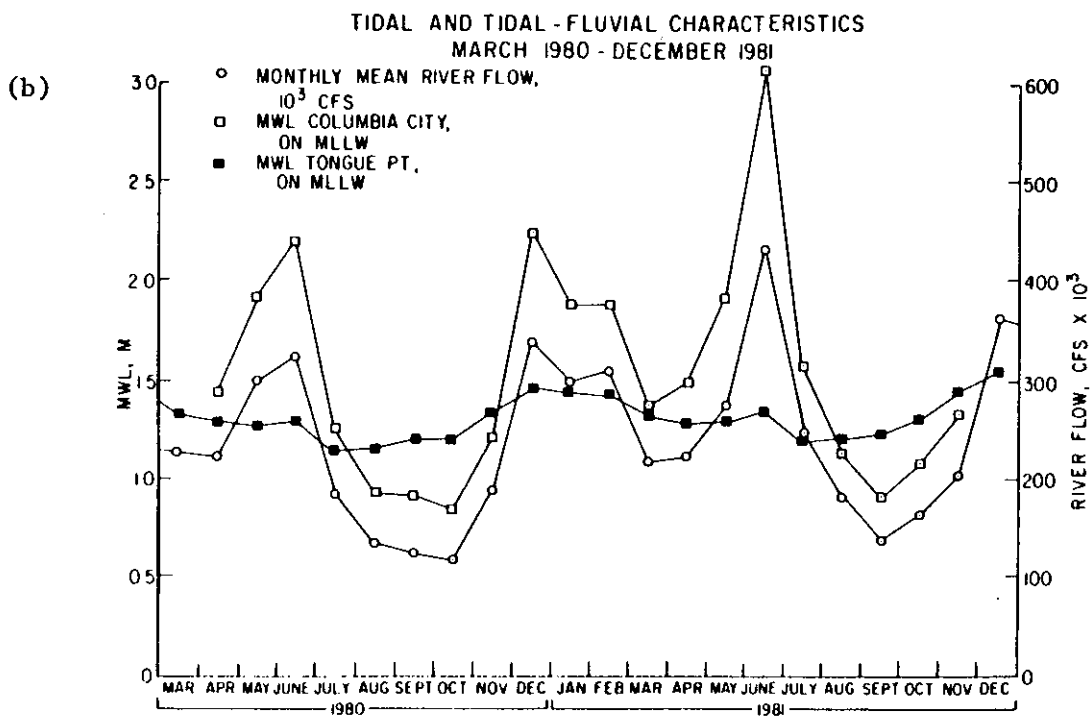
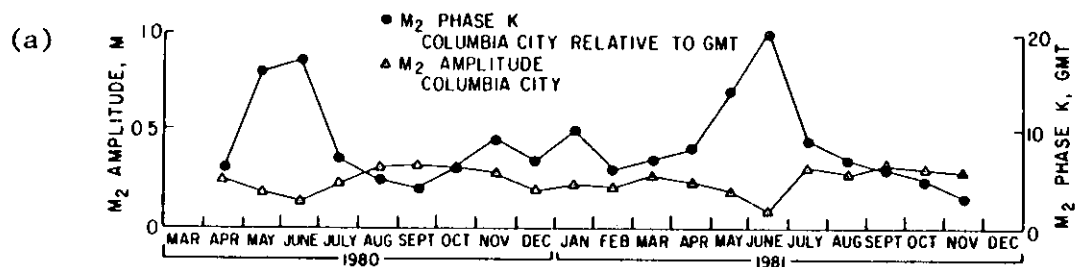


Figure 31. The effect of river flow on river stage. The lower line defines the slope of CRD. (provided by the U.S. Army Corps of Engineers, Portland District).

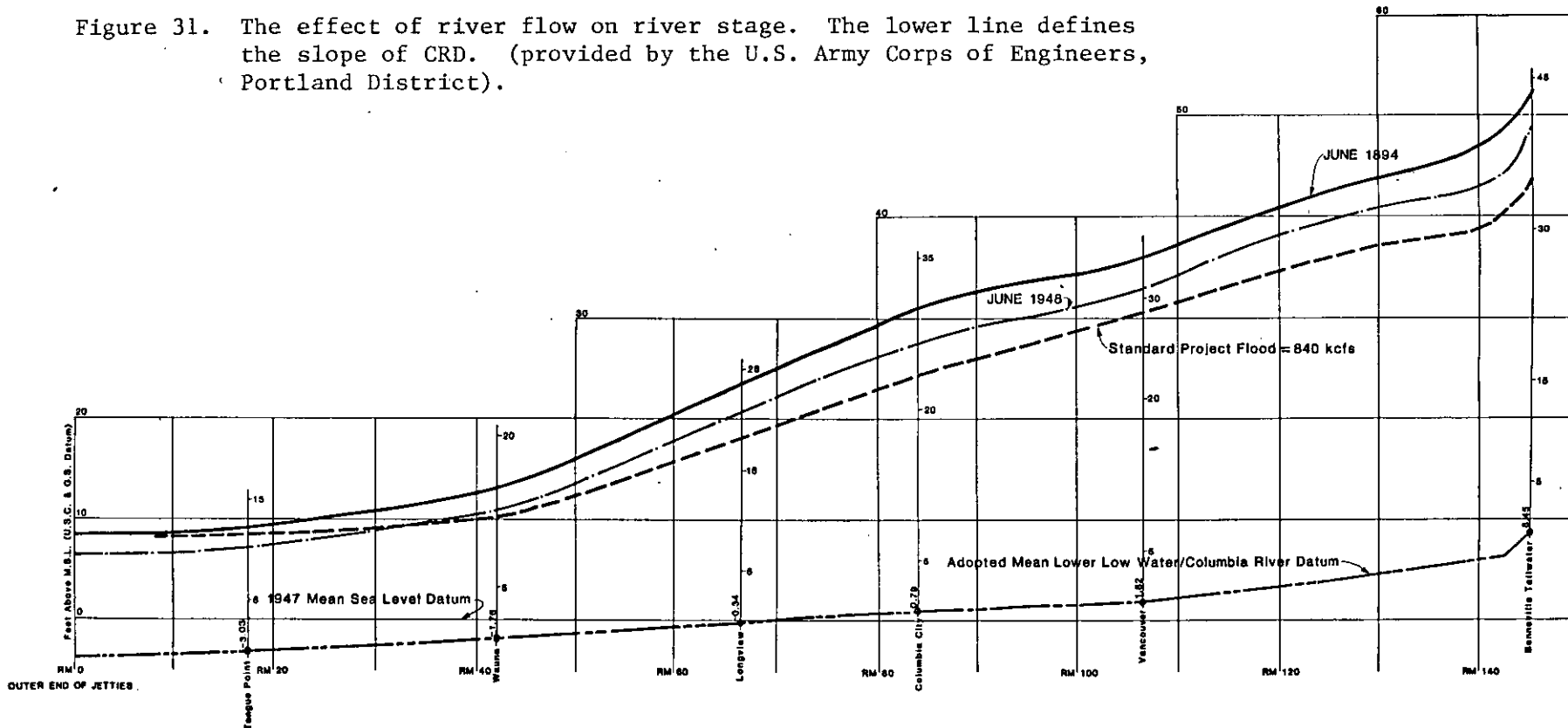
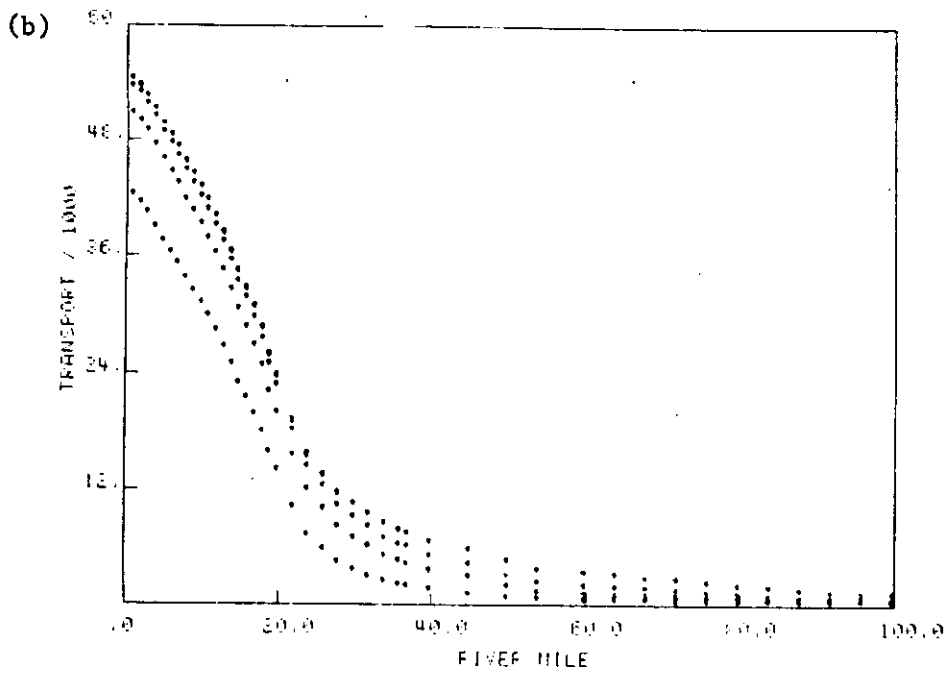
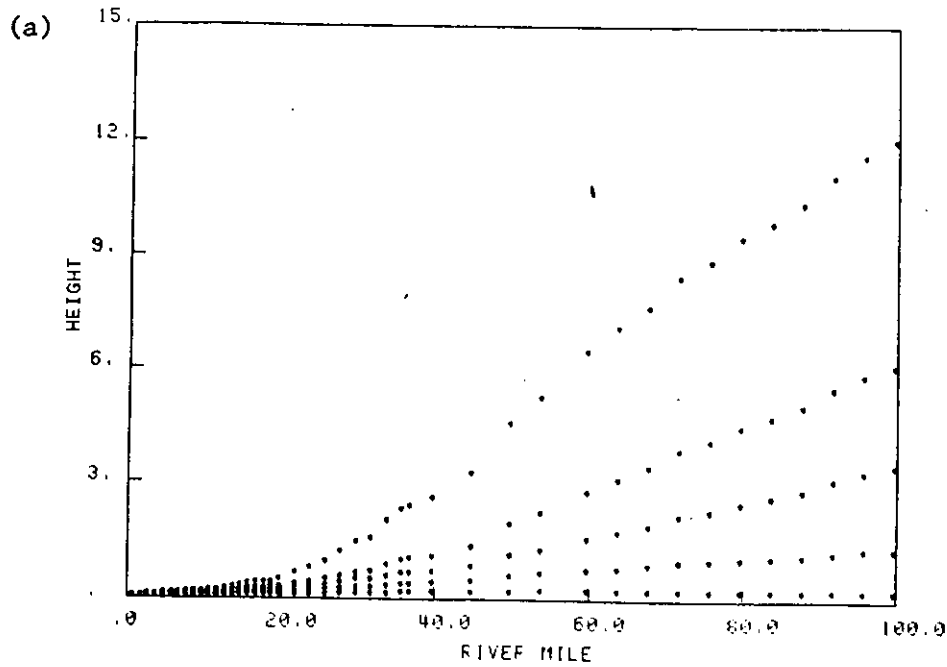


Figure 32. Predicted stage in m (a), and tidal transport amplitude in  $10^3 \text{ m}^3/\text{s}$  (b) as a function of river mile for river flows (bottom to top) of 0, 100, 300, 500 and 1,000 kcfs (0, 2831, 8495, 14159, and 28,317  $\text{m}^3/\text{s}$ ) and a 2.0m tidal range.



Second, the increased adverse pressure gradient pushes the salinity intrusion downriver strengthening the horizontal salinity gradient and the baroclinic circulation. Third, stratification is increased in the estuary; this decreases the vertical mixing and further enhances the baroclinic circulation. Fourth, the non-linear nature of bottom friction means that the friction on the tidal flow is greatly increased when the riverflow increases. This increase in friction causes the change in M2 amplitude at Columbia City and other stations in the fluvial part of the system.

### 3.3.2 Model Results

One of the primary purposes of the one-dimensional, harmonic model was to investigate in a systematic manner the interaction between the tides and the riverflow. Although the diurnal constituents were not included directly in the model, multiple tidal constituents and large range tides can be simulated by using the combined amplitude of two or more semidiurnal constituents. Thus, a spring tide (M2 and S2 in phase) can be approximated by using as a boundary condition at the mouth M2+S2.

To systematically investigate tidal-fluvial interactions, the one-dimensional model was run with riverflows of 0, 100, 300, 500, and 1000 kcfs (0, 2,832, 8,500, 14,160, and 28,320 m<sup>3</sup>/s) and tidal amplitudes of 0.5, 1.0, 1.5, and 2.0 m (tidal ranges of 1.0, 2.0, 3.0, and 4.0 m); this encompasses all likely tidal ranges and riverflows. Model results are summarized in Table 4. River stage and tidal transport amplitude as functions of river mile are shown for all five riverflows in Figures 32a and b for a tidal range of 2.0 m. Tidal prism and Stokes drift transport at the mouth are given in Tables 5a and 5b.

The variations of tidal height amplitude and tidal transport at the upriver stations with riverflow and tidal range (Table 4 and Figures 13 to 17) show the effects of friction and geometry. Increasing the tide at the entrance does not cause a proportional effect at Tongue Pt. and beyond (Figures 17a and b), because of greatly increased friction on larger range tides. Higher riverflow also increases the frictional damping considerably. The decrease in tidal amplitude with increasing riverflow is much more severe upriver; the decrease in tidal amplitude is only ~20% at Tongue Pt. between 0 and 1000 kcfs (0 and 28,320 m<sup>3</sup>/s) but is more than 75% at Columbia City. The tidal transport amplitude drops off by ~60 to ~80% in the first 20 river miles (Figure 32b and Table 4), because the width and tidal range decrease upriver. Increasing the riverflow from 0 to 1000 kcfs (0 to 28,320 m<sup>3</sup>/s) decreases the transport at the mouth (the total tidal prism) by ~25%. The tidal transport at the mouth decreases with increasing riverflow, because high riverflow decreases the tidal range upriver. As the tidal range increases, flood tide transports (tidal transport minus riverflow transport) and ebb tide transports (tidal transport plus riverflow) diverge. More and more of the tidal prism is satisfied by the holdup of riverflow. At the river mile where the flood tide transport is zero, the flood tidal transport (averaged over half a tidal cycle) is exactly balanced by riverflow. Even though flood currents are observed during some part of the tidal cycle, no net upriver transport occurs during the six lunar hours of flood tide, and the ebb transport is twice the tidal transport. The tidal prism upstream of this point is entirely satisfied by holdup of riverflow.

Figure 32b can be also be used to predict the point upriver of which the currents no longer reverse, that is, the point where the flow is always in the downriver direction. This point varies for a 2.0 m tidal range from ~RM-9 for 1000 kcfs riverflow to ~RM-44 for 100 kcfs (2,830 m<sup>3</sup>/s). Stronger tides and lower riverflows (which occur sporadically during the low-flow season; Lutz et al. 1975) will cause reversals much farther upriver. A 4.0 m tidal range would cause reversals almost all the way to Vancouver at RM-105. A very weak tide (~1.2 m

Table 4. Tidal properties as a function of riverflow and tidal range - model predictions

Tidal Range = 2.0 m, Riverflow = 0 kcfs

<u>Station</u>	<u>RM</u>	<u>Tidal Current</u>		<u>Riverflow</u>	<u>Height</u>		<u>Stokes Drift</u>	<u>Stage</u>	<u>Phase difference</u>
		<u>Amplitude m/s</u>	<u>Phase, deg.</u>	<u>m/s</u>	<u>Amplitude m</u>	<u>phase</u>	<u>m/s</u>	<u>m</u>	<u>Heights - flow, deg.</u>
Entrance	1	1.40	168	0	1.00	225	.030	.00	57
Tongue Pt.	19	.66	188	0	1.18	252	.022	.03	64
Wauna	40	.48	249	0	.90	290	.012	.12	41
Columbia City	84	.29	333	0	.45	363	.004	.18	30

Tidal Range = 2.0 m, Riverflow = 500 kcfs

Entrance	1	1.31	165	-.36	1.00	225	.025	.01	60
Tongue Pt.	19	.56	184	-.35	1.11	252	.015	.24	68
Wauna	40	.26	242	-.96	.70	296	.004	1.26	54
Columbia City	84	.04	346	-1.35	.14	394	.000	4.74	48



Table 4. (continued)

Tidal Properties as a Function of Riverflow and Tidal Range - Model Predictions

Tidal Range = 4.0 m, Riverflow = 500 kcfs

<u>Station</u>	<u>Rm.</u>	<u>Tidal Current</u>		<u>Riverflow</u> m/s	<u>Height</u>		<u>Stokes</u> <u>Drift</u> m/s	<u>Stage</u> m	<u>Phase difference</u> Heights - flow, deg.
		<u>Amplitude</u> m/s	<u>Phase,</u> deg.		<u>Amplitude</u> m	<u>phase</u>			
Entrance	1	2.3	166	-.32	2.00	225	.084	.02	59
Tongue Pt.	19	.95	184	-.29	2.12	252	.039	.36	68
Wauna	40	.54	235	-.88	1.45	289	.014	1.48	54
Columbia City	84	.11	332	-1.32	.35	381	.001	4.73	49

Tidal Range = 4.0 m, Riverflow = 1000 kcfs

Entrance	1	2.07	164	-.65	2.00	225	.070	.03	61
Tongue Pt.	19	.76	183	-.59	1.95	253	.027	.60	70
Wauna	40	.28	243	-1.68	.97	299	.004	2.88	56
Columbia City	84	.03	345	-2.11	.14	394	.000	9.48	49

Table 4. (continued)

Tidal Properties as a Function of Riverflow and Tidal Range - Model Predictions

Tidal Range = 2.0 m, Riverflow = 1000 kcfs

<u>Station</u>	<u>Rm.</u>	<u>Tidal Current</u>		<u>Riverflow</u> m/s	<u>Height</u>		<u>Stokes</u> <u>Drift</u> m/s	<u>Stage</u> m	<u>Phase difference</u> Heights - flow, deg.
		<u>Amplitude</u> m/s	<u>Phase,</u> deg.		<u>Amplitude</u> m	<u>phase</u>			
Entrance	1	1.10	165	-.72	1.00	225	.021	.02	60
Tongue Pt.	19	.41	189	-.70	.98	255	.010	.43	66
Wauna	40	.11	257	-1.76	.38	313	.001	3.01	56
Columbia City	84	.01	361	-2.10	.05	410	.000	9.71	49

Tidal Range = 4.0 m, Riverflow = 0 kcfs

Entrance	1	2.31	168	0	2.00	225	.089	.01	57
Tongue Pt.	19	.98	189	0	2.15	254	.048	.12	65
Wauna	40	.70	250	0	1.53	293	.026	.38	43
Columbia City	84	.38	339	0	.66	371	.008	.52	32

tidal range) would result in no inward transport at the mouth for a riverflow of 1000 kcfs ( $28,320 \text{ m}^3/\text{s}$ ). Density-driven flood currents would probably still be observed at depth near the entrance.

It is useful for many purposes to compare riverflow volume during a 12.42 hour tidal cycle to half-tidal cycle transport volumes. The ratio of tidal transport volume over half a tidal cycle (tidal transport amplitude  $\times \frac{2}{\pi} \times 6.21$  solar hrs) to freshwater flow volume over a 12.42 hr tidal cycle is given in Table 5a. The ebb/flood transport volume is the tidal transport volume  $\pm \frac{1}{2}$  (the riverflow volume). A ratio of 0.5 in Table 5a corresponds to the condition where the riverflow volume over half a tidal cycle is equal to the tidal transport; the tidal prism is entirely filled by the holdup of riverflow. Except under high riverflow and low tidal range, the tidal exchange is considerably larger than the riverflow volume. Included in Table 5b is the Stokes drift volume ratio; this inward Stokes drift flow volume is very nearly compensated during each tidal cycle by the Stokes drift return flow. The Stokes drift is large relative to riverflow only at low riverflow levels and large tidal ranges, but under these conditions, the Stokes drift compensation flow is a significant fraction of the total outflow.

The calculation of the ratios in Table 5a involves several assumptions that are not strictly fulfilled. The most important is that width is not a function of stage. Table 5a probably underestimates tidal prisms for larger range tides, particularly during the winter months, when sea level is high. The distortion in the shape of the tidal wave by frictional effects is also not represented, but this should have little effect on the calculated volumes.

The pattern of tidal height and tidal current phases (and the phase difference between them) is complex. There are at least four governing factors: channel width, friction, the riverflow, and average depth; these factors interact in a complex manner. Increasing friction (caused by increases in either river or tidal flow) tends to make the wave more progressive. The progressive nature of the wave is indicated by the phase difference in Table 4; a perfectly progressive wave (no reflected wave) would have a phase difference of zero. A standing wave (reflected wave equal to incoming wave) would have a phase difference of 90 deg. The strength of the reflected wave (which is dependent on the geometry) affects the phase of the tidal height, in that a standing wave has high water nearly simultaneous throughout the estuary.

Increasing depth (as occurs as the river stage increases), causes a progressive wave to travel faster; the phase speed is  $(gd)^{\frac{1}{2}}$ . The speed of the riverflow has a doppler shift effect, the incoming wave is shifted to a shorter wavelength and the outgoing wave is shifted to a longer wavelength. The model predicts that increasing riverflow makes the wave much slower (height phase larger) and more progressive (phase difference smaller), but changes in stage and river flow speed are relatively unimportant below Tongue Pt. The travel time of high water from the entrance to Columbia City varies from 138 deg ( $\sim 4.75$  hours) to 185 deg ( $\sim 6.4$  hours), depending on river flow and tidal range. The model also predicts that riverflow has a stronger effect on this travel time at smaller tidal ranges, for reasons which are not clear.

Figure 32a shows the river stage predicted by the model for river flows from 0 to 1000 kcfs (0 to  $28,320 \text{ m}^3/\text{s}$ ) and a tidal range of 1.0 m. (The stage is the mean water level; the tides are then added to this mean water level). These results may be compared to the observations in Figure 31. The zero river-flow stage is not zero, because of the Stokes drift. It can be seen in Figure 32a that the stage at Tongue Pt. is very little affected by fluctuations in riverflow of between 100 and 500 kcfs ( $2,830$  and  $14,160 \text{ m}^3/\text{s}$ ); the difference is only  $\sim 14$

Table 5a . Tidal prism ( $\text{km}^3$ ) and ratio of tidal prism to riverflow volume

Tidal Range (m)		Riverflow (kcfs)	0	100	300	500	1,000.
		( $10^3 \text{ m}^3/\text{s}$ )	0	2.83	8.50	14.2	28.30
		( $\text{km}^3 / \text{tidal}^\dagger$ cycle)	0	.127	.38	.633	1.27
1.0	prism		0.44	0.44	0.41	0.37	0.29
	ratio		-	3.5	1.1	0.6	0.2
2.0	prism		0.79	0.79	0.78	0.74	0.62
	ratio		-	6.2	2.0	1.2	0.5
3.0	prism		1.12	1.12	1.11	1.08	0.96
	ratio		-	8.8	2.9	1.7	0.8
4.0	prism		1.44	1.44	1.43	1.41	1.29
	ratio		-	11.3	3.8	2.2	1.0

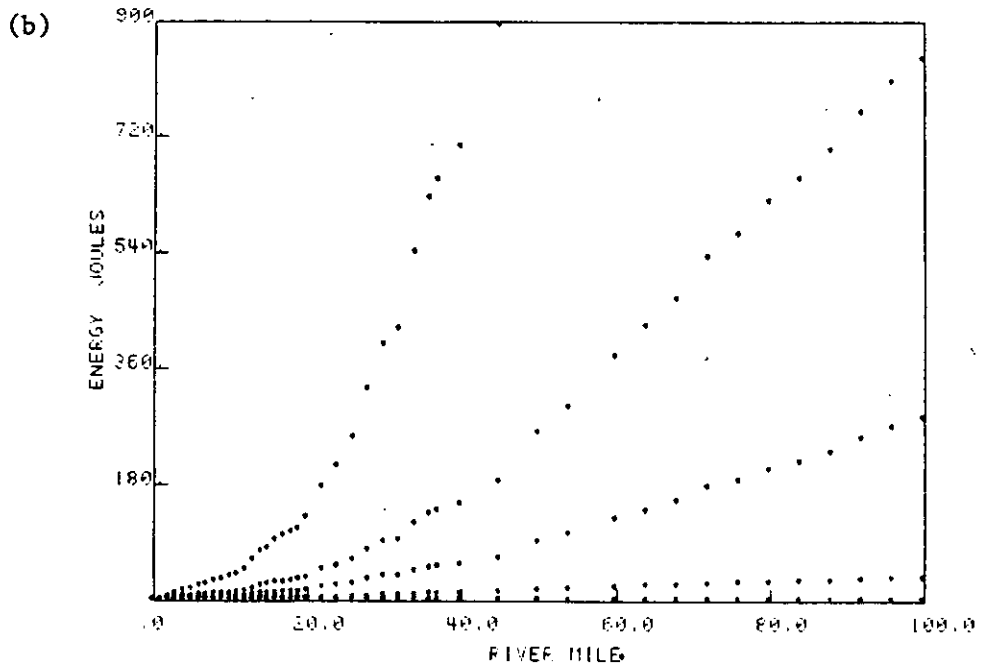
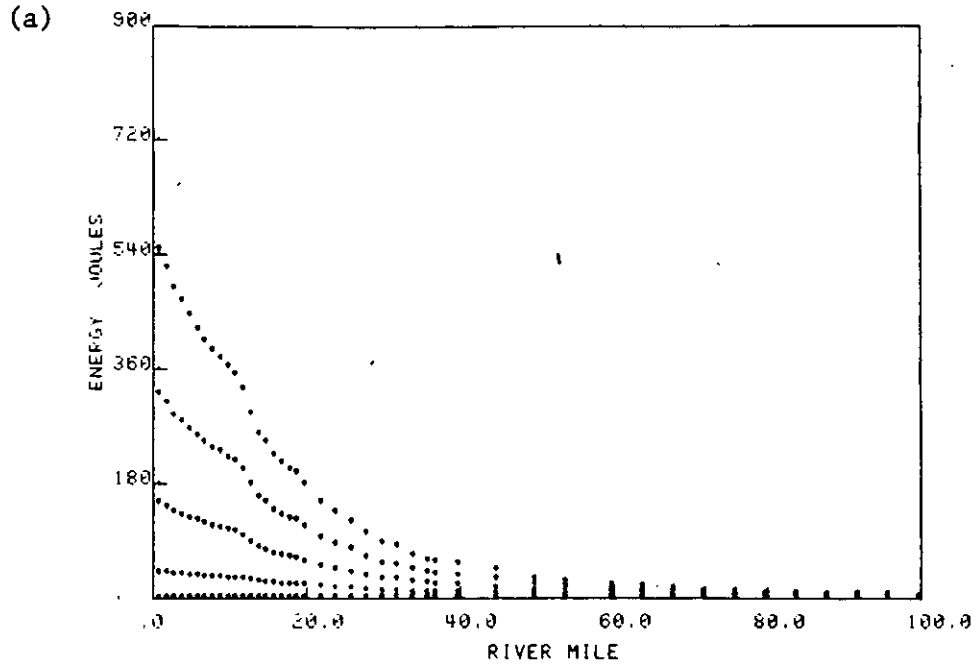
<sup>†</sup>One tidal cycle = 12.42 hours

Table 5b. Stokes drift volume (km<sup>3</sup>) and ratio of Stokes drift volume to riverflow volume

		Riverflow (kcfs)	0	100.	300.	500.	1,000.
		(10 <sup>3</sup> m <sup>3</sup> /s)	0	2.83	8.50	14.2	28.30
		(km <sup>3</sup> /tidal cycle <sup>†</sup> )	0	.127	.38	.633	1.27
Tidal Range (m)							
1.0	volume		.015	.015	.013	.012	.010
	ratio		-	.118	.035	.019	.008
2.0	volume		.053	.053	.050	.044	.037
	ratio		-	.417	.130	.070	.029
3.0	volume		.106	.108	.104	.097	.080
	ratio		-	.853	.275	.153	.062
4.0	volume		.174	.176	.174	.165	.137
	ratio		-	1.385	.459	.260	.108

<sup>†</sup>One tidal cycle = 12.42 hours

Figure 33. Model predictions of (a) tidal energy flux, and (b) mean flow potential energy flux, both in  $10^6$  joules, as functions of river mile for (a) (bottom to top) tidal ranges of 0, 1, 2, 3 and 4m, and (b) river flows of 0, 100, 300, 500 and 1000 kcfs (0, 2832, 8495, 14,160 and 28,320  $m^3/s$ ).



cm. A flow of 1000 kcfs (which corresponds to the flood of 1948) raises the stage at Tongue Pt. less than 30 cm. Increases in stage are much larger upriver; the model predicts stages of 4.7 and 9.7 m above MSL at Columbia City for flows of 500 and 1000 kcfs (14,160 and 28,320 m<sup>3</sup>/s), respectively. Figure 31 and 1981 tidal data show that these predictions are somewhat high. The maximum stage in June 1981 was ~4.1 m, and the highest stage at Columbia City for the 1948 flood was ~8.3 m above MSL. The reason for the overprediction is believed to be the fact that the model does not include a realistic flood plain.

### 3.4. THE ENERGY BUDGET

#### 3.4.1 Interpretation of Energy Budget Terms

The M2 tide and the riverflow provide most of the energy for circulatory processes. We discuss here how energy from these two sources appears in the energy budget, as represented by Eq. (23) of Section 2.4.2. As discussed in Section 1.3, the Stokes drift and the associated tidal energy input are large in systems with progressive or partially progressive tides. This occurs because the flow is deeper on flood tide than on ebb. This flood-to-ebb difference in elevation causes a net inflow (the Stokes drift; Section 1.3) and an energy flux. The tidal energy flux is simply the potential energy difference caused by the difference in surface elevation (and therefore potential energy) of the flood and ebb flows. The stronger the dissipation, the more progressive the wave is, and the greater the elevation difference and energy transport into the system. The tidal energy flux is shown as a function of river mile in Figure 33a.

The analogous potential energy term for the riverflow arises from the river slope; as the water flows downhill, gravitational potential energy is released. This term is largest in the upriver areas where the surface slope is large and increases sharply with increasing riverflow, as in Figure 33b. The mean flow kinetic energy flux term results from the decrease in flow velocity of the mean flow in the downstream direction as the cross-sectional area increases. The dissipation is the loss of energy caused by friction on the bottom and sides of the estuary channels. It is associated both with the form drag of bedforms, shoals, curves, etc., and skin friction of the sediment itself.

To summarize the balance of Eq. (23), both the tides and riverflow contribute potential energy and dissipation terms, but only the mean flow contributes a kinetic energy flux term. Interactions (between the tidal and mean flow) occur both in the dissipation and kinetic energy flux terms. The interaction terms in the dissipation occur because the dissipation is proportional to  $[|q|q^2]$ , where the total transport  $q = q_0 + q_1$ ,  $q_0$  is the mean flow,  $q_1$  is the tidal transport amplitude,  $| |$  indicates the absolute value, and the brackets indicate a tidal cycle average. The tidal dissipation arises from  $[|q_1|q_1^2]$ , the mean flow dissipation from  $[|q_0|q_0^2]$ , and the interaction dissipation from the mixed terms. The kinetic energy flux is also cubic in  $u$ , but without the absolute value; odd powers of the tidal velocity average to zero over a tidal cycle, thus there is no purely tidal kinetic energy flux term and only one interaction term ( $[q_0q_1^2]$ ).

The flood-ebb difference in energy dissipation can be seen as follows. On flood tide, the river and tidal flow are in opposite directions. Thus, the flood dissipation is proportional to  $|q_1 - q_0|(q_1 - q_0)^2$ . On ebb tide, the river and tidal flow are in the same direction, and the dissipation is given by  $(q_1 + |q_0|)^3$ . Because the dissipation varies with the cube of the speed, ebb tide dissipation will be substantially larger than the flood time dissipation, if  $\frac{|q_0|}{q_1}$  is substantial.

#### 3.4.2 Neap-Spring Effects

TABLE 6. Total tidal and mean flow potential energy fluxes and total dissipation

Tidal Range, m	<u>Riverflows</u>	0	100	300	500	1000
	kcms m <sup>3</sup> /s	0	2832	8395	14,160	28,320
1.0	Tidal Energy Flux, 10 <sup>6</sup> Joules		40			
	Potential Energy Flux, 10 <sup>6</sup> Joules		28			
	Total Dissipation, 10 <sup>6</sup> Joules		67			
2.0	Tidal Energy Flux, 10 <sup>6</sup> Joules	150	149	141	127	105
	Potential Energy Flux, 10 <sup>6</sup> Joules	0	35	284	824	3318
	Total Dissipation, 10 <sup>6</sup> Joules	150	181	418	947	3461
3.0	Tidal Energy Flux, 10 <sup>6</sup> Joules		319			
	Potential Energy Flux, 10 <sup>6</sup> Joules		42			
	Total Dissipation, 10 <sup>6</sup> Joules		354			
4.0	Tidal Energy Flux, 10 <sup>6</sup> Joules	549	546	540	505	422
	Potential Energy Flux, 10 <sup>6</sup> Joules	0	50	300	816	3261
	Total Dissipation, 10 <sup>6</sup> Joules	549	585	811	1283	3659



The energy budget provides a useful framework in which to study neap-spring variations. Let us consider the simplest, no riverflow case, since variations in riverflow act primarily to change the fraction of the system where neap-spring effects are important without altering the basic processes at work. The energy budget then contains only two terms, tidal input and dissipation. The tidal energy coming into the system from the ocean is proportional to the Stokes drift at the entrance,  $q_1 h_1 \cos \delta$ , where  $\delta$  is the phase difference between the tidal transport  $q_1$  and the tidal height  $h_1$ . Since  $q_1$  is proportional to the tidal amplitude, the tidal energy varies with the square of the tidal range at the entrance:  $h_1^2 \cos \delta$ . The dissipation inside the estuary varies with tidal range cubed. It is not immediately obvious how the tidal energy input and dissipation remain in balance, over the tidal month, because they vary with different powers of the tidal range. One possible mechanism is variation of  $\delta$ , the phase difference between the heights and currents, at the entrance (Heath 1981). It is improbable that this effect could, by itself, account for the spring-to-neap difference in the energy balance, because  $\cos \delta$  would have to change by a factor of two, as the tidal range doubled, to account for the entire discrepancy.

The tidal model of Section 3.3 predicts negligible phase changes at the entrance for a doubling of the tidal range (Table 4 and Figures 17a and b), and the model and the observed spatial distribution of the semidiurnal constituent amplitudes (Table 1) strongly suggest that another mechanism is more important. The other mechanism for balancing tidal input and dissipation is the spatial variation of tidal range in the estuary, as a function of the tidal range at the mouth. The tide is essentially composed of phase and amplitude modulated semidiurnal and diurnal tidal waves. The amplitude and phase modulation is accounted for in a harmonic analysis by introduction of various diurnal and semidiurnal tidal constituents whose frequencies are determined from astronomical considerations. It was stated in Sections 3.1 and 3.2 that the semidiurnal tidal wave is described primarily by three tidal constituents, M2, S2 and N2, that spring/neap tides were described by  $M2 \pm S2$ , that perigean/apogean tides were described by  $M2 \pm N2$ , and that S2 and N2 both decrease more rapidly in the upriver direction than does M2 (Table 1). We can now interpret this rapid decrease of N2 and S2. The spring tide wave is described by  $M2 + S2$ . The greater dissipation in the interior of the estuary requires that the spring tide increase in tidal amplitude inside the estuary be less than proportional to that at the entrance. The more rapid decrease upriver of S2 than M2 provides exactly that response. The neap tide wave ( $M2 - S2$ ) is less rapidly damped than M2 alone or  $M2 + S2$ , as is required by the relatively small dissipation on neap tides. The situation is similar with  $M2 + S2 + N2$  and  $M2 - N2 - S2$ . (Figures 17a and b). We can be reasonably confident that the model realistically reproduces neap-to-spring changes in system energetics, because it reproduces correctly the distribution of  $M2 + S2 + N2$  and  $M2 - S2 - N2$  and other constituent combinations.

### 3.4.3 Energy Budget Calculations

#### Variations with River Flow and Tidal Range

The energy budget was evaluated using the one-dimensional tidal model for selected cases in the same series of riverflows and tidal ranges used in Section 3.3; the riverflows were 0, 100, 300, 500 and 1000 kcfs (0, 2832, 8345, 14,160, and 28,320  $m^3/s$ ), and the tidal ranges were 1.0, 2.0, 3.0 and 4.0 m. These results are summarized in Table 6, which shows the total tidal energy flux, total mean flow potential energy flux, and total dissipation for the entire system for the various cases. It is evident from Table 6 that the largest energy fluxes are associated with large tides and riverflows, and that major freshets provide by far the largest energy fluxes. The total dissipation for a 1000 kcfs flow (28,320  $m^3/s$ ) is about 6 times that for the largest reasonable tide of 4 m. This very large mean

Figure 34. Model predictions of total energy flux unit area (E) and dissipation/unit area (D) both in Joules/m<sup>2</sup>, as a function of river mile for (a), a tidal range 2m and river flow of 300 kcfs (8495 m<sup>3</sup>/s) (b), a tidal range of 4m and a river flow of 300 kcfs (2832 m<sup>3</sup>/s), and (c), a tidal range of 4m and river flow of 500 kcfs (14,160 m<sup>3</sup>/s). Imbalances between D and E indicate errors in the model. The present, annual maximum energy level corresponds roughly to (c); note energy minimum at ~RM-14 to 25.

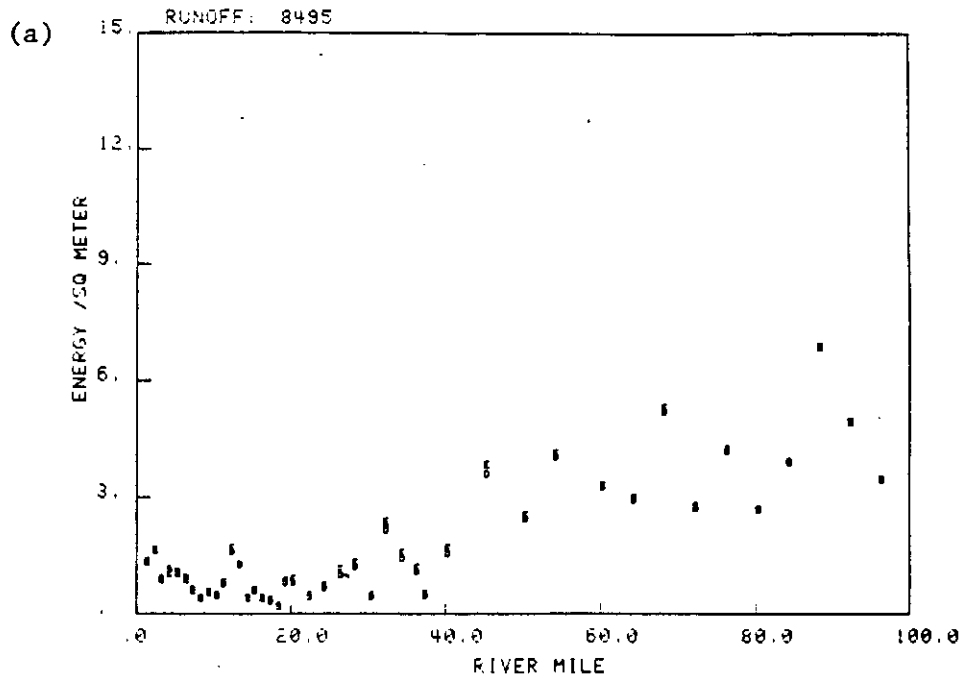
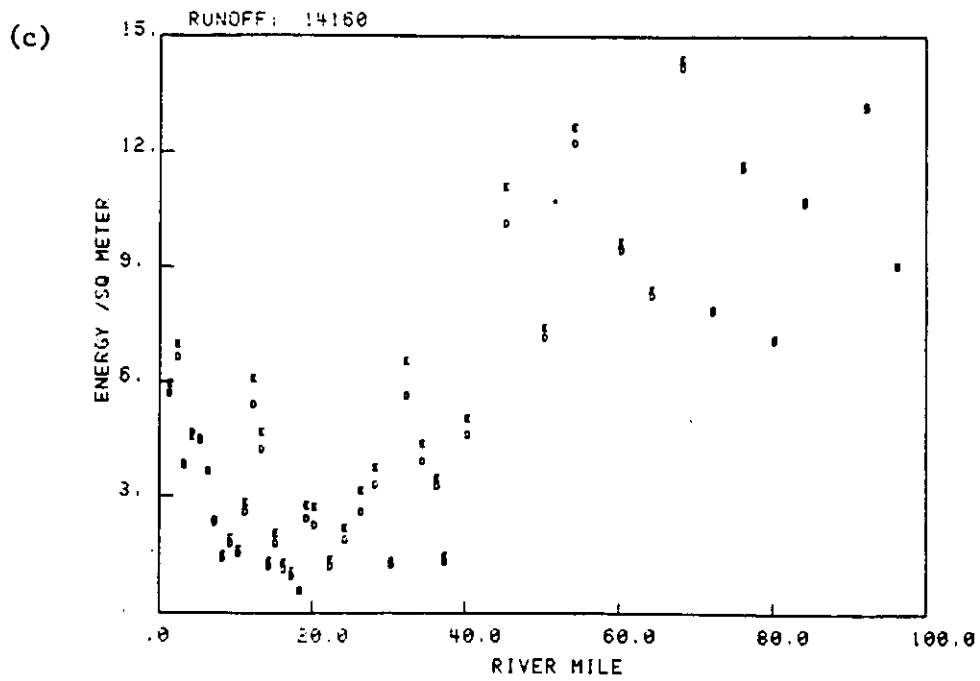
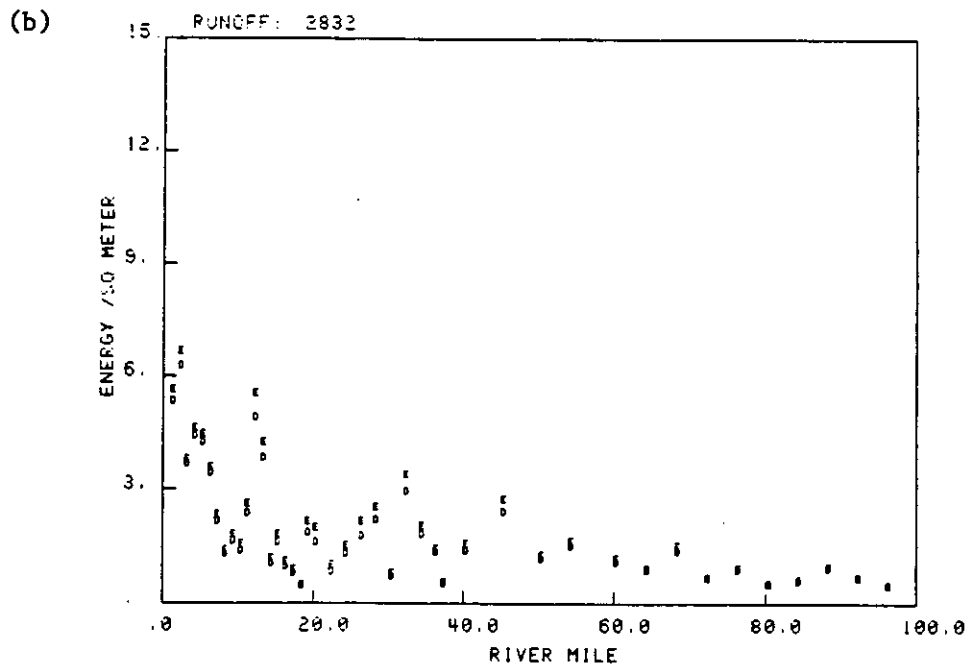


Figure 34. (continued).



flow potential energy is the result of the high river stage that accompanies floods; most of this potential energy does not reach the estuary, however, because it is lost to dissipation upstream of the estuary proper. The spatial distribution of dissipation in the system for the various cases is discussed further, below.

Examination of the model results shows that not all of the terms included in Eq. (24) are important; only the M2 tidal energy flux, the mean flow potential energy flux, and the tidal and riverine dissipations need be considered here. We can approximate the energy balance of Eq. (24) to about 10% as:

$$\begin{aligned} \Delta \text{ M2 tidal energy flux} + \Delta \text{ mean flow potential energy flux} & \quad (27) \\ & = \text{ mean flow dissipation} + \text{ tidal dissipation} \end{aligned}$$

Consideration of the distribution with river mile of the various terms allows further simplification. It can be seen from Figures 33a and b, which show the tidal energy flux and the mean flow potential energy flux as functions of river mile for various riverflows and tidal ranges, that tidal energies are generally large only seaward of RM-20 and riverine terms large only upriver of RM-20. Thus, in the high-energy cases (i.e., river flow and/or tidal range large) which are important for sediment transport, the energy balance at most locations in the system is either:

$$\Delta \text{ tidal energy flux} = \text{ tidal dissipation} \quad (28)$$

(in the estuary) or

$$\Delta \text{ mean flow potential energy} = \text{ mean flow dissipation} \quad (29)$$

(in the fluviably-dominated section)

Eq. (28) is the energy balance for a strongly-tidal estuary without major riverflow, and Eq. (29) is the expression for a non-tidal river. Eq. (27) is necessary only in the tidal-fluvial reaches (~RM-18 to ~RM-50, depending on the riverflow). Of the terms included in Eq. (24), but neglected in Eq. (27), the tidal-fluvial interaction terms in the potential energy and dissipation, and the riverine kinetic energy flux are the most important; they are large only when the riverflow is large and are always less than 10% of the dominant riverine terms. In the riverine part of the system, they may be much larger than the tidal terms, however. Thus, the energy budget shows the same division of the system into estuarine, tidal-fluvial and fluvial reaches that is found in many other aspects of the physics, geology, and biology of the system.

Total dissipation (the sum of all terms on the right hand side of Eq. (23) and energy inputs (the sum of all terms on the left hand side of Eq. (23) are shown as a function of river mile for 3 typical cases in Figures 34a, b and c. Three points should be made in regard to these figures. First, the model does not conserve energy perfectly; dissipation and energy inputs do not balance, although they balance within 2% at most sections and ~18% in the worst cases. It is believed that terms not evaluated are small, and that the errors result from the approximations used to calculate the non-linear, convective acceleration term  $\frac{q}{a} \frac{\partial q}{\partial x}$ .

Second, there is a broad area of minimum energy between ~RM-18 and ~RM-30. As is clear from Figures 33a and b, this reach of the estuary is never exposed to high energy fluxes, even by the largest tides or freshets. This relatively low energy level occurs in the widest part of the river/estuary system and may account for the formation of the islands of Cathlamet Bay. The implications of the energy minimum are discussed further in the Integration Report.

Third, there are numerous, sharp maxima and minima in the dissipation vs. river mile curves (Figures 34a, b and c). The dissipation maxima correspond to shallow sections of the estuary. In most cases, a distinct shoal in the channel can be observed that corresponds to each maxima, e.g., the inner tidal delta at RM-2, lower Desdemona Shoal between RM-6 and RM-9, Flavel Bar at RM-12 to RM-13, etc. It may seem paradoxical that a shoal could exist in a reach where large amounts of energy are lost to bottom friction. But considered from the point of view of a sediment particle moving downstream, a dissipation maximum is first (as the particle reaches the upstream side of the maximum) a reach of increasing energy, and then one of decreasing energy. Thus, at least in the fluvial part of the system where sediment is generally moving seaward, the downstream side of a dissipation maximum (topographic high) might correspond to an area of deposition, as would the upstream side of a dissipation minimum (topographic low). This corresponds to the convergences and divergences in the mean flow, that are also associated with topographic highs and lows as discussed in Ianniello (1979, 1981) and Section 3.2. Salinity gradients in the estuary proper greatly complicate sedimentary processes, and this simple model may not be adequate to explain processes there.

#### Errors and Processes Not Considered

Errors occur in the energy budget (which was based on Eq. (23)) because some terms in Eq. (22) were ignored, and because the diurnal tide is neglected even in Eq. (22). The buoyancy flux, the temporal change term, and direct work by/on the moon are believed to be less than 1% of the tidal energy flux. The diurnal tidal components account for perhaps 20% of the tidal energy in the estuary proper and less upriver of RM-20. MK3 and M4 account for perhaps as much as 6-7% of the total tidal energy, but only in the upriver areas, where the riverflow terms are usually dominant. Thus, the tidal constituents neglected in the calculations are too small to invalidate the calculations.

Errors in the representation of the M2 tide and riverflow by tidal model may also occur; the tidal energy flux is very sensitive to the phase difference between the tidal height and the tidal flow. Comparison of model results (Figures 13 to 15 and 17a and b) with the data (Figures 20 and 21) suggests that the tide may be somewhat more progressive (heights and flow more in phase) than represented by the model. In the worst reasonable case, the model could be off by as much 10 deg in phase, which would result in the model underestimating the tidal energy flux by ~25%.

Finally, since the model over-estimates river stage by as much as ~17% under the highest flow condition, the mean flow potential energy flux at the upriver end is overestimated by the same amount for this case. Errors are much smaller than this below RM-50 and throughout the system for all but the 1000 kcfs (28,320 m<sup>3</sup>/s) case. None of these errors is large enough to invalidate or modify any of the conclusions drawn.

The energy budget in the lower estuary may also be modified by atmospheric processes, such as storm surges, wind driven currents, and ocean waves, which have not been included in the calculations. The energy flux into the estuary over a tidal cycle for a storm surge of 25 cm (which is somewhat greater than the storm-induced increase in elevation that occurred during any 12.42 hr tidal cycle in the 1979-81 period) can be estimated; it is small, about 10% of the M2 tidal flux at the entrance. Data and modeling results (Hamilton 1984) suggest that currents driven by winds over the estuary are even less important to the energy budget. The effect of ocean waves on the energy budget has not been quantitatively estimated, but it is unlikely to be large, even at the entrance. Thus, atmospheric processes do not greatly modify the energy budget of the system. This does not necessarily mean that these processes are unimportant for sediment transport. Sediment transport is strongly non-linear; once a certain

threshold is reached, it increases very rapidly as the bottom stress increases. The combination of large tides, high river flow, large waves, and a storm surge that accompany some winter freshets may be quite effective in moving sediment near the entrance.

### 3.5 THE SALINITY DISTRIBUTION

Previous sections have considered the tidal and mean flows from a dynamical point of view. In this section the salinity distribution is considered from a descriptive point of view, since knowledge of this property is often required by estuarine scientists and managers. The salinity varies daily, tidal monthly, and seasonally; it was necessary to consider all three time scales. T-S (temperature and salinity) characteristics were defined, and seasonal average salinity distributions were compiled for the high and low-flow seasons using all available (1980 and 1981) time series data. Salinity intrusion was examined for a low-riverflow period (October 1980 neap to spring cycle) and for extreme high-flow periods in June 1959 and in June 1981.

The salinity distribution was determined from time series of Aanderaa current meter salinity data, with available profile data used as appropriate. The use of current meter data to produce salinity sections provides synopticity not usually available with profile data and allows assessment of temporal variability. The wide spacing of current meter moorings, however, renders tentative interpretations based only on current meter results. The uncertainty is greatest at the surface, where the salinity is highly variable and no current meter data are available. Cross-channel variability, caused by channel curvature and the earth's rotation, also introduces errors that are probably greatest at and below RM-6, where the channel is wide.

#### 3.5.1 Water Masses and Mixing

In order to describe oceanographic mixing processes, it is customary to define end-member water types that have extreme water properties and that mix together to create the observed temperature and salinity properties in an area (the water masses). Water types in the Columbia River and adjacent ocean waters have been defined by Conomos et al. (1972). The three water types are River Water (RW), Surface Ocean Water (SOW), and Sub-surface Ocean Water (SSOW).

River Water (RW) has a salinity of zero, but highly variable temperature characteristics. National Marine Fisheries Service (NMFS) records from Trojan (RM-72) show temperatures ranging from 0.2 deg C in January 1979 to 23.1 deg C in August 1977. CREDDP and NOS records for 1980 and 1981 show temperatures above 20 deg C for periods of several weeks during the summers of both 1980 and 1981.

SOW is defined (Conomos et al. 1972) as the warmest water of near-oceanic salinity in the area. Pure SOW is found in the top 15 m more than 15 km offshore. SSOW is the coldest and most saline water type. It is generally found at least 20 to 30 m below the surface. It is closest to the surface inshore, because of coastal and river plume-induced upwelling. The temperature and salinity characteristics of SOW and SSOW are defined in Table 7.

Processes within the estuary are sufficiently variable, that is difficult to define "typical" T-S digrams. A T-S diagram for a near bottom current meter off Clatsop Spit for an upwelling situation illustrates the influence of RW, SOW and SSOW (Figure 35). The mixing of RW and SOW defines one line, and the mixing of SSOW and SOW defines another. In the absence of upwelling offshore, only the line defining mixing between RW and SOW would appear. It is interesting that very little mixing takes place between SSOW and RW. Were such mixing occurring, the T-S pattern would more closely resemble a triangle. Such mixing does occur at meters closer to the surface during the same period.

---

\*Personal communication, R. J. McConnell, NMFS, Hammond, Or.

Table 7. Defining properties of Surface Ocean Water (SOW) and Subsurface Ocean Water (SSOW), near mouth of Columbia River.

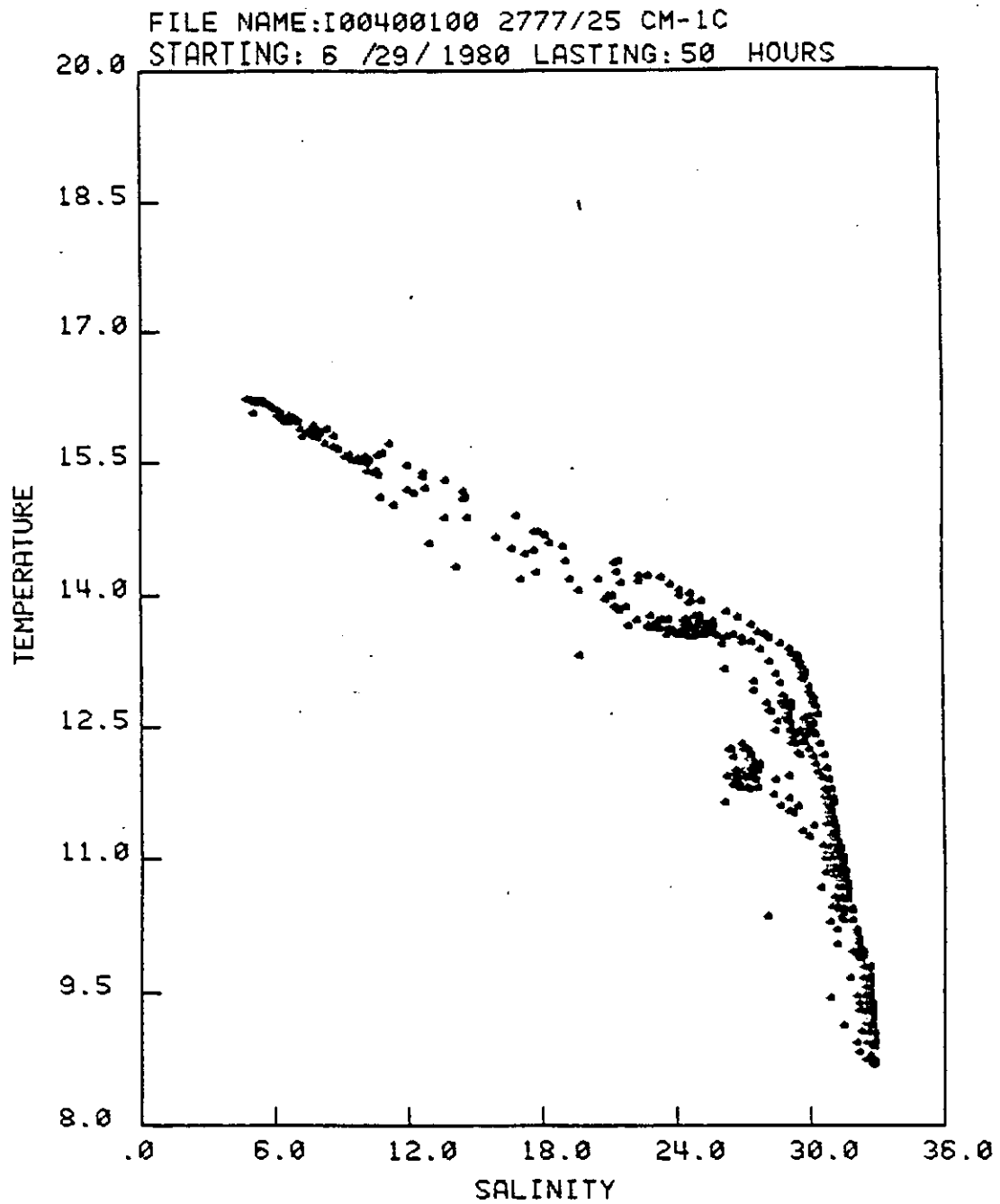
	<u>SOW</u>		<u>SSOW</u>	
	<u>Salinity ppt</u>	<u>Temp °C</u>	<u>Salinity ppt</u>	<u>Temp °C</u>
June 11-20, 1965*	31.76 ± 0.1	12.8 ± 0.2	33.64 ± 0.17	7.57 ± 0.13
Sept. 14-26, 1965*	31.92 ± 0.45	13.6 ± 0.3	33.36 ± 0.21	7.80 ± 0.11
June 15-20, 1966*	31.65 ± 0.55	12.5 ± 0.7	33.76 ± 0.09	7.25 ± 0.16
Aug. 13-23, 1966*	31.78 ± 0.85	13.83 ± 0.86	33.63 ± 0.23	7.49 ± 0.21
Jan. 13-Feb. 20, 1958†	32.0 - 32.5	10.2 - 10.9	not observed	

\*from Conomos et al., 1972

†from U.S. Navy Hydrographic Office, 1960



Figure 35. The mixing of RW with SOW, and SOW with SSOW.



### 3.5.2 Seasonal-Average Salinity Distributions

All available data for March 25 to October 31, 1980, and April 30 to October 31, 1981, were used to construct high and low-flow seasonal mean, minimum, and maximum salinity distributions for the North and South channels. The seasonal mean flow for the high-flow season was  $\sim 310$  kcfs ( $\sim 8800$  m<sup>3</sup>/s); that for the low-flow season was  $\sim 155$  kcfs ( $\sim 4400$  m<sup>3</sup>/s). The winter salinity distribution is not presented, because insufficient winter data are available.

Some biological processes have time scales of weeks to months and may be expected to respond to the seasonal average salinity. The analysis of Section 1.1, however, emphasized the importance of non-linear processes in maintaining the circulation and salinity distributions. Many biological processes are undoubtedly also non-linear. The response of a non-linear process to average conditions is not likely to be the same as the average of the (non-linear) responses to the series of individual states that form the average. Great care should be exercised in drawing conclusions concerning the circulatory and other processes from the average salinity distributions; The observed time series of salinity are more indicative of circulatory processes and may be more useful for biological studies as well.

#### The High-Flow Season

Figures 36a, and b and 37a and b show the high-flow ( $\sim 310$  kcfs or  $8,800$  m<sup>3</sup>/s) season maximum and mean salinity distributions for the South and North channels, respectively. No minimum salinity plots are shown because the salinity is known (Section 3.5.4) to go to zero above  $\sim$ RM-2 on the ebb tide under spring tide, freshet conditions, although this condition was not actually observed during the 1980-81 period.

The mean salinity plots for the high-flow season show substantial top to bottom salinity differences (10 to  $>20$  ppt), and the stratification is fairly uniform with depth (Figures 36b and 37b). The mean horizontal salinity gradient (Figure 38) is somewhat variable with depth and horizontal distance, but the apparent uniformity of the salinity distribution is largely a result of the averaging. The density structure at most times during the high-flow seasons shows sharp horizontal and vertical gradients. The stratification and horizontal salinity gradient are less uniform in the maximum salinity case than the mean salinity case, because of the salt-wedge like structure of the incoming flow.

The mean salinity plots show some influence of the sills in both channels, between RM-6 and RM-9. There is also greater maximum salinity intrusion in the North Channel at mid-depth than in the South Channel, despite the very shallow sill depths. This results from greater freshwater flow volume in the North Channel. That the maximum salinity (Figure 39) for the high-flow season is greater between RM-6 to RM-11 than that for the low-flow season probably reflects the greater importance of baroclinic circulation in this part of the estuary and seasonal differences in upwelling. Note also that the salinity range exceeds 30 ppt between  $\sim$ RM-8 and  $\sim$ RM-13. Salinity ranges up to 33 ppt occasionally occur at individual current meters during a single tidal day.

#### The Low-Flow Season

Figures 40a to c and 40d to f show the minimum, maximum, and mean salinity distributions for the low-flow season ( $\sim 155$  kcfs or  $\sim 4,400$  m<sup>3</sup>/s) for the South and North Channels, respectively. Top to bottom salinity differences are less ( $\sim 5$  to  $\sim 15$  ppt), the slope of the isohalines is sharper, the horizontal density gradients are weaker, and the mean salinity intrusion length ( $\sim 25$  miles) is much greater than in the high-flow season. The maximum salinity (Figure 40b) suggests salinity intrusion of  $\sim 5$  ppt to Pillar Rock (RM-27) and beyond. Minimum salinity intrusion is substantial, and North Channel-South Channel

Figure 36. Maximum (a) and mean (b) salinity for the South Channel for the high flow season (mean river flow 310 kcfs or 8778 m<sup>3</sup>/s), based on all available 1980 and 1981 data.

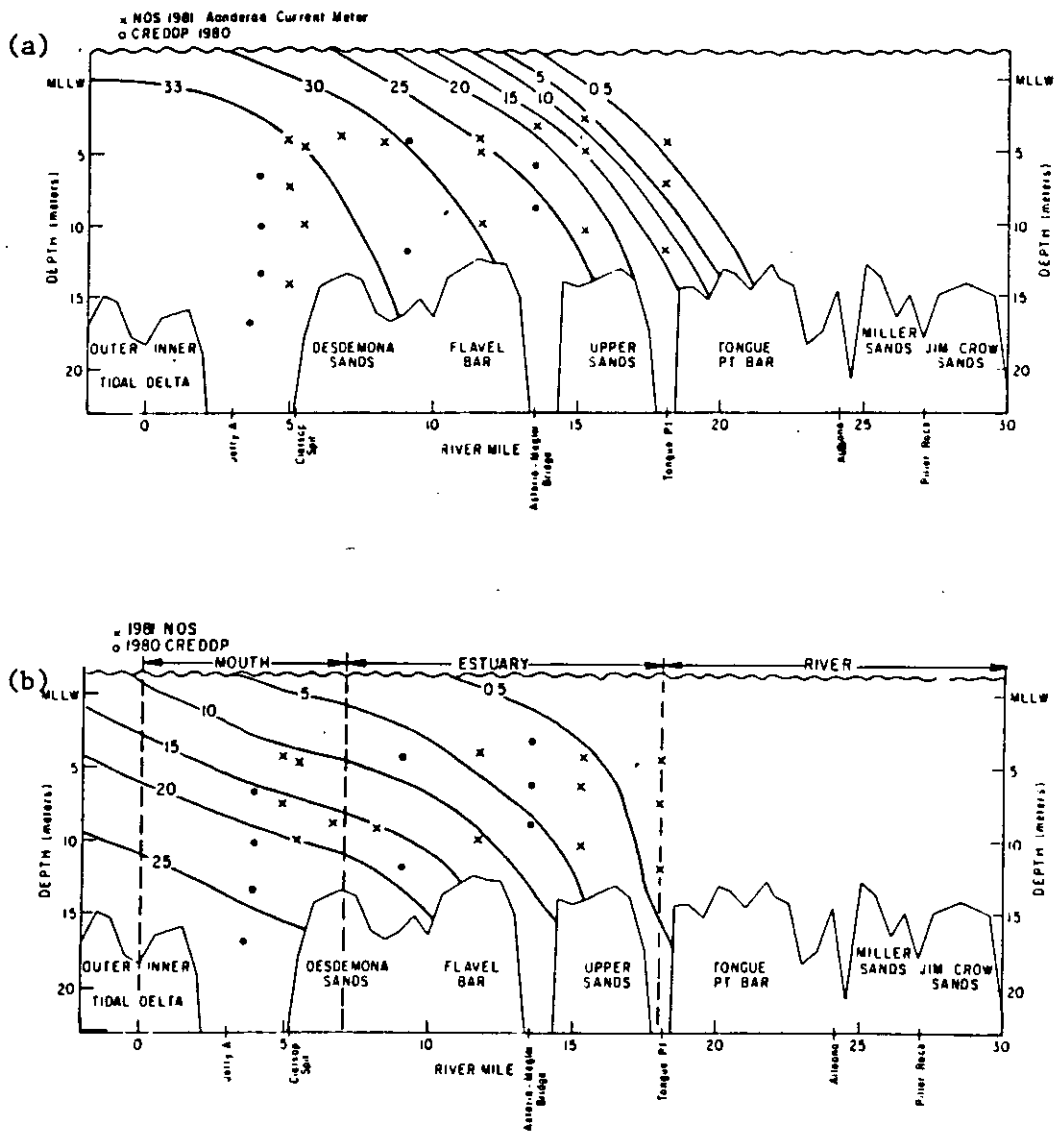


Figure 37. Maximum (a), and mean salinity (b), for the North Channel for the high flow season (mean river flow 310 kcfs or 8778 m<sup>3</sup>/s), based on all available data.

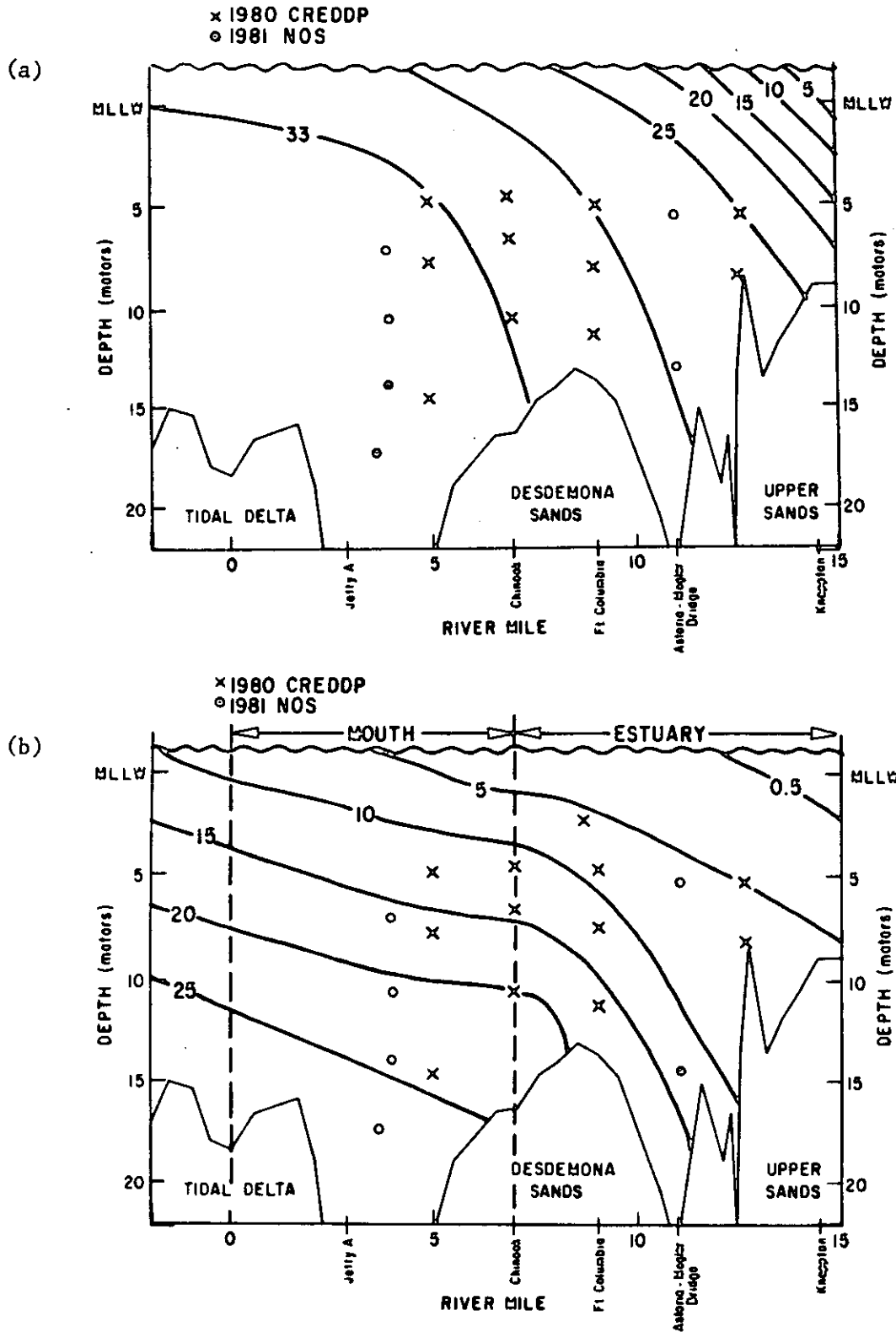


Figure 38. Seasonal mean salinity at MLLW and 12m in the South Channel for the high flow season (310 kcfs) and the low flow season (155 kcfs), based on all 1980-81 data.

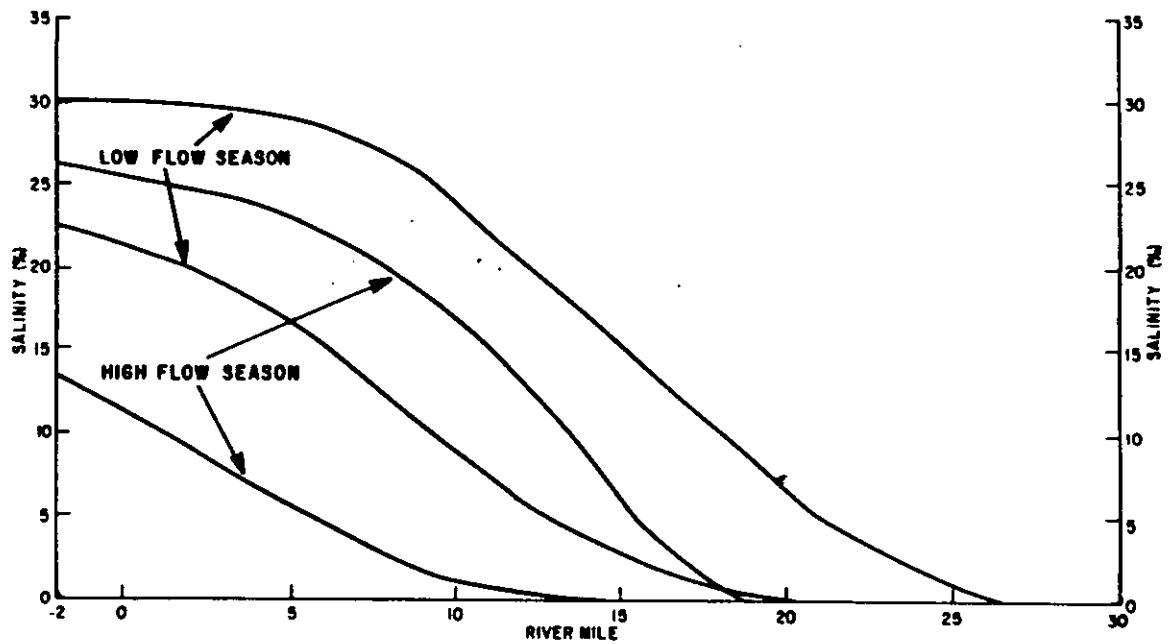


Figure 39. Seasonal minimum and maximum salinity in the South Channel for the high flow seasonal (310 kcfs) and the low flow seasonal (155 kcfs).

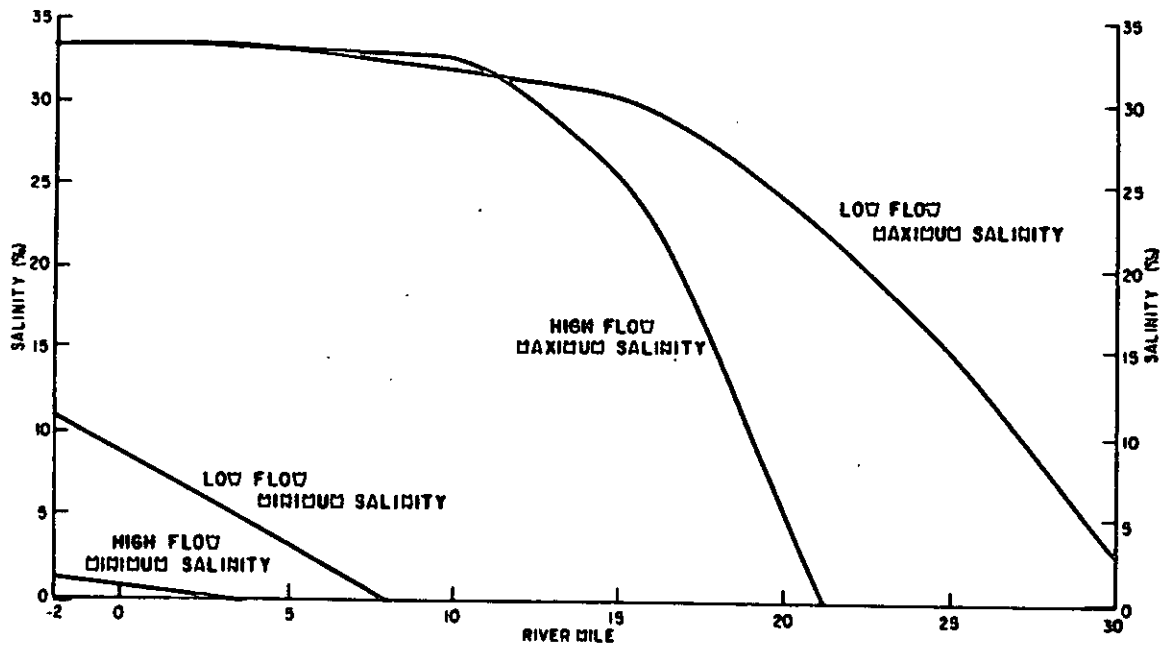


Figure 40. Seasonal (a) minimum, (b) maximum and (c) mean salinity in the South Channel and (d) to (f) in the North Channel for the low-flow season (155 kcfs).

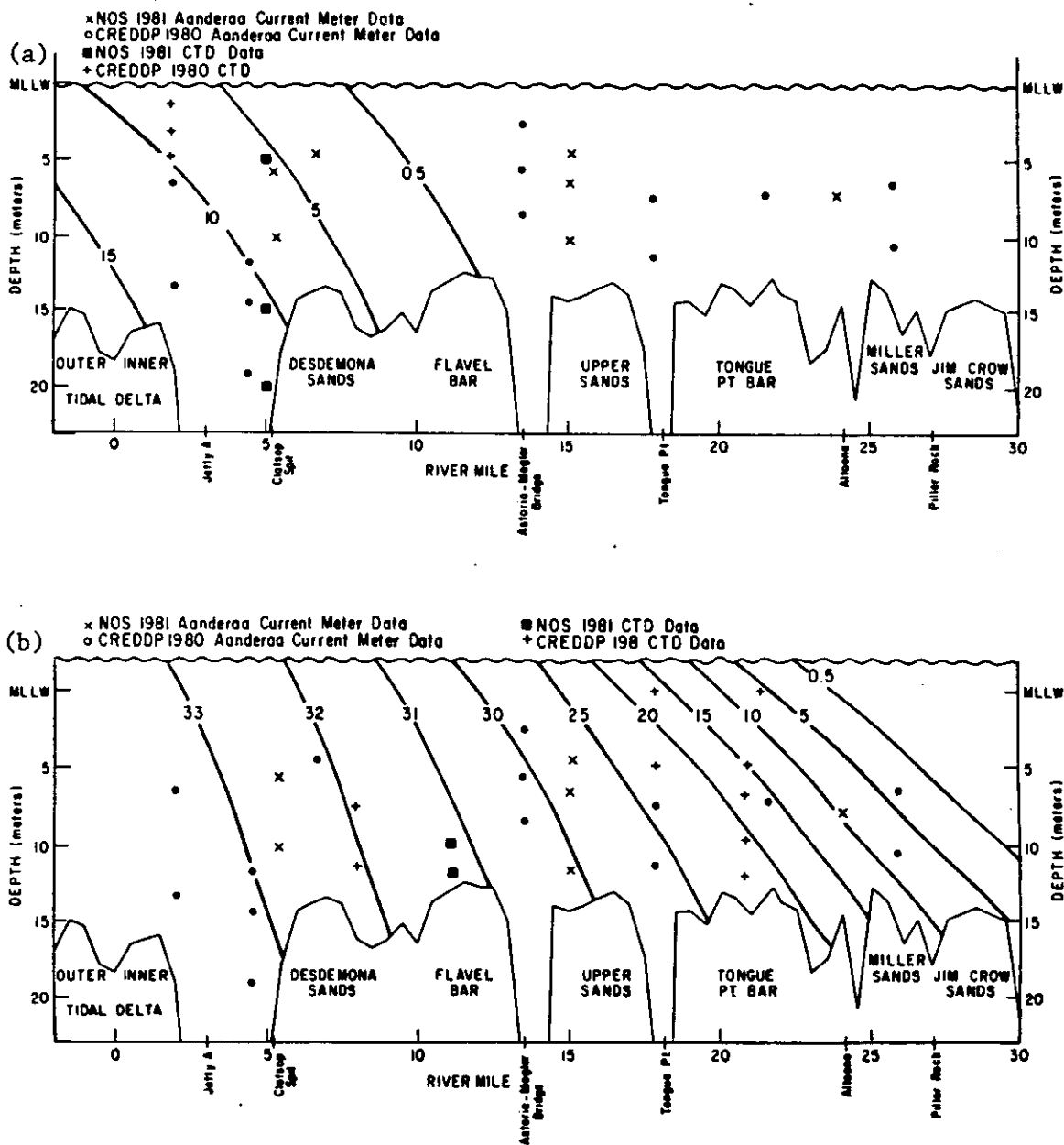


Figure 40. (continued).

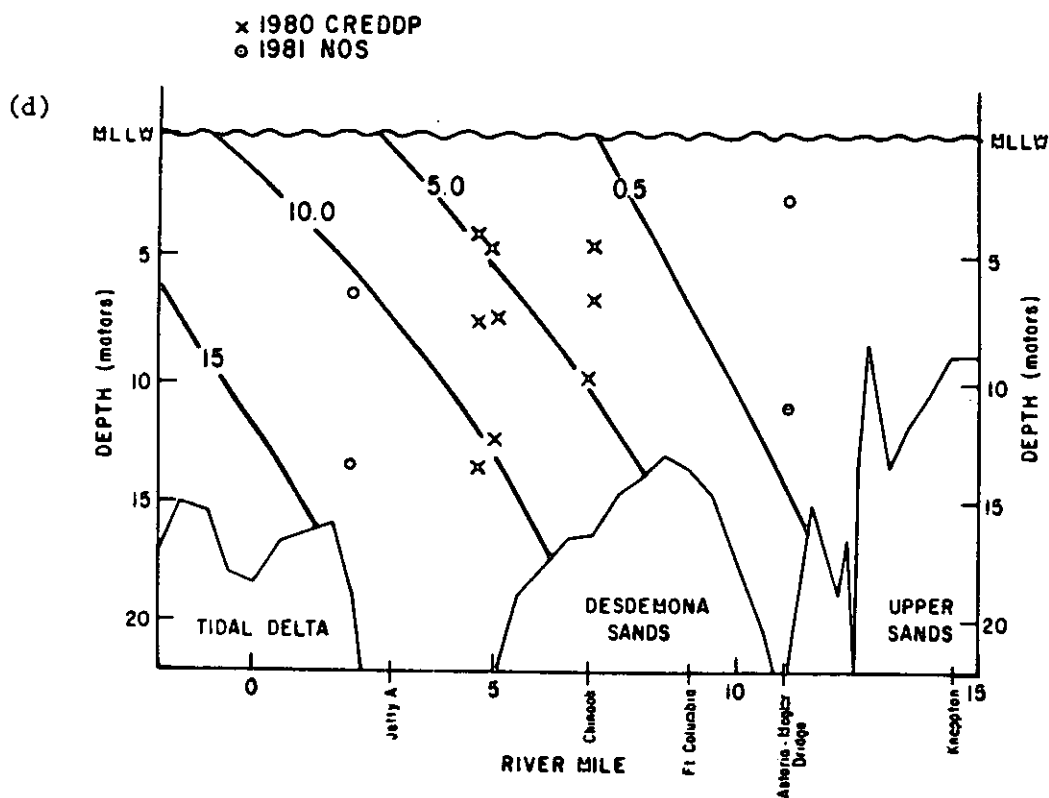
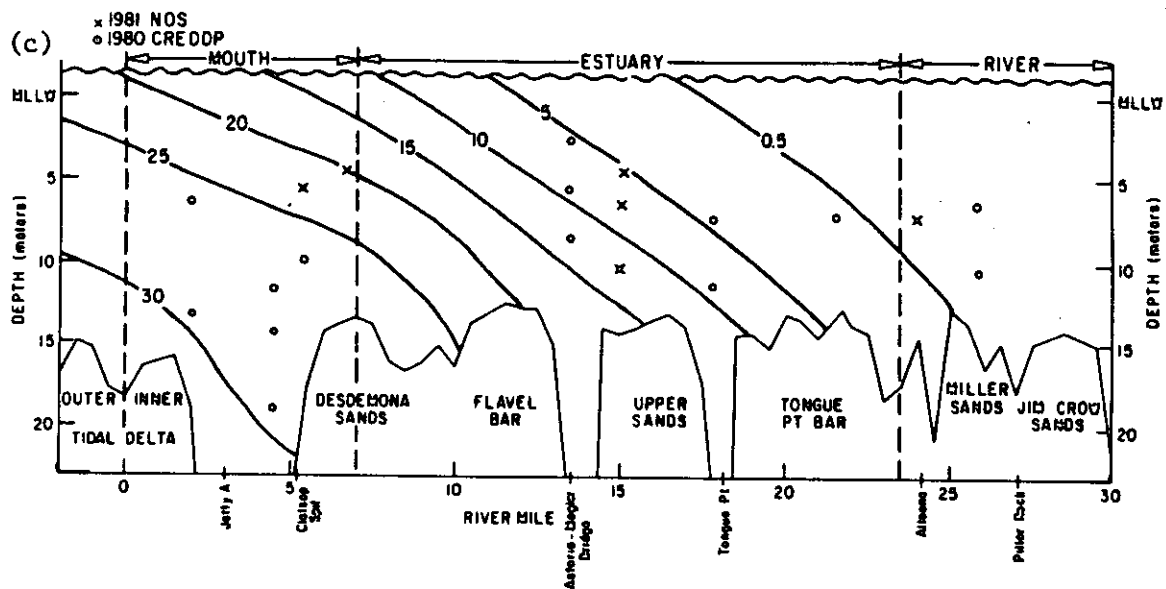




Figure 40. (continued).

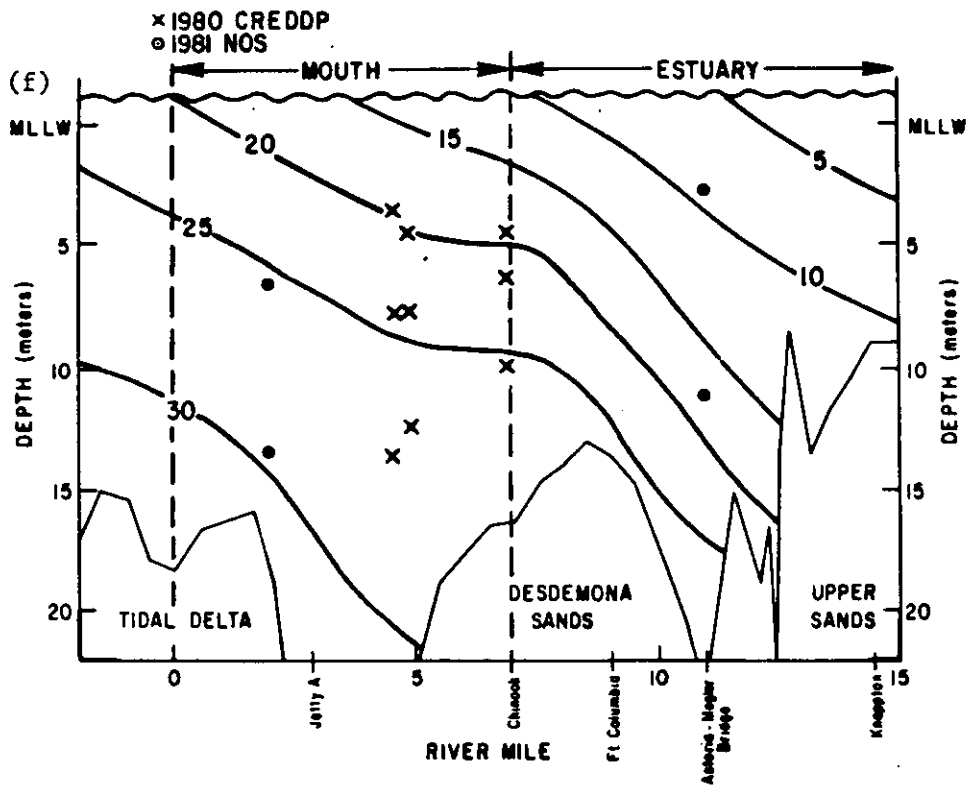
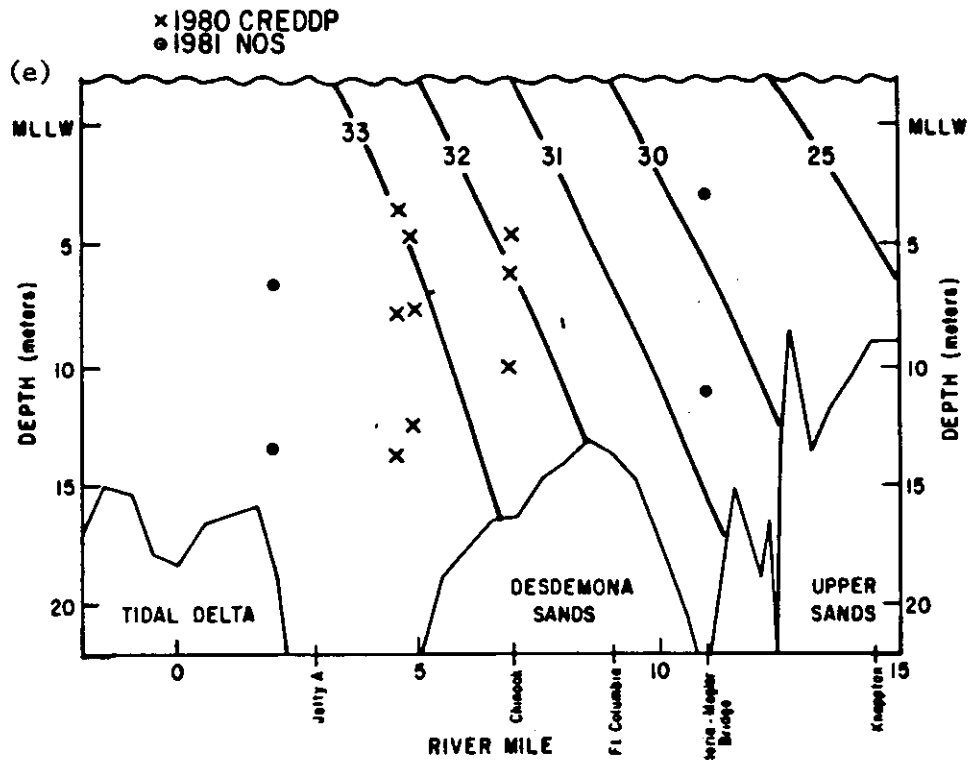


Table 8. Salinity characteristics, Columbia River Estuary at Astoria-Megler Bridge, selected spring and neap tides, March - October 1980.

A. Low Flow Neap Tides

<u>Station Data</u>				<u>Salinity Results, ppt</u>				<u>Diurnal Tide Range</u>	<u>Riverflow</u>
<u>Station</u>	<u>Meter</u>	<u>Depth, M</u>	<u>Date</u>	<u>Mean</u>	<u>Minimum</u>	<u>Maximum</u>	<u>Range</u>	<u>Meters</u>	<u>CFS x 10<sup>3</sup></u>
5B	4422/51	15	7/21/80	24.97	14.60	30.73	16.13	2.0	160
5A	4423/6	9	"	20.79	5.57	29.27	19.58	2.0	160
5A	2776/11	3	"	2.99	0.07	9.96	9.89	2.0	160
5B	4422/51	15	8/19/80	22.51	11.61	29.03	17.42	2.0	130
5A	4423/6	9	"	18.24	7.65	26.71	19.06	2.0	130
5A	2276/11	3	"	7.48	3.31	15.52	12.21	2.0	130
5B	4423/7	15	10/17/80	22.65	7.11	28.51	21.40	2.0	140
5A	2276/12	9	"	19.25	7.10	28.59	21.49	2.0	140
5A	4422/100	3	"	7.81	2.60	15.26	12.66	2.0	140
5B	1665/13	15	4/8/80	19.96	2.18	26.81	24.63	2.1	170
5A	2775/10	9	"	14.05	3.06	24.60	21.54	2.1	170
5A	3227/7	3	"	4.00	0.85	10.68	9.83	2.1	170

Table 8. (continued)

B. Low Flow Spring Tides

<u>Station Data</u>				<u>Salinity Results, ppt</u>				<u>Diurnal Tide Range</u>	<u>Riverflow</u>
<u>Station</u>	<u>Meter</u>	<u>Depth, M</u>	<u>Date</u>	<u>Mean</u>	<u>Minimum</u>	<u>Maximum</u>	<u>Range</u>	<u>Meters</u>	<u>CFS x 10<sup>3</sup></u>
5B	4422/51	15	7/28/80	18.51	3.22	30.49	27.27	3.1	160
5A	4423/6	9	"	13.18	1.70	28.22	26.52	3.1	160
5A	2776/11	3	"	8.10	1.19	23.23	22.04	3.1	160
5B	4422/51	15	8/10/80	18.33	4.50	29.81	25.31	2.9	150
5A	4423/6	9	"	13.66	3.70	25.07	21.37	2.9	150
5A	2776/11	3	"	8.95	1.92	22.10	20.18	2.9	150
5B	4422/51	15	8/26/80	16.10	3.01	29.66	26.65	3.0	112
5A	4423/6	9	"	12.08	1.45	24.38	22.93	3.0	112
5A	2776/11	3	"	8.77	0.91	21.08	20.17	3.0	112
5B	4423/7	15	10/24/80	16.41	3.25	30.22	26.97	3.4	140
5A	2776/12	9	"	12.81	1.53	24.37	22.84	3.4	140
5A	4422/100	3	"	9.81	0.99	24.65	23.66	3.4	140

Table 8. (continued)

C. Moderate Flow Neap Tides

<u>Station Data</u>				<u>Salinity Results, ppt</u>				<u>Diurnal Tide Range</u>	<u>Riverflow</u>
<u>Station</u>	<u>Meter</u>	<u>Depth, M</u>	<u>Date</u>	<u>Mean</u>	<u>Minimum</u>	<u>Maximum</u>	<u>Range</u>	<u>Meters</u>	<u>CFS x 10<sup>3</sup></u>
5B	1665/13	15	4/22/80	18.17	1.13	26.44	25.31	2.0	200-220
5A	3227/7	3	"	1.29	0.00	4.67	4.67	2.0	200-220
5B	1665/13	15	5/5/80	14.66	0.05	26.14	26.09	2.3	290
5A	3227/7	3	"	1.77	0.00	7.69	7.69	2.3	290
5B	4422/50	15	6/20/80	21.38	3.99	28.05	24.06	1.7	360
5A	4423/5	9	"	11.16	0.59	26.43	25.84	1.7	360
5A	2776/10	3	"	2.03	0.06	10.81	10.75	1.7	360

110

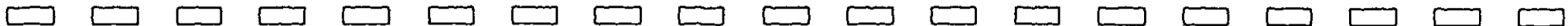


Table 8. (continued)

D. Moderate Flow Spring Tides

<u>Station Data</u>				<u>Salinity Results, ppt</u>				<u>Diurnal Tide Range</u>	<u>Riverflow</u>
<u>Station</u>	<u>Meter</u>	<u>Depth, M</u>	<u>Date</u>	<u>Mean</u>	<u>Minimum</u>	<u>Maximum</u>	<u>Range</u>	<u>Meters</u>	<u>CFS x 10<sup>3</sup></u>
5B	4422/50	15	6/29/80	13.26	0.01	28.16	28.15	3.0	300
5A	4423/5	9	"	6.03	6.00	25.14	25.14	3.0	300
5A	2776/10	3	"	2.04	0.01	10.77	10.76	3.0	300
5B	4422/51	15	7/11/80	12.02	0.10	25.53	25.43	3.2	220
5A	4423/6	9	"	6.91	0.00	21.43	21.43	3.2	220
5A	2776/11	3	"	3.50	0.00	14.45	14.45	3.2	220
5B	1665/13	15	4/15/80	10.99	0.00	28.07	28.07	3.3	190
5A	3227/7	3	"	3.29	0.00	15.82	15.82	3.3	190

Figure 41. October 1980 neap tide (a) minimum, (b) maximum and (c) mean salinity and (d) salinity range for the south channel.

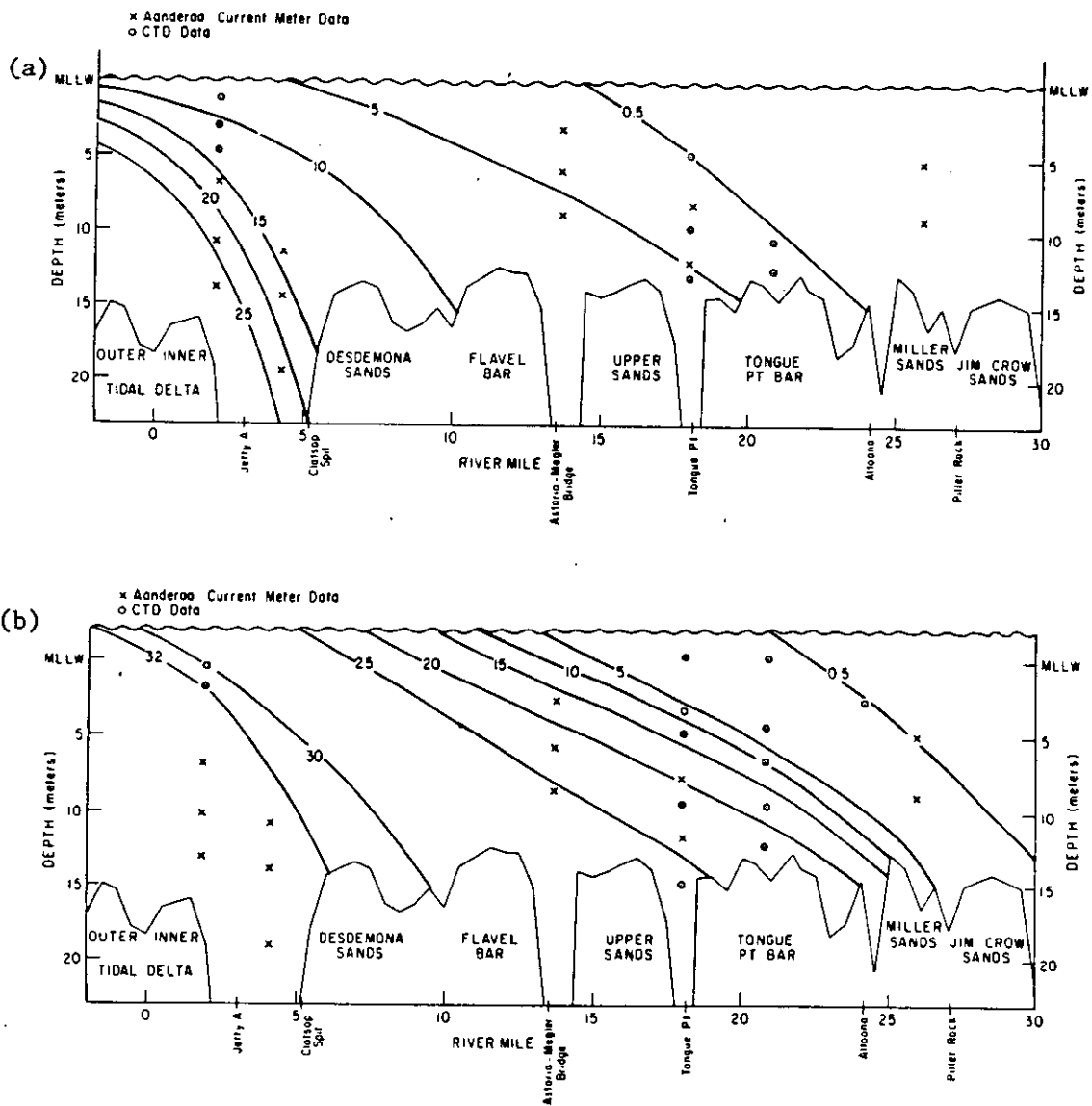
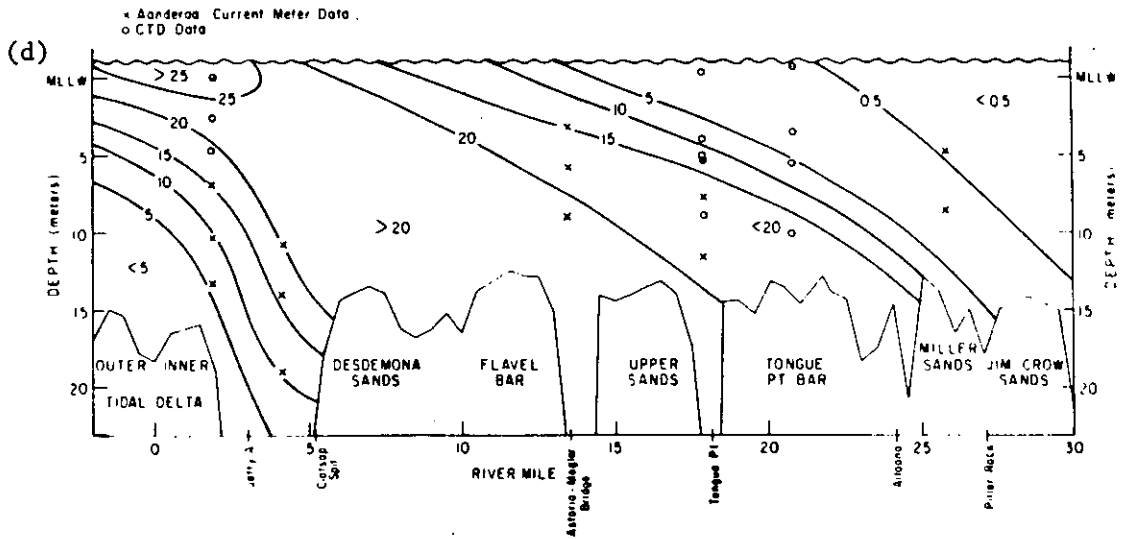
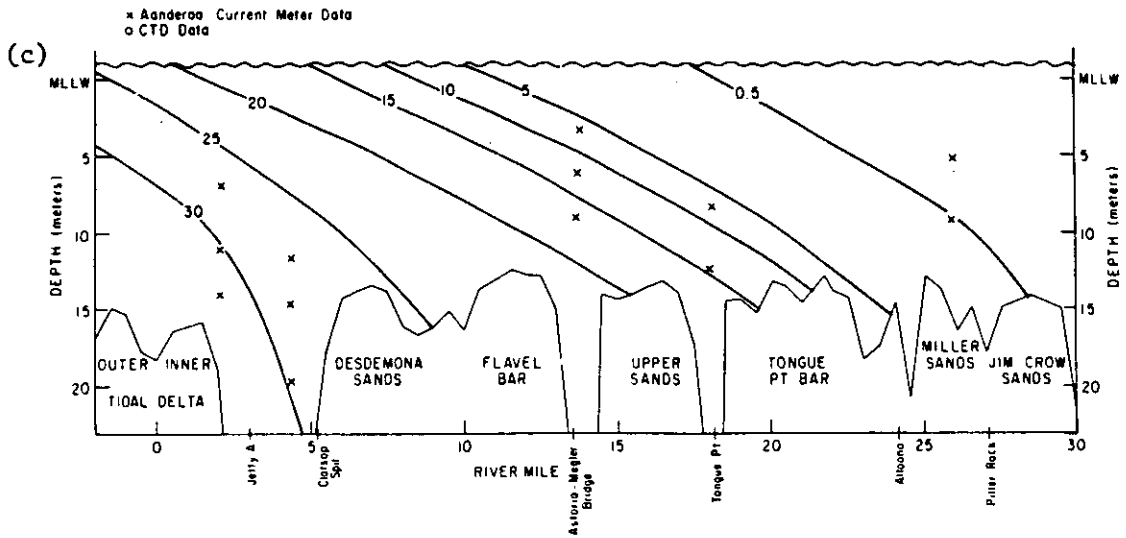


Figure 41. (continued).



differences are less prominent. The mean salinity gradient (Figure 38) is less variable than in the high-flow case, but far from constant. The extreme salinities (Figure 39) indicate that the mean salinity provides a poor indication of the behavior of the system for both seasons.

### 3.5.3 The Low-Flow Salinity Distribution

Strong neap-to-spring transitions in the salinity distribution occur during low-flow periods (McConnell et al. 1981; Jay 1982). An example of this transition is provided by the profile and current meter data for October 1980. The riverflow during the period was 120 to 150 kcfs or 3,400 to 4,250 m<sup>3</sup>/s. Further discussion of these data is presented in Jay (1982). This low-flow period best exemplifies the neap-to-spring transition in mixing processes that occurs during most low-flow periods.

#### The October 1980 Neap-Tide Period

The four-day, neap-tide period October 16 to 19 was a period of minimum vertical mixing, maximum stratification, and maximum salinity intrusion length. The minimum tidal range occurred on the night of October 16-17, with a diurnal range of <2.0 m. Comparison of maximum salinities at the Astoria-Megler Bridge for this and earlier neap tides suggests that this is one of perhaps 3 or 4 periods of maximum salinity intrusion for the year; Table 8). Plots for South Channel during this period of minimum, maximum, and mean salinity intrusion and salinity range are found in Figures 41a to d. The corresponding distribution of the mean flow, as predicted by the two-dimensional, laterally-averaged model of Hamilton (1984), is shown in Figure 28a. Minimum and maximum salinity correspond roughly to end of ebb and end of flood pictures, but the data used are not truly synoptic, because maximum salinity occurred on a later tidal cycle above Tongue Pt. than in the lower estuary.

The strength of the stratification during the neap tide period is shown in the typical late flood salinity and velocity profiles for Tongue Pt. (Figures 42a and b). The flow is divided into distinct upper and lower layers by the sharp interface at ~8 m. The lower, saline layer is still advancing slightly, and the upper layer has started to ebb. A smaller density interface occurs at ~6.4 m. On ebb, stratification is reduced, as both vertical mixing and advection reduce bottom salinity (Figure 43a and b). Early in the ebb, vertical mixing causes the salinity at mid-depth to increase despite outward advection.

Near the entrance, maximum stratification occurs at the end of the ebb, as water of oceanic salinity (>32 ppt) moves upriver beneath a surface layer that is still ebbing. It was noted in Section 3.2 that the surface ebb may continue for as much as two hours after the onset of flood, lower in the water column (Figures 25a and b). Minimum stratification occurs later on the flood, when salinities of >30 ppt occur at all depths below MLLW.

One very prominent feature of Figures 41a to d is the temporal and spatial variability of the horizontal salinity gradient  $\frac{\partial S}{\partial x}$ . The greatest horizontal gradients are found at the end of flood at and above Tongue Pt. (Figure 41b) and at the end of ebb near the entrance (Figure 41a). Strong gradients are present at each location for only part of the tidal cycle. The horizontal gradient also varies by at least a factor of five between the surface and 5 m at Tongue Pt. at the end of a flood. The lack of synopticity in the data used distorts somewhat the form of the salinity intrusion; salinity gradients ( $\frac{\partial S}{\partial x}$  and  $\frac{\partial S}{\partial z}$ ) at the head of the salt wedge are probably much sharper than shown in Figure 41b.

The observed (Figure 41d) distribution of the salinity range can be explained as the result of typical estuarine mixing processes. Nearly pure



Figure 42. (a) Salinity, temperature and sigma - t, and (b) speed and direction at station 6SA on neap tide. Weak flood prevails at bottom, but ebb has begun in the surface layer. Very strong stratification occurs at about 8m, isolating the upper layer from the influence of the bottom boundary.

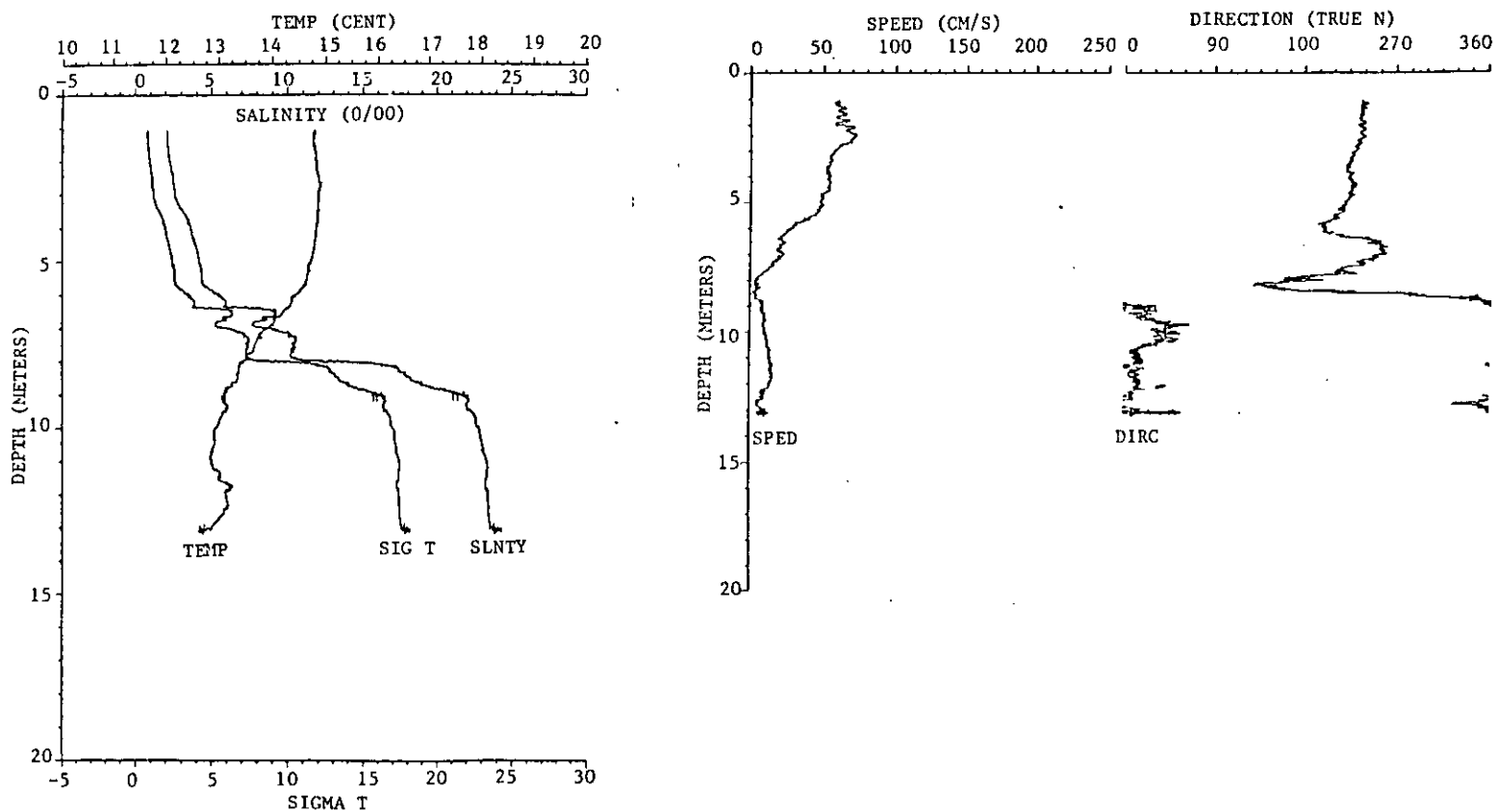
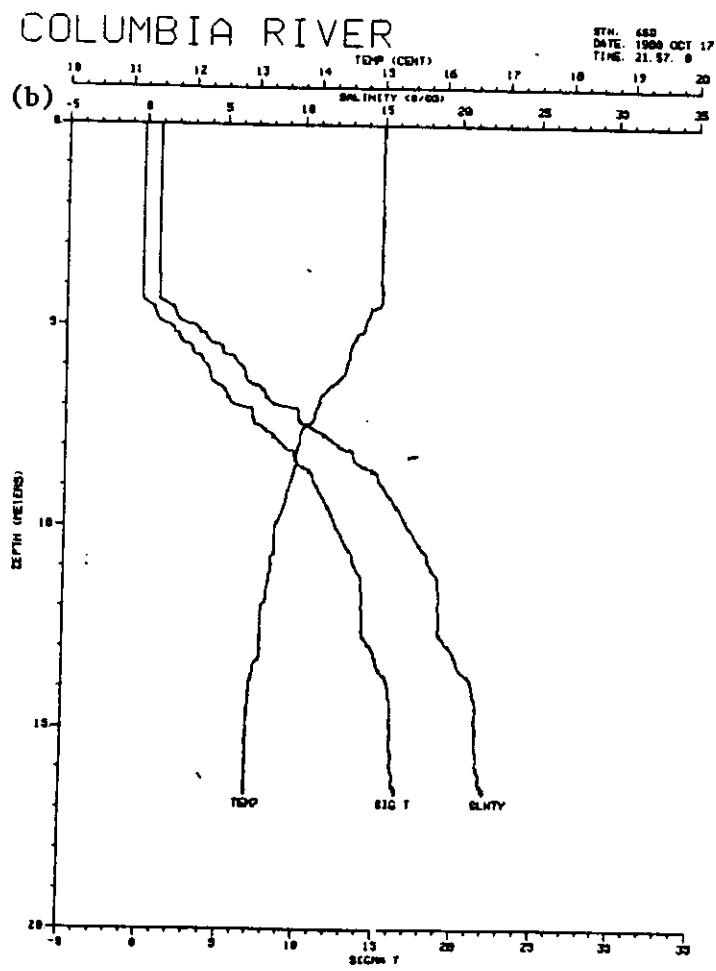
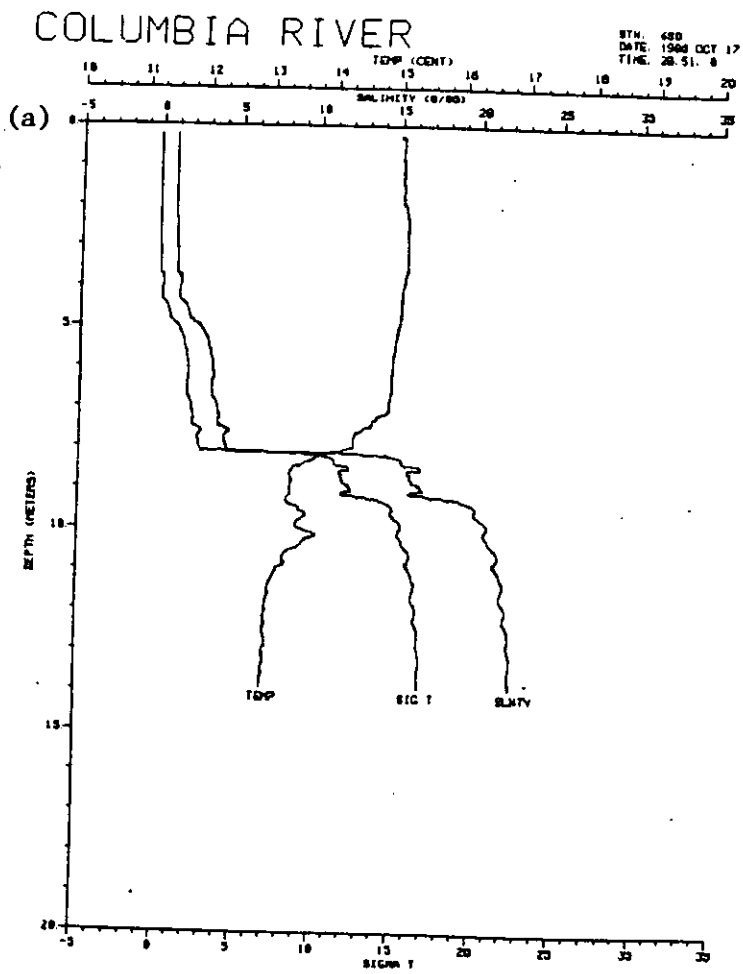


Figure 43. (a) Salinity, temperature and sigma-t (a) on late flood, and (b) on early ebb at station 6SD on neap tide. Velocities in (a) are low throughout the water column, because tide advance of the salt wedge has nearly ceased. Note multiple layers in the salt wedge. The increased energy level on ebb tide has caused substantial vertical mixing; salinity has increased between 5 and 8m in (b).



oceanic water is found at the bottom near the entrance during most stages of the tide. River water enters at the surface near the upstream end. Under conditions of weak mixing the result is an intermediate, high variance water mass that is beneath the river water at the upstream end of the estuary and over the oceanic water at the ocean end. The area down stream of the Astoria-Megler Bridge is one of very large (>25 ppt) salinity range under most conditions; the shape and position of this maximum varies.

#### The October 1980 Spring-Tide Period

The October 1980 spring-tide period was one of maximum mixing and minimum stratification. Figures 44a to d show the minimum, maximum, and mean salinity intrusion and salinity range for October 24 to 26. The mean flow predicted by the two-dimensional, laterally-averaged model (Hamilton 1984) is shown in Figure 28b. The diurnal range was >3.4 m. This condition of strong tides and low runoff probably represents the extreme well-mixed condition in the Columbia River Estuary; this period has the highest mean and maximum surface salinities and minimum mean vertical stratification at the Astoria-Megler Bridge for any 1980 spring tide for which data are available (Table 8). Contours in Figures 44a to d are accordingly more nearly vertical than during other periods.

The differences between Figures 41a to d for the neap tide and Figures 44a to d for the spring tide stem from greater vertical mixing and greater tidal excursion on spring tide. The shorter salinity intrusion length and lesser stratification on spring tide are caused by the greater vertical mixing. The increased vertical mixing is clearly evident in the salinity and velocity profiles taken near Hammond (Figures 45a and b). The velocity profile (Figure 45b) is that of a turbulent boundary layer modified by weak stratification. The decreased ebb bottom salinities at the entrance on the spring tide (Figure 44a) are related to both the increased vertical mixing and the greater excursion.

The spring-to-neap differences in extreme (Figure 46) and time-averaged (Figure 47) salinities emphasize the difference in salinity intrusion length and in dynamics. Salinity intrusion on the neap tide was ~7 to 8 RM further than on spring tide. The spring and neap mean salinities of Figure 46 should be contrasted to Figure 3a; only the time averaged spring tide salinity gradient (Figure 47) is comparable to Figure 3a. The spring tide salinity gradient is more uniform than the low-flow mean conditions (Figure 38), because of the strong vertical mixing on a spring tide. The neap tide mean salinity gradient is much more variable than the spring tide mean because of the weaker mixing and stronger baroclinic circulation on neap tide.

#### 3.5.4 The High-Flow Salinity Distribution

High riverflows in excess of 500 kcfs ( $14,130 \text{ m}^3/\text{s}$ ) occur only a few days per year under the present flow regulation system. Salinity data are available for only two such periods, June 18-20, 1959, a spring tide, and June 9-12, 1981, a neap tide. The major difference between these two periods is not the difference in tidal range; it is that the flow was nearly steady in June 1959, but varied rapidly between June 7 and June 15, 1981.

##### Steady, High River Flow

Salinity intrusion during periods of steady, high riverflow can be investigated using data from June 1959, during which time the riverflow was 535 to 570 kcfs ( $15,150$  to  $16,140 \text{ m}^3/\text{s}$ ). Figures 48a and b are based on data collected from boats over a three-day period and show the maximum and mean salinity during this period. The lack of synopticity is important, because the tidal range increased from ~2.8 to ~3.1 m (spring tide) during the observation period, and because a change in offshore water masses occurred. Salinities of >33 ppt were

Figure 44. (a) minimum, (b) maximum and (c) mean salinity and (d) salinity range in the South Channel for the October 1980 spring-tide period. Salinity intrusion length and stratification are both less than on neap tide.

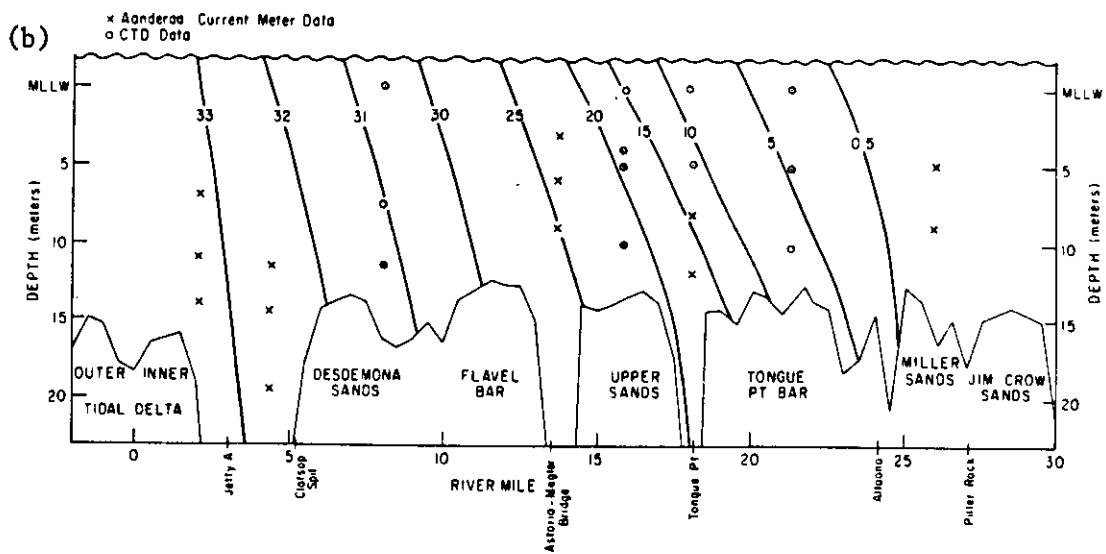
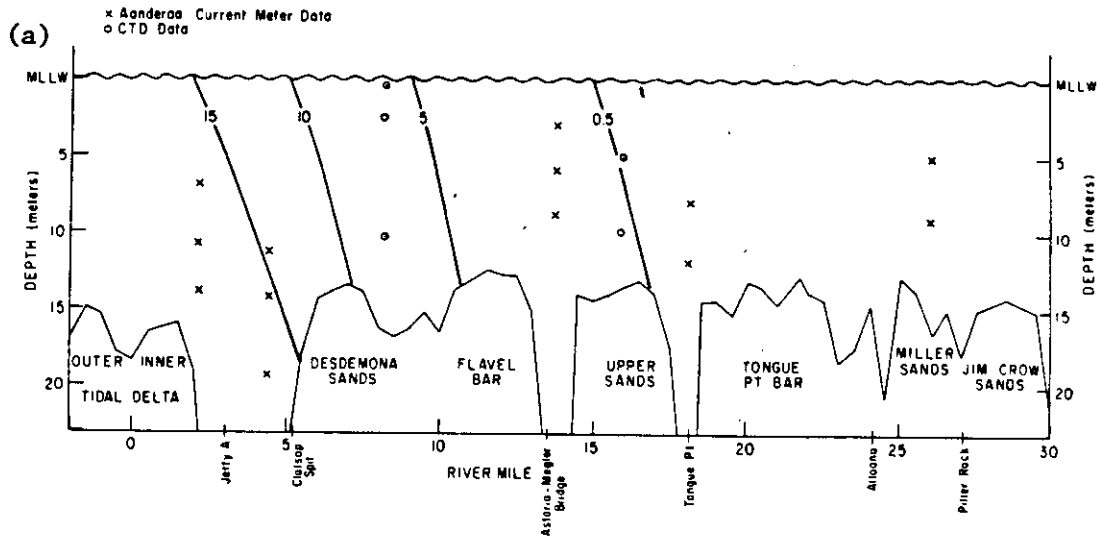


Figure 44. (continued).

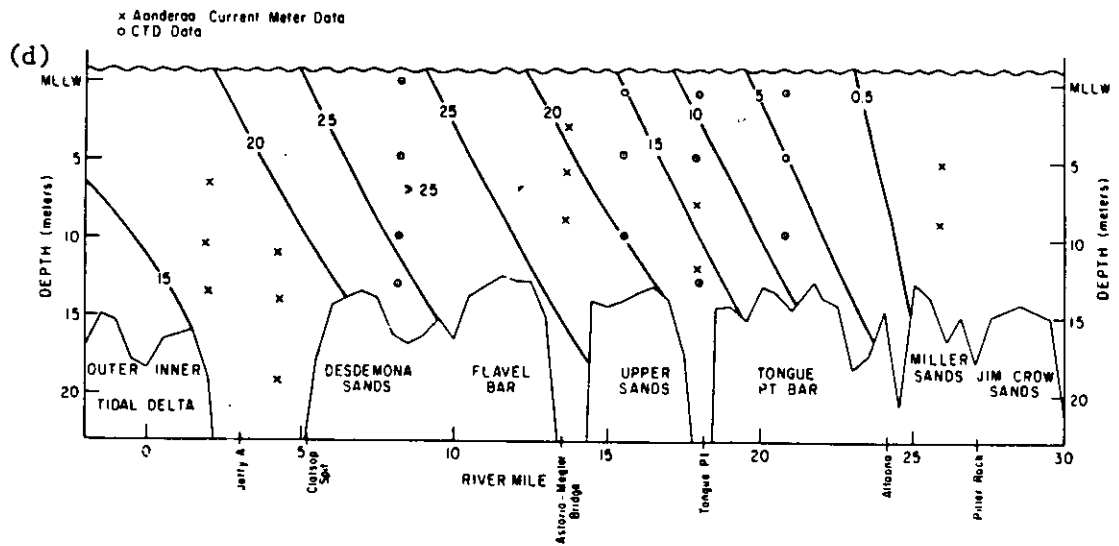
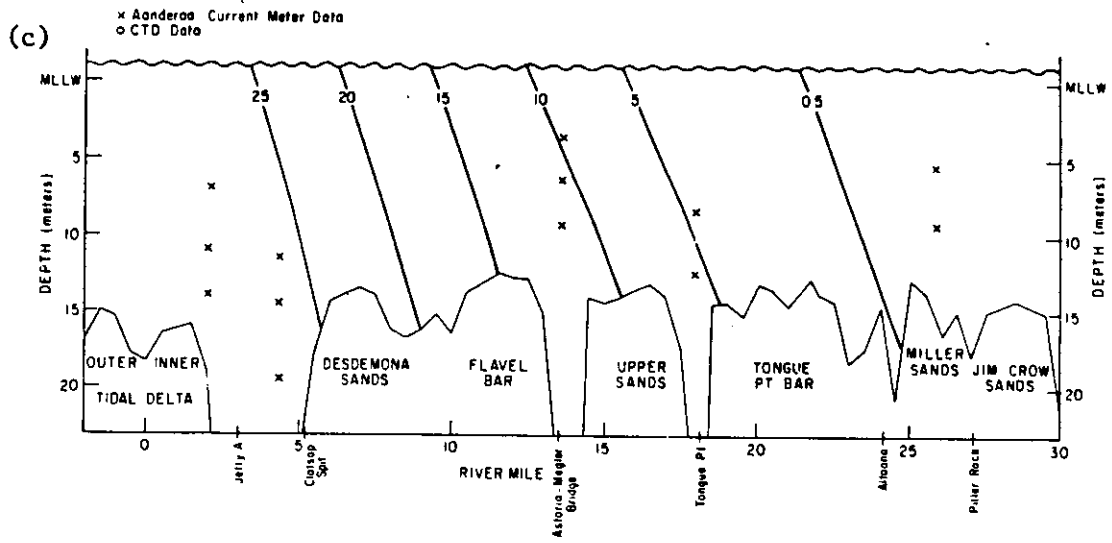


Figure 45. (a) Salinity, temperature and sigma - t, and (b) speed and direction profiles at station 4-SB during flood tide, during a period of very large tidal range. The stratification is small and much of the observed variation in the speed and direction profiles is noise introduced by surface and boat motion.

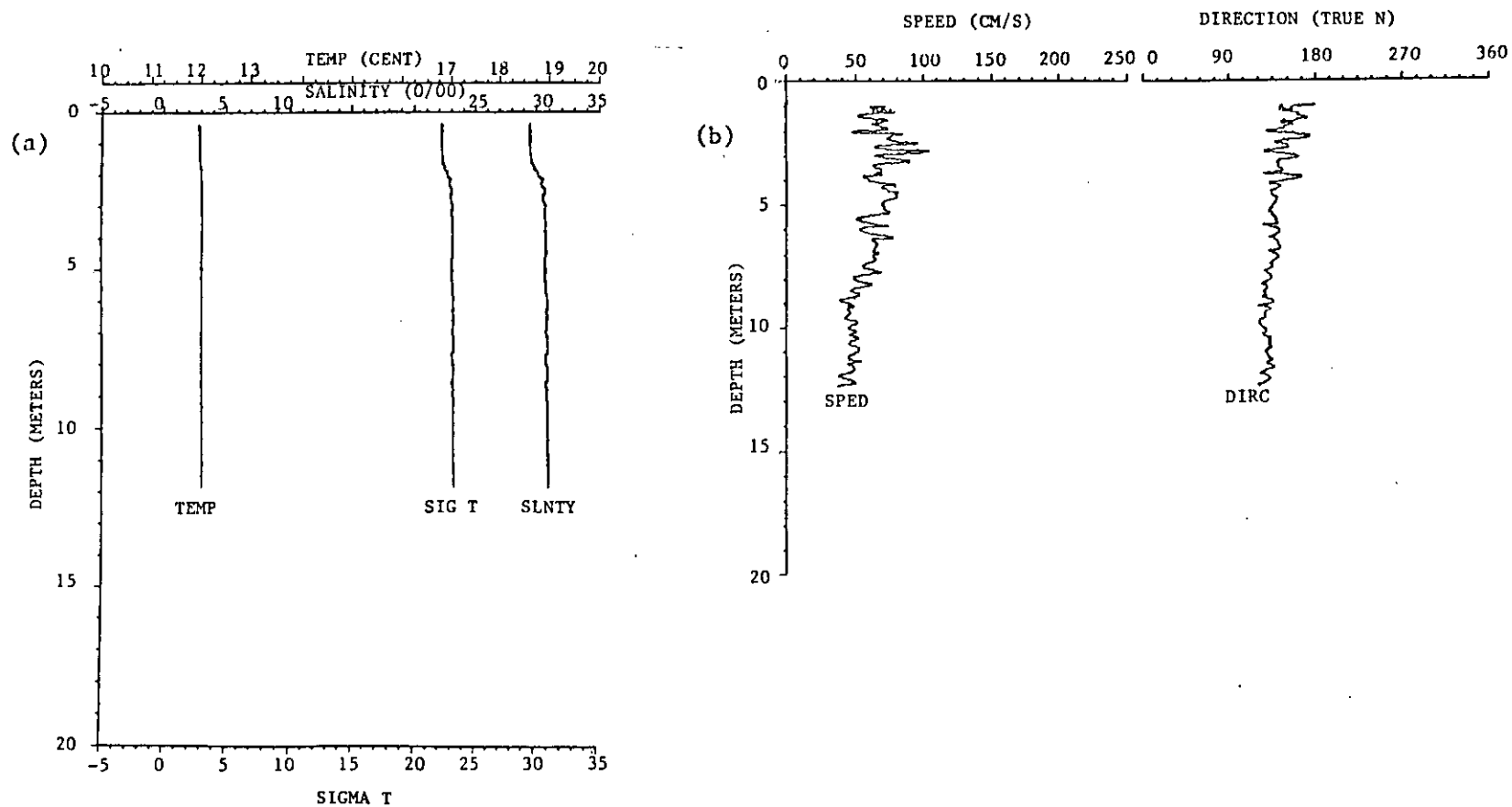


Figure 46. Maximum (above) and minimum (below) salinity intrusion for spring tide, neap tide and "event period" in October 1980; river flow 120 to 150 kcfs (3400 to 4250 m<sup>3</sup>/s). Reduced maximum salinity intrusion during the event period was caused by a wind-induced increase in surface slope.

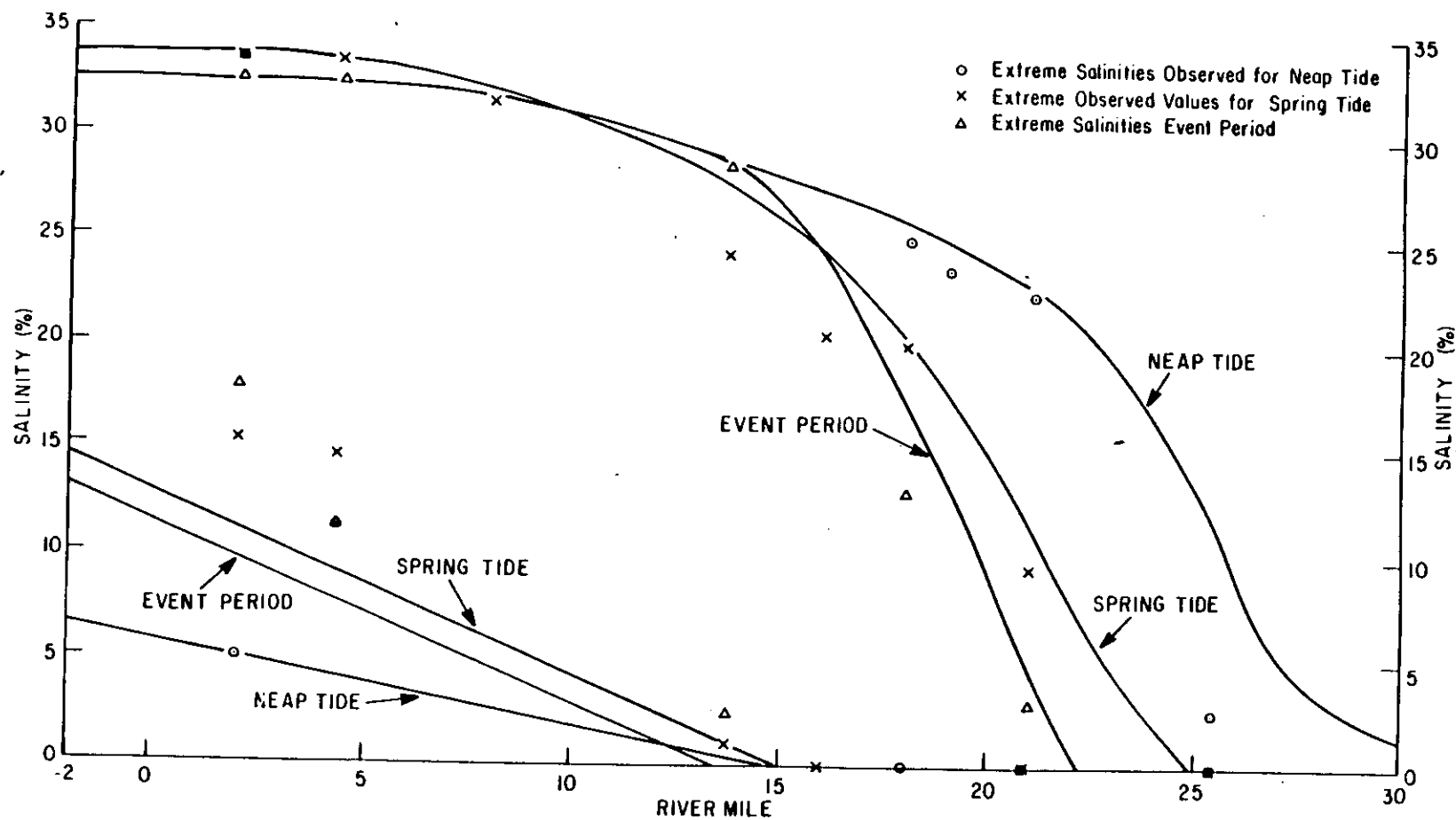


Figure 47. October 1980 mean salinity at MLLW (below) and 12 m (above) for neap and spring tide in the South Channel.

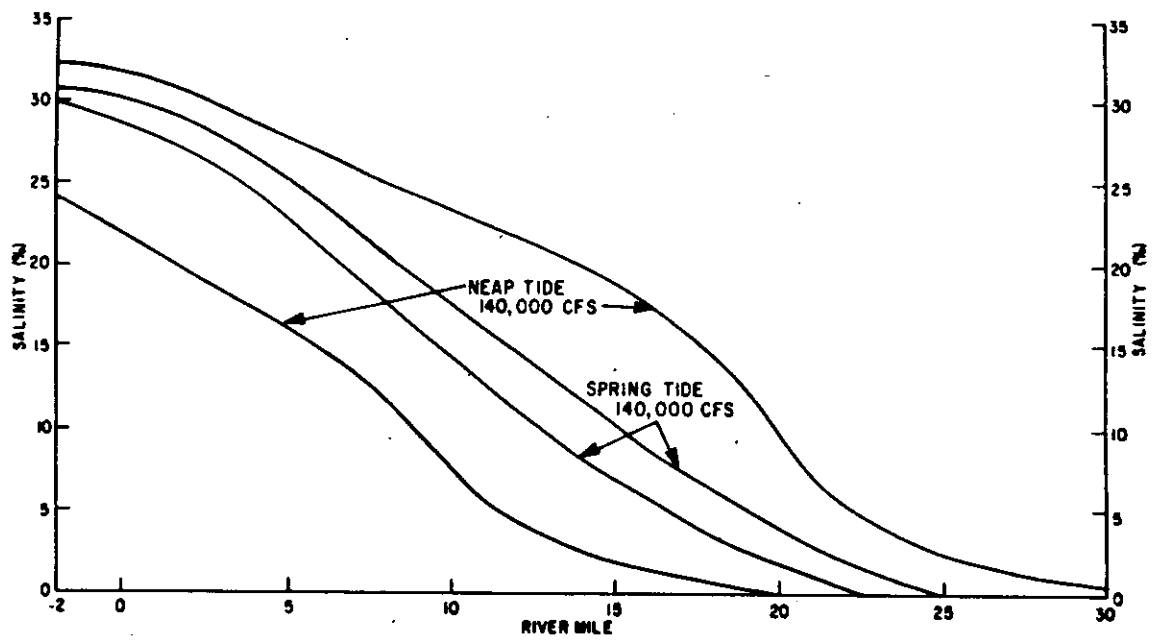




Figure 48. Maximum (a) and mean salinity (b) in the South Channel during the 1959 spring freshet, as taken from US Army Engineers (1960). Salinity was entirely absent from the system for several hours at the end of ebb.

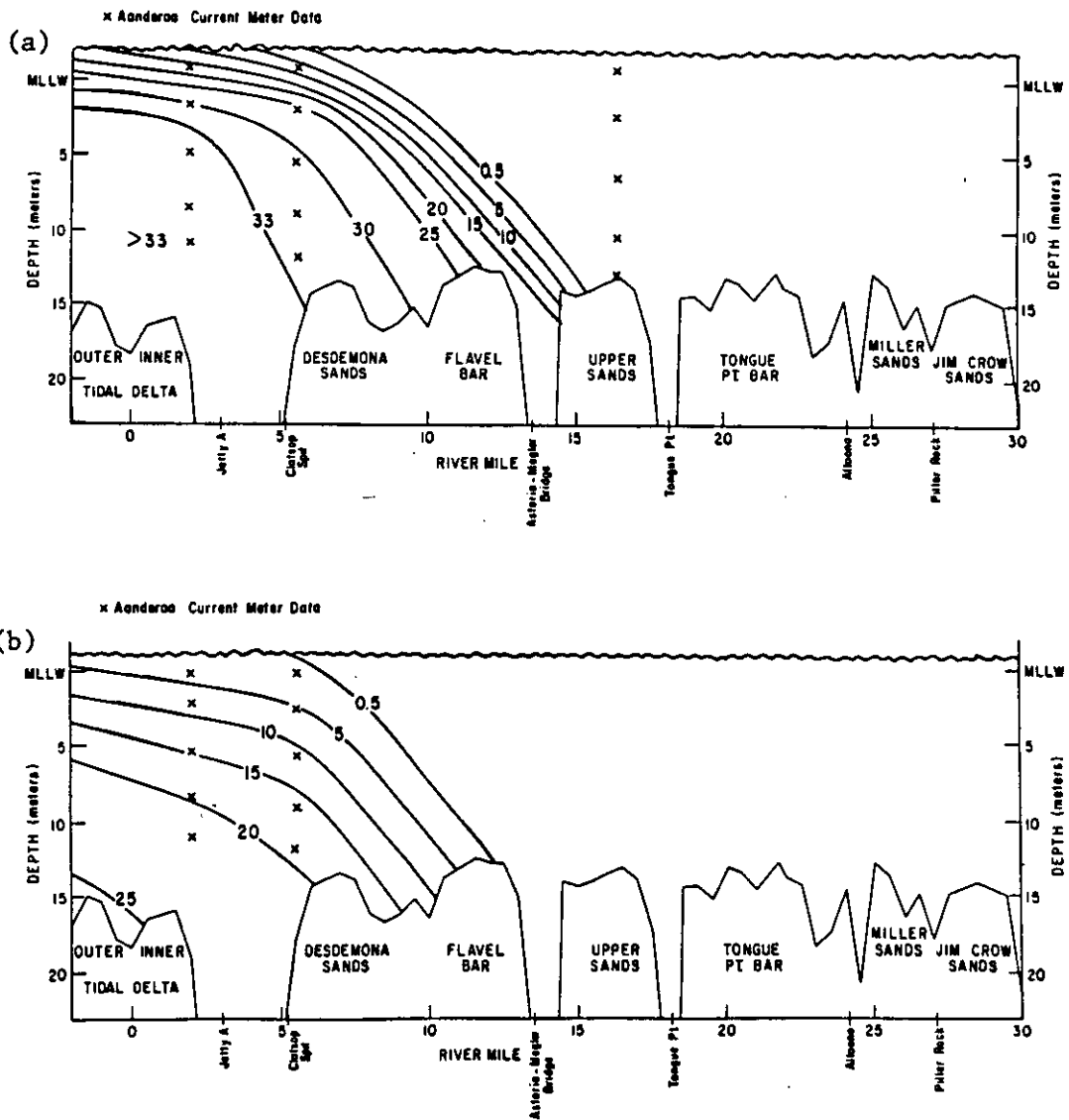


Figure 49. Acoustic Echo Sounding Profile of the Fraser River Estuary Salt Wedge. Above, a) the situation early in the ebb; below, b) the situation late in the ebb. The lower, continuous trace is the bottom, showing sand waves up to ~3m in height. The upper trace is the boat hull, and the intermediate trace is the interface between the salt wedge and the overlying freshwater.

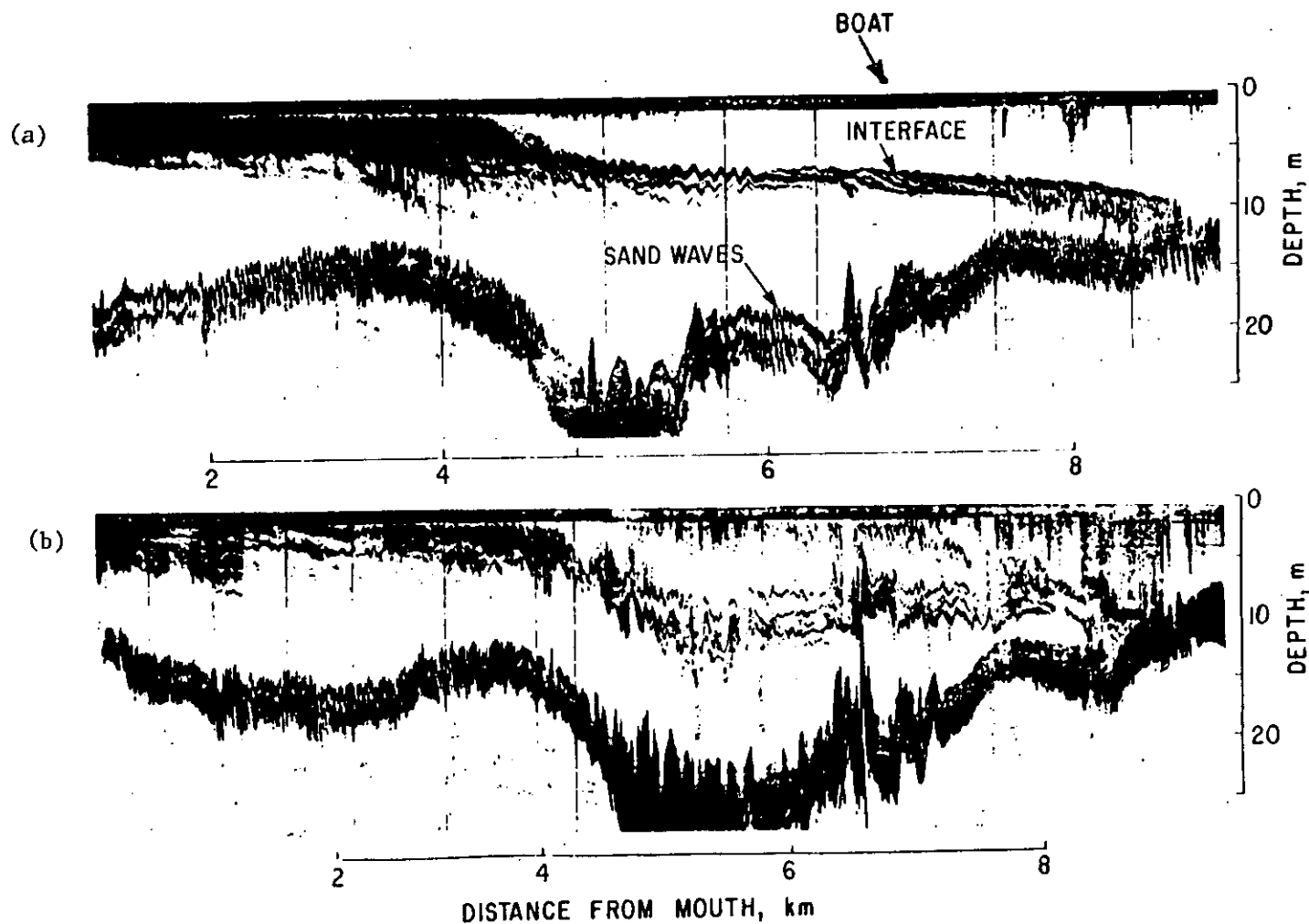
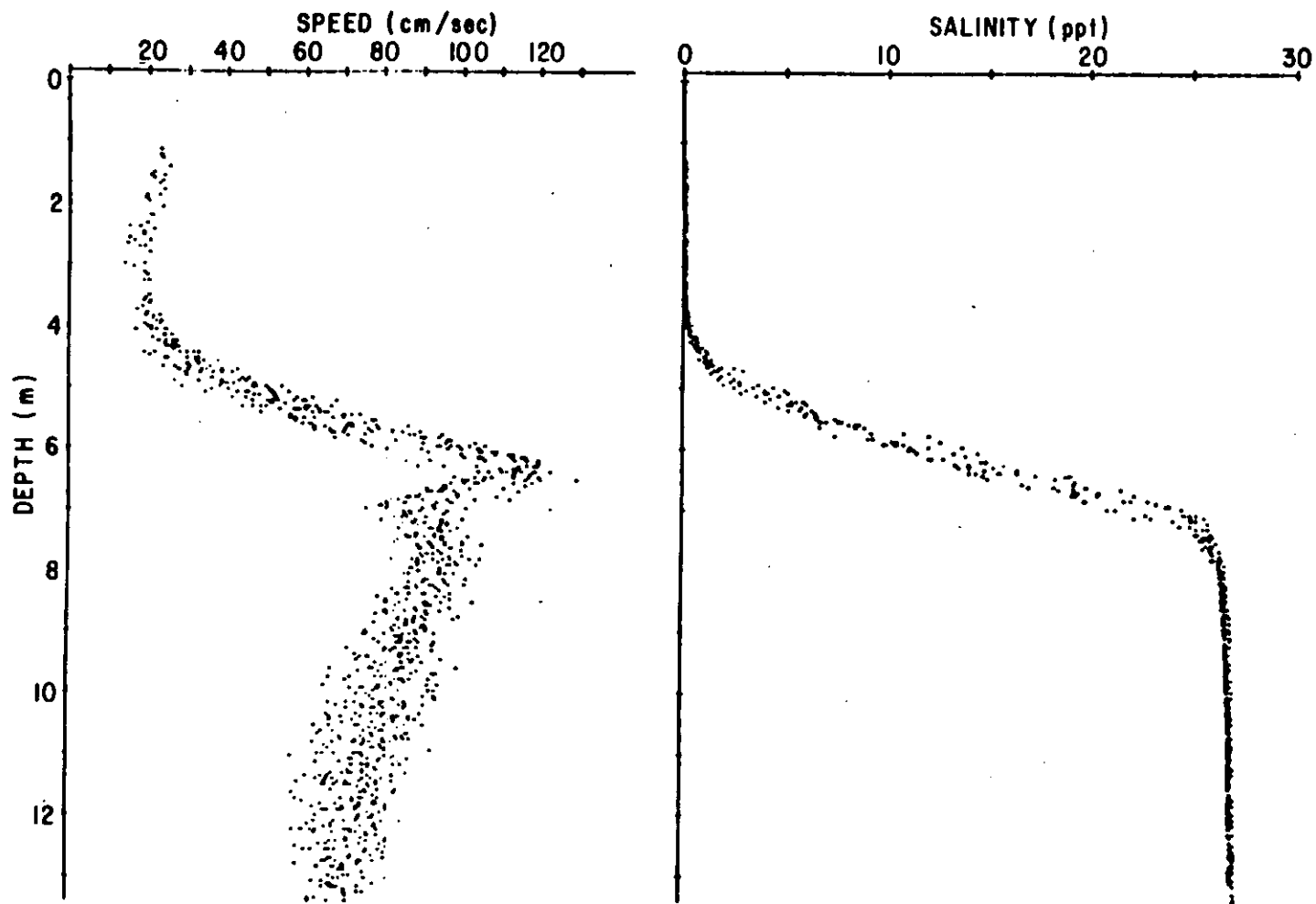


Figure 50. Profiles of (a) current speed and (b) salinity in the Fraser River salt wedge.



observed at the Clatsop Spit section (~RM-5.5) on June 19, whereas the salinity at the entrance section (RM-2) did not exceed 32 ppt the previous day. For several hours at the end of ebb the salinity observed did not exceed 0.5 ppt at any station. Thus, no minimum salinity plot is necessary, and the salinity range and maximum salinity are identical (Figure 48a). The salinity data in Figures 48a and b have been contoured using present day bathymetry, although controlling depths at the entrance and in the navigation channel at that time were ~1 to 2 m shallower.

The June 1959 situation (Figures 48a and b) is notable for the very large salinity range (as much as 33 ppt), for strong stratification, and for a very large horizontal salinity gradient (up to 10 ppt/km). The strong gradients exist because the salinity intrusion occurs as a salt wedge. The total absence of freshwater at the end of ebb can be attributed to the large tidal range; the salt wedge is mixed and advected totally out of the estuary. The strong stratification is the result of the very large riverflow. There is undoubtedly a strong baroclinic circulation which allows strong flood intrusion of salt water despite the great riverflow.

It is difficult, using the available, widely-spaced, non-synoptic salinity data, to obtain a detailed image of the salinity intrusion into the estuary under salt wedge conditions, because of the large spatial variability in  $\frac{\partial S}{\partial x}$  and  $\frac{\partial S}{\partial z}$ . A more detailed, synoptic picture can be obtained using acoustic scattering off particles trapped in regions of strong density gradients (as observed by an acoustic echo sounder; Gardner et al. 1980). This method has not yet been used in the Columbia River Estuary, but the profiles presented in Figures 42 and 43 and in Section 3.6 are sufficiently similar to those observed in the Fraser River Estuary, that results from that system (provided by R. Geyer, University of Washington), will be used to illustrate the processes that are believed also to occur in the Columbia River Estuary.

Figure 49a and b shows the Fraser River salt wedge near its maximum upriver extent during a period of moderate riverflow and strong tides. Figure 49a shows a transect taken at the beginning of the surface ebb, with minimal or flood currents at the bottom. The "nose" of the wedge is nearly vertical and the downstream increase in height of the wedge is evident. There is a stretch of some 4 km where a two-layer system is present. Figure 49b shows internal waves and other events late in the ebb that act to break down the wedge. The salt wedge disappears during the ebb tide, more because it is mixed into the overlying water mass, than because it is advected out of the system. At the end of ebb, salinity intrusion is found only within a few km of the mouth.

The velocity and density profiles for a position some distance seaward of the head of the wedge show strong shear and stratification (Figures 50a and b). The bottom layer is nearly the same salinity as the water entering the estuary from the Straits of Georgia; the surface water is nearly fresh. The form of the velocity profile shows the effects of the baroclinic pressure gradient, stratification and bottom boundary friction. The shear in the bottom layer is greatest very close to the bed and decreases sharply with distance away from the bed. This is typical of a weakly stratified boundary layer. The velocity increases from the surface down, because the barotropic (surface-slope-induced) and baroclinic (density-induced) pressure gradients act in the same direction and the baroclinic gradient increases with depth. This baroclinic flow meets the boundary layer flow at the depth of the interface; the details of the velocity structure within this layer need not concern us here. The very large shear that occurs at the interface can occur only because of the strong stratification; turbulent momentum transfer is very weak within the interface layer.

Some caution must be exercised in extending observations from the Fraser to the Columbia River Estuary. The Fraser River Estuary is a nearly-straight, narrow channel, without the complications of large sand flats and channel networks. The salt wedge there occurs very consistently, but the occurrence of a salt wedge in the Columbia River Estuary is more sporadic. Conditions for its occurrence have not been precisely defined; but weak tides and strong runoff favor the formation of a salt wedge. Observations in the Columbia River Estuary also suggest that highly stratified conditions may not be present at all locations downstream of the head of the wedges and that the water in the wedge is significantly less saline than the water entering the estuary.

#### High and Variable River Flow

Salinity intrusion during high and variable flow conditions has been investigated using data collected during a brief period of high riverflow in mid-June 1981 (Figure 4); the flow rose very quickly from ~400 kcfs (11,330 m<sup>3</sup>/s), peaked at ~560 kcfs (15,900 m<sup>3</sup>/s) on June 10 and 11, and then dropped back to ~400 kcfs. The total duration of flow greater than ~500 kcfs (14,130 m<sup>3</sup>/s) was only four days. Comparison of the June 1981 data (Figures 51a to d) with the June 1959 data (Figures 48a and b) reveals that a transient flow increase produces a very different salinity regime from a steady flow of the same magnitude. The June 1981 situation is notable for the lack of stratification, because saline bottom water was absent. One reason for the low salinity bottom water is the occurrence of an offshore downwelling event on June 8; not only is salt water pushed out of the estuary by the sharp increase in riverflow, but the T-S characteristics are greatly altered. The time-series data (Figure 52) for stations off Clatsop Spit show a marked increase in temperature (~3 deg C) which starts June 8, ~2-1/2 days before the peak flow. The great differences between the June 1959 and June 1981 situations must, however, be caused by some factor in addition to downwelling; SSOW was not present on June 18, 1959, and yet flood salinities at Clatsop Spit exceeded 31 ppt. Nor is the difference in tidal range the major factor; the neap tide in June 1981 would favor greater stratification, not less.

It is believed that low salinities and minimal stratification during June 1981 were caused primarily by the transient response of the system to a change in riverflow. Time series records show that salinities at mid-depth off Clatsop Spit were sharply reduced on June 10, but for only about 24 hours (Figure 52). There was a substantial decrease at Ft. Columbia for about 5 days. Thus salinities returned to near normal (for a downwelling period) at Clatsop Spit while the flow was still above 500 kcfs (14,130 m<sup>3</sup>/s) but remained depressed for a much longer period near the surface and at upriver stations. We hypothesize that the initial decrease of salinity at all depths is caused by an adjustment of surface slope of the system at the onset of high flow. This adjustment is barotropic (occurs at all depths) and pushes a large part of the saline water mass out of the estuary in a short time (less than one day). There then occurs a baroclinic adjustment (that is a function of depth) driven by the density structure that brings salinity back into the deeper parts of the estuary near the entrance. Salinities remain depressed near the surface and upriver because of the high riverflow. After the baroclinic adjustment occurs, stratification is greatly enhanced and  $\frac{\partial S}{\partial x}$  increased.

If Figures 51a to d (June 1981) capture the system in the midst of an adjustment to a change in external forcing, Figures 48a and b (June 1959) represent the quasi-equilibrium state that would occur after this series of adjustments of flow to runoff. Such an equilibrium was never reached in June 1981, because the flow immediately dropped and the system remained out of adjustment with its external forcing. Figure 53 compares the mean salinity gradients for the June

Figure 51. Minimum (a), maximum (b) and mean salinity (c), and salinity range for the South Channel, during the 1981 spring freshet.

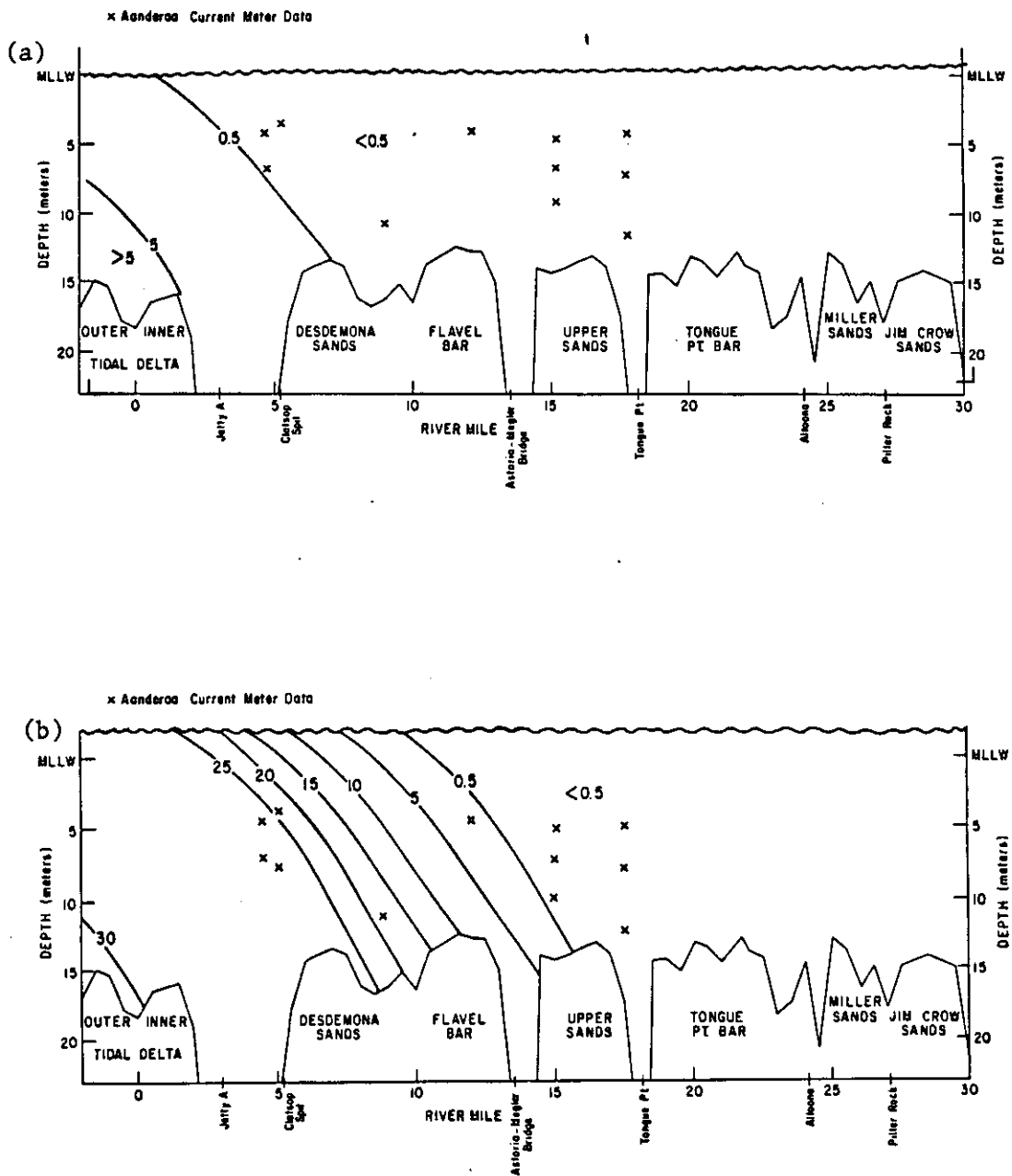


Figure 51. (continued).

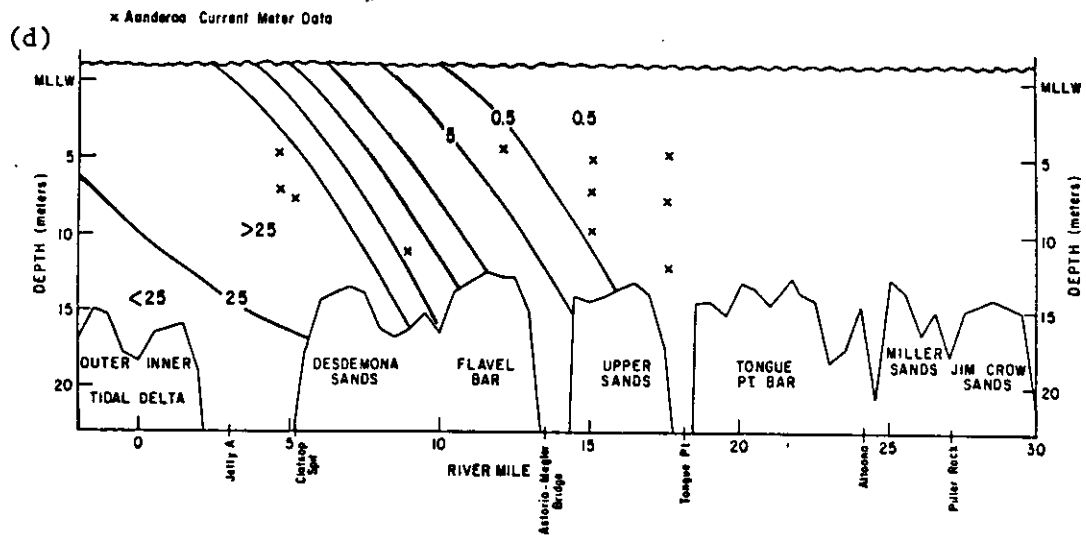
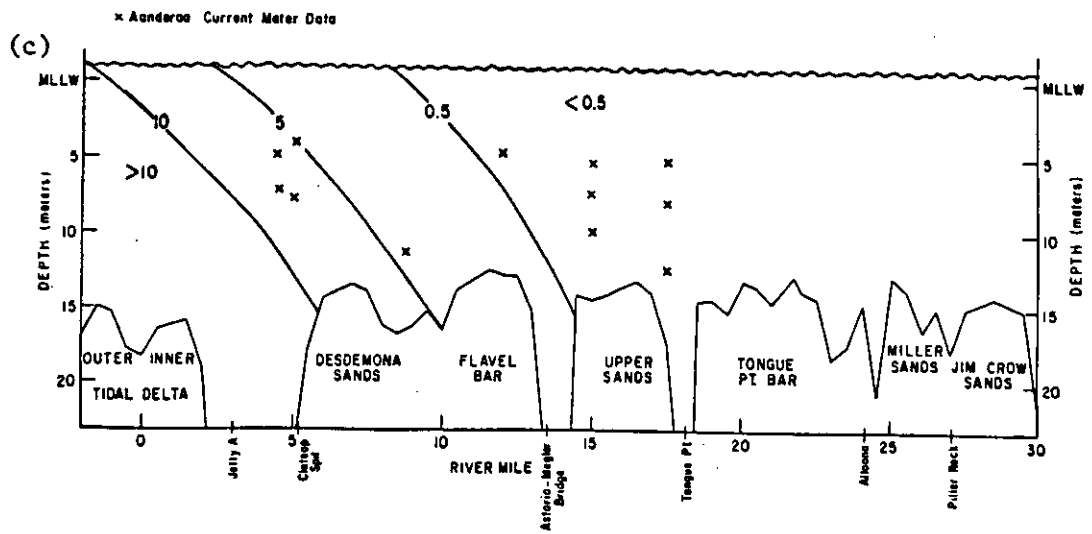


Figure 52. Time series of (bottom to top) speed, direction, salinity and temperature at 7m at station CM-1 (RM-5, North Channel) during the spring freshet period, 1981. Note the decreased salinity on 6/10/81, at peak of freshet. Decreased salinities after 6/18/81 reflect absence of upwelling (note warm temperatures), which also affects T-S characteristics from 6/9 to 6/14/81.

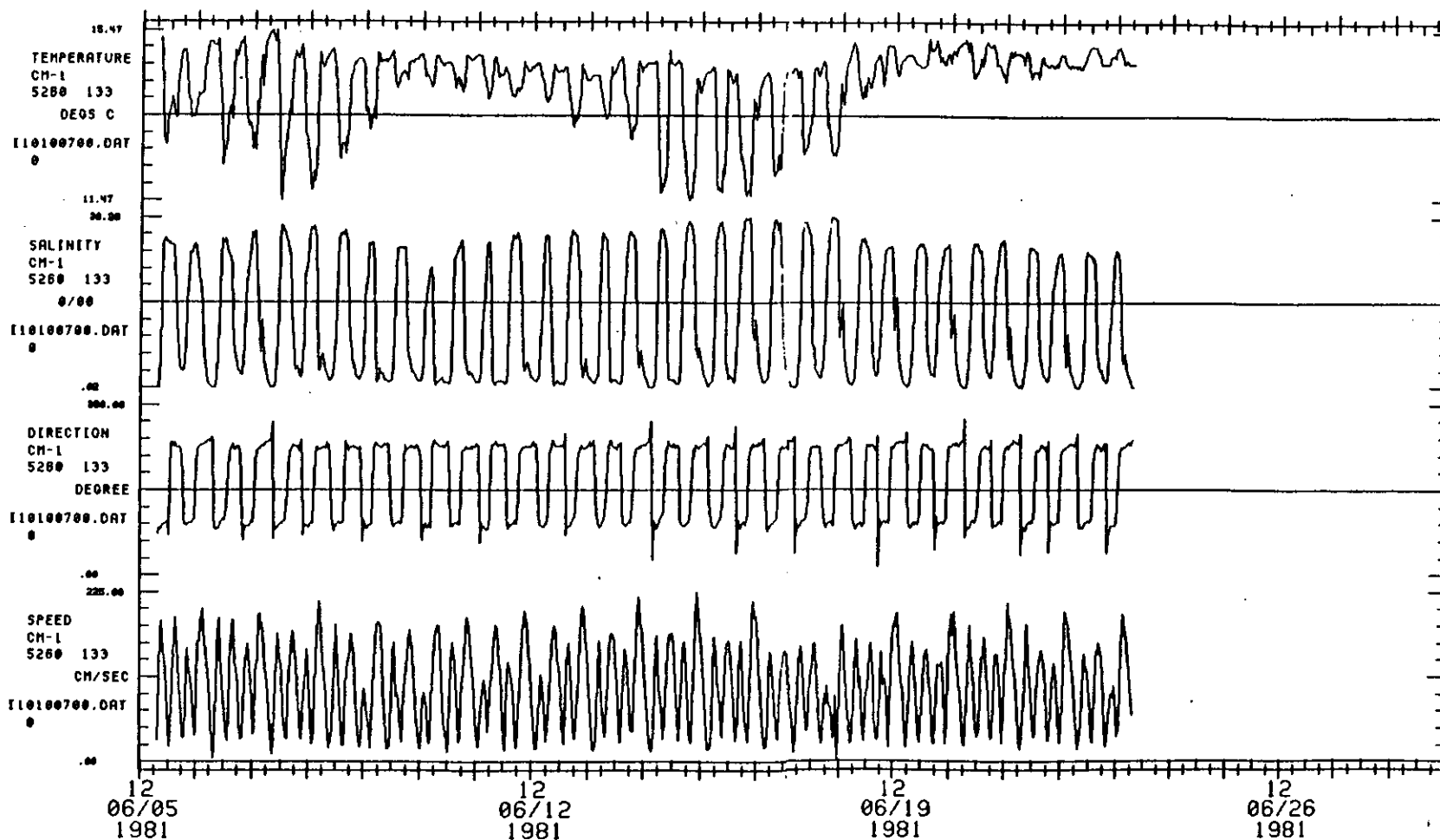
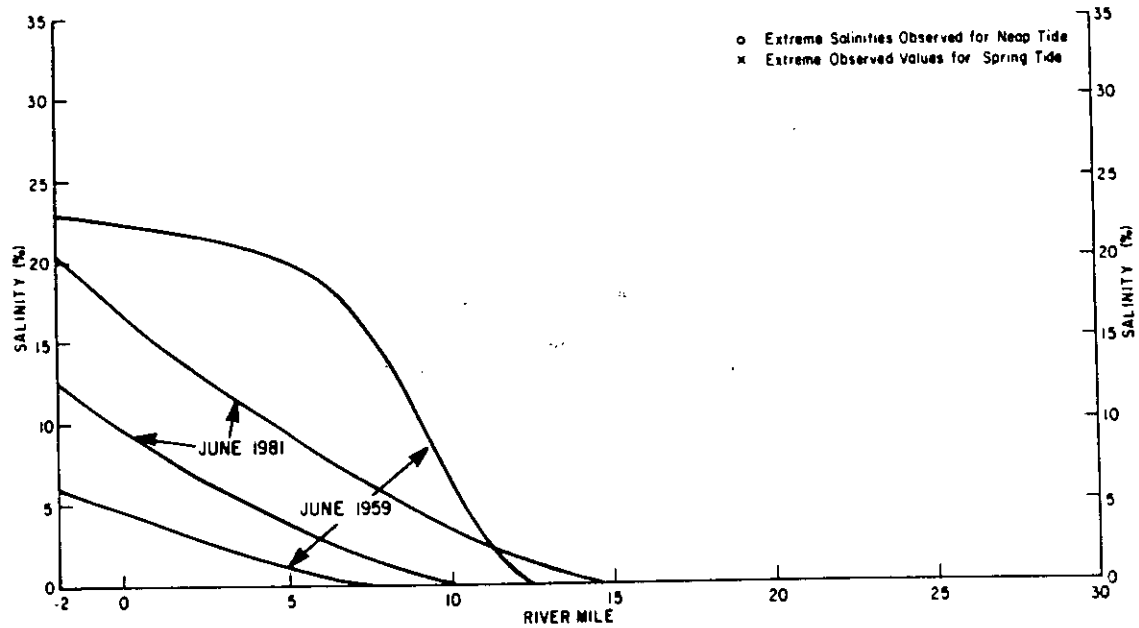




Figure 53. Salinity at MLLW (below) and 12m (above) for high-flow periods during June 1959 and June 1981.



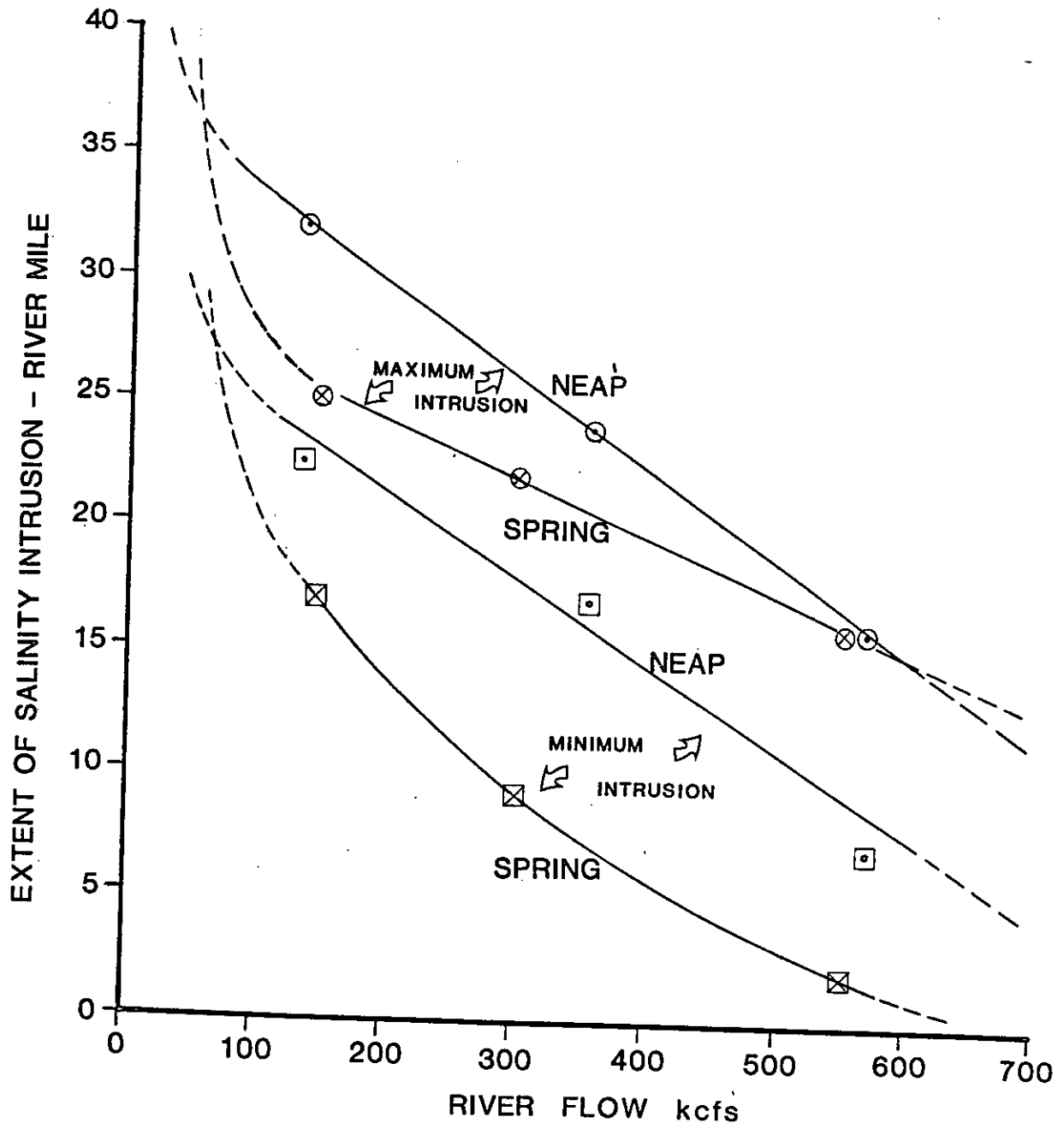


Figure 54. Maximum and minimum salinity intrusion length for spring and neap tides, as a function of riverflow.

1959 and 1981 periods. It can be seen that the gradient is steeper, as much as ~3.2 ppt/RM (and more variable in the vertical) in the 1959 equilibrium case. The gradient for the 1981 case (Figure 53) closely resembles that for much lower flows, but shifted in the downriver direction (Figure 47). This further supports the idea that the June 1981 data represent the transient response of the system, previously in equilibrium with a smaller flow, to a much higher flow.

In summary, the initial response of the system to a sharp increase in riverflow is very different from the final equilibrium with the high flow. Although extreme, high-flow events are now much less frequent than prior to regulation of the flow by dams, the total absence of salt from the system for about half a tidal cycle is still possible, when strong riverflow coincides with strong tides.

### 3.5.5 Neap-to-Spring Transitions, River Flow and Tidal Range

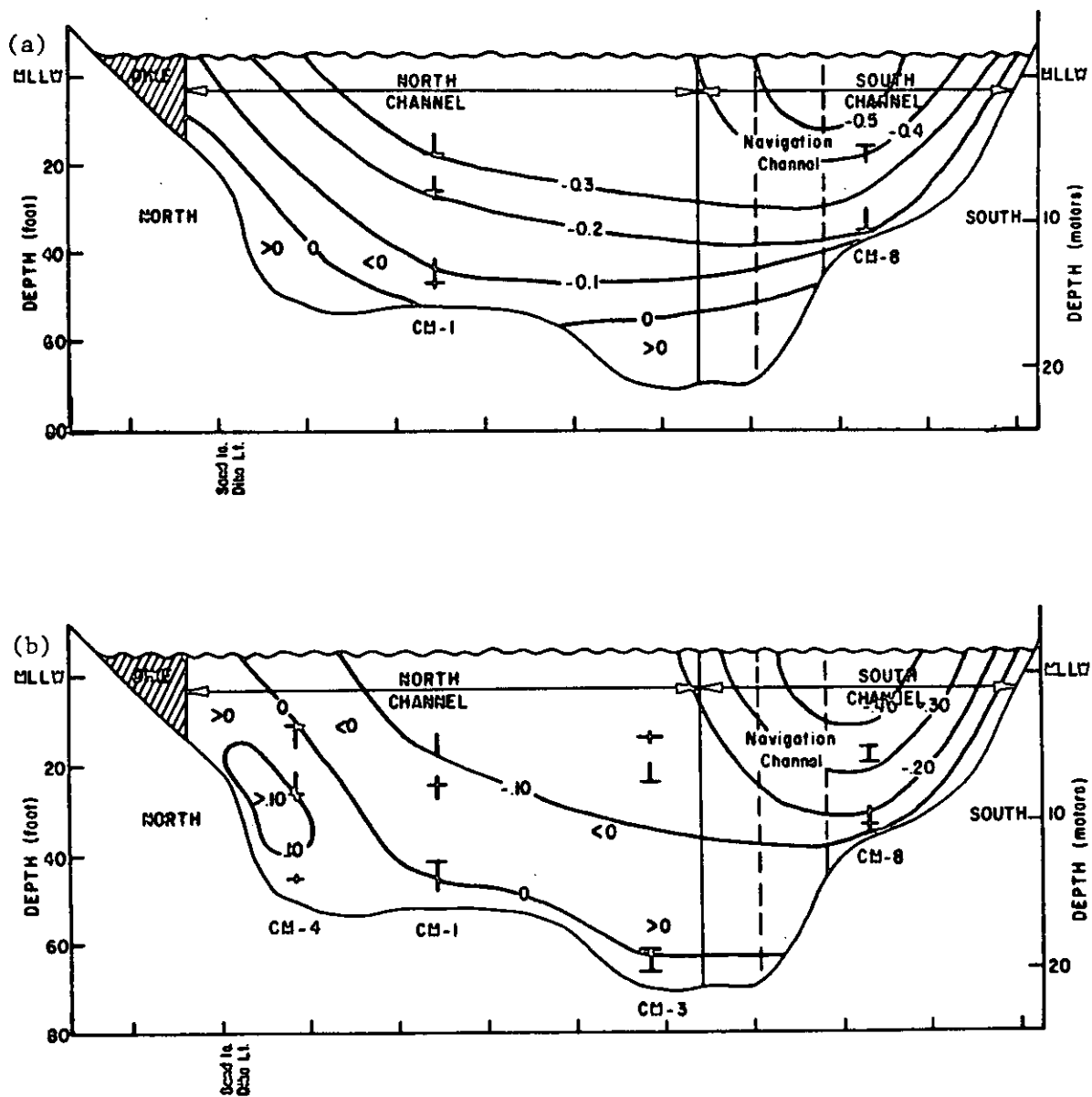
The salinity intrusion under moderate riverflow (300-350 kcfs or 8500-9900 m<sup>3</sup>/s) has been discussed in the Chapter 3 of the Integration Report, salinity sections for moderate riverflow observed during June 1980 are included in Appendix E, and the mean salinity at MLLW and 12 m is shown in Figure 3b. Salinity intrusion lengths (Figure 54) and stratification are intermediate between those for low-flow periods (Section 3.5.3) and freshet periods (Section 3.5.4). Figure 54, which shows neap and spring values of maximum and minimum salinity intrusion length as functions of riverflow, has been prepared on the basis of limited data and reasonable assumptions about the asymptotic behavior of the system at very high and very low river flows. It summarizes the present state of knowledge concerning neap-spring transitions.

At extremely low riverflow (Figure 54), the neap-spring transition that is so prominent in the present, low-flow season data would disappear, because riverflow is necessary for the occurrence of the stratification that makes the transition possible. Salinity intrusion in this hypothetical situation would be greatest on spring tide, because of the greater tidal excursion. Increasing the riverflow would result in a situation where the system is highly stratified on neap tide, and relatively well-mixed on spring tide; this is the existing low-flow situation, where salinity intrusion is greatest on neap tides. A further increase in riverflow would cause the estuary to be moderately to highly stratified under all tidal conditions, because the tidal mixing is insufficient, for all real tidal ranges, to bring about a well-mixed system. This is the present high-flow situation, which minimizes neap-spring differences in salinity intrusion length, because modest neap-spring changes in stratification more or less offset changes in tidal excursion. At the highest riverflow, salinity intrusion would again be greatest on spring tide, because the system would be strongly stratified (probably a salt wedge) for all tidal ranges, and because the greater tidal excursion on spring tides would bring the salt water further into the system. In summary, the present neap-spring transition, with its enhanced neap-tide salinity intrusion, is something that can occur only within the range of riverflow defined approximately in Figure 54. Were the bathymetry or tidal range to be altered, then the range of flows leading to a neap-spring transition would also be changed.

### 3.6 TRANSPORT PROCESSES

The transport of a conservative substance, such as salt, can be used as an indicator of the behavior of non-conservative substances, such as suspended sediment or organisms, for which insufficient data are available to calculate transports. Salt transport calculations also provide a means of testing the prediction (Section 1.2) that salt is maintained in the estuary, in the face of strong outward flow by the tides working on the salinity gradient. We have therefore used the extensive Aanderaa current meter salinity and velocity records to calculate salt transport at selected cross-sections.

Figure 55. Mean flow of water through Clatsop Spit - Sand Island Section in m/s during (a) high-flow season, and (b) low flow season.



### 3.6.1 Transport at Clatsop Spit: The Seasonal Pattern

The Clatsop Spit-Sand Is. cross-section provided the entrance boundary condition for the 1981 NOS study. As such, it was repeatedly and heavily instrumented. It is the only estuary cross-section at which more than a single current meter mooring was routinely deployed. The densest sampling occurred in August and September 1981, during which 4 stations were occupied. Results for the spring season are based on two stations. The number of hours of usable data for each meter for each season was shown in Figures 11a and b.

#### Mean Flow Properties

The tidal current characteristics at the Clatsop Spit-Sand Is. cross-section were discussed in Section 3.2. The tidal flow varies in strength and phase by a factor of about three (Figure 22b) and about one hr (Figure 22a), respectively, from bottom to top, as a result of the influence of bottom friction and the density structure. The strongest tidal flow is at the surface in the middle of the North Channel. Most of the tidal prism of the lower estuary, particularly the mid-estuary sand flats, is filled from the North Channel side; this interpretation is consistent with sedimentological results (Sherwood et al. 1984).

The mean flow is distributed differently in the cross-section than the tidal flow (Figures 55a and b). Outward flow is concentrated at the surface in the South Channel, where flows reach 0.4 m/s during the low-flow season and 0.5 m/s during the high-flow season. During the high-flow season there is also substantial (0.3 m/s) outflow at the surface of the North Channel. The outflow is strongest in the South Channel, because the flow in the river channel upstream of Altoona is diverted into the South Channel by a series of navigation structures and sand islands. The outflow at the surface in the North Channel probably reflects water transported in subsidiary channels across the sand flats from the South to the North Channel, between RM-10 and RM-20.

One striking feature of Figures 55a and b is the weakness of the upstream bottom flow during both seasons. The seasonal average net upstream flow does not exceed  $\sim 0.11$  m/s anywhere in the section for either season; it is strongest along the north side of the North Channel, where it extends to the surface during the low-flow season, but is absent in both seasons in the South Channel. Much of the shear in the mean flow is presumably caused by frictional and stratification effects, just as is the case with the tidal flow (Section 3.2); these vary in the along-and cross-channel directions, according to the topography. The two-dimensional, laterally-averaged model also showed net downstream flow at the bottom in this reach in the South Channel (Hamilton 1984). It is probable that the curvature of the channel near Jetty A is responsible for the inward flow predominance on the north side. The inward flow is directed toward the north side of the channel at Jetty A. The outward flow is directed primarily by the relatively constricted channel topography of the North and South Channels.

#### Salt Transport - The Seasonal Picture

The forces maintaining the salt balance have been discussed in Section 1.2. Figures 56a and b to 59a and b show the salinity distribution, the tidal advective (or oscillatory) salt transport, the mean flow salt transport, and the total salt transport (that is, the right hand side of Eq. (26), which, neglecting the turbulent transport, is the sum of tidal and mean flow transport, the Stokes drift transport, and two other small terms not shown individually) for the high and low-flow seasons. The stratification and shear are somewhat greater in the South Channel in both seasons, and the tidal currents are weaker. This does not result in upstream bottom flow or inward salt transport, because of the very large, net outward flow of water in the South Channel. The salinity is slightly higher (Figures 56a and b) on the north side, which is consistent with the larger net inflow there.

Figure 56. Salinity distribution at the Clatsop Spit - Sand Island Section in ppt during (a) high-flow season and (b) low-flow season.

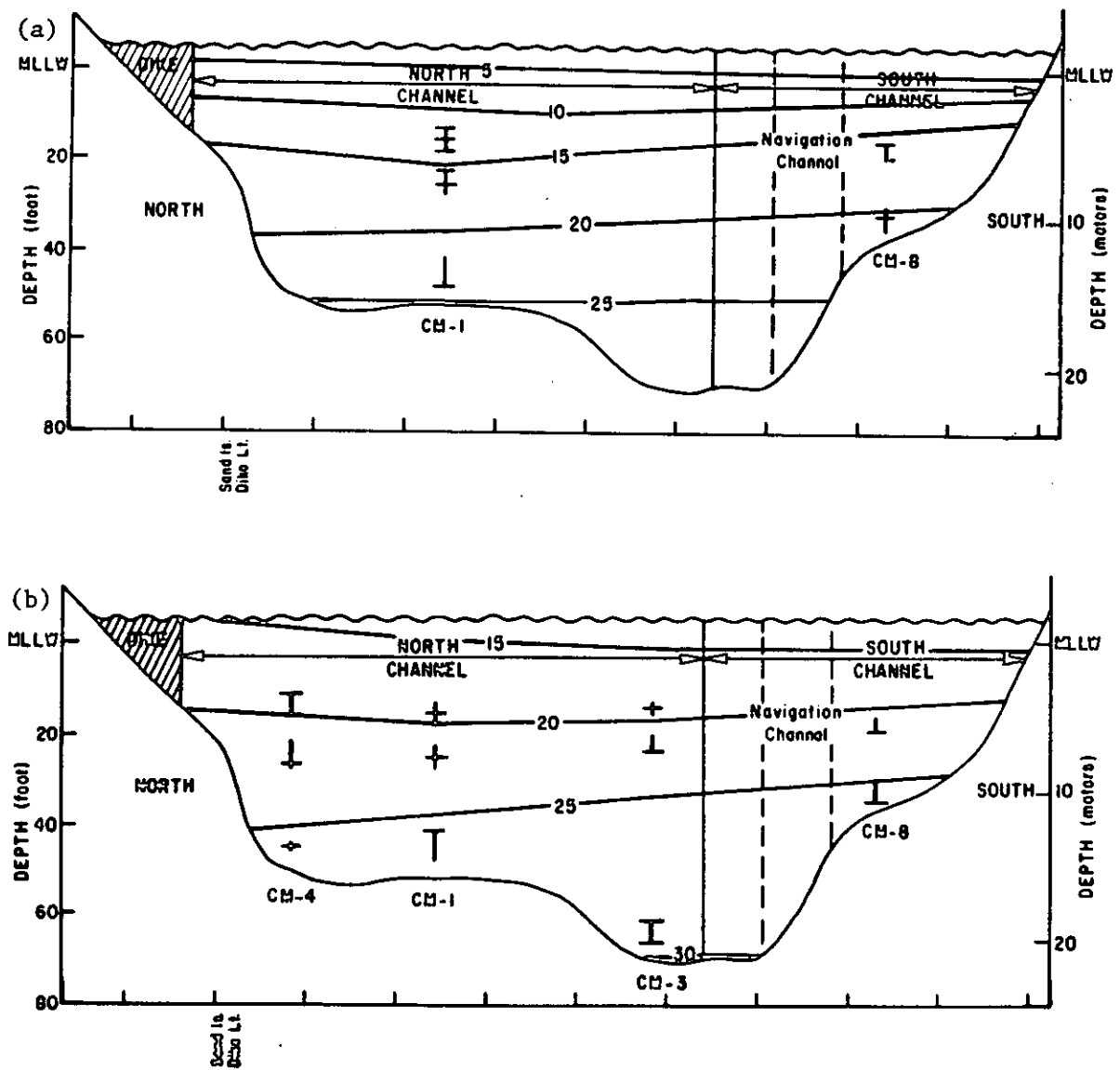


Figure 57. Tidal advective salt transport in  $\text{kg}/\text{m}^2\text{s}$  through the Clatsop Spit - Sand Island Section during (a) high-flow season, and (b) low-flow season.

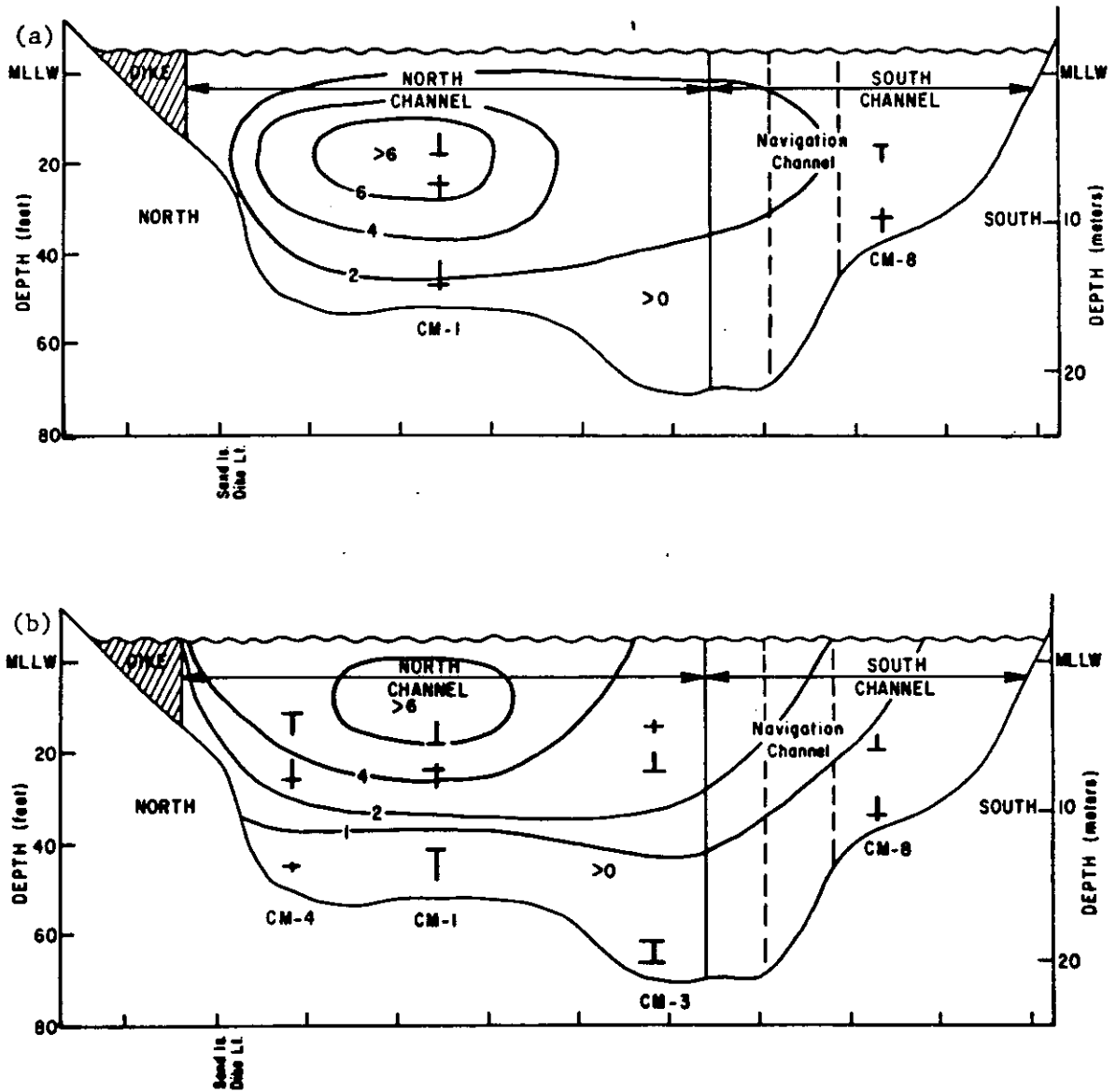


Figure 58. Mean flow salt transport in  $\text{kg}/\text{m}^2$ s through the Clatsop Spit - Sand Island Section during (a) high-flow season, and (b) low-flow season.

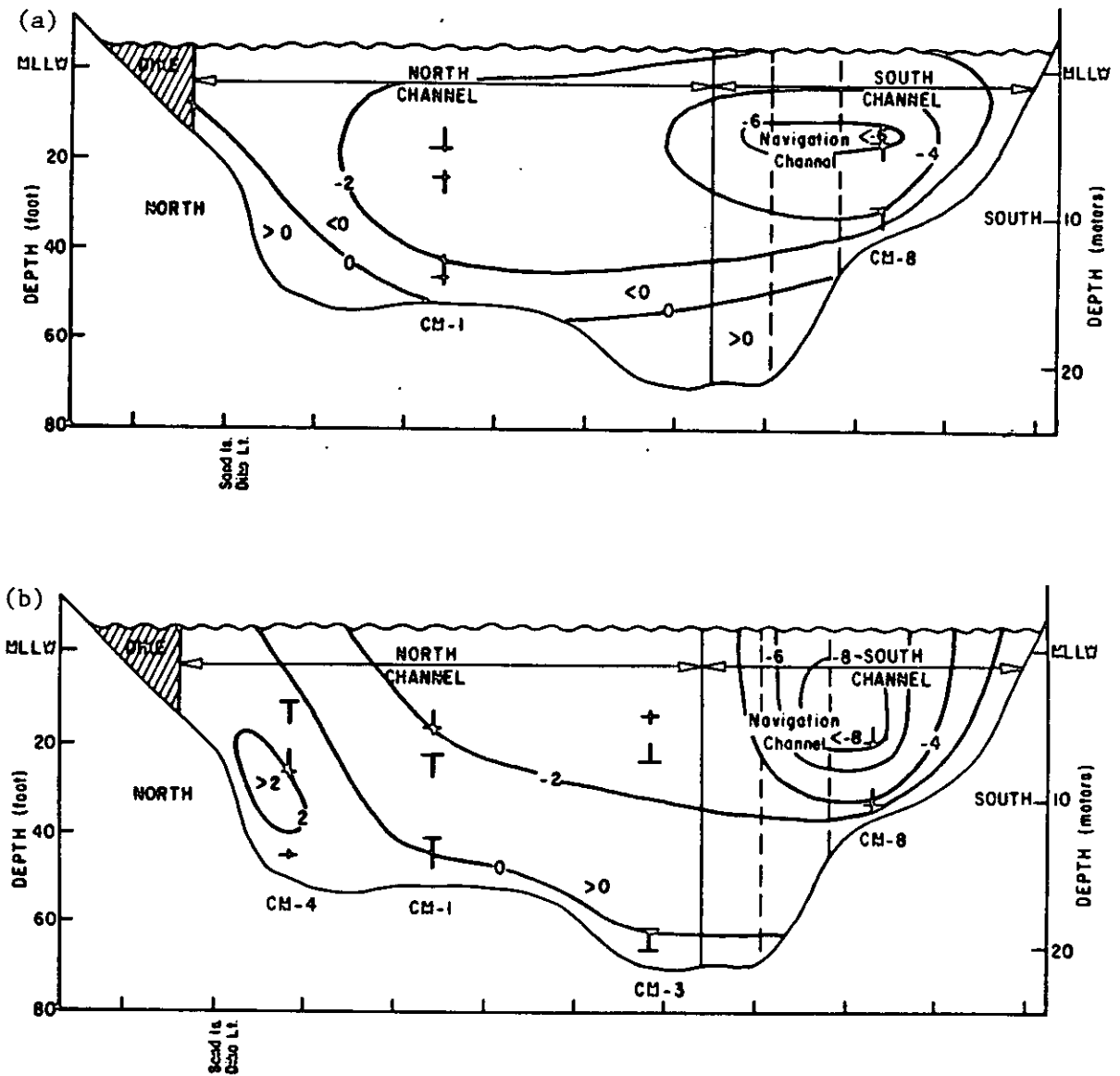
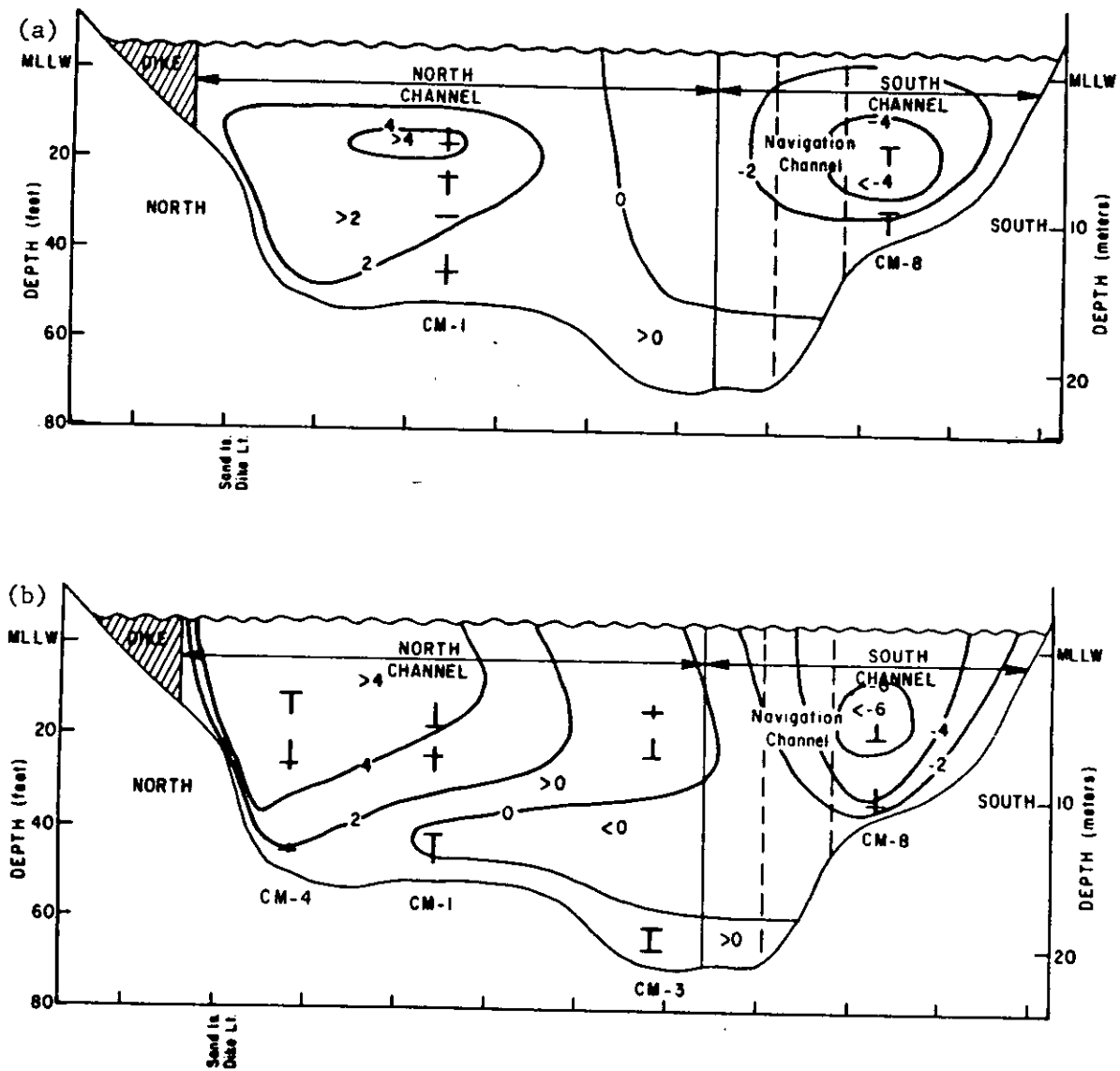




Figure 59. Total salt transport in  $\text{kg/m}^2\text{s}$  through the Clatsop Spit - Sand Island Section during (a) high-flow season, and (b) low-flow season.



Inward salt transport occurs in a jet in the middle of the North Channel (Figures 57a and b). The depth of the strongest transport is ~3 to ~5 m below MLLW in the low-flow season and ~5 to ~6 m in the high-flow season. The strongest tidal currents occur at the same lateral position, but at the surface. The salt transport drops off at the surface because the surface salinity is low, particularly in the high-flow season. Outward salt transport by the mean flow occurs in a jet in the South Channel at a depth of ~3 to ~5 m in the high-flow season and ~2 to ~4 m in the low-flow season (Figures 58a and b). As with the tidal transport in the North Channel, the outward transport in the South Channel occurs at slightly greater depth during the high-flow season, because surface salinities are lower then. Inward transport by the mean flow is strongest along the north side during the low-flow season. Salt transport near the bottom is weak in all seasons.

The total salt transport by all processes (Figures 59a and b) is inward in the North Channel and outward transport in the South Channel in both seasons. There are at least four important implications here. First, Figures 57a and b to 59a and b are a striking confirmation of the analysis of Section 1.2, which argued that the salt balance was maintained (in the face of strong outward transport of salt by the mean flow) by inward tidal transport of salt. The inward transport by the mean flow is of secondary importance in maintaining this balance.

Second, inward and outward salt transports are laterally separated. The lateral separation is in part a function of the topography of this particular section, which is just seaward of the junction of the North and South Channels. A section closer to the entrance might show a different lateral pattern, but Desdemona Sands (upstream of the Clatsop Spit-Sand Is. Section) provides a partial barrier to transport between channels. Net upstream transport should be found at stations in the North Channel, and downstream transport at stations in the South Channel, for some distance upstream of Clatsop Spit. The observed separation does not fit the lateral gravitational circulation mechanism proposed by Fischer (1976), because Fischer's postulated mechanism did not include tidal processes. Conservation of salt requires that the salt transported into the North Channel somehow reach the South Channel, so that it may return to the ocean. The most probable mechanism for this process is the same channels that transport water from South to North Channel across the mid-estuary flats, between RM-10 and RM-20. Although they have a net water transport toward the North Channel, these channels are ideally situated to have a salt transport in the opposite direction. They run diagonally from low river mile in the North Channel to high river mile in South Channel. They transport nearly-fresh water to the North Channel on ebb tide and relatively-saline water to the South Channel on flood. The strength of the transport in these shallow channels may be augmented by the phase difference in tidal forcing at the two ends. Stokes drift may also play an important role in the transport of water and salt across the flats.

Third, the vertical separation of inward and outward transports is small. This suggests that vertical mixing, vertical tidal transport, and entrainment do not have to lift a parcel of saline water very far while it is in the estuary.

Fourth, the seasonal differences are small. This is in part a result of the flow pattern for 1981. There was a distinct freshet, but flow was unusually low during May and high during August, so that the average flow for the two seasons (as defined here) varies only by a factor of two. A larger seasonal contrast in flow would cause larger seasonal changes in salt transport. Transports further upstream show much stronger seasonal changes because, as discussed in Section 3.5, salinities upstream show much larger seasonal variations. We shall see below that seasonal changes are also minimized by the fact that the tidal and mean flow transports tend to fluctuate in opposite directions.

### Salt Transport at Clatsop Spit: Temporal Variations

The temporal variations in salt transport at Clatsop Spit have been examined by plotting time series of salt transport parameters for individual meters. The picture that emerges is one of complex, compensating changes in different parts of the cross-section. There is an increase of stratification on neap tides so that the salinity is lower at the upper meters. There is also some redistribution in the vertical of mean flow that is related to both changes in stratification and Stokes drift. In general, the tidal monthly changes at most Clatsop Spit meters were less dramatic than further up-estuary.

The longest continuous record for the Clatsop Spit-Sand Is. Section is for a mid-depth (~6 to 8 m) meter at CM-1, for which 4 continuous deployments are available during the high-flow season (Figure 60). The strongest tidal monthly changes at Clatsop Spit were also found in this record. Figure 60 covers slightly more than two tidal months and includes the 1981 spring freshet. The most striking features are the increase in outward flow and decrease in average salinity during the freshet and the regular neap-to-spring changes in salt transport terms. The total salt transport is inward at all times despite the outward mean flow, because this meter is located just below the center of the jet of inward tidal transport. There is an increase in both tidal and mean flow salt transport during the freshet period. The outward mean flow salt transport increases slightly with increasing riverflow, but not in direct proportion to the flow. This occurs because an increase in outflow is associated with a decrease in salinity. The tidal transport at mid-depth increases as the riverflow increases and the flow becomes more stratified. Figures 61a and b show salinity and temperature profiles for periods corresponding to the end of the weaker ebb and the end of the weaker flood for June 17 and 18. Salinity intrusion occurs on this occasion as a salt wedge, with two definite layers and a more or less sharp interface. Surface salinity remains essentially fresh during the entire 12 hour period; bottom salinities vary only slightly. The striking feature of the profiles is the vertical excursion of the interface between the two layers. The vertical excursion of this interface during the tidal cycle is closely related to the upstream salt transport by tidal processes, because the difference between flood and ebb salinities at mid-depth is very large. As the interface moves up and down with the tide, there is a large correlation between salinity and velocity and a correspondingly large tidal advective salt transport.

With regard to tidal-monthly changes, the inward tidal transport increases substantially with the increased stratification on neap tides, without a large increase in average salinity. Small adjustments in both mean flow and salinity also cause substantial neap-to-spring adjustments in mean flow salt transport. These neap-to-spring changes in mean flow salt transport partially compensate for the neap tide increases in tidal transport so that the total salt transport is less variable during the tidal month than either term individually. There is a slight tendency for a larger total inward salt transport at this station on a neap tide, which is in part compensated at other meters at this section and which in part contributes to the increase in average salinity during the neap at stations further up the estuary.

In summary, large changes in mean flow and tidal-cycle-average salinity during the spring season do not result in large changes in salt transport at the Clatsop Spit-Sand Is. section, because the mean flow and the average salinity change in opposite directions. The mean flow salt transport and the tidal salt transport also tend to change in opposite directions during the neap to spring cycle so that the total salt transport is more stable than the individual terms contributing to it.

#### 3.6.2 Salt Transport at Other Transects

Figure 60. Time series of salt and water transport parameters at mid-depth at CM-1 (~RM-5, middle of North Channel), spring 1981.

The time period includes the spring freshet (day ~40); however, tidal monthly changes dominate salt transport terms.

RNGE = tidal range	TADV = mean flow salt transport
HBAR = low-passed tidal height	TSV = tidal oscillatory salt transport
SBAR = low-passed salinity	TSTK = salt transport by stokes drift
QBAR = mean flow	TNET = net salt transport
QSTK = stokes drift	
QNET = net drift	

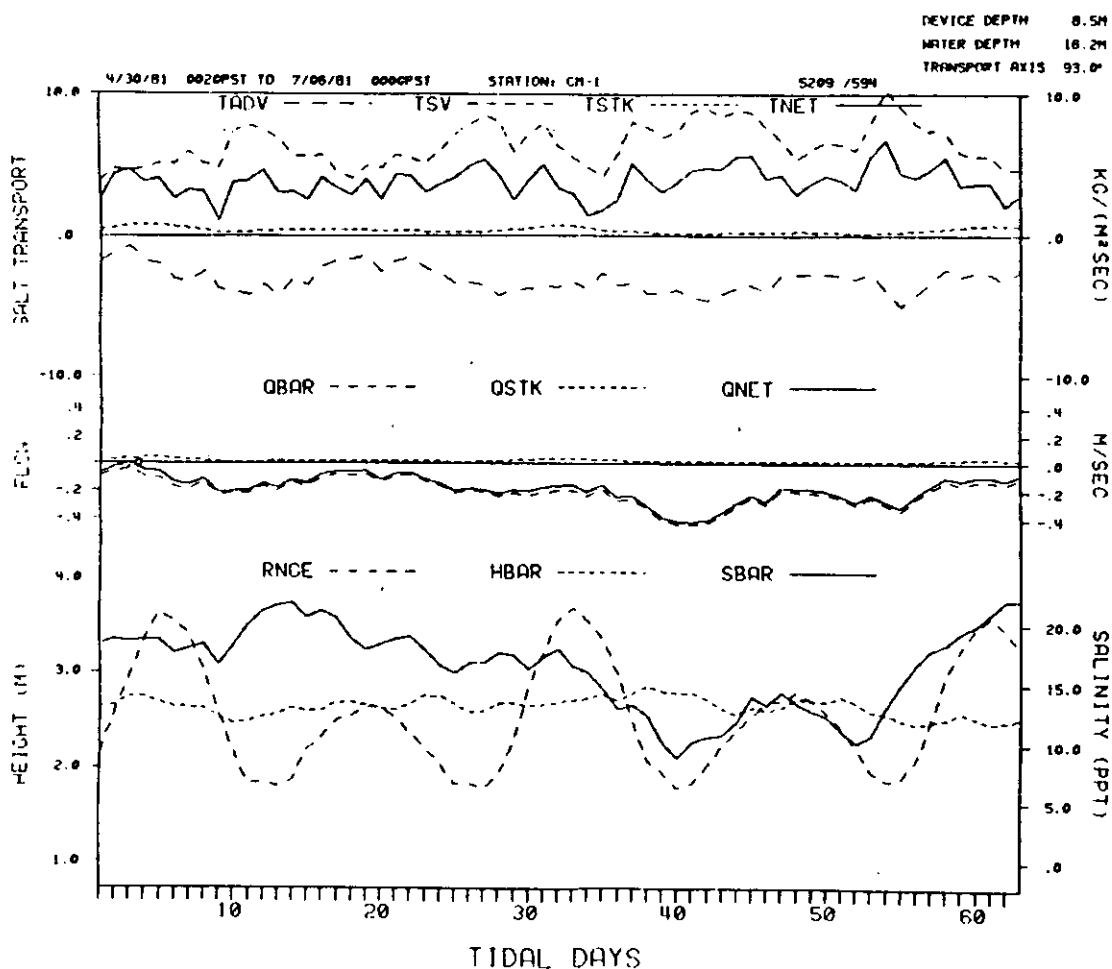
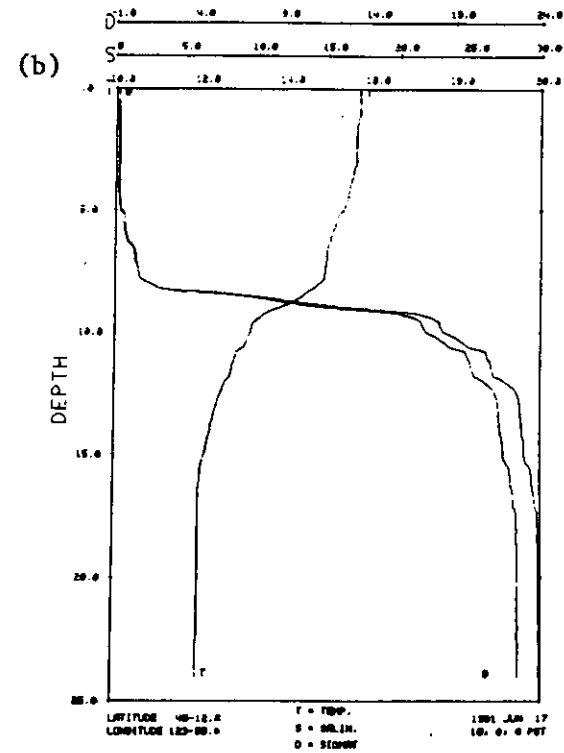
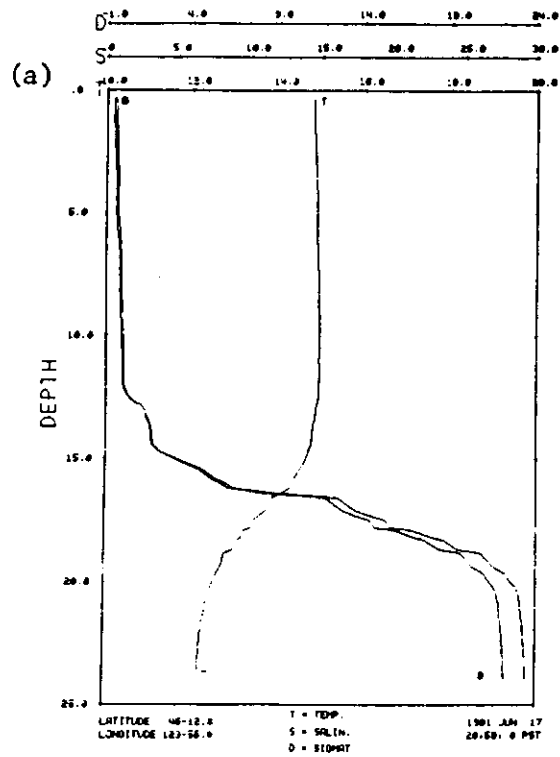


Figure 61. Temperature (T), salinity (S), and sigma-t (D) profiles at (a) the end of weaker ebb, and (b) the end of weaker flood.



### Salt Transport Near RM-2

The results of Hansen (1965a and b), Hughes (1968) and Hughes and Rattray (1981) demonstrate that lateral flow variability is important near the entrance. There appears to be an eddy north of the navigation channel, in the triangular area between Jetty A and North Jetty. Probably there is little net transport of either salt or water in this eddy. The 1975 current data discussed by Sternberg et al. (1977) show that the most saline water enters the estuary through a deep channel south of the navigational channel at the end of the jetties.

Calculations based on 10 tidal days of data for meters at depths of 7 and 14 m and 2 tidal days at 12 m depth at CM-2S (south side of the navigation channel, RM-2) during October 1981 show that neap-to-spring variability is more important at this station than at the Clatsop Spit-Sand Is. Section. During the weak tides (<1.8 m) at the beginning of the deployment, upstream salt transport is greatest at the deepest meter, and is primarily the result of mean upstream bottom flow. Mean flow salt transport at the upper meter (~7 m, mid-depth) is strongly outward early in the deployment and decreases as the tidal range increases and shear decreases. The level of strongest inward salt transport shifts toward the surface during the period, as the gravitational circulation becomes less important and tidal and the Stokes drift transports becomes larger. This is the only cross-section where Stokes drift transports larger than  $1 \frac{\text{kg}}{\text{m}^2\text{s}}$  have been observed; they may reach  $2 \frac{\text{kg}}{\text{m}^2\text{s}}$  at the surface. This is also the only station below the Astoria-Megler Bridge where salt transport by the mean flow is of major importance during the neap tide. This is consistent with the very strong horizontal salinity gradients found here during some stages of the tide (Section 3.5) on neap tides.

### Salt Transport at Astoria (~RM-15)

Station CM-9 was one of the two highest priority stations during the 1981 NOS sampling. Extensive records are available for mid-depth meters, but results are spotty for near-surface and near-bottom meters. Figure 62 shows the salt transport parameters for a 110 tidal day period from May 5 to August 31, 1981 for successive deployments of meters at ~5 to ~7 m below MLLW. Mean flow ranges from more than 0.4 m/s in the downstream direction to near zero ppt late in the record. Significant upstream flow never occurs, and the net downstream flow is small only after two neap tides late in the record. Salinities range from near zero ppt for 20 days during the freshet to ~13 ppt just after a neap tide in August.

Salt transports early in the record are small and variable. Salinity and salt transport terms vanish during the June 1981 freshet period. The post-freshet period is the most interesting. As at Clatsop Spit, there is a tendency (with important exceptions) for changes in the mean and the tidal salt transports to compensate one another, but the salt transports are greatest on spring rather than neap tides. The net salt transport is small and slightly inward, until the last 20 days of the record, during which two interesting events occur, following two neap tides. These two events are similar to that observed in detail during the October 1980 CREDDP cruise and are believed to have occurred on several other neap tides in 1980. At or after the period of minimum tidal range, the salinities increase dramatically (in one case in Figure 62, from ~4 to ~13 ppt). This increase is accompanied by a sharp decrease in downstream mean flow salt transport and a resulting strong, upstream total salt transport. The near-bottom salinity may increase by as much as 15 ppt. Near-surface meters show very little change in salinity; thus, the stratification is greatly increased.

These events have been interpreted in Section 3.5 as instances in which the system undergoes a transition from a partially-mixed to a highly-stratified condition. This neap-spring transition is a function of the decrease in tidal energy

Figure 62. Time series of salt and water transport parameters at mid-depth at CM-9 (~RM-15, off Astoria, in the South Channel), spring and summer 1981. The salinity is ~0 ppt. for ~20 days during the spring freshet (days 32 to 52). There is an increase in salinity after each neap tide; apparently only the last two neap tides resulted in formation of a salt wedge and dramatically increased salinity intrusion and salt transport. Symbols are as in Figure 60

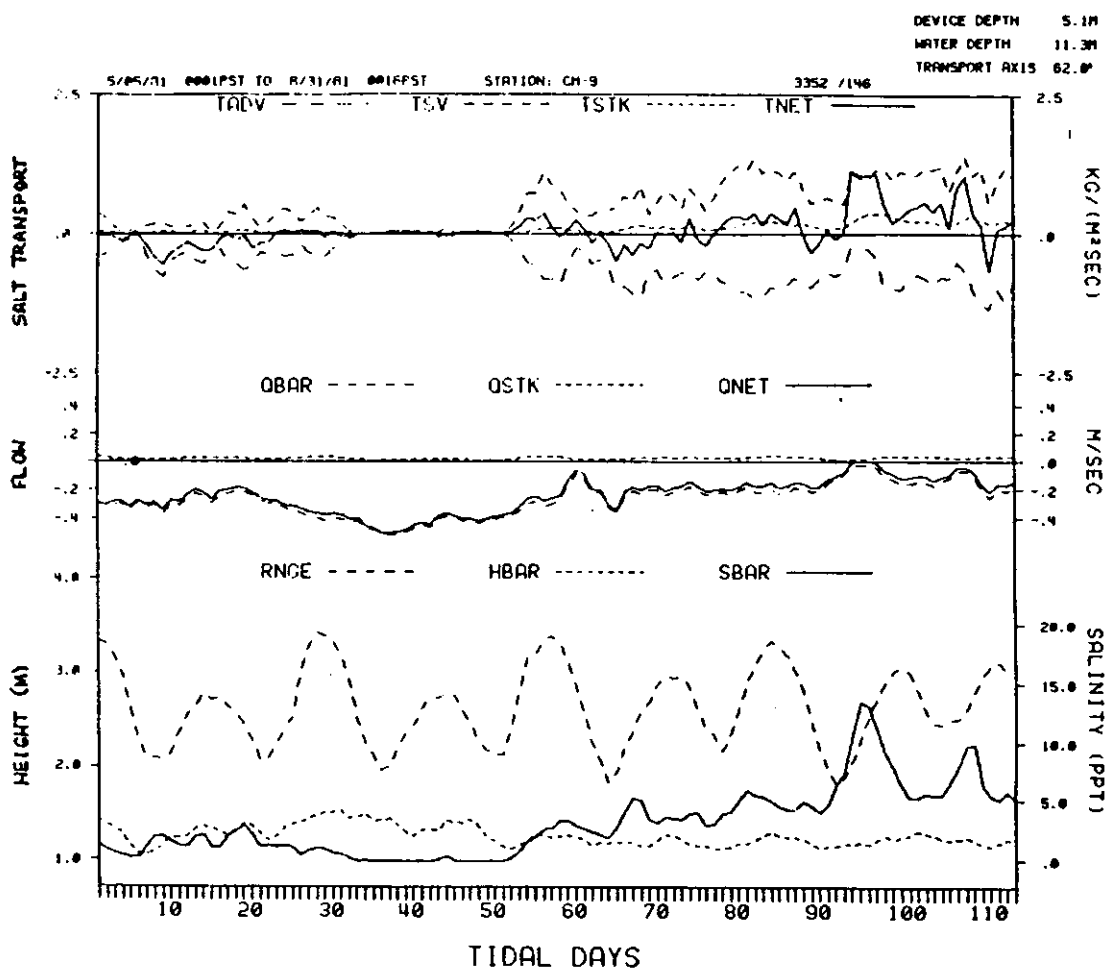


Table 9. Seasonal cycle of Mean Water Level (MWL)<sup>†</sup> at Tongue Pt.

	1960-78	Observed 1980-81		1980-81		1980-81, Corrected	
	<u>Average,m</u>	<u>Average,m</u>	<u>Std.dev.,m</u>	<u>Average,m</u>	<u>Std.dev.,m</u>	<u>Average,m</u>	<u>Std.dev.,m</u>
Jan.	1.47	1.47	.17	1.46	.11	1.34	.11
Feb.	1.43	1.45	.15	1.43	.11	1.35	.11
Mar.	1.39	1.34	.14	1.34	.10	1.36	.09
Apr.	1.33	1.29	.09	1.31	.06	1.30	.07
May	1.31	1.28	.08	1.29	.07	1.31	.07
Jun.	1.34	1.33	.10	1.34	.09	1.30	.08
July	1.28	1.18	.06	1.20	.05	1.34	.05
Aug.	1.22	1.19	.05	1.18	.03	1.28	.03
Sep.	1.22	1.22	.07	1.22	.06	1.31	.05
Oct.	1.28	1.27	.14	1.27	.09	1.31	.09
Nov.	1.38	1.41	.19	1.40	.12	1.33	.11
Dec.	1.48	1.53	.18	1.53	.11	1.42	.11
Mean	1.337	1.327	0.166	1.328	0.134	1.330	.092

<sup>†</sup>Heights are in m, relative to MLLW (1960-78 epoch), which is 0.713 above gauge datum.  
Data for the 1960-78 period are from NOS.



for mixing on the weaker tides. Note that each of the last four neap tides is accompanied by an increase in salinity, which is amplified as the riverflow and tidal range decrease. Only the last two have major effects on transport processes, presumably because the other events are too weak to cause large changes in stratification. It appears that neap-spring transitions and the resulting strong salinity intrusion events are somewhat sporadic. Figure 62 suggest that the transition does not occur if the riverflow or the tidal energy is too high, but necessary and sufficient conditions have not yet been defined.

The timing of the maximum salinity relative to the neap tide is also quite interesting. The maxima in Figure 62 all occur a few days after the neap, as the tidal energy level increases. Jay (1982) also found a tendency for the maximum salinity to occur a day or two later at the upstream end of the estuary than at the Astoria-Megler Bridge. W.R. Geyer (personal communication) has found that the Fraser River salt wedge intrudes further upriver as the tidal range increases. Apparently the salt wedge in the Columbia River Estuary continues to move upstream as the tidal excursion increases after the minimum tidal range, until the mixing is intense enough that a salt wedge can not be maintained. The pattern of sills and holes above the Astoria-Megler Bridge, the diurnal inequality, the rate at which the tidal range increases, and the riverflow all probably influence the non-linear transition between highly-stratified and partially-mixed conditions. This complex transition remains poorly understood.

In summary, the monthly variation in tidal energy is the primary factor governing salt transport processes above the Astoria-Megler Bridge, during the low-flow season. These processes are confined to the deeper part of the navigation channel and probably have little effect on shallower parts of the estuary. The details of neap-to-spring changes remain poorly understood.

### 3.7 RESIDUAL FLOW PROCESSES

It was argued in Section 1.3 that the residual (or low-frequency) circulation is driven by the tides, riverflow, salinity (density structure), and winds and pressure (atmospheric forcing). The purpose of this section is to describe statistically the system's barotropic response to this low-frequency forcing. Atmospheric forcing is found, through examination of the statistical relationship between the forcing and the estuarine response (tidal heights, surface slopes and residual currents), to be of less importance than the other factors in determining the barotropic residual circulation (that part of the residual circulation driven by the surface slope).

#### 3.7.1 Seasonal Cycles

The statistical calculations reported below required removal of the seasonal signal from all variables, as described in Section 2.5. This seasonal signal, however, also contains useful information. The seasonal cycle of MWL (mean water level) is indicative of processes occurring within the estuary and in the adjacent coastal ocean (Section 1.3). The long-term seasonal properties of mean water level (MWL) at Tongue Pt. are compared with those for the 1980-81 periods in Table 9. It can be seen that maximum MWL occurs in December and is some 25 cm (1960-78 average) to 35 cm (1980-81 average) higher than that in August. The standard deviation of MWL for the winter months is also 2 to 3 times as great as that for the summer months. A part of the MWL variance at Astoria is caused by the seasonal variation in atmospheric pressure; the adjustment of MWL for IBE reduces the variance by about 35%, without affecting the the magnitude of the annual cycle for 1980-81.

Removal of the seasonal riverflow signal from the annual MWL cycle reduces its magnitude (1980-81 average) from  $\sim 35$  cm to  $\sim 14$  cm, a seasonal cycle somewhat smaller than the cycle ( $\sim 20$  cm) due to coastal and oceanic effects, as

Table 10. Seasonal cycle of riverflow 1969-82 and 1980-81.

	Riverflow 1969-82	Riverflow 1980-81	
	<u>Average, m<sup>3</sup>/s x 10<sup>3</sup></u>	<u>Average, m<sup>3</sup>/s x 10<sup>3</sup></u>	<u>Std.dev., m<sup>3</sup>/s x 10<sup>3</sup></u>
Jan.	9.17	8.61	2.41
Feb.	8.31	7.10	1.84
Mar.	8.45	6.09	0.84
Apr.	8.29	6.57	1.06
May	10.03	8.39	1.34
Jun.	10.53	10.43	2.13
Jul.	6.87	6.12	1.40
Aug.	4.65	4.45	0.84
Sep.	4.07	3.77	0.38
Oct.	4.33	4.16	0.68
Nov.	5.97	5.34	0.96
Dec.	8.80	10.45	2.97
Mean	<u>7.46</u>	<u>6.76</u>	<u>2.68</u>

determined by Hickey and Pola (1983) from 25 years of data. This remaining  $\sim 14$  cm seasonal cycle in adjusted MWL is presumably accounted for by oceanic processes; the upwelling/downwelling cycle, seasonal changes in alongshore pressure gradient, seasonal changes in deep ocean currents, and coastal steric effects (Section 1.3).

The tidal-fluvial model discussed in Section 3.3 predicts a long-term mean seasonal sea level cycle at Tongue Pt. of  $\sim 8$  to 9 cm, without coastal effects. The sum of the effects predicted by this model and the predicted offshore effects ( $\sim 20$  cm) is  $\sim 29$  cm, slightly larger than the observed 25 cm. This suggests that steric effects (not included in the calculations of Hickey and Pola 1983) caused by the plume can not be of major importance.

Removal of both IBE and seasonal runoff effects reduces the MWL variance to about 30% of the value for the uncorrected MWL (Table 9). The remaining variance is presumably caused by short term atmospheric and riverflow effects; it is these short term effects that we investigate below. Table 9 shows that, even after the removal of seasonal effects, the variance in MWL is highest in the winter, with a secondary peak in June. Comparison with Tables 10 and 11a and b suggests strongly that this variance cycle can be explained by the seasonal variance cycles of riverflow and atmospheric parameters.

The seasonal cycle of riverflow is shown in Table 10 and in Figures 4 and 30. It is evident (Table 10) that the years 1980 and 1981 were somewhat dryer than the long-term (1969 to 1982) average. The riverflow deficit was greatest in February to May; the June freshet period was about average and the December freshet period was wetter than the long-term average. The variance in river flow is greatest in December and January. Winter freshets do not occur every year; when they do, they are brief and intense. The variance in May is not particularly large; it is a month of relatively reliable, high flow. June variance is higher, because major spring freshets do not occur every year, but when they do, they occur in June.

Both available sets of wind data were used in compiling Table 11a and b, because of uncertainties as to which set of wind data was most closely related to circulation in the estuary (Section 2.5). The seasonal wind and pressure cycles that drive the continental shelf circulation and that contribute to the MWL cycle are clearly seen. It can also be seen in Table 11a and b that the calculated geostrophic winds, are much stronger than the observed Newport winds. In this regard, it is most useful to compare wind stress statistics. Means and standard deviations of both components of the geostrophic winds are 2.6 to 3.9 times as large, but the seasonal pattern of means and standard deviations are quite similar. The mean and standard deviations of the alongshore wind stress are two to three times as strong as the onshore component in both data sets. Average winds are directed north in the winter and south in the summer. Winds are somewhat offshore in the mean during some of the winter months. Strong winds are always, at Newport, and almost always in the geostrophic winds, directed to the north and east. It is certain that the Newport winds do not adequately represent the drainage winds down the Columbia Gorge from the interior during the winter. These are somewhat better represented in the geostrophic winds.

The Newport winds and the geostrophic winds were compared to each other and to available estuary observations to determine how closely related the various wind data were. All winds were low-passed to remove signals at daily and higher frequencies. Table 12 shows correlation coefficients between the wind components from the various sources. Newport winds compared very favorably in both u and v-components with the winds at Desdemona Sands at about RM-13. The v-component at the data buoy (offshore at the former position of the Columbia River lightship) was related to both u and v-components at Newport. The onshore u-component at the data buoy was not related to either component at

Table 11a. Seasonal cycles of atmospheric parameters, Geostrophic winds<sup>†</sup> 1980-81 (46°N 124°W).

	pressure, mbar	wind u, m/s	wind v, m/s	windstress, u				windstress, v			
				average newton/m <sup>2</sup>	std. dev. newton/m <sup>2</sup>	# of obs. >.4 newton/m <sup>2</sup>	# of obs. <-.4 newton/m <sup>2</sup>	average newton/m <sup>2</sup>	std. dev. newton/m <sup>2</sup>	# of obs. >.4 newton/m <sup>2</sup>	# of obs. <-.4 newton/m <sup>2</sup>
Jan.	1015.9	-2.67	5.64	-.049	.094	2	0	.132	.198	17	0
Feb.	1015.2	-0.65	5.91	-.003	.091	1	0	.108	.129	9	6
Mar.	1017.4	2.17	0.20	.028	.069	1	0	.007	.079	1	0
Apr.	1018.1	2.52	0.19	.033	.053	0	0	.003	.063	0	0
May	1017.5	2.43	-3.31	.024	.027	0	0	-.038	.048	0	0
Jun.	1018.9	2.28	-2.69	.021	.028	0	0	-.033	.052	0	0
July	1018.8	1.38	-5.77	.014	.027	0	0	.066	.040	0	0
Aug.	1016.3	1.16	-4.61	.011	.022	0	0	-.048	.041	0	0
Sep.	1016.8	0.82	-0.75	.008	.038	0	0	-.002	.052	0	0
Oct.	1017.2	-0.24	2.14	-.003	.054	0	0	.044	.109	4	0
Nov.	1016.7	1.20	5.89	.024	.085	0	0	.103	.117	6	1
Dec.	1016.6	0.92	6.03	.014	.087	0	0	.119	.161	13	1
Mean	1017.14	0.96	0.68	.0104	.065	4	0	.0263	.123	49	8

<sup>†</sup>Calculated by NMFS from 6-hourly data. High-frequency fluctuations removed with a lanczos low-passed filter with half-power point at (32 hours)<sup>-1</sup>.

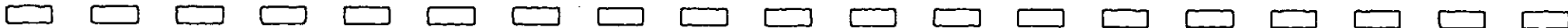
Table 11b. Seasonal cycles of atmospheric parameters, Newport, OR winds 1980-81 (44° 40'N 124° 04'W)

	pressure, mbar	wind u, m/s	wind v, m/s	windstress, u		# of obs. 2		windstress, v		# of obs. 2	
				average 2 newton/m <sup>2</sup>	std. dev. newton/m <sup>2</sup>	>.2 newton/m <sup>2</sup>	<-.2 newton/m <sup>2</sup>	average 2 newton/m <sup>2</sup>	std. dev. newton/m <sup>2</sup>	>.2 newton/m <sup>2</sup>	<-.2 newton/m <sup>2</sup>
Jan.	-	-1.57	-0.43	-.007	.040	0	0	.022	.049	2	0
Feb.	-	-1.30	1.42	-.007	.022	0	0	.024	.062	8	0
Mar.	-	1.02	0.64	.011	.026	0	0	.008	.038	3	0
Apr.	-	1.25	0.48	.013	.028	0	0	.008	.043	0	0
May	-	1.17	-0.58	.006	.010	0	0	-.004	.022	0	0
Jun.	-	1.02	-0.46	.007	.013	0	0	-.004	.026	0	0
July	-	0.98	-2.41	.008	.014	0	0	-.020	.033	0	0
Aug.	-	0.90	-0.98	.005	.008	0	0	-.007	.019	0	0
Sep.	-	0.15	0.36	.001	.005	0	0	.004	.024	0	0
Oct.	-	-0.56	0.47	-.003	.013	0	0	.010	.042	3	0
Nov.	-	-0.73	1.96	-.001	.024	0	0	.025	.053	8	0
Dec.	-	-0.42	1.93	.003	.031	1	0	.034	.081	13	0
Mean	-	0.17	0.20	.0030	.023	1	0	.0067	.047	37	0

Table 12. Maximum correlations and lags between wind data from various sources<sup>†</sup>

	Data Buoy Winds 46°11'N 124°11'W		Newport, OR Winds 44°40'N 124°04'W		Desdemona Sands Winds 46°12'N 123°52'W	
	u	v	u	v	u	v
Geostrophic u	.50/1	.65/0	.57/0	.63/-1	.65/-1	.85/-2
Winds, v	.17/0	.71/0	-.30/-1	.48/1	.40/-2	.52/0
Newport u	-.17/2	-.82/0			.71/-1	.31/-2
Winds, v	.245/2	.83/0			.25/1	.82/-1

<sup>†</sup>Results presented as correlation between variable in left-hand column and variable in top row, at lag indicated: corr/lag.



Newport. Lags for maximum correlations were small in all cases. The geostrophic winds (Table 12) were substantially better related to data buoy onshore winds and slightly less related to alongshore winds than were the Newport winds, and geostrophic winds were less related to both components of the Desdemona Sands winds. Local winds could not be tested against each other, because the observations were not from the same time period; it appears, however, that there are substantial differences between the winds at the data buoy and at Desdemona Sands.

The geostrophic and Newport winds were fairly well correlated with each other in both components. In all cases with the geostrophic winds and in all but one case with the Newport winds, off-diagonal correlations sometimes exceeded the diagonal correlations. That is, the u-component at one station was more closely related to the v-component at another station, than to the u-component at that station. This suggests that the wind direction changes as it encounters the coast.

In summary, the Newport winds are a better representation of winds in the estuary than the geostrophic winds. The geostrophic winds are a slightly better representation of the winds over the continental shelf, primarily because the Newport winds are so poorly related to the onshore component at the mouth of Columbia River. Which wind data should be used in statistical calculations depends on the relative importance of local (over the estuary) and large-scale forcing.

### 3.7.2 Tests of Hypotheses

The  $O(1)$  vertically-integrated force balance in an estuary expresses the relationship between acceleration of the flow, surface slope (barotropic forcing), bottom stress, and surface wind stress. The statistical properties of the surface slope are, therefore, a good indication of the causes of the barotropic part of the residual flow. Tidal heights are examined, because of the importance of sea level height to other estuarine parameters and because there is broad knowledge in the oceanographic literature of the behavior of tidal heights. We can not expect, with this simple approach, to evaluate the importance of the baroclinic forcing in residual flow processes. The hypotheses we test are therefore related to the barotropic part of the estuarine circulation. The hypotheses are:

- o Atmospheric effects dominate the barotropic part of the residual circulation.
- o Local atmospheric forcing is more important than continental-shelf-scale atmospheric forcing in the barotropic residual circulation.

Tables 13a and b show the correlations between tidal height and surface slope and various forcing functions, and Table 14 shows the percent of the variance of height and slope observations attributable to deviation from the mean of each forcing variable (as determined by a linear regression model with zero time lag between all variables). The correlations in Table 13a between height and tidal range are greatest at Wauna, but there is a very strong pattern of correlation between height and tidal range at all stations and all lags. Heights are greatest at all stations except Jetty A slightly after (three to six lags) the time of maximum tidal range. One lag in all calculations is six hours, so that the maximum tidal height occurs about one day after the tides of greatest range. The lowest tidal heights occur (with one exception) about one quarter of a tidal month (25 to 31 lags) before or after the time of greatest range. The temporal structure of the correlations leaves little doubt as to the causal nature of the connection between height and tidal range. The relationship between slope and tidal range is also strong (and greatest in the estuary proper). Figure 63a shows

Table 13a. Maximum correlation and lags between height and various forcing functions<sup>†</sup>

Station	Heights <sup>†</sup>		Tidal Range*		River Flow		Pressure		Bakun x-wind stress		Bakun y-wind stress		Newport x-wind stress		Newport y-wind stress	
	# of Observations	Period	corr.	lag	corr.	lag	corr.	lag	corr.	lag	corr.	lag	corr.	lag	corr.	lag
Jetty A	760	5/80 to 11/80	-.256 +.309	4 37	.210	-1	-.418	5	+.393	1	.352	5	-.156	7	.506	0
Jetty A	860	5/81 to 12/81	-.143	-31	.131	-8	-.387	5	+.239	-2	.500	0	.144	-7	.476	3
Tongue Pt.	2800	1/80 to 12/81	-.331 +.290	-27 4	.429	-8	-.356	7	.400	-1	.407	4	.16	-2	.480	0
Wauna	1200	1/81 to 11/81	-.527 .512	-28 3	.597	0	-.244	12	+.323	0	.330	5	-.1	-14	-.146	+3
Columbia City	1880	8/80 to 11/81	.224 .126	-25 6	.862	1	-.212	16	.296	16	.16	18	not calculated			

<sup>†</sup> Seasonal signal and tidal period signal removed from all parameters.

<sup>†</sup> Inverse barometer effect and seasonal effect removed.

\* 1 lag is 6 hours. Positive (negative) lags indicate that the forcing function leads (lags) height or slope.



Table 13b. Maximum correlation and lags between river slope and various forcing functions<sup>†</sup>

Reach	Slopes		Tidal Range*		River Flow		Pressure		Bakun x-wind stress		Eakun y-wind stress		Newport x-wind stress		Newport y-wind stress	
	# of Observations	Period	corr. lag		corr. lag		corr. lag		corr. lag		corr. lag		corr. lag		corr. lag	
			corr.	lag	corr.	lag	corr.	lag	corr.	lag	corr.	lag	corr.	lag	corr.	lag
Tongue Pt. -Jetty A	760	5/80 to 11/80	-.500	-29	.147	-23	.111	-3	.11	1	-.319	-2	.329	-1	.230	-4
			.788	1												
			.542	33												
Tongue Pt. -Jetty A	850	5/81 to 12/81	-.499	-29	.347	-29	.219	-27	.17	0	.18	-2	.16	-30	.13	-3
			.678	1												
			-.489	32												
Wauna -Tongue Pt.	1200	1/81 to 11/81	.376	-30	.699	1	.12	-2	.17	13	.14	14	not calculated			
			.387	1												
			-.247	33												
Columbia City -Wauna	1200	1/81 to 11/81	-.105	.16	-.949	2	-.16	18	.19	16	.223	29	not calculated			

<sup>†</sup>Seasonal signal and tidal period signal removed from all parameters.

\* 1 lag is 6 hours. Positive (negative) lags indicate that the forcing function leads (lags) height or slope.

Table 14. Percent of variance in low-passed heights and slopes accounted for by forcing functions, as determined by regression analysis<sup>†</sup>

Station Period	# of Observations	Forcing Variable					Total
		Tidal Range	River Flow	x-stress*	y-stress*	Pressure	
<u>Tidal Height</u>							
Jetty A 5/81-12/81	870	-	-	3.7	23.0	3.4	31.2
Tongue Pt. 1/80-12/81	2800	7.4	16.2	16.1	12.7	-	51.1
Wauna 2/81-11/81	1200	25.0	37.2	4.5	2.8	-	69.8
Columbia City 8/80-11/81	1880	5.6	73.9	-	-	-	80.3
<u>Slope</u>							
Tongue Pt.- Jetty A 5/81-12/81	860	51.3	5.2	2.7	2.3	-	61.8
Wauna- Tongue Pt. 2/81-11/81	1200	19.4	47.4	2.1	-	2.2	71.2
Columbia City- Wauna 2/81-11/81	1200	-	88.0	-	-	-	89.3

<sup>†</sup>All variables low-passed to remove tidal variations and decimated to 6-hour intervals. Regression performed with zero time lag between forcing and tidal height (or slope). Variables accounting for less than 1% of the variance omitted.

\*Geostrophic winds only used in the regression analysis.

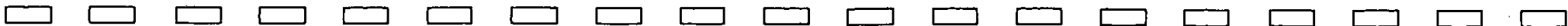
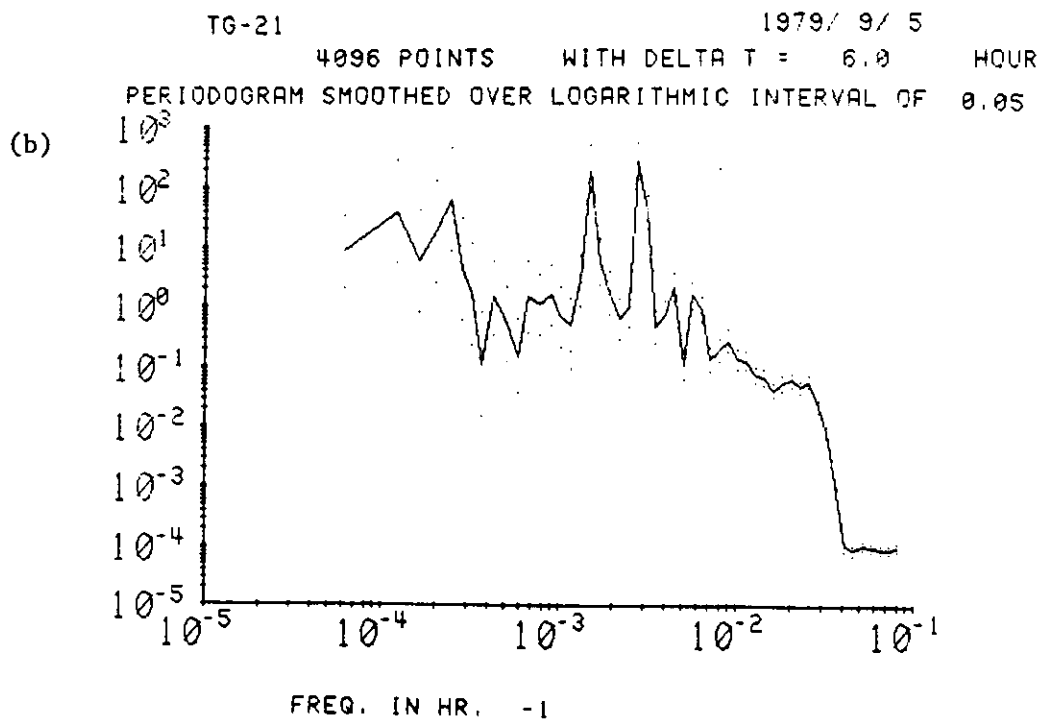
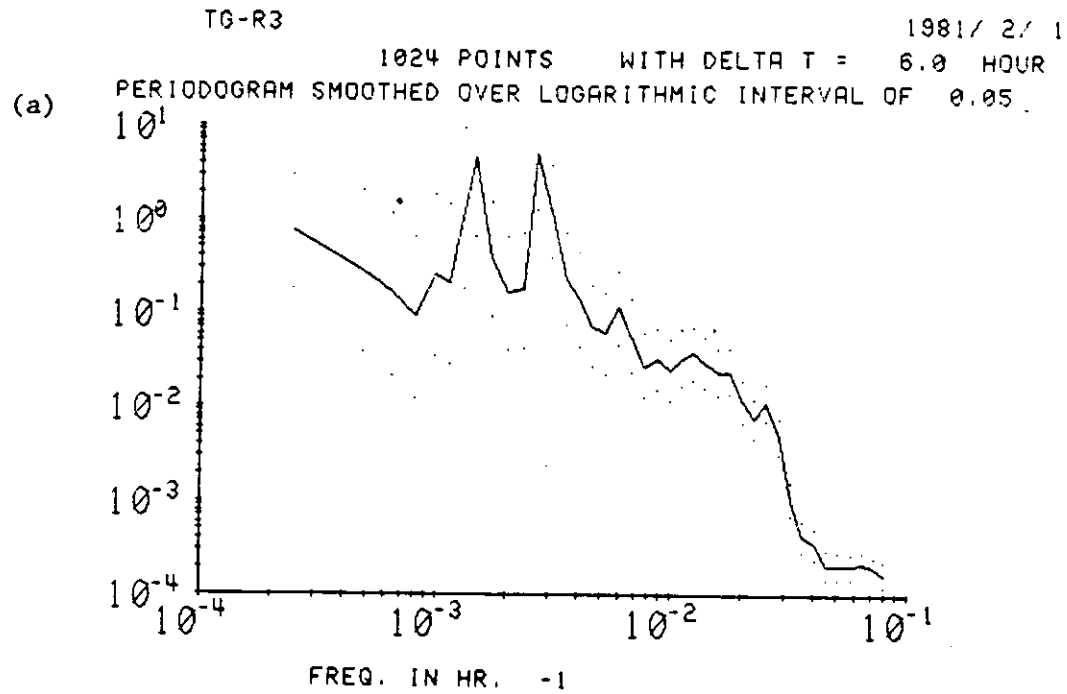


Figure 63. Power spectrum of (a) low-passed Wauna - Tongue Pt. slope, and (b) low-passed Tongue Pt. tidal range. Daily tides and seasonal trends have been removed from both (a) and (b); river flow effects have been removed from (a). Dots indicate 95% confidence intervals.



the spectrum of Wauna-Tongue Pt. slope (after removal of daily tides, seasonal trend and river flow effect). The dominant periodicities are the same (~15 and ~28 days) as seen in the Tongue Pt. tidal range (Figure 63b).

The correlation with riverflow increases upriver in both the heights and slopes. This correlation is also very broadly based in time, but the response is not necessarily in phase with the forcing. The response to riverflow is very much weaker below than above Tongue Pt., as predicted by the model of Section 3.3.

The regression results for tidal range and riverflow (Table 14) are very similar to the correlation results in Tables 13a and b. The importance of tidal range is greatest at Wauna (in the heights) and in the estuary (in the slopes). The importance of riverflow grows upriver for both heights and slopes. The highly organized time structure of the correlation between height and slope and these forcing functions means that the regression model is quite successful, even though zero lag, rather than the optimum lag, was used in all cases in the regression model.

The tidal and riverflow forcing are important in both the tidal heights and slopes; we can therefore expect the barotropic part of the residual flow to respond very strongly to these forcing functions. A very different situation pertains with the atmospheric forcing, where the response of the tidal heights to atmospheric forcing is much stronger than that of the slopes. That tidal height is correlated with pressure, even after the removal of IBE, means that the response of coastal sea level to pressure is somewhat greater than that predicted by the IBE (as found also by Chelton and Davis 1982 and other workers). This response decreases upriver. The response of the slope to pressure does not show the same systematic structure in space and time as the response of the slope to riverine and tidal forcing.

The response to wind stress is also dependent on the wind data used. Both the Newport and the geostrophic wind data suggest that the tidal heights at the entrance respond most strongly to the alongshore wind stress (Table 13a); that is, that coastal Ekman dynamics govern the response of the tidal heights in the lower estuary. The geostrophic wind data also show a substantial response of the tidal heights to the onshore component of the wind. This response is greatest at Tongue Pt. and presumably is the result of local sea surface setup in the estuary.

The response of the slopes in Tables 13a and b and 14 to atmospheric forcing is smaller in magnitude and temporally less well-organized than the response of the tidal heights to the same forcing. There is some indication in Tables 13a and b that both the coastal upwelling and downwelling cycle and local setup of water inside the estuary (by the onshore component of the wind stress) are of some importance in the lower estuary. On the whole, atmospheric forcing plays a less prominent role in determining residual slope (and, therefore, barotropically driven flows) than tidal heights; that is, the barotropic residual circulation is dominated by tidal and riverflow forcing. Our first hypothesis, that atmospheric processes dominate the residual flow, is thus disproved. The second hypothesis, that coastal-scale forcing is more important than local forcing, can not be proven or disproved; it appears that they are of about equal (though minor) importance inside the estuary.

There are some qualifications that must be included with the statement that the barotropic residual circulation is dominated by tides and riverflow. First, most of the tidal height and slope records are incomplete and include more summer than winter data; atmospheric forcing is most important in winter. The atmospheric response is greatest at Tongue Pt., where data for two complete years are available. The fall of 1981 was, however, quite stormy, and storm effects are well-represented in the 1981 data. Second, it is possible that wind data from a different station would yield better results. Nonetheless, the

qualitative examination of time-series data further demonstrates the dominance of riverine and tidal forcing.

It is reasonable to pose the question as to how the atmospheric forcing can be important in the heights and not the slopes -- conservation of mass requires that flows be associated with the changes in estuary surface level. The point is that these flows are too small to dominate the residual circulation. This is in marked contrast to systems such as Chesapeake Bay, where the atmospheric processes dominate residual flows (Elliot and Wang 1977). Consider the 0.5 m increase in sea level of a large storm between November 10 and 14, 1981. This was the sharpest such event of the 1979-81 period. This 50 cm change is about half the amplitude of the M2 tide but occurred over about eight tidal cycles. The volume exchange during a tidal cycle was therefore only  $\sim 1/16$  of that associated with M2 tide. A similar effect (in terms of volume of water transported) would be achieved by a riverflow change of  $\sim 30-35$  kcfs (about  $900-1000 \text{ m}^3/\text{s}$ ), according to Table 5a. Changes in riverflow of that magnitude are hard to detect in the Tongue Pt.-Jetty A slope. The relatively large effect of the onshore component of the wind on surface slope is primarily a result, then, not of sea-level changes but of redistribution of water in the estuary.

Another way of considering the difference between the response of the slope and the response of currents is in terms of the wave speed of a surface slope (barotropic) adjustment. Consider an impulsive change in sea level at the mouth of the estuary. The surface slope adjustment to this change in sea level will move upstream at  $c = (gd)^{\frac{1}{2}}$ , the shallow water wave phase speed. Using the tidal model results as typical, the phase difference for the M2 tide between Jetty A and Tongue Pt. is only  $\sim 20$  deg in phase or  $\sim 40$  minutes. From the point of view of low passed heights or slopes, (filtered and decimated to six-hour intervals), and relative to the several day period of most atmospheric disturbances, this adjustment occurs essentially instantaneously. Thus the flows associated with changes in sea level are small, and the changes are felt nearly simultaneously throughout the system.

## 4. SUMMARY AND RECOMMENDATIONS

### 4.1 SUMMARY OF PRESENT KNOWLEDGE

CREDDP circulatory studies were carried out in six areas: theory of estuarine circulation, tidal processes, system energetics, density (i.e. salinity) distribution, salt transport, and low-frequency flow processes.

The major theoretical results are the definition of modes of estuarine circulation and an analysis of the forces maintaining the salinity distribution. The circulation modes are defined by application of a scaling analysis and perturbation expansion. This analysis separates the primary  $O(1)$  tidal circulatory processes, from the secondary, modifying features. The primary tidal circulation occurs at diurnal and semidiurnal frequencies and constitutes the first estuarine circulation mode. It is driven both by the surface slope and the time-varying density distribution. The secondary  $O(\epsilon)$  circulation modifies the primary tidal circulation. It can be divided into three modes that occur at different frequencies: the tidal overtones (that occur at frequencies higher than semidiurnal and are produced by the distortion of the tidal wave as it moves upriver), the secondary tidal circulation (at diurnal and semidiurnal frequencies), and the residual (or time-averaged) circulation, which varies during the tidal month and seasonally. The residual circulation is driven by the riverflow, the salinity distribution, tidal energy transferred from the primary tidal circulation, and, to a lesser extent, atmospheric effects.

With regard to the tidal circulation, data analysis and model results show that:

- Tidal range decreases rapidly in the upriver direction on the tides of higher range; that is, an increase in tidal range at the mouth results in a less than proportional increase upriver. Conversely, tidal range drops off slowly with river mile on tides of lesser range. This occurs because the dissipation of tidal energy varies with the cube of the tidal range, but the tidal energy flux into the estuary varies approximately with the square of the tidal range.
- There is more energy available for mixing on the ebb than on the flood, because of the strength of the riverflow. The greater mixing on ebb and the effects of salinity intrusion combine to make the vertical structure of the ebb currents very different than that of flood currents; this is the ebb-flood asymmetry. The vertical distribution of the mean flow is determined by the differences between the ebb and flood flows. The large shear on ebb, the greater vertical uniformity of the flood flow and the horizontal salinity gradient combine to generate net upstream bottom currents in the lower estuary.
- The vertical structure of the currents is also strongly influenced by along-channel changes in depth and width. Net upstream bottom flow associated with reaches of strong horizontal salinity gradients is often not continuous from the entrance to the upstream limits of salinity intrusion. Its continuity is often interrupted by pockets of net downstream bottom flow caused by interaction of the flow with topographic features. This suggests that the estuarine turbidity maximum, which is dependent upon the upstream bottom flow, may form preferentially in certain parts of the estuary and may be spatially discontinuous.
- Tidal transports and tidal velocities are greater in the North Channel than in the South Channel. Most of the tidal prism of the lower estuary is filled by the flow in the North Channel.

- o Freshets reduce the tidal range and greatly increase the river stage above RM-20, because the riverflow increases the friction. Tides and stage below Tongue Pt. are much less affected by such changes in riverflow.
- o Energy budget calculations based on the tidal model show that the tidal energy entering the mouth of the estuary from the ocean is the dominant source of energy for circulatory processes in the estuary proper (below about RM-18). The energy budget for this reach is essentially tidal energy flux in, dissipation out. The dominant source of energy in the river is fluvial potential energy, and the energy budget for this part of the system is fluvial potential energy flux in, dissipation out. Most of this energy is dissipated above RM-30 so that below RM-18, energy from the riverflow is less important than tidal energy under all riverflow conditions. Both tidal and fluvial energy inputs must be considered in the area of minimum energy between about RM-18 and RM-30 that corresponds to the islands and other depositional features of Cathlamet Bay. Much more energy is available for circulation and sediment transport in the fluvial part of river during the larger floods (e.g. 1894 and 1948) than is ever supplied to the estuary proper by any tidal condition.

Use of the perturbation expansion to define salinity distribution modes provides important insight into the factors that govern salinity intrusion into the estuary. The analysis indicates that the salinity distribution is maintained primarily by the tidal currents (including the density-driven part thereof) working on the salinity gradient, not by the mean upstream bottom flow. Salt must be transported vertically as well as horizontally, if the salinity distribution is to be maintained. It appears that mixing and tidal transport, rather than entrainment, are primarily responsible for this vertical transport, but details of vertical salt transport remain unclear.

During periods of low riverflow there is a neap-to-spring transition that changes the density structure from well or partially-mixed (spring tide) to highly stratified (neap tide). This transition is less prominent under high-flow conditions. The transition may be abrupt because of the interaction of vertical mixing and stratification; increased stratification during periods of decreasing tidal range before the neap tide inhibits mixing which, in turn, allows further increases in stratification. The process is reversed as tidal range increases after the neap. Salinity intrusion length is greatest under low-flow, neap tide conditions, because the stratification allows upstream movement without significant mixing with overlying river water. Salt has been observed in this study to penetrate beyond RM-25, but salinity intrusion probably extends to about RM-30 several times per year. At the end of ebb on an extreme high-flow spring tide, no salt is found anywhere upriver of RM-2.

The high-flow ( $\sim 310$  kcfs or  $8,800 \text{ m}^3/\text{s}$ ) and low-flow ( $\sim 155$  kcfs or  $4,400 \text{ m}^3/\text{s}$ ) seasonal mean, minimum, and maximum salinity distributions have been defined for North and South Channels. These seasonal distributions should be useful in understanding biological processes having seasonal time scales, but averaging obscures physical processes which are better understood in terms of the actual states of the system. The seasonal averages suggest that salinity intrusion into the North Channel is somewhat greater than that into the South Channel under high-flow conditions, because of the stronger riverflow in the South Channel. The difference is less pronounced under low-flow conditions.

Salinity intrusion into peripheral bays is not well defined except in Baker and Youngs Bays. The salinity intrusion into Grays and Cathlamet Bays is inherently hard to predict, because these bays are adjacent to the main channels near the upstream limits of salinity intrusion. Whether intrusion occurs in these bays depends on the salinity in the main channel at the sill depth of the

peripheral bay or channel. Because the peripheral bays are shallow, wind-driven circulation is more important there than in deeper parts of the estuary.

Salt and water transport calculations show that most of the net outflow of water is near the surface in the South Channel. Upstream bottom flow is strongest in the North Channel. Salt enters the estuary primarily by tidal mechanisms in a near-surface jet in the North Channel, at the same lateral position as the strongest tidal currents. Unlike the tidal currents, the maximum salt transport is below the surface (but above mid-depth) because the salinity is low at the surface. The mean or residual circulation appears to be important in inward salt transport only on neap tides and in those parts of the estuary where horizontal salinity gradients are unusually strong. Salt transports near the bottom are otherwise small. The large, near-surface, mean outflow (primarily riverflow) in the South Channel transports salt out of the estuary.

The response of the barotropic (surface slope-driven) part of the low-frequency or residual flow and to changes in riverflow, atmospheric effects (wind and pressure), and tidal energy was investigated by use of the statistical properties of the atmospheric data, tidal heights and surface slopes. Record lengths of up to two years were used. The primary conclusions of the residual flow work were:

- o Atmospheric pressure fluctuations, wind-driven changes in elevation of the coastal ocean, and along-channel winds over the estuary are all important to sea levels in the system, but atmospheric forcing is too weak to dominate the mean or residual flow in the estuary.
- o The dominant factors controlling the residual circulation (slopes, currents, and salinity) in the estuary proper (below Tongue Pt.) are the tidal forcing and river inflow. Tidal processes and riverflow are about equally dominant in controlling slopes in the Wauna-Tongue Pt. reach. River flow is strongly dominant above Wauna.

#### 4.2 AREAS OF INADEQUATE KNOWLEDGE

The CREDDP field program and the very large NOS data set that became available less than a year before the end of the program have left us with one of the most intensive and extensive physical data bases available for any estuary of comparable size, but one which is still incompletely analyzed. There are, however, certain areas in which even this data base is inadequate and certain important processes that have not been examined at all. One geographic area that has been found to be critical to the salt and mass balance of the estuary is the mid-estuary flats. Substantial exchanges of water and salt are believed to occur in the subsidiary channels that cross these flats, but no data are available to assess these transports. century (Gibbs 1973), and severe working conditions have limited the acquisition of data seaward of Jetty A. Despite plans to deepen the entrance channel, knowledge of this area can not be considered sufficient for modeling of estuarine processes, prediction of tidal currents and severe wave conditions, channel design studies, or management of dredging. We would like to know whether critical conditions are reached at any stage of the tide for propagation of internal waves; such hydraulic control at the entrance (or at the sills in both channels between RM-6 and RM-9) would affect circulatory processes throughout the estuary. The answer to this question requires more velocity and density profiles.

Another geographic area where the data are inadequate is the peripheral bays. Data of all kinds are absent in Grays Bay and incomplete in the other bays. The bays are difficult to study either with moored instruments or profiling gear because they are shallow. Moreover, atmospheric forcing is probably more



important there, making any short segment of data more difficult to relate to the mean conditions. Knowledge of how the circulation of the main body of the estuary works has now reached the point that sampling and modeling efforts can be profitably directed toward the peripheral bays.

Moored-instrument studies have inadequately sampled near-surface processes in all parts of the estuary. The large amount of floating debris, wave action, and vandalism problems render near-surface moorings unattractive; most studies have kept "surface" meters at 3 to 5 m on MLLW. Profiling instruments show large shears and stratification near the surface under certain conditions. Prediction of severe wave conditions near the mouth requires near-surface current and density observations because the largest shears and phase differences in the tidal currents are found near the entrance.

Studies to date have focused on synoptic-scale processes, not the details of turbulent mixing, internal waves, etc. To a certain extent it is productive to conduct smaller-scale, mechanistic studies in simpler systems; some results from these estuaries may then be used in the more complex Columbia River Estuary. However, the ability to do this is presently inhibited by the almost total absence of some relatively simple measurements. Profile data are lacking during the high-flow season, and no acoustic echo sounding transects are available for any season. The acoustic echo sounding records are probably the easiest and most productive work that could be carried out. They provide a wealth of qualitative information concerning the form and extent of salinity intrusion, vertical mixing, transport processes, and so on. These records, combined with CTD profiling, would be an inexpensive way to determine the extent of salinity intrusion into peripheral bays. A more complete understanding of the neap-to-spring transition in density structure and salinity intrusion length may also require detailed measurements of flow and density on a scale fine enough to allow calculation of turbulent fluxes of momentum and salt.

Evaluation of the function and distribution of fronts is important. Fronts are known to be of high biological productivity in many bodies of water; they have so far been ignored in studies of the Columbia River Estuary.

The one-dimensional model should be refined to include the diurnal tides and the tidal overtones, and the North and South channels should also be treated individually. These changes would improve the tidal flows and energy budget calculated from the model.

## LITERATURE CITED

- Allen, G. P.; Solomon, J. C.; DuPenhoat, Y.; De Grondpre, C. 1980. Effects of tides on mixing and suspended sediment transport in macrotidal estuaries. *Sed. Geol.* 26: 69-80.
- Allen, J. S. 1980. Models of wind-driven currents on the continental shelf. *Ann. Rev. Fluid Mech.* 12: 389-433.
- Anderson, G. C.; Barnes, C. A.; Buddinger, T. F.; Love, C. M.; McManus, D. A. 1961. The Columbia River discharge area of the Northeast Pacific Ocean, a literature survey. University of Washington, Department of Oceanography.
- Bakun, A. 1975. Daily and weekly upwelling indices, West Coast of North America, 1967-73. NOAA Tech. Rep. 16, NMFS SSRF-693.
- Barnes, C. A.; Duxbury, A. C.; Morse, B.-A. 1972. The Columbia River Estuary and Adjacent Ocean Waters Bioenvironmental Studies. Circulation and selected properties of the Columbia River effluent at sea. Seattle: University of Washington Press.
- Callaway, R. J. 1971. Applications of some numerical models to Pacific Northwest estuaries. Proceedings: 1971 Technical Conference on Estuaries of the Pacific Northwest, Circ. #42. Engineering Experiment Station, Oregon State University, Corvallis, OR.
- Chelton, D. B.; Davis, R. E. 1982. Monthly mean sea-level variability along the west coast of North America. *J. Phys. Oceanogr.* 12: 757-784.
- Columbia River Estuary Data Development Program (CREDDP). 1984. The Columbia River Estuary: atlas of physical and biological characteristics. Astoria, OR.
- Conomos, T. J.; Gross, M. G.; Barnes, C. A.; Richards, F. A. 1972. The Columbia River Estuary and Adjacent Ocean Waters Bioenvironmental Studies. River-ocean nutrient relations in summer. Seattle: University of Washington Press.
- Creech, C. 1977. Five-year climatology (1972-1976) off Yaquina Bay, Oregon. Oregon State U. Sea Grant Pub. #ORES-U-77-011, Corvallis, OR.
- Dronkers, J. J. 1964. Tidal Computations in Rivers and Coastal Waters. Amsterdam: North-Holland Publishing Company.
- Dyer, K. R. 1973. Estuaries: A Physical Introduction. London: John Wiley & Sons.
- Elliot, A. J.; Wang, D.-P. 1978. Hydrodynamics of Estuaries and Fjords. The

Effect of meteorological forcing on the Chesapeake Bay: The coupling between an estuarine system and its adjacent coastal waters. New York: Elsevier Scientific Publishing Co.

- Fischer, H. P. 1976. Mixing and dispersion in estuaries. *Ann. Rev. of Fluid Mech.*: 107-133.
- Foreman, M. G. G. 1977. Manual for Tidal Heights Analysis and Prediction. Pacific Marine Science Report 78-6. Patricia Bay, Sidney, B.C.: Institute of Ocean Sciences.
- Foreman, M. G. G. 1978. Manual for Tidal Currents Analysis and Prediction, Patricia Bay, Sidney, B.C.: Institute of Ocean Sciences.
- Foreman, M. G. G.; Henry, R. F. 1979. Tidal Analysis Based on High and Low Water Observations. Pacific Marine Science Report 79-15. Patricia Bay, Sidney, B.C.: Institute of Ocean Sciences.
- Gardner, G. B.; Nowell, A. R. M.; Smith, J. D. 1980. Turbulent processes in estuaries. Reprinted from *Estuarine and Wetland Processes*. New York: Plenum Publishing Corp.
- Haas, L. W. 1977. The effect of spring-neap tidal cycle on the vertical salinity structure of the James, York and Rappahannock Rivers, Virginia, U.S.A. *Est. Coast. Mar. Sci.* 5: 485-496.
- Halpern, D.; Pillsbury, R. D.; Smith, R. L. 1974. An intercomparison of three current meters operated in shallow water. *Deep-Sea Res.* 21: 489-497.
- Hamilton, P. 1983. Numerical modeling of the depth dependent salinity intrusion for the Coal Point Deepening Project in the Columbia River Estuary. Final report. Portland: U.S. Army Engineer District.
- Hamilton, P. 1984. Columbia River Estuary hydrodynamic modelling, final report. Astoria: Columbia River Data Development Program.
- Hamilton, P.; Rattray, M., Jr. 1978. *Estuarine Transport Processes. Theoretical aspects of estuarine circulation*. Columbia: University of South Carolina Press.
- Hansen, D. V. 1965a. Currents and Mixing in the Columbia River Estuary, *Ocean Sci. Ocean Engin.; Technol. Soc. and Am. Soc. Limnol. Oceanogr.* 2: 943-955.
- Hansen, D. V. 1965b. Estuaries. Salt balance and circulation in partially mixed estuaries. Publication No. 83. Washington, D.C.: American Association for the Advancement of Science.
- Hansen, D. V.; Rattray, M., Jr. 1965. Gravitational circulation in straits

- and estuaries. *J. Mar. Res.* 23: 104-122.
- Hickey, B. M. 1979. The California Current system--hypotheses and facts. *Prog. Oceanog.* 8: 191-279.
- Hickey, B. M.; Pola, N. E. 1983. The seasonal alongshore pressure gradient on the West Coast of the United States. *J. Geophys. Res.* 88: 7623-7633.
- Hopkins, T. S. 1971. On the barotropic tide over the continental shelf off the Washington-Oregon Coast. Seattle: University of Washington, Dept. Of Oceanogr. Special Report #46.
- Hughes, F. W. 1968. Salt flux and mixing processes in the Columbia River Estuary during high discharge. Seattle: University of Washington, M.S. Thesis.
- Hughes, F. W.; Rattray, M., Jr. 1980. Salt flux and mixing in the Columbia River Estuary. *Est. Coast. Mar. Sci.* 10: 479-493.
- Ianniello, J. P. 1977a. Non-linearly induced residual currents in tidally dominated estuaries. Ph.D. dissertation, The University of Connecticut.
- Ianniello, J. P. 1977b. Tidally induced residual currents in estuaries of constant breadth and depth. *J. Mar. Res.* 35: 755-786.
- Ianniello, J. P. 1979. Tidally induced residual currents in estuaries of variable breadth and depth. *J. Phys. Oceanogr.* 9: 962-974.
- Ianniello, J. P. 1981. Comments on tidally induced residual currents in estuaries: dynamics and near-bottom flow characteristics. *J. Phys. Oceanogr.* 11: 126-134.
- Irish, J. D.; Bendiner, D. J.; Levin, M. D.; Zeh, J. 1976. WHIMPER, a library of time series programs. Seattle: University of Washington, Dept. of Oceanography Tech. Rept. #342.
- Jay, D. 1982. Columbia River Estuary salinity distribution. Submitted to Portland: US Army Corps of Engineers.
- Jay, D. 1983. Interim Report: circulatory processes in the Columbia River Estuary. Seattle: University of Washington.
- Kalvaitis, A. P. 1981. Uncertainty estimates for oceanographic and meteorological measurements. ESO Technical Report TE3-81-008.
- Kreiss, H. 1957. Some remarks about non-linear oscillations in tidal channels. *Tellus* 9: 53-68.

- Lavelle, J. W.; Mojfield, H. 1983. Effects of time varying viscosity on oscillatory turbulent channel flow. *J. Geophys. Res.* 88: 7607-7616.
- Long, C. E. 1981. A simple model for time-dependent stably stratified turbulent boundary layers. Seattle: University of Washington, Special Report No. 95.
- Longuet-Higgins, M. S. 1969. On the transport of mass by time-varying ocean currents. *Deep-Sea Res.* 16: 431-447.
- Lutz, G. A.; Hubbell, D. W.; Stevens, H. H., Jr. 1975. Discharge and flow distribution, Columbia River Estuary. Washington, D. C.: U. S. Government Printing Office, Geological Survey Professional Paper 433-P.
- Marmer, H. A. 1951. Tidal Datum Planes. Washington, D. C.: U. S. Government Printing Office, Special Publication No. 135. Revised (1951) Edition.
- McConnell, R. J.; Snyder, G. R.; Durkin, J. T.; Blahm, T. H. 1981. Concentration, extent and duration of salinity intrusion into the Columbia River Estuary September-October 1977-78. *Proceedings of the National Symposium on Freshwater Inflow to Estuaries, FWS/OBS-81/04*, 2: 41-54.
- Narayanan, S.; Berryman, D.; Blaskovich, A. 1982. Columbia River Estuary study. Submitted to Victoria, B.C.: US Army Corps of Engineers.
- National Oceanic and Atmospheric Administration 1980. The relationship between the upper limit of coastal wetlands and tidal datums along the Pacific coast. Rockville: National Ocean Survey.
- Ocean Engineering Programs School of Engineering, Oregon State University, Corvallis, Oregon 1975. Physical characteristics of the Youngs Bay estuarine environs. Submitted to ALUMAX Pacific Aluminum Corporation.
- Officer, C. B. 1976. *Physical Oceanography of Estuaries (and Associated Coastal Waters)*. New York: Wiley-Interscience.
- Orem, H. M. 1968. Discharge in the lower Columbia River Basin, 1928-65. Washington, D. C.: US Geological Survey Circular 550.
- Phillips, O. M. 1980. *The Dynamics of the Upper Ocean*. Cambridge: Cambridge University Press.
- Rattray, M., Jr.; Dworski, J. G. 1980. Comparison of methods of analysis of the transverse and vertical circulation contributions to the longitudinal advective salt flux in estuary. *Est. Coast. Mar. Sci.* 11: 515-536.

- Robe, R. Q. 1968. Salt flux in and classification of the Columbia River Estuary during high and low discharge. Seattle: University of Washington, unpublished ms.
- Ryan, T. A., Jr.; Joiner, B. L.; Ryan, B. F. 1976. Minitab Student Handbook. North Scituate, Mass: Duxbury Press.
- Ryan, T. A., Jr.; Joiner, B. L.; Ryan, B. F. 1980. Minitab Reference Manual. Pennsylvania State University.
- Sherwood, C.; Creager, J. S.; Roy, E. H.; Gelfenbaum, G.; Dempsey, T. 1984. Sedimentary processes and environments in the Columbia River Estuary. Astoria: CREST/CREDDP
- Simmons, H. B. 1966. Estuarine and Coastline Hydrodynamics. Field experience in estuaries. New York: McGraw-Hill.
- Sternberg, R. W.; Creager, J. S.; Glassley, W.; Johnson, J. 1977. Aquatic disposal field investigations, Columbia River disposal site, Oregon. Appendix A: Investigation of the hydraulic regime and physical nature of bottom sedimentation. Vicksburg: U.S. Army Engineer Waterways Experiment Station.
- Townsend, C. K.; Hull, W. V.; 1981. OPR-N805-AR-81, Circulatory Survey, Columbia River Estuary, OR.
- Uncles, R. J.; Jordan, M. D. 1980. A one-dimensional representation of residual currents in the Severn Estuary and associated observations. Est. Coast. Mar. Sci. 10:
- U.S. Army Engineers. 1960. 1959 Current Measurement Program, Columbia River at Mouth, Oregon and Washington, Vol. IV. Portland: Corps of Engineers.
- U.S. Coast and Geodetic Survey 1952. Manual of harmonic constant reductions. Special Publication No. 260, US Government Printing Office.
- U.S. Navy Hydrographic Office 1958. Inshore survey results, Columbia River approaches. Washington, D. C.: H. O. Misc. 15359-21S.
- Werner, F.; Hickey, B. M. 1983. The role of a longshore pressure gradient in Pacific Northwest coastal dynamics. J. Phys. Oceanogr. 13: 395-410.
- Webster, I.; Juhasz, T. 1980. Columbia River Estuary study, circulation and hydrography, current studies 1980. Dobrocky Seatech, Ltd.
- Williams, C. F. 1933. Mouth of Columbia River current survey 1932-33. Portland: War Dept., Office of District Engineer. dummy page

APPENDIX A

Field Sampling Locations, 1977 to 1981

Table 15. CREDDP Current Meter Mooring Deployments March–November 1980.

<u>Station Designation</u>	<u>Latitude (N)</u>	<u>Longitude (W)</u>	<u>Nominal Depths (m) of Instrument</u>	<u>Installation Method</u>	<u>Date of Installation</u>	<u>Date of Recovery</u>
* CM-1C	46° 15' 30"	124° 01' 17"	5 11 17	Subsurface mooring	June 20, 1980	July 1, 1980
CM-1D	46° 15' 02"	124° 01' 12"	5 9 12	Subsurface mooring	June 20, 1980	July 3, 1980
CM-2S	46° 15' 13"	124° 03' 21"	6 10 14	Subsurface mooring	October 15, 1980	October 27, 1980
CH-3S	46° 14' 50"	124° 00' 28"	5 9 12	Subsurface mooring	October 15, 1980	October 27, 1980
CM-4A	46° 12' 08"	123° 56' 25"	5 12	Subsurface mooring	June 25, 1980	July 3, 1980
CM-4B	46° 14' 20"	123° 54' 13"	5 9	Subsurface mooring	June 20, 1980	June 25, 1980
CM-5A	46° 11' 52"	123° 51' 05"	3 6 9	Fixed to bridge	March 25, 1980	May 21, 1980
CM-5A	46° 11' 52"	123° 51' 05"	3 6 9	Fixed to bridge	June 20, 1980	July 5, 1980
CM-5A	46° 11' 52"	123° 51' 05"	3 6 9	Fixed to bridge	July 5, 1980	October 14, 1980
CH-5A	46° 11' 52"	123° 51' 05"	3 6 9	Fixed to bridge	October 16, 1980	October 30, 1980



Table 15. (continued).

<u>Station Designation</u>	<u>Latitude (N)</u>	<u>Longitude (W)</u>	<u>Nominal Depths (m) of Instrument</u>	<u>Installation Method</u>	<u>Date of Installation</u>	<u>Date of Recovery</u>
CM-5B	46 <sup>0</sup> 14' 21"	123 <sup>0</sup> 52' 21"	6 15	Fixed to bridge	March 27, 1980	May 21, 1980
** CM-5B	46 <sup>0</sup> 14' 21"	123 <sup>0</sup> 52' 21"	7 16	Fixed to bridge	June 20, 1980	July 4, 1980
CM-5B	46 <sup>0</sup> 14' 21"	123 <sup>0</sup> 52' 21"	6 15	Fixed to bridge	July 4, 1980	October 14, 1980
CM-5B	46 <sup>0</sup> 14' 21"	123 <sup>0</sup> 52' 21"	6 15	Fixed to bridge	October 16, 1980	October 30, 1980
CM-6S	46 <sup>0</sup> 13' 07"	123 <sup>0</sup> 46' 04"	5 9	Subsurface mooring	October 16, 1980	October 27, 1980
CM-7D	46 <sup>0</sup> 15' 35"	123 <sup>0</sup> 37' 10"	5 9	Subsurface mooring	June 19, 1980	July 3, 1980
*** CM-7E	46 <sup>0</sup> 13' 03"	123 <sup>0</sup> 38' 27"	5	Subsurface mooring	June 21, 1980	July 4, 1980
CM-7F	46 <sup>0</sup> 10' 48"	123 <sup>0</sup> 39' 23"	5	Subsurface mooring	June 21, 1980	July 4, 1980
CM-7M	46 <sup>0</sup> 13' 52"	123 <sup>0</sup> 40' 04"	5	Subsurface mooring	October 15, 1980	October 29, 1980
CM-7N	46 <sup>0</sup> 15' 36"	123 <sup>0</sup> 37' 08"	5 9	Subsurface mooring	October 16, 1980	October 27, 1980
CM-7S	46 <sup>0</sup> 12' 01"	123 <sup>0</sup> 40' 56"	9	Subsurface mooring	October 15, 1980	October 29, 1980

\* Top two meters lost to ship damage to mooring.

\*\* Instruments were deployed 1m deeper during the period.

\*\*\* Mooring possibly dragged to shallower water during the period.

Table 16. CREDDP Velocity and Density Profiles Collected in October 1980.

<u>Vessel</u>	<u>Station(s)</u>	<u>Number of Casts Completed</u>	<u>Time Period</u>	<u>Comments</u>
U and I	6SA	19	Oct. 16, 07:20 - Oct. 16, 19:05	
Thorfinn	6SA	42	Oct. 16, 14:00 - Oct. 18, 10:45	
U and I	6SB, 6SC, 6SD	12	Oct. 16, 19:29 - Oct. 17, 03:00	
U and I	6SB, 6SA, 6SD	15	Oct. 17, 01:02 - Oct. 17, 10:32	
U and I	6SE, 6SB, 6SA	9	Oct. 17, 10:52 - Oct. 17, 14:03	
U and I	6SE, 6SC, 6SD	8	Oct. 17, 14:26 - Oct. 17, 16:16	
U and I	6SE, 6SA, 6SC, 6SD	22	Oct. 17, 16:47 - Oct. 18, 05:30	
U and I	2N	35	Oct. 18, 08:30 - Oct. 19, 01:30	Station moved 300 m east
Thorfinn	2S	42	Oct. 18, 11:00 - Oct. 19, 08:30	Anchor dragging Oct. 19, 23:30
U and I	3F	11	Oct. 19, 02:30 - Oct. 19, 12:05	
Thorfinn	3F	24	Oct. 19, 09:30 - Oct. 19, 20:00	
U and I	3H	25	Oct. 19, 13:28 - Oct. 20, 01:00	Moved to east side of buoy 21, Oct. 19, 17:30
Thorfinn	3I	61	Oct. 19, 21:00 - Oct. 20, 13:53	Double casts now taken at each station
U and I	3E	14	Oct. 20, 01:35 - Oct. 20, 04:34	
U and I	3J	48	Oct. 20, 05:17 - Oct. 20, 16:58	

Table 16. (continued).

<u>Vessel</u>	<u>Station(s)</u>	<u>Number of Casts Completed</u>	<u>Time Period</u>	<u>Comments</u>
Thorfinn	5NA	56	Oct. 20, 16:00 - Oct. 21, 07:31	
U and I	5NA, 5NB, 4NB, 4NA	102	Oct. 20, 19:00 - Oct. 21, 16:47	Dragged anchor Oct. 21, 01:00
Thorfinn	5NC	99	Oct. 21, 08:35 - Oct. 22, 09:03	
U and I	5NA, 5NB, 5NC	96	Oct. 21, 17:15 - Oct. 22, 09:17	
U and I	6SF, 6SA, 6SB, 6SE	16	Oct. 22, 14:59 - Oct. 22, 17:54	
Thorfinn	6SE	157	Oct. 22, 15:20 - Oct. 24, 06:31	
U and I	6SA, 6SB, 6SF	18	Oct. 22, 19:29 - Oct. 22, 22:55	
U and I	6SA	50	Oct. 22, 23:30 - Oct. 23, 08:02	Dragged anchor in ebb Oct. 23, 02:30
U and I	6SF, 6SA, 6SB	76	Oct. 23, 15:44 - Oct. 24, 05:31	
U and I	5SA, 5SB	98	Oct. 24, 07:28 - Oct. 25, 22:31	8 casts taken at station 5SB
Thorfinn	5SB	100	Oct. 24, 10:25 - Oct. 25, 10:30	
U and I	4SB, 4SA, 3H	186	Oct. 25, 22:50 - Oct. 27, 07:34	12 casts taken at station 3H. Dragged anchor into shipping lane, Oct. 26, 10:00
U and I	11A, 11B, 11C.	134	Oct. 27, 18:00 - Oct. 28, 23:14	

Table 17. 1981 NOS and U.S. Geological Survey Tidal Height Stations.

A. 1981 NOS Stations

<u>Station Location</u>	<u>Latitude (N)</u>	<u>Longitude (W)</u>
Jetty A, WA	46°16.0'	124°02.2'
Chinook, WA	46°16.3'	123°56.8'
Ft. Steven, OR	46°12.4'	123°57.0'
Astoria, Youngs Bay, OR	46°10.3'	123°50.5'
Tongue Pt., OR	46°12.5'	123°46.0'
Knappton, WA	46°16.2'	123°02.8'
Altoona, WA	46°16.0'	123°39.3'
Knappa, Knappa, Slough, OR	46°11.3'	123°35.3'
Skamokowa, WA	46°16.1'	123°06.1'
Cathlamet, WA	46°12.1'	123°23.1'
Wauna, OR	46°09.6'	123°24.3'
Beaver, OR	46°10.8'	123°11.2'
Kalama, WA	46°00.4'	122°50.8'

B. 1980-81 U.S. Geological Survey Tidal Height Stations

<u>Station Location</u>	<u>Latitude (N)</u>	<u>Longitude (W)</u>
Jetty A, WA	46°16.0'	124°02.2'
Wauna, OR	46°09.4'	123°24.5'
Columbia City, OR	46°54.0'	122°48.0'

Table 18. NOS 1981 Current Meter Mooring Deployments.

Period	Station Number	Depth (Feet)	Observation Levels (Feet)	Mooring Type
1, 2, 3, 4, 8, 9, 12, 13, 14	C1	75	-15, -25, +25, +5	T/B.P.
8, 9, 10, 11	C2	45	+10	Special
8, 9	C3	40	-15, -25, +5	T/B.P.
8, 9	C4	65	-15, -25, +5	T/B.P.
1, 2, 8, 9, 12, 13	C5*	25	+5	B.P.
3	C6	10	+5	B.P.
3	C7	20	+5	B.P.
1, 2, 8, 9, 12, 13	C8*	10	+5	B.P.
Project	C9	40	-15, -25, +5	T/B.P.
1, 2, 12, 13	C10	35	-15, +5	T/B.P.
4	C11	14	+5	B.P.
1, 2, 3, 4, 14	C12	45	-15, -25, +5	T/B.P.
3, 4, 14	C13	12	+5	B.P.
1, 2, 3, 4, 12, 13, 14	C14	40	-15, -25, +5	T/B.P.
3, 4, 14	C15	15	+5	B.P.
1, 2, 3, 4, 12, 13, 14	C16	30	-15, +5	T/B.P.
1, 2, 8, 9, 12, 13	C17	40	-15, -25, +5	T/B.P.
1, 2, 8, 9, 12, 13	C18	40	-15, -25, +5	T/B.P.
4	C19	25	+5	B.P.
1, 2, 12, 13	C20	40	-15, -25, +5	T/B.P.
10	C21	25	+5	B.P.
10	C22	20	+5	B.P.
10, 11, 12, 13	C23	40	-15, -25, +5	T/B.P.
10, 11	C24	25	+5	B.P.
10, 11	C25	35	-15, +5	T/B.P.
10, 11	C26	20	+5	B.P.
10, 11	C27	35	-15, +5	T/B.P.
11	C28	15	+5	B.P.
11	C29	35	-15, +5	T/B.P.
11	C30	15	+5	B.P.
5, 6	C31	40	-15, -25, +5	T/B.P.
5	C32	13	+5	B.P.
5	C33	15	+5	B.P.
5	C34	40	-15, -25, +5	T/B.P.
6	C35	20	+5	B.P.

\* Stations C5 and C8 have an Aanderra current meter at +5 feet on a bottom platform and an Aanderra tide gauge bracketed to the platform.

Table 18. (continued).

<u>Period</u>	<u>Station Number</u>	<u>Depth (Feet)</u>	<u>Observation Levels (Feet)</u>	<u>Mooring Type</u>
5, 6	C36	40	-15, -25, +5	T/B.P.
5, 6	C37	40	-15, -25, +5	T/B.P.
6	C38	20	+5	B.P.
Project	C39	55	-15, -25, +5	T/B.P.
7	C40	40	-15, -25, +5	T/B.P.
7	C41	35	-15, +5	T/B.P.
7	C42	30	-15, +5	T/B.P.
6, 7	C43	35	-15, +5	T/B.P.
7	C44	30	-15, +5	T/B.P.
7	C45	35	-15, +5	T/B.P.
6, 7	C46	35	-15, +5	T/B.P.

T = Taut-line Mooring

B.P. = Bottom Platform

Special = High Velocity Mooring for Current Station No. 2

Table 19. NOS 1981 CTD Profile Stations.

A. Time-Series Stations

<u>Station</u>	<u>Number of Casts</u>	<u>Time Period</u>	<u>Latitude</u>	<u>Longitude</u>
TS-20	30	May 21-22, 1981	46°12'54"	123°46'48"
TS-12A	54	May 27-28, 1981	46°13'0.0"	123°57'60"
TS-12B	50	June 17-18, 1981	46°12'12.0"	123°56'18.0"
TS-12C	19	Aug. 25-26, 1981	46°11'36.0"	123°54'42.0"
TS-1	35	Sept. 2-3, 1981	46°15'0.0"	123°59'30.0"
TS-12C	42	Sept. 3-4, 1981	46°11'30.0"	123°54'36.0"
TS-20	27	Nov. 17-18, 1981	46°12'42.0"	123°47'22.8"
TS-1	52	Nov. 18-19, 1981	46°14'54.0"	123°59'24.0"
TS-10	27	Nov. 19-20, 1981	46°11'18.0"	123°53'42.0"

B. Transect Stations

<u>Station</u>	<u>Number of Casts</u>	<u>Time Period</u>	<u>Latitude</u>	<u>Longitude</u>
ST-2	5	various	46°15'21.0"	124°4'12.0"
ST-202	5	"	46°15'21.0"	124°2'6.60"
ST-1	1	"	46°15'6.6"	123°59'30.0"
ST-17	1	"	46°14'6.0"	123°59'6.0"
ST-18	2	"	46°14'54"	124°1'12.0"
ST-12	3	"	46°12'45"	123°56'36"
ST-14	1	"	46°14'30.0"	123°55'12.0"
ST-10	3	"	46°11'24"	123°53'51"
ST-206	2	"	46°11'30"	123°52'15"

Table 20. Corps of Engineers Endeco 105 Current Meter Station Locations for June 15 - 29, 1977.

Station No.	Location		Meter Depth ft-mllw	Water Depth ft-mllw
	N. Lat.	W. Long.		
Transect 1 at RM 5.5				
M1	46°14'53.0"	124°01'48.6"	17 11 6	2
M2	46°15'02.2"	124°01'50.9"	31 16 6	36
M3	46°15'33.2"	124°01'1.3"	57 29 7	62
Transect 2 at RM 2				
M4	46°15'37.9"	124°05'01.4"	43 23 8	48
M5	46°14'58.0"	124°04'40.6"	35 19 7	41
M6	46°14'44.7"	124°04'34.3"	31 16 6	36

Current speed and direction are at synchronous, 15 minute intervals for all meters; monthly average freshwater flow about 156,000 cfs.



Table 21. Corps of Engineers Endeco 105 Current Meter Station Locations for March 9 - April 6, 1978.

Station No.	Location and Oregon State Grid	Oregon State Grid		Water Depth ft-mllw	Meter Depth Below ft-mllw
		X	Y		
T1	Main Channel, So. of Sand Island	1,117,318	960,690	52	5 47
T2	So. Channel, off Tansy Point	1,134,515	940,811	44	5 39
T3	No. Channel, off McGowan	1,140,499	954,471	55	5 28 50
T4	No. Channel, off Megler	1,156,153	956,554	30	15
T5	So. Channel, off Alderborok	1,168,114	944,825	39	5 34
T6	N.E. of Lois Island, North Channel	1,188,345	941,664	33	16
T7	Ship Channel, RM 20.5	1,186,134	956,859	42	21
T8	Ship Channel, Harrington Point	1,201,946	961,140	37	18
T9	Woody Island Channel, near Snag Is.	1,207,647	945,671	40	20
T10	Ship Channel, RM 30	1,230,424	958,982	40	20
T11	Ship Channel, RM 37	1,259,248	945,370	32	5 27
T12	Clifton Channel, Bradwood	1,256,881	937,453	13	7

Current speed and direction are at synchronous, 30 minute intervals for all meters.

A-10



APPENDIX B

Tidal Height and Tidal Current  
Harmonic Analysis Results

Table 22. Tidal current Harmonic Constants for CM-1, Mid-depth.

FILE I10101902 DAT RAYDPT = 1.000  
 STATION ID CM-1 METER NUMBER 005209/594 MOD 2 METER DEPTH 8.5  
 LATITUDE 046 15'09.00" N LONGITUDE 123 59'40.00" W  
 FROM 4 03HR 1/ 5/81 TO 7.03HR 6/ 7/81  
 ALL TIMES AND PHASES CONVERTED TO GMT  
 NO PTS= 1588 DURATION = 1588 HRS NO. VALID X,Y PTS= 1587 1587  
 MODAL MODULATION, BUT NO INFERENCE. CORRECTIONS HAVE BEEN MADE  
 ANALYSIS RESULTS IN CURRENT ELLIPSE FORM

NAME	SPEED	MAJOR	MINOR	AMP	RATIO	INC	DEC T	Q	G+	G-	KAPPA
1 Z0	0.00000000	21.951	0.000	21.951	0.154	18.3	251.7	180.0	161.7	198.3	100.0
2 NM	0.00151215	2.476	0.919	2.641	0.019	24.0	66.0	4.5	340.5	28.5	8.9
3 MSF	0.00282193	6.198	-0.052	6.198	0.043	4.2	85.0	33.9	29.7	38.2	42.1
4 ALP1	0.03439657	1.387	-0.341	1.428	0.010	162.5	287.5	293.1	130.6	95.7	268.2
5 2G1	0.03570635	2.161	-1.043	2.400	0.017	93.6	356.4	315.5	221.8	49.1	294.3
6 Q1	0.03721850	1.859	-0.806	2.026	0.014	141.4	308.6	26.4	245.0	167.8	9.6
7 O1	0.03873065	11.989	-0.837	12.018	0.084	169.5	280.5	325.0	155.5	134.5	312.6
8 NO1	0.04026860	2.771	1.426	3.117	0.022	142.9	307.1	349.8	206.9	132.8	341.8
9 K1	0.04178075	26.529	-2.196	26.619	0.187	162.8	287.2	349.3	186.5	152.1	345.6
10 J1	0.04329290	1.079	0.490	1.185	0.008	124.9	325.1	31.5	266.6	156.5	32.2
11 O01	0.04483084	2.684	0.433	2.719	0.019	12.3	77.7	110.4	98.1	122.7	115.6
12 UPS1	0.04634299	1.425	-0.894	1.682	0.012	154.7	295.3	228.8	74.1	23.5	238.3
13 EPS2	0.07617731	2.459	-0.159	2.464	0.017	179.1	270.9	106.7	287.6	285.8	78.1
14 MU2	0.07768947	8.656	0.378	8.665	0.061	1.1	88.9	347.5	346.4	348.7	323.3
15 N2	0.07899925	26.930	-1.425	26.967	0.189	164.2	285.8	339.4	175.2	143.6	319.0
16 M2	0.08051140	142.585	-5.503	142.691	1.000	166.9	283.1	11.5	204.7	178.4	355.4
17 L2	0.08202355	14.313	-1.551	14.397	0.101	176.2	273.8	39.9	223.7	216.2	28.2
18 S2	0.08333334	22.545	-0.866	22.562	0.158	163.7	286.3	21.1	217.4	184.9	13.1
19 ETA2	0.08507364	1.580	-0.139	1.586	0.011	153.5	296.5	8.2	214.7	161.6	5.2
20 M03	0.11924206	14.025	0.348	14.029	0.098	169.7	280.3	243.6	73.9	53.3	215.0
21 M3	0.12076710	1.430	-0.488	1.511	0.011	171.5	278.5	38.4	227.0	209.9	14.2
22 MK3	0.12229215	11.207	1.258	11.278	0.079	163.0	287.0	228.7	65.7	31.7	208.7
23 SK3	0.12511408	1.697	0.620	1.807	0.013	170.6	279.4	216.7	46.1	27.3	205.1
24 MN4	0.15951064	2.494	0.841	2.632	0.018	121.2	328.8	215.3	94.2	336.5	178.7
25 M4	0.16102280	5.194	2.407	5.725	0.040	120.2	329.8	252.3	132.2	12.5	220.1
26 SN4	0.16233258	0.673	-0.151	0.690	0.005	141.9	308.1	13.9	232.0	155.8	345.4
27 MS4	0.16384473	2.135	0.770	2.267	0.016	169.5	280.5	301.7	132.3	111.2	277.6
28 S4	0.16666667	1.694	0.038	1.695	0.012	159.5	290.5	154.7	355.3	314.2	138.8
29 2MK5	0.20280355	5.665	-0.918	5.738	0.040	18.0	72.0	82.0	64.0	100.0	46.1
30 2SK5	0.20844741	0.644	0.261	0.695	0.005	130.2	319.8	330.2	200.0	100.4	310.6
31 2MN6	0.24002205	3.530	-0.789	3.617	0.025	173.0	277.0	267.5	94.4	80.5	214.8
32 M6	0.24153420	3.008	-0.656	3.079	0.022	164.9	285.1	292.7	127.8	97.5	244.3
33 2MS6	0.24435614	1.557	-0.125	1.562	0.011	16.7	73.3	93.7	77.0	110.4	53.5
34 2SM6	0.24717806	0.558	-0.042	0.560	0.004	157.0	293.0	337.2	180.2	134.1	305.1
35 3MK7	0.28331494	3.720	-0.110	3.721	0.026	163.6	286.4	129.5	375.9	293.1	77.5
36 M8	0.32204559	2.348	0.824	2.488	0.017	164.2	285.8	164.9	0.6	329.1	100.4

B-1

Table 23. Tidal Height Harmonic Constants for Tongue Pt. for 1981.

FILE I00800401.DAT RAYOPT = 0.950  
 STATION ID T9-21 METER NUMBER 000021  
 METER USE NUMBER 031 MODIFICATION '1 LATITUDE 046 12'30.00" N LONGITUDE 123 46'00.00" W  
 ANALYSIS OF HOURLY TIDAL HEIGHTS 8.00H 1/ 1/81 TO 7.00H 1/ 1/82 GMT  
 DURATION = 8760 HRS NO. OBS. = 8760 NO. PTS. ANAL. = 8759 MIDPT = 0.00H 2/ 7/81  
 ALL TIMES AND PHASES CONVERTED TO GMT

NO	NAME	FREQUENCY	A	RATIO	°	KAPPA
1	Z0	0.00000000	1.3472	1.4233	0.00	0.00
2	SA	0.00011407	0.1358	0.1434	8.36	8.69
3	SSA	0.00022816	0.0721	0.0762	159.99	160.65
4	MSM	0.00130978	0.0397	0.0419	324.68	328.45
5	MM	0.00151215	0.0403	0.0426	94.34	98.69
6	MSF	0.00282193	0.0387	0.0408	40.24	48.37
7	MF	0.00305009	0.0157	0.0166	191.78	200.56
8	ALP1	0.03439657	0.0040	0.0042	336.90	312.19
9	Z01	0.03570635	0.0031	0.0033	245.49	224.55
10	SI01	0.03590872	0.0080	0.0084	315.45	295.10
11	G1	0.03721890	0.0411	0.0435	241.21	224.63
12	RHO1	0.03742087	0.0050	0.0053	196.30	180.30
13	O1	0.03873065	0.2380	0.2515	241.04	228.81
14	TAU1	0.03895881	0.0149	0.0158	10.68	359.11
15	BET1	0.04004044	0.0103	0.0109	246.73	238.28
16	NO1	0.04026860	0.0271	0.0286	258.98	251.19
17	CHI1	0.04047097	0.0067	0.0071	275.46	268.25
18	PI1	0.04143851	0.0107	0.0113	270.50	266.08
19	P1	0.04155259	0.1129	0.1193	255.46	251.36
20	S1	0.04166667	0.0076	0.0080	279.29	275.53
21	K1	0.04178075	0.4005	0.4231	255.87	252.43
22	PSI1	0.04189482	0.0098	0.0104	211.58	208.47
23	PHI1	0.04200891	0.0034	0.0036	236.57	233.79
24	THE1	0.04309053	0.0051	0.0054	301.75	302.09
25	J1	0.04329290	0.0175	0.0185	278.33	279.25
26	SO1	0.04460268	0.0141	0.0149	55.87	60.56
27	OO1	0.04483084	0.0114	0.0120	301.96	307.30
28	UPS1	0.04634299	0.0014	0.0015	54.45	64.15
29	OO2	0.07597495	0.0015	0.0016	52.00	23.28
30	EPS2	0.07617731	0.0078	0.0083	7.84	339.70
31	2N2	0.07748710	0.0136	0.0144	206.48	182.11
32	MU2	0.07768947	0.0163	0.0172	8.14	344.35
33	N2	0.07899925	0.1790	0.1891	241.89	221.88
34	NU2	0.07920162	0.0378	0.0399	241.10	221.67
35	H1	0.08039733	0.0080	0.0084	153.33	137.34
36	M2	0.08051140	0.9466	1.0000	264.04	248.38
37	H2	0.08062547	0.0046	0.0048	138.62	123.29
38	MKS2	0.08073956	0.0094	0.0100	209.23	194.22
39	LDA2	0.08182118	0.0198	0.0209	267.16	255.28
40	L2	0.08202395	0.0441	0.0466	265.23	253.93
41	T2	0.08321926	0.0152	0.0160	301.97	294.11
42	S2	0.08333334	0.2337	0.2469	294.94	287.41
43	R2	0.08344740	0.0023	0.0025	340.21	333.00
44	K2	0.08356149	0.0748	0.0790	287.82	280.95
45	MSN2	0.08484548	0.0102	0.0108	128.10	124.93
46	ETA2	0.08507364	0.0010	0.0010	321.57	319.05
47	MO3	0.11924206	0.0307	0.0324	95.67	67.79
48	M3	0.12076710	0.0033	0.0035	141.97	118.48
49	SO3	0.12206399	0.0175	0.0185	131.44	111.68
50	MK3	0.12229215	0.0235	0.0248	113.36	94.26
51	SK3	0.12511408	0.0077	0.0082	134.93	123.96
52	MN4	0.15951064	0.0059	0.0062	62.49	26.81
53	M4	0.16102280	0.0113	0.0119	99.21	67.89
54	SN4	0.16233258	0.0024	0.0025	83.53	55.98
55	MS4	0.16384473	0.0075	0.0079	106.85	83.65
56	MK4	0.16407289	0.0032	0.0033	302.39	279.85
57	S4	0.16666667	0.0022	0.0023	152.90	137.84
58	SK4	0.16689482	0.0019	0.0020	106.82	92.41
59	2MK5	0.20280355	0.0106	0.0112	110.73	75.97
60	2SK5	0.20844741	0.0007	0.0007	194.89	176.38
61	2MN6	0.24002205	0.0065	0.0069	105.45	54.11
62	N6	0.24153420	0.0119	0.0125	126.87	79.89
63	2MS6	0.24435614	0.0087	0.0092	157.78	118.93
64	2MK6	0.24458429	0.0032	0.0034	132.18	93.98
65	2SM6	0.24717806	0.0021	0.0023	206.28	175.55
66	MSK6	0.24740623	0.0018	0.0019	179.12	149.05
67	3MK7	0.28331494	0.0012	0.0013	206.12	155.70
68	M8	0.32204959	0.0010	0.0011	216.56	153.92

Table 24. Tidal Height Harmonic Constant Reduction for Tongue Pt. for 1981.

FILE 100B00401.DAT RAYOPT = 0.950  
 STATION ID TQ-21 METER NUMBER 000021  
 METER USE NUMBER 031 MODIFICATION 1 LATITUDE 046 12'30.00" N LONGITUDE 123 46'00.00" W  
 ANALYSIS OF HOURLY TIDAL HEIGHTS 8.00H 1/ 1/81 TO 7.00H 1/ 1/82 GMT  
 DURATION = 8760 HRS NO. OBS. = 8760 NO. PTS. ANAL. = 8759 MIDPT = 0.00H 2/ 7/81  
 ALL TIMES AND PHASES CONVERTED TO GMT

TIDAL RANGES IN METERS AND RATIOS OF TIDAL RANGES

MEAN RANGE = 2.031 GREATER DIURNAL RANGE = 2.617 LESSER DIURNAL RANGE = 1.446  
 SPRING RANGE = 2.435 NEAP RANGE = 1.566 PERIGEAN RANGE = 2.415 APOGEAN RANGE = 1.743  
 GREATER TROPIC RANGE = 2.810 LESSER TROPIC RANGE = 1.107

GREATER DIURNAL/MEAN = 1.288 LESSER DIURNAL/MEAN = 0.712 QT DIURNAL/LS DIURNAL = 1.810  
 SPRING/MEAN = 1.199 NEAP/MEAN = 0.771 SPRING/NEAP = 1.555  
 PERIGEAN/MEAN = 1.189 APOGEAN/MEAN = 0.858 PERIGEAN/APOGEAN = 1.386  
 QT TROPIC/MEAN = 1.383 LS TROPIC/MEAN = 0.545 QT TROPIC/LS TROPIC = 2.539

AGES AND GREENWICH INTERVALS IN HOURS

PHASE AGE = 38.40 PARALLAX AGE = 48.69 DIURNAL AGE = 21.51 HW INTERVAL = 8.58 LW INTERVAL = 2.46

AMPLITUDE RATIOS

$(K1+O1)/M2 = 0.675$   $(M2+S2+N2)/(O1+K1+P1) = 1.809$   $O1/K1 = 0.594$

INEQUALITIES IN METERS

DIURNAL INEQUALITIES: DHQ = 0.213 DLQ = 0.373

TROPIC INEQUALITIES: HWQ = 0.557 LWQ = 1.146  $K1+O1 = 0.639$   $K1-O1 = 0.162$

TIDAL DATUM LEVELS IN METERS

DATUM	ON MWL	ON MLLW	ON TIDE GAUGE
MHHW	1.240	2.617	2.988
MLHW	0.815	2.191	2.162
MHLW	-0.631	0.745	0.716
MLLW	-1.376	0.000	-0.029
MHW	1.027	2.404	2.375
MWL	0.000	1.376	1.347
MLW	-1.004	0.373	0.343

MTL-MWL = 0.012

APPENDIX C

Tidal Constants (Table 25) and  
Tidal Height Observation Stations (Table 26),  
compiled from NOS records

Table 25. Tidal intervals, Ranges and Inequalities - Columbia River Estuary from the Records of the Coast and Geodetic Survey 1852-1959.

A. Oregon Stations (RM 0-150)

RM	Station	Greenwich intervals in hrs <sup>*</sup>		Mn	Ranges in ft <sup>+</sup>		Inequalities in ft <sup>‡</sup>	
		HWI	LWI		Diurnal	Extreme	DHO	DLQ
7.5	PT. ADAMS ** (FT. STEVENS) 16 mos., 1940-42	8.73	2.43	6.41	8.35	13.7	0.70	1.24
10.7	WARRENTON ** SKIPANON RIVER 62 tides, 1935	8.99	2.75	6.5	8.3	--	0.65	1.15
12.0	ASTORIA, YOUNGS BAY ** 3 yrs, 1931-34 1 yr harmonic analyses, 1935	8.97	2.82	6.70	8.55	14.8	0.66	1.16
		8.92	2.84	6.69	8.63	--	0.71	1.23
12.0	YOUNGS RIVER *** 37 tides, 1935	9.16	3.10	6.90	8.60	--	0.60	1.10
12.8	LEWIS & CLARK R. *** 13 tides, 1935	9.14	3.30	6.90	8.70	--	0.60	1.10
13.0	ASTORIA, PORT DOCKS ** 1958, 3 mos.	9.08	3.01	6.25	7.99	--	0.66	1.08
14.5	ASTORIA, 9th STREET ++ 3 yrs, 1873-76	9.11	3.11	6.43	8.26	14.03	0.65	1.18
18.2	TONGUE PT. ** 1 yr harmonic analyses, 1974 1 yr harmonic analyses, 1939	9.12	3.02	6.46	8.32	--	0.69	1.17
		9.24	3.15	6.44	8.27	--	0.69	1.15
20	SETTLERS PT. ** 2 mos., 1935	9.57	3.94	6.30	8.00	--	0.70	1.00
26	CARLSON IS. 64 tides, 1935	9.73	4.50	5.69	7.07	--	0.62	0.76
30	ALDRICH PT. 70 tides, 1936	10.04	4.82	5.54	6.85	--	0.61	0.70
38.9	CLIFTON 54 tides, 1936	10.34	5.32	5.10	6.24	--	0.56	0.58

Table 25. (continued).

RM	Station	Greenwich intervals in hrs <sup>*</sup>		Mn	Ranges in ft <sup>+</sup>		Inequalities in ft <sup>#</sup>	
		HWI	LWI		Diurnal	Extreme	DHQ	DLO
39.8	BUGBY HOLE 27 tides, 1937	10.57	5.30	5.11	6.26	--	0.57	0.58
42	WAUNA <sup>**</sup> 14 mos., 1940-42	10.49	5.38	5.17	6.33	--	0.59	0.57
43	WESTPORT 34 tides, 1937	10.63	5.51	4.92	5.96	--	0.56	0.48
54	LACODA 53 tides, 1937	11.24	6.41	4.14	4.95	--	0.48	0.33
61	WALKER IS. 42 tides, 1937	11.60	6.76	3.71	4.42	--	0.44	0.27
	RINEARSON SLOUGH <sup>** #</sup> 2 tides, 1877	--	--	3.60	4.40	11.0	0.40	0.40
67.4	RAINIER <sup>** #</sup> 56 tides, 1877	11.98	7.68	3.20	3.70	--	0.20	0.30
	DOBELBOWER 22 tides, 1937	11.99	7.52	3.29	4.04	--	0.47	0.28
74	GOBLE 1 mo., 1937	12.22	7.84	2.97	3.57	--	0.42	0.19
84	COLUMBIA CITY 38 tides, 1937	0.45	8.47	2.38	2.72	--	0.35	0.09
86	ST HELENS <sup>**</sup> 13 mos., 1940-42	0.30	8.80	1.97	2.51	--	0.42	0.14
87	WARRIOR ROCK 40 tides, 1937	0.83	8.81	2.15	2.60	--	0.36	0.09
86.7	MULTNOMAH CHANNEL <sup>#</sup> (north end) 16 tides, 1937	1.15	9.18	1.83	2.24	--	0.30	0.08
	KELLEY PT. <sup>**</sup> 11 mos., 1940-42	2.22	10.33	1.43	1.96	--	0.40	0.13
	WARRENDALE <sup>**</sup> 2 mos., 1940-42	6.98	1.67	0.39	0.61	--	0.12	0.10



Table 25. (continued).

## B. Washington Stations (RM 0--150)

RM	Station	Greenwich intervals in hrs <sup>*</sup>			Ranges in ft <sup>+</sup>		Inequalities in ft <sup>‡</sup>	
		HWI	LWI	Mn	Diurnal	Extreme	DHQ	DLQ
2	NORTH JETTY** 138 tides, 1958	8.46	2.00	5.68	7.57	--	0.67	1.22
≈3	FT. CANBY** 3 mos., 1926	8.77	2.88	5.81	7.57	12.1	0.70	1.06
≈3.5	ILWACO** 1 mo., 1958	8.98	3.09	6.19	8.00	--	0.69	1.12
≈6	CHINOOK** 109 tides, 1958	8.85	2.33	6.23	8.32	--	0.69	1.40
≈13	HUNGRY HARBOR** 113 tides, 1935	9.27	2.92	6.43	8.26	--	0.63	1.20
23.5	HARRINGTON PT** 120 tides, 1935	9.59	4.12	5.75	7.17	--	0.62	0.80
24.3	ALTOONA** 22 mos., 1940-42	9.55	3.93	6.11	7.66	--	0.65	0.90
28.5	BROOKFIELD 73 tides, 1936	10.05	4.61	5.49	6.84	--	0.60	0.75
30.6	THREE TREE PT.†† 11 tides, 1868	10.07	3.69	5.50	6.90	--	0.50	0.90
33.3	SKAMOKAWA 2 mos., 1950	10.14	4.81	5.56	6.87	--	0.61	0.70
39.5	CATHLAMET 16 mos., 1940-42	10.44	5.31	5.22	6.40	--	0.59	0.59
48.3	CAPE HORN 55 tides, 1937	10.84	5.80	4.62	5.60	--	0.52	0.46
50.5	EAGLE CLIFF** 16 mos., 1940-42	10.92	6.08	4.49	5.47	--	0.55	0.43
53.7	OAK POINT 65 tides, 1937	11.22	5.29	4.24	5.10	--	0.52	0.34
	STELLA** 15 mos., 1940-42	11.22	6.57	4.00	4.89	--	0.53	0.36
66	LONGVIEW** 15 mos., 1940-42	11.65	7.30	3.27	3.99	--	0.48	0.24

Table 25. (continued).

RM	Station	Greenwich intervals in hrs <sup>*</sup>		Ranges in ft <sup>+</sup>			Inequalities in ft <sup>‡</sup>	
		HWI	LWI	Mn	Diurnal	Extreme	DHQ	DLQ
75	KALAMA <sup>**</sup> 15 mos., 1940-42	12.10	7.97	2.54	3.20	--	0.43	0.18
	MARTINS BLUFF 39 tides, 1937	0.05	8.04	2.56	3.04	--	0.31	0.17
96	WILLOW BAR <sup>‡‡‡</sup> 9 mos., 1941	1.21	9.54	1.50	2.03	--	0.40	0.13
106	VANCOUVER <sup>‡‡‡</sup> 9 mos., 1940-42	2.53	10.70	1.33	1.84	--	0.38	0.13
	ELLSWORTH <sup>‡‡‡</sup> 10 mos., 1940-42	2.97	11.13	0.99	1.43	--	0.31	0.13
121.7	WASHOUGAL 6 mos., 1940-42	4.14	12.26	0.54	0.90	--	0.23	0.13

The assistance of the National Ocean Survey in providing the data listed herein is gratefully acknowledged.

\* The Greenwich Interval is the time between lunar passage over Greenwich and the following high water (HWI) or low water (LWI).

+ The mean range, Mn = MHW - MLW.  
The diurnal range = MHHW - MLLW = Mn + DHQ + DLQ.  
The extreme range is the difference between highest and lowest observed tides.

‡ DHQ = MHHW - MHW  
CLQ = MLW - MLLW

\*\* Accepted values are available. The values given are usually the accepted values but may, instead, be derived from harmonic analyses or differ from the accepted values by a few hundredths of a foot. The latter case arises where I have used the reported values rather than the accepted values.

‡‡ Observations reduced by comparison to a station other than Tongue Pt. Values may be obsolete.

Willamette River stations have been omitted.

Table 26. Tidal Height Stations in the Columbia River and Estuary Occupied by the Coast and Geodetic Survey 1852-1959.

A. Oregon Stations (RM 0 - 150)

River Mile	Station	Date	Length of Record	Comments	Comparison Station
7.5	Ft. Stevens (Pt. Adams)	1850	2 yrs	no data provided	Presidio Astoria Tongue Pt. Tongue Pt. (1941-59)
		1852		no data provided	
		1868		no data provided	
		1905-06	2 yrs		
		1926	4 mos.		
		1936	58 tides		
		1940-42	2 yrs	BAV*	
		1958	5 mos.		
≈10.7	Warrenton (Skipanon River)	1935	62 tides	BAV	Tongue Pt. (1941-59)
≈12.0	Astoria, Youngs Bay	1931-42	11 yrs	BAV	Tongue Pt. (1941-59)
≈12.8	Lewis & Clark River	1935	13 tides	BAV	Youngs Bay
≈12	Youngs River	1935	13 tides	BAV	Youngs Bay
≈13	Astoria, Port Docks	1958	3 mos.	BAV	Tongue Pt. (1925-41)
≈14.5	Astoria, 9th St.	1853-66	12-1/2 yrs		Tongue Pt. Tongue Pt.
		1873-76	3 yrs		
		1883	7 mos.		
		1884	3 mos.		
		1926	21 tides		
		1936	57 tides		
		1958	67 tides		
18.2	Tongue Pt. <sup>+</sup>	1868	56 tides		--
		1925-43	18 yrs		--
		1941-59	18 yrs	BAV, primary station	
≈20	Settlers Pt.	1935	2 mos.	BAV, CRD <sup>‡</sup>	Tongue Pt. (1941-59)
		1947	71 tides		
≈26	Karlson Is.	1935	64 tides	BAV, CRD	Tongue Pt.
		1936	36 tides		Tongue Pt.
≈30	Aldrich Pt.	1936	70 tides	CRD	Tongue Pt.
≈38.9	Clifton	1936	54 tides	CRD	Tongue Pt.
		1937	2 tides	CRD	Tongue Pt.

Table 26. (continued).

River Mile	Station	Date	Length of Record	Comments	Comparison Station
42	Wauna	1937	34 tides	CRD	Tongue Pt.
43	Westport Sl.	1937	34 tides	CRD	Tongue Pt.
54	Lacoda (Bradbury Sl.)	1937 1958	53 tides 11 mos.	CRD	Oak Pt. Tongue Pt.
61	Walker Is.	1937	42 tides	CRD	Tongue Pt., Oak Pt.
	Rinearson Sl.	1877	11 tides	BAV	Cathlamet
67.4	Rainier	1877	56 tides	BAV	not available
	Dobelbower	1937	28 tides	CRD	Tongue Pt.
74	Goble	1937	1 mo.	CRD	Tongue Pt.
84	Columbia City	1937	58 tides	CRD	Tongue Pt.
86	St. Helens	1877	67 tides		not available
		1881	?		" "
		1886	106 tides		" "
		1940-42	13 mos.	BAV, CRD	Tongue Pt.
87	Warrior Rock	1937	40 tides	CRD	Columbia City
86.7	Multnomah Channel (north end)	1937	16 tides	CRD	Warrior Rock, Columbia City
	Kelley Pt.	1940-42	11 mos.	BAV, CRD	Tongue Pt.
	Warrendale	1940-42	2 mos.	BAV, CRD	Kelley Pt.

Table 26. (continued).

## B. Washington Stations (RM 0 - 150)

River Mile	Station	Date	Length of Record	Comments	Comparison Station
2	North Jetty	1926	47 tides	Superseded	Tongue Pt., Presidio Tongue Pt. (1941-59)
		1958	138 tides	BAV	
≈3	Ft. Canby	1852	16 tides	BAV	Presidio, Tongue Pt. (1941-59) Tongue Pt. Tongue Pt. (1941-59)
		1853	93 tides		
		1868	132 tides		
		1877	65 tides		
		1926	3 mos.		
		1952	8 tides		
		1958	?		
3.5	Ilwaco	1933	163 tides	BAV	Tongue Pt. (1941-59) Tongue Pt. (1941-59)
		1958	1 mo.		
≈6	Chinook	1933	44 tides	Superseded BAV	Ilwaco Tongue Pt. Tongue Pt. Tongue Pt. Tongue Pt. (1941-59)
		1935	33 tides		
		1936	48 tides		
		1952	46 tides		
		1958	109 tides		
≈13	Hungry Harbor	1933	113 tides	BAV	Tongue Pt. (1941-59) Tongue Pt.
		1936	50 tides		
23.5	Harrington Pt.	1935	120 tides	CRD	Tongue Pt.
24.3	Altoona	1940-42	22 mos.	BAV	Tongue Pt. (1941-59) Tongue Pt. Tongue Pt.
		1950	61 tides		
		1958-59	1 yr		
28.5	Brookfield	1936	73 tides	CRD	Tongue Pt. Tongue Pt.
		1950	111 tides		
30.6	Three Tree Pt.	1868	11 tides		
33.3	Skamokawa	1936	54 tides	BAV, CRD	Tongue Pt. Tongue Pt. Tongue Pt.
		1940-42	14 mos.		
		1950	2 mos.		
39.5	Cathlamet	1875	94 tides	BAV, CRD	Tongue Pt. Tongue Pt. Tongue Pt.
		1876	39 tides		
		1877	56 tides		
		1936	43 tides		
		1937	29 tides		
		1940-42	16 mos.		

Table 26. (continued).

River Mile	Station	Date	Length of Record	Comments	Comparison Station
48.3	Cape Horn	1937	55 tides	CRD	Tongue Pt.
50.5	Eagle Cliff	1876	56 tides		
		1937	37 tides		Tongue Pt.
		1940-42	16 mos.	BAV, CRD	Tongue Pt.
53.7	Oak Pt.	1877	56 tides		
		1937	65 tides	CRD	Tongue Pt.
	Stella	1937	37 tides		Tongue Pt.
		1940-42	15 mos.	BAV, CRD	Tongue Pt.
66	Longview	1937	56 tides		Tongue Pt.
		1940-42	15 mos.	BAV, CRD	Tongue Pt.
75	Kalama	1877	14 tides		Rainier
		1940-42	15 mos.	BAV, CRD	Tongue Pt.
	Martins Bluff	1937	39 tides	CRD	Tongue Pt.
96	Willow Bar	1941-42	9 mos.	CRD, BAV	St. Helens, Kelley Pt.
106	Vancouver	1940-42	9 mos.	CRD, BAV	Kelley Pt.
	Ellsworth	1940-42	10 mos.	CRD, BAV	Kelley Pt.
121.7	Washougal	1940-42	6 mos.	CRD, BAV	Kelley Pt.

The assistance of the National Ocean Survey in providing the materials above is gratefully acknowledged. The listing is likely not exhaustive.

\* BAV = Basis of Accepted Values, as recorded in material received from National Ocean Survey.

+ Additional data up to present have been collected at Tongue Pt., which is the primary station and for which predictions are tabulated in the Tide Tables. No tabulations have been made for most of the years. However, harmonic analysis results are available for selected years.

‡ CRD = Columbia River Datum, which is related to tide staff. Recent adjustments (1964) to CRD have been made, but most historical materials use values listed.

Stations in the Willamette River have been omitted from the listing, as have some stations above Longview, for which results were never tabulated.

APPENDIX D

Tidal Inundation Time for the 1940-61 Period,  
as Calculated by National Ocean Survey

THE FREQUENCY REPRESENTS THE TOTAL NUMBER OF TIMES THE WATER LEVEL (TIDE) IS EQUAL TO OR BELOW A GIVEN ELEVATION. THE PERCENT FREQUENCY IS THAT NUMBER OF TIDES DIVIDED BY THE TOTAL NUMBER OF TIDES, AT ALL ELEVATIONS, TIMES 100.

THE DURATION REPRESENTS THE TOTAL NUMBER OF HOURS THE WATER REMAINS AT OR IS BELOW A PARTICULAR ELEVATION. A PERCENT DURATION IS THIS NUMBER OF HOURS DIVIDED BY THE TOTAL NUMBER OF HOURS DATA IS COLLECTED, TIMES 100.

MLLW = 2.34 FEET ABOVE STATION DATUM.  
MLW = 3.46 FEET ABOVE STATION DATUM.  
MTL = 6.78 FEET ABOVE STATION DATUM.  
MHW = 10.09 FEET ABOVE STATION DATUM.  
MHHW = 10.76 FEET ABOVE STATION DATUM.  
NGVD = 5.56 FEET ABOVE STATION DATUM.

1960 - 1978 TIDAL EPOCH

MLLW = 2.51 FEET ABOVE STATION DATUM.

1941-1959 TIDAL EPOCH



Table 27. Tidal inundation time for the 1940-61 period, calculated by the National Ocean Survey.

FREQUENCY AND DURATION OF LOW WATERS 9439040 FROM 1 1940 TO 7 1961				
ELEVATION ABOVE DATUM FEET (METERS)	CUMULATIVE FREQUENCY (NO. OF LOW WATERS)	CUMULATIVE FREQUENCY (PERCENTAGE)	CUMULATIVE DURATION (HOURS)	CUMULATIVE DURATION (PERCENTAGE)
.2 (.06)	1	.00	1	.00
.3 (.09)	1	.00	1	.00
.4 (.12)	6	.00	7	.00
.5 (.15)	18	.10	21	.00
.6 (.18)	27	.10	34	.00
.7 (.21)	47	.30	60	.00
.8 (.24)	87	.60	105	.00
.9 (.27)	132	.90	173	.00
1.0 (.30)	208	1.40	264	.10
1.1 (.34)	284	2.00	377	.20
1.2 (.37)	388	2.70	534	.30
1.3 (.40)	510	3.60	735	.40
1.4 (.43)	626	4.40	919	.50
1.5 (.46)	801	5.60	1218	.60
1.6 (.49)	1003	7.10	1588	.90
1.7 (.52)	1216	8.60	2013	1.10
1.8 (.55)	1461	10.30	2498	1.40
1.9 (.58)	1721	12.20	2498	1.40
2.0 (.61)	2057	14.50	3738	2.10
2.1 (.64)	2373	16.80	4437	2.50
2.2 (.67)	2698	19.10	5205	2.90
2.3 (.70)	3067	21.70	6121	3.50
2.4 (.73)	3412	24.20	7099	4.00
2.5 (.76)	3826	27.10	8194	4.60
2.6 (.79)	4177	29.60	9291	5.30
2.7 (.82)	4555	32.50	10491	6.00
2.8 (.85)	4941	34.60	11676	6.60
2.9 (.88)	5332	37.10	12962	7.40
3.0 (.91)	5593	39.60	14345	8.20
3.1 (.94)	5938	42.10	15660	8.90
3.2 (.98)	6288	44.60	17115	9.80
3.3 (1.01)	6591	46.70	18606	10.60
3.4 (1.04)	6900	48.90	20117	11.50
3.5 (1.07)	7179	50.90	21595	12.30
3.6 (1.10)	7476	53.00	23176	13.20
3.7 (1.13)	7761	55.00	24746	14.10
3.8 (1.16)	8032	56.90	26341	15.00
3.9 (1.19)	8280	58.70	27880	15.90
4.0 (1.22)	8547	60.60	29632	16.90
4.1 (1.25)	8816	62.50	31329	17.90
4.2 (1.28)	9107	64.60	33067	18.90
4.3 (1.31)	9361	66.40	34772	19.90
4.4 (1.34)	9644	68.40	36540	20.90
4.5 (1.37)	9947	70.50	38450	22.00
4.6 (1.40)	10218	72.50	40339	23.10
4.7 (1.43)	10502	74.50	42265	24.20
4.8 (1.46)	10794	76.50	44306	25.30
4.9 (1.49)	11091	78.60	46269	26.50
5.0 (1.52)	11374	80.70	48427	27.70
5.1 (1.55)	11650	82.60	50453	28.90

Table 27. (continued).

FREQUENCY AND DURATION OF LOW WATERS 9439040 FROM 1 1940 TO 7 1961				
ELEVATION ABOVE DATUM FEET (METERS)	CUMULATIVE FREQUENCY (NO. OF LOW WATERS)	CUMULATIVE FREQUENCY (PERCENTAGE)	CUMULATIVE DURATION (HOURS)	CUMULATIVE DURATION (PERCENTAGE)
5.2 (1.58)	11293	84.30	52614	30.10
5.3 (1.62)	12138	86.10	54796	31.30
5.4 (1.65)	12397	87.90	56967	32.60
5.5 (1.68)	12610	89.40	59166	33.80
5.6 (1.71)	12801	90.80	61358	35.10
5.7 (1.74)	13001	92.20	63598	36.40
5.8 (1.77)	13148	93.20	65759	37.60
5.9 (1.80)	13272	94.10	67867	38.80
6.0 (1.83)	13387	94.90	70064	40.10
6.1 (1.86)	13501	95.70	72118	41.30
6.2 (1.89)	13598	96.40	74269	42.50
6.3 (1.92)	13696	97.10	76404	43.70
6.4 (1.95)	13763	97.60	78484	44.90
6.5 (1.98)	13810	97.90	80548	46.10
6.6 (2.01)	13857	98.30	82663	47.30
6.7 (2.04)	13901	98.60	84694	48.50
6.8 (2.07)	13940	98.90	86779	49.70
6.9 (2.10)	13964	99.00	86779	49.70
7.0 (2.13)	14073	99.80	85839	49.10
7.1 (2.16)	14068	99.80	83626	47.90
7.2 (2.19)	14060	99.70	81724	46.80
7.3 (2.23)	14047	99.60	79660	45.60
7.4 (2.26)	14027	99.50	77586	44.40
7.5 (2.29)	14008	99.30	75556	43.20
7.6 (2.32)	13974	99.10	73533	42.10
7.7 (2.35)	13934	98.80	71383	40.80
7.8 (2.38)	13884	98.50	69308	39.70
7.9 (2.41)	13802	97.90	67145	38.40
8.0 (2.44)	13724	97.30	65088	37.20
8.1 (2.47)	13613	96.50	62825	35.90
8.2 (2.50)	13493	95.70	60723	34.70
8.3 (2.53)	13352	94.70	58508	33.50
8.4 (2.56)	13212	93.70	56356	32.20
8.5 (2.59)	13023	92.40	54127	31.00
8.6 (2.62)	12827	91.00	51879	29.70
8.7 (2.65)	12611	89.40	49579	28.40
8.8 (2.68)	12389	87.90	47341	27.10
8.9 (2.71)	12132	86.00	45123	25.80
9.0 (2.74)	11891	84.30	42943	24.60
9.1 (2.77)	11570	82.00	40674	23.20
9.2 (2.80)	11227	79.60	38444	22.00

Table 27. (continued).

FREQUENCY AND DURATION OF INUNDATION 9439040 FROM 1 1940 TO 7 1961				
ELEVATION ABOVE DATUM FEET (METERS)	CUMULATIVE FREQUENCY (NO. OF HIGH WATERS)	CUMULATIVE FREQUENCY (PERCENTAGE)	CUMULATIVE DURATION (HOURS)	CUMULATIVE DURATION (PERCENTAGE)
9.3 ( 2.83)	10907	77.30	36215	20.70
9.4 ( 2.87)	10538	74.70	33994	19.40
9.5 ( 2.90)	10137	71.90	31801	18.20
9.6 ( 2.93)	9672	68.60	29675	16.90
9.7 ( 2.96)	9242	65.90	27572	15.70
9.8 ( 2.99)	8747	62.00	25902	14.60
9.9 ( 3.02)	8276	58.70	23477	13.40
10.0 ( 3.05)	7793	55.20	21646	12.30
10.1 ( 3.08)	7273	51.60	19716	11.20
10.2 ( 3.11)	6802	48.20	17998	10.30
10.3 ( 3.14)	6282	44.50	16284	9.30
10.4 ( 3.17)	5807	41.20	14683	8.40
10.5 ( 3.20)	5343	37.90	13173	7.50
10.6 ( 3.23)	4908	34.80	11842	6.70
10.7 ( 3.26)	4431	31.40	10490	6.00
10.8 ( 3.29)	4013	28.40	9333	5.30
10.9 ( 3.32)	3600	25.90	8233	4.70
11.0 ( 3.35)	3191	22.60	7174	4.10
11.1 ( 3.38)	2829	20.00	6221	3.50
11.2 ( 3.41)	2499	17.70	5518	3.10
11.3 ( 3.44)	2227	15.80	4808	2.70
11.4 ( 3.47)	1963	13.90	4141	2.30
11.5 ( 3.51)	1690	11.90	3521	2.00
11.6 ( 3.54)	1486	10.50	3055	1.70
11.7 ( 3.57)	1301	9.20	2598	1.40
11.8 ( 3.60)	1140	8.00	2211	1.20
11.9 ( 3.63)	985	6.90	1845	1.00
12.0 ( 3.66)	825	5.80	1532	.80
12.1 ( 3.69)	690	4.80	1269	.70
12.2 ( 3.72)	566	4.00	1038	.50
12.3 ( 3.75)	471	3.30	841	.40
12.4 ( 3.78)	401	2.80	701	.40
12.5 ( 3.81)	319	2.20	555	.30
12.6 ( 3.84)	252	1.70	438	.20
12.7 ( 3.87)	204	1.40	339	.10
12.8 ( 3.90)	164	1.10	264	.10
12.9 ( 3.93)	123	.80	197	.10
13.0 ( 3.96)	92	.60	145	.00
13.1 ( 3.99)	69	.40	100	.00
13.2 ( 4.02)	52	.30	68	.00
13.3 ( 4.05)	39	.20	50	.00
13.4 ( 4.08)	26	.10	34	.00
13.5 ( 4.11)	20	.10	25	.00
13.6 ( 4.15)	13	.00	16	.00
13.7 ( 4.18)	7	.00	9	.00
13.8 ( 4.21)	4	.00	6	.00
13.9 ( 4.24)	2	.00	3	.00
14.0 ( 4.27)	2	.00	3	.00
14.1 ( 4.30)	2	.00	2	.00
14.2 ( 4.33)	1	.00	1	.00

APPENDIX E

Salinity Intrusion Plots

Figure 64. June 1980 (a) minimum, (b) maximum, (c) mean salinity, and (d) salinity range in the South Channel during neap tide.

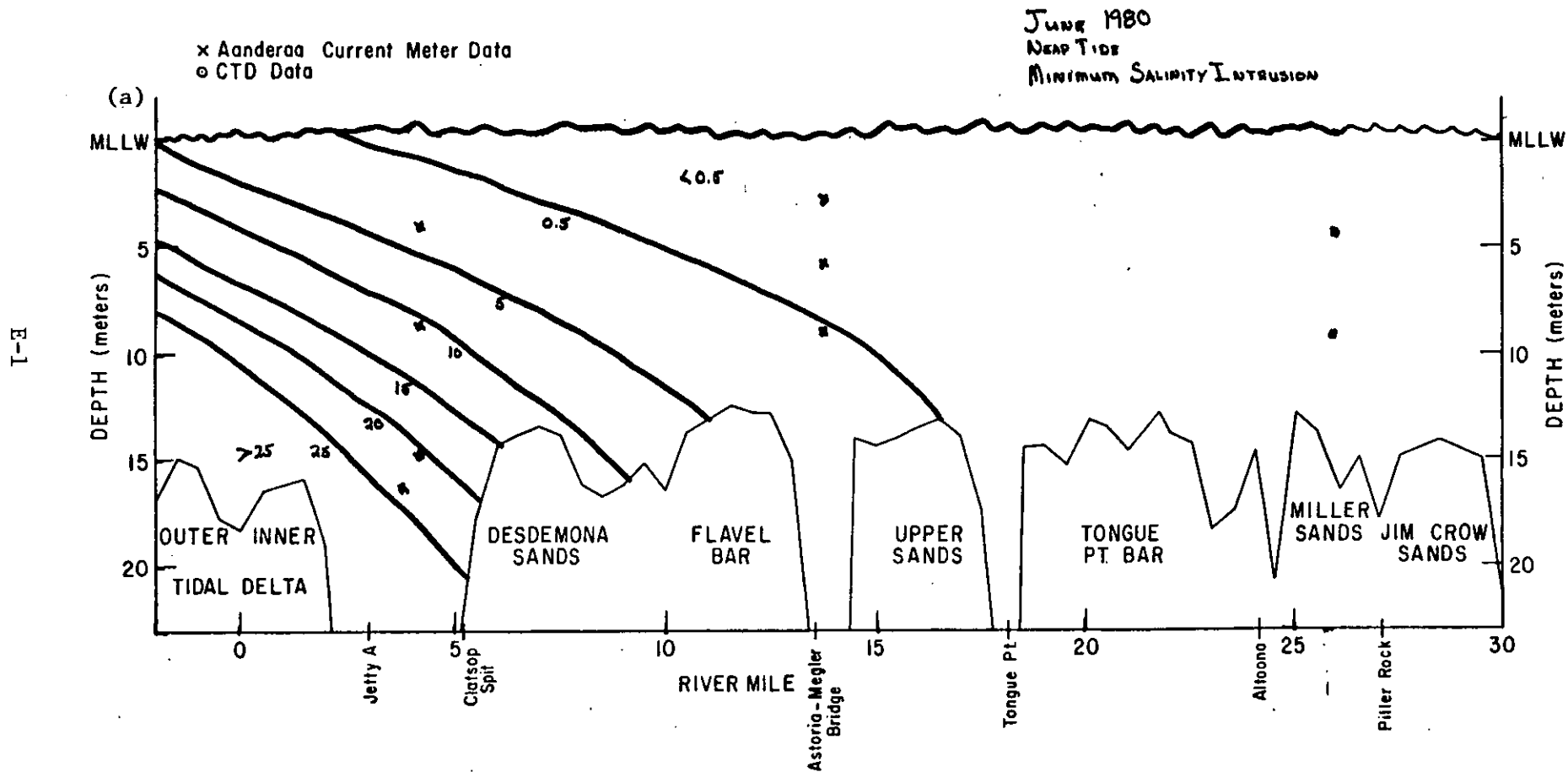
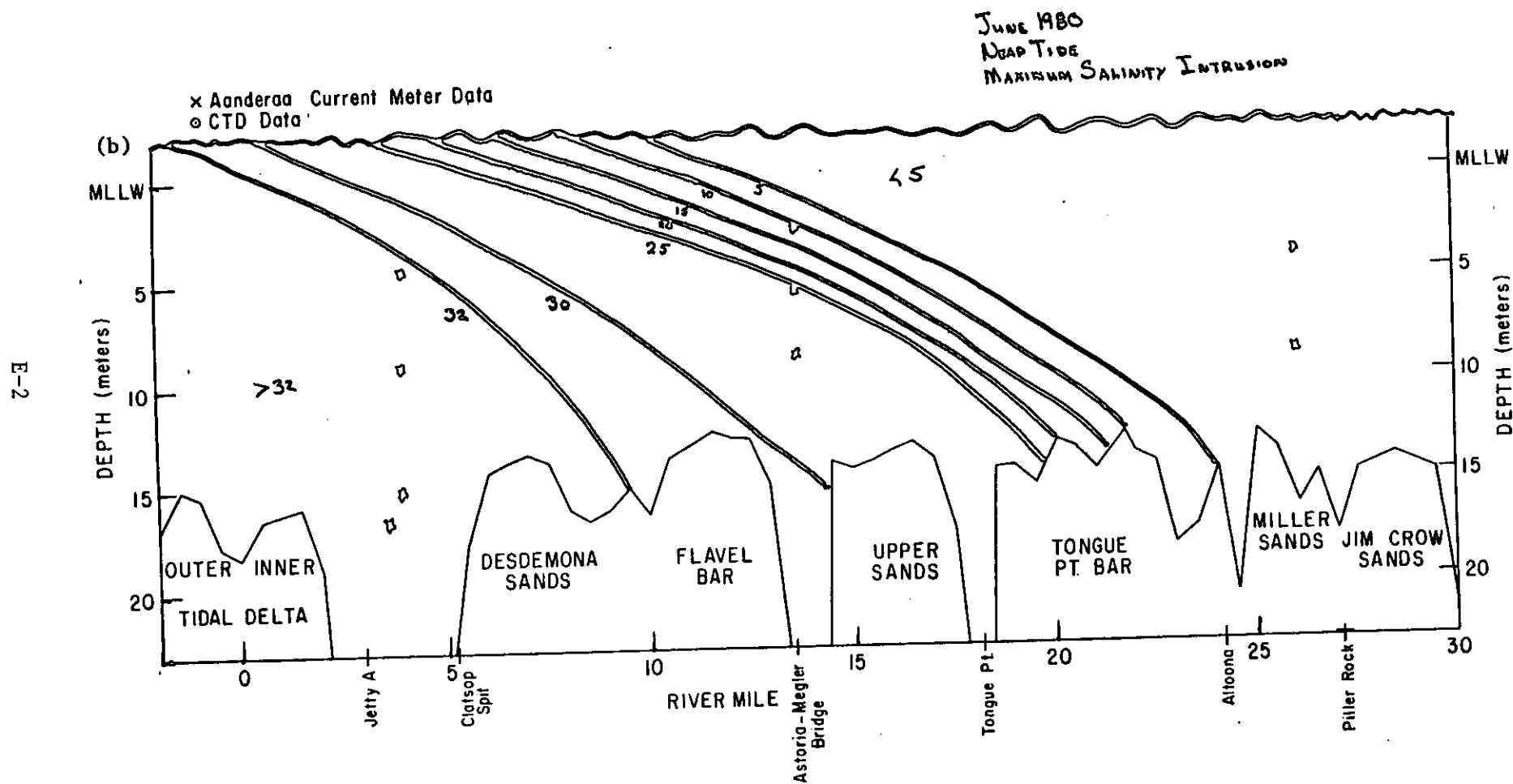


Figure 64. (continued).



E-2



Figure 64. (continued).

E-3

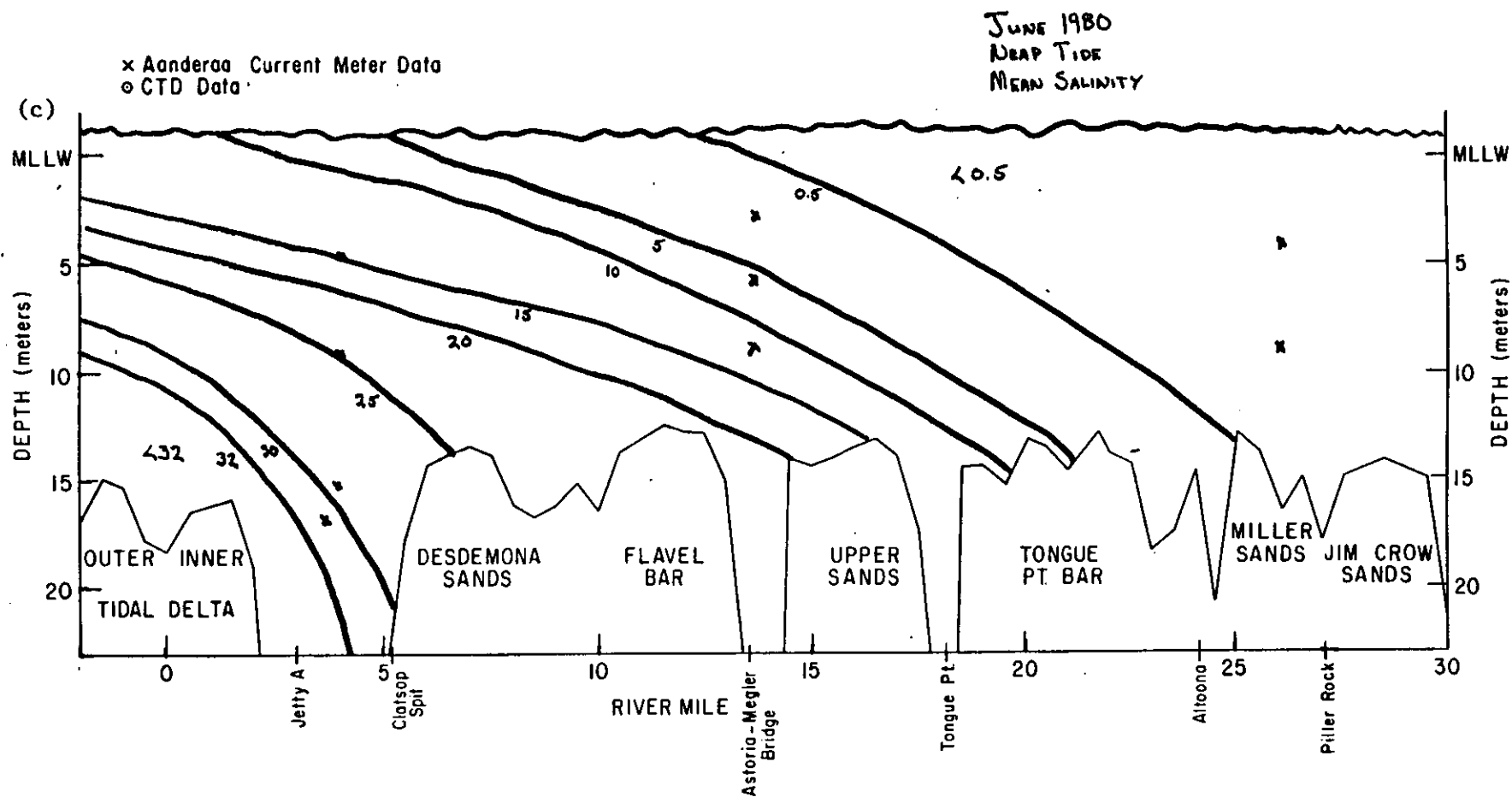






Figure 65. June 1980 (a) minimum, (b) maximum, (c) mean salinity, and (d) salinity range in the South Channel during spring tide.

E-5

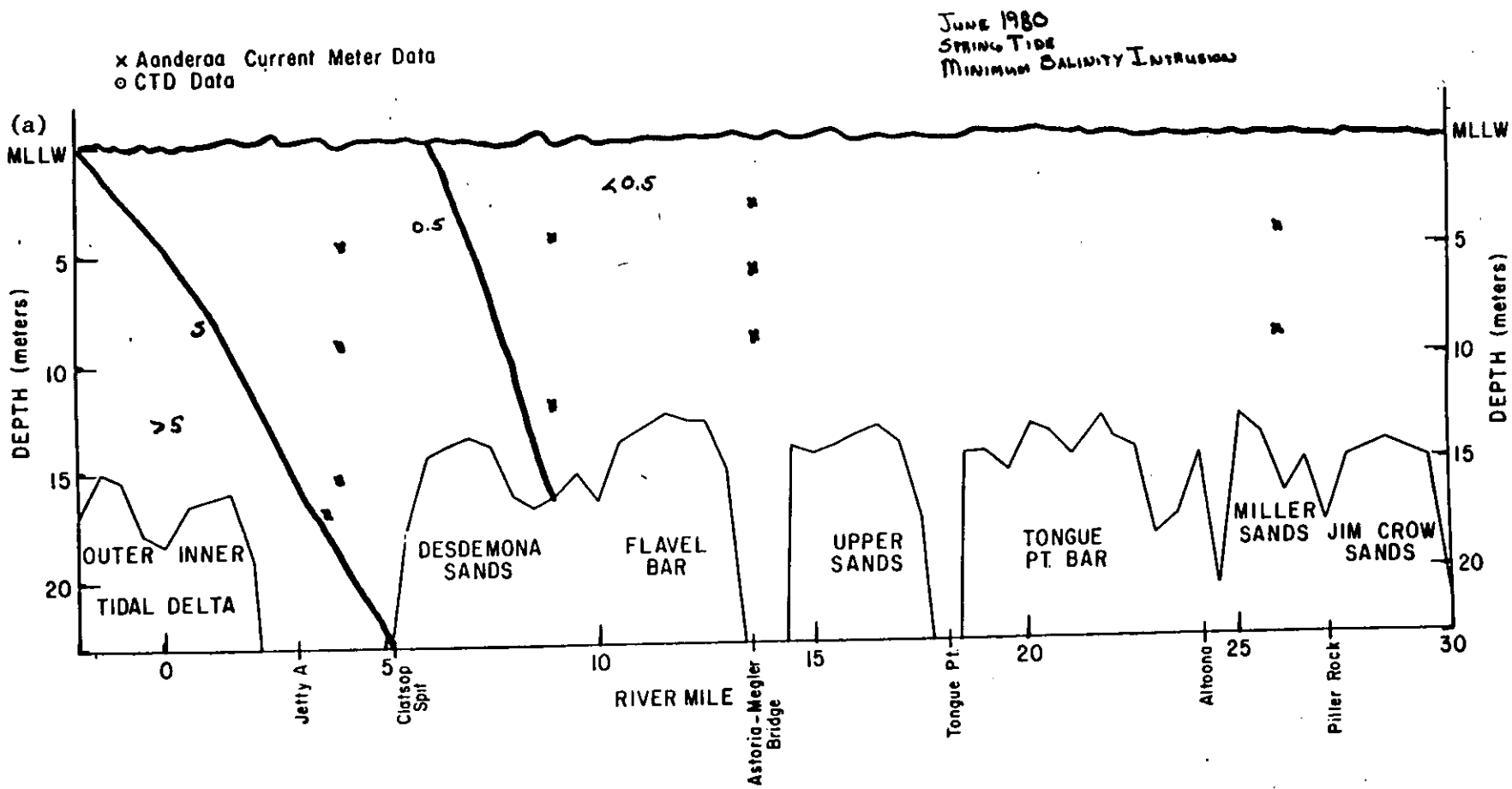


Figure 65. (continued).

NAVIGATIONAL CHANNEL  
 JUN 1980  
 SPRING TIDE  
 MAXIMUM SALINITY INTRUSION

E-6

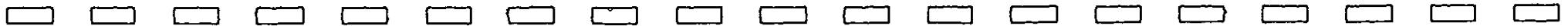
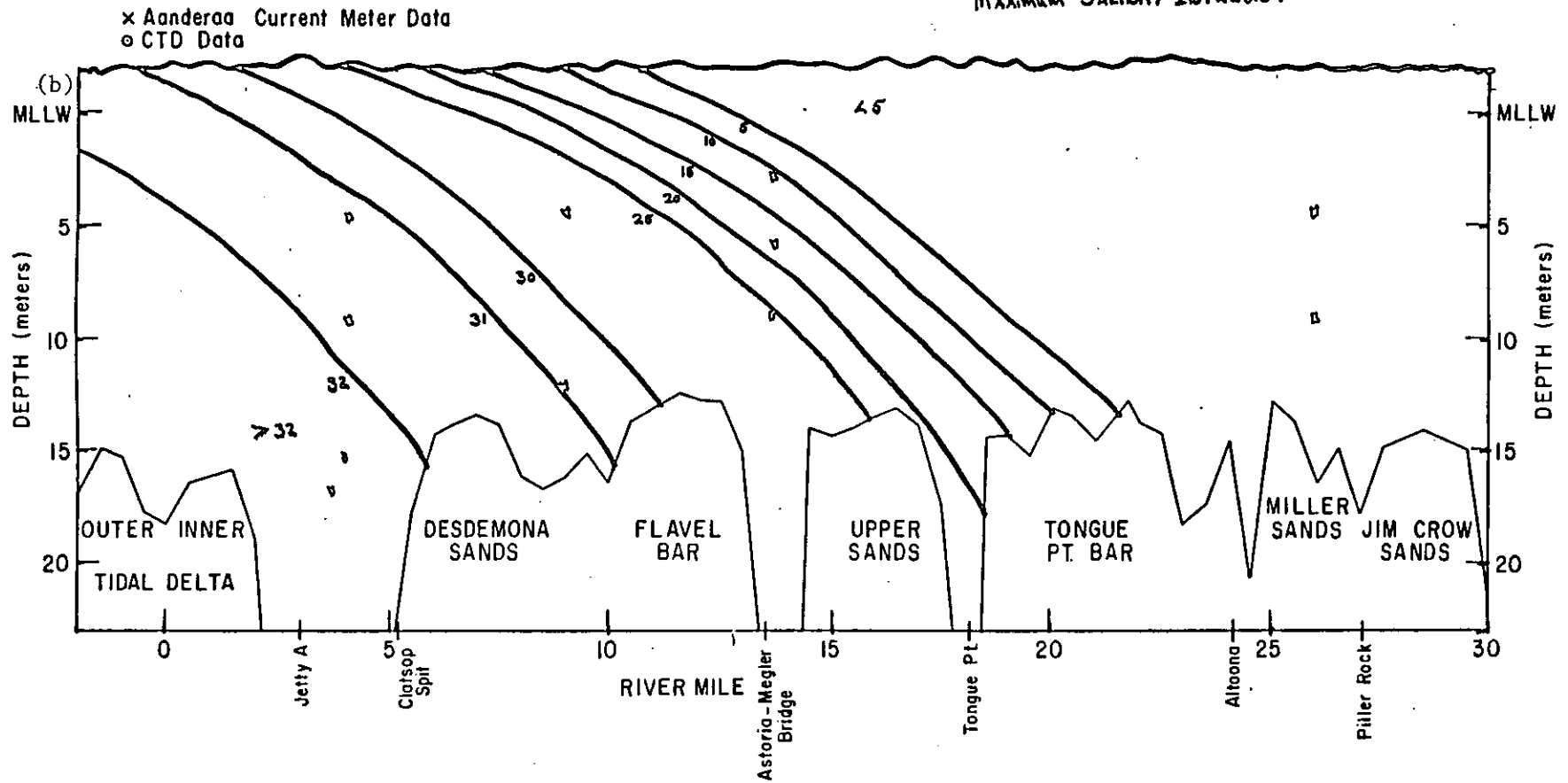


Figure 65. (continued).

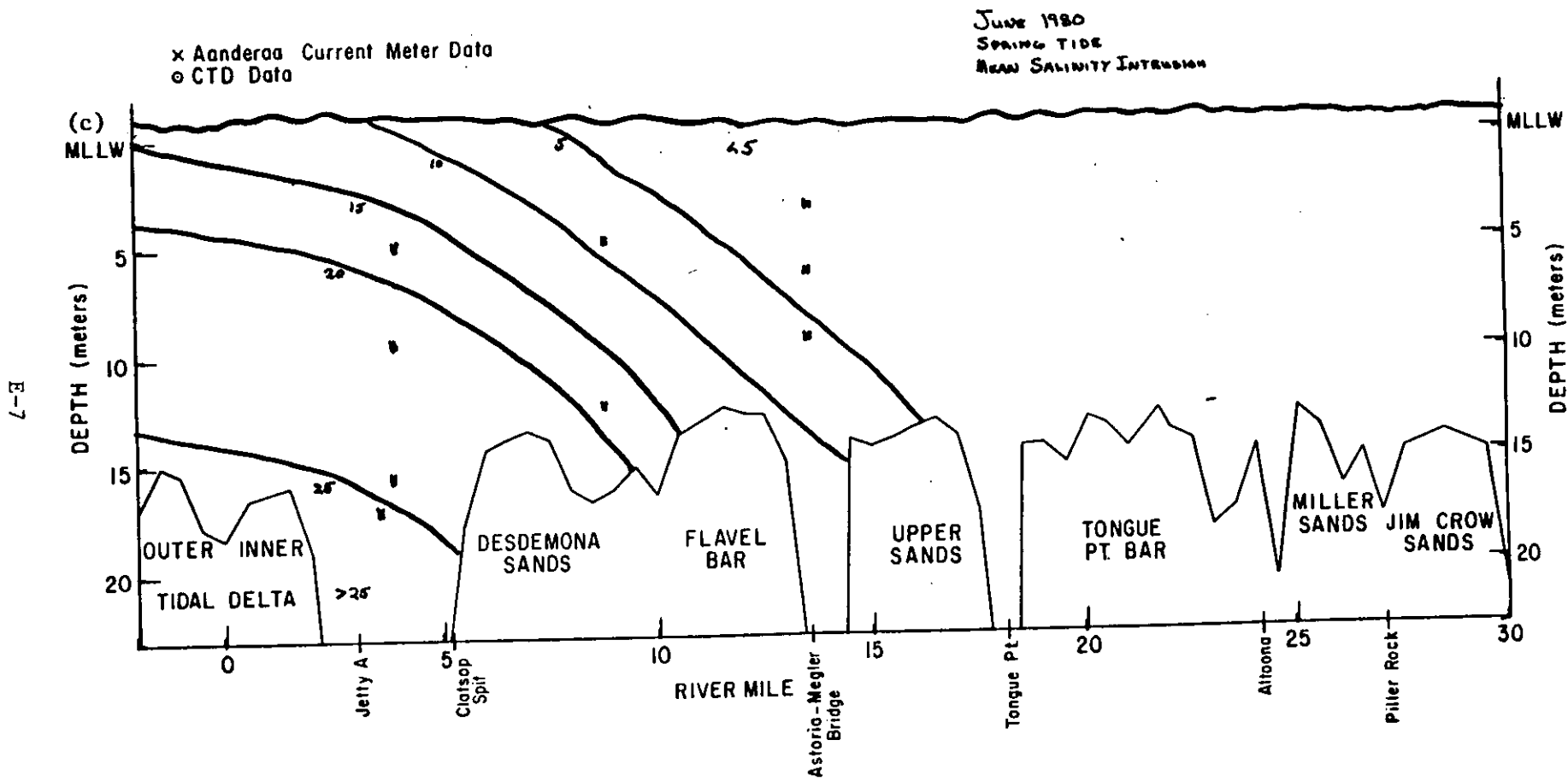


Figure 65. (continued).

### NAVIGATIONAL CHANNEL

JUNE 1980  
SPRING TIDE  
SALINITY RANGE

x Aanderaa Current Meter Data  
o CTD Data

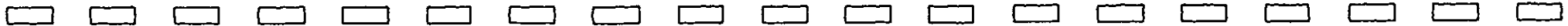
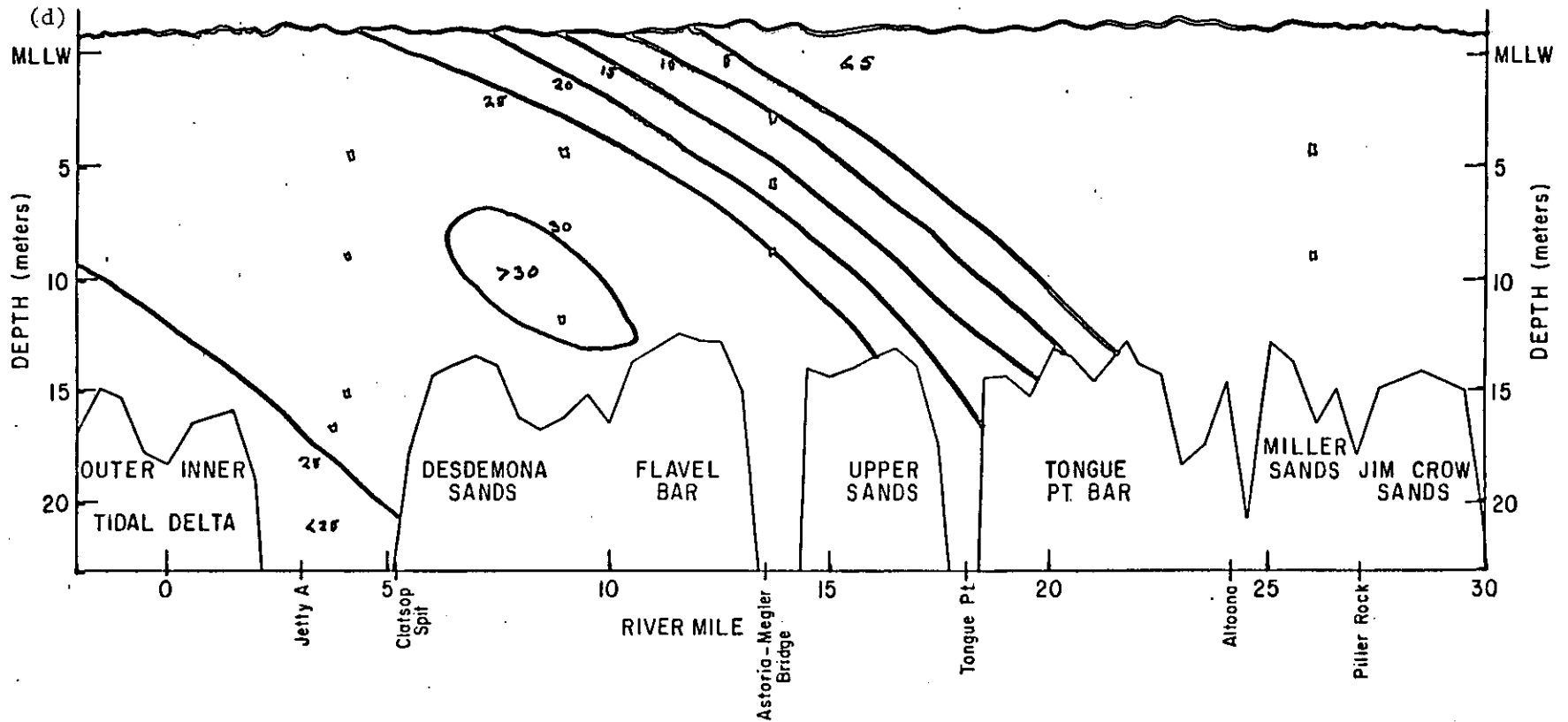


Figure 66. June 1980 (a) minimum, (b) maximum, (c) mean salinity, and (d) salinity range in the North Channel for neap tide.

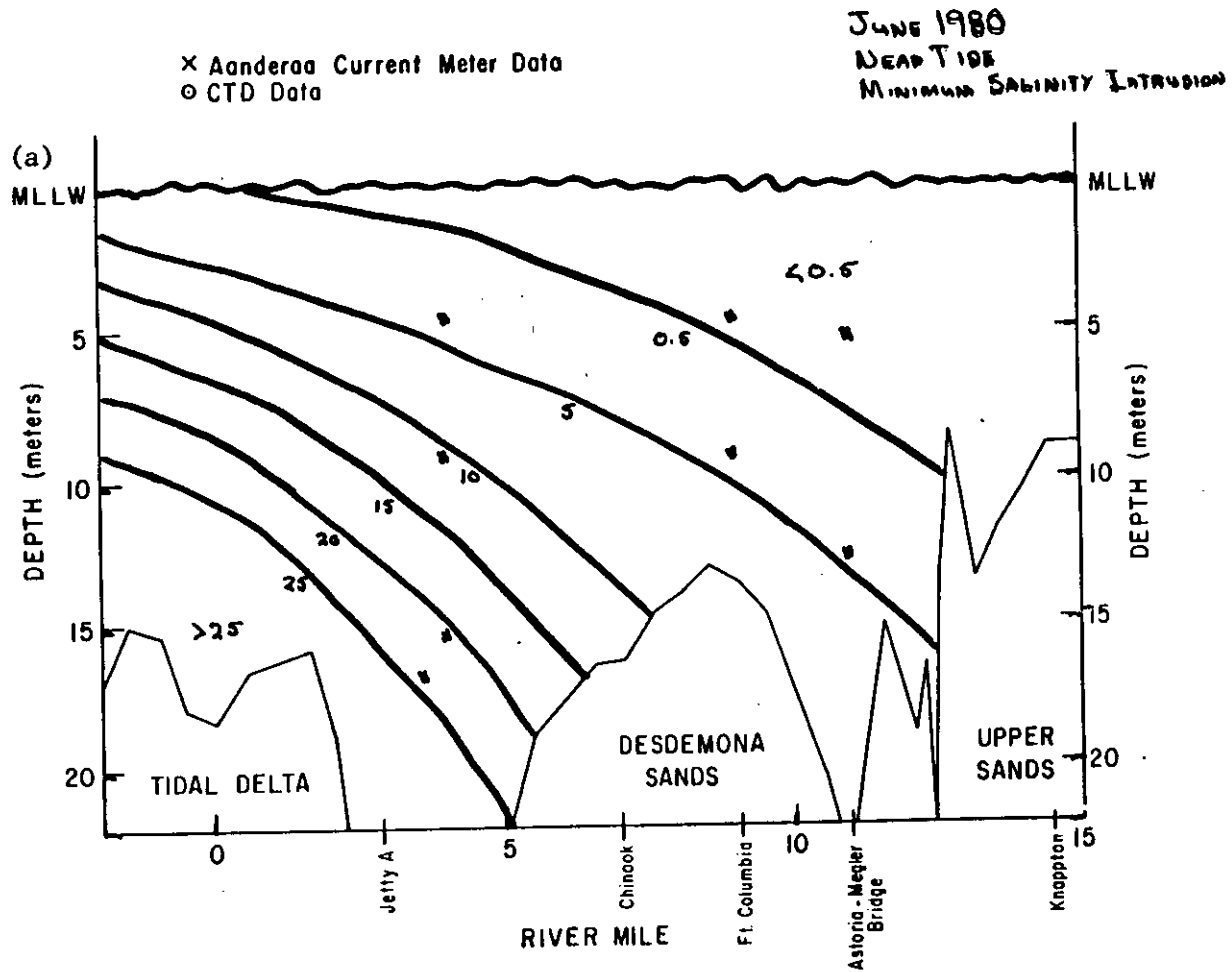
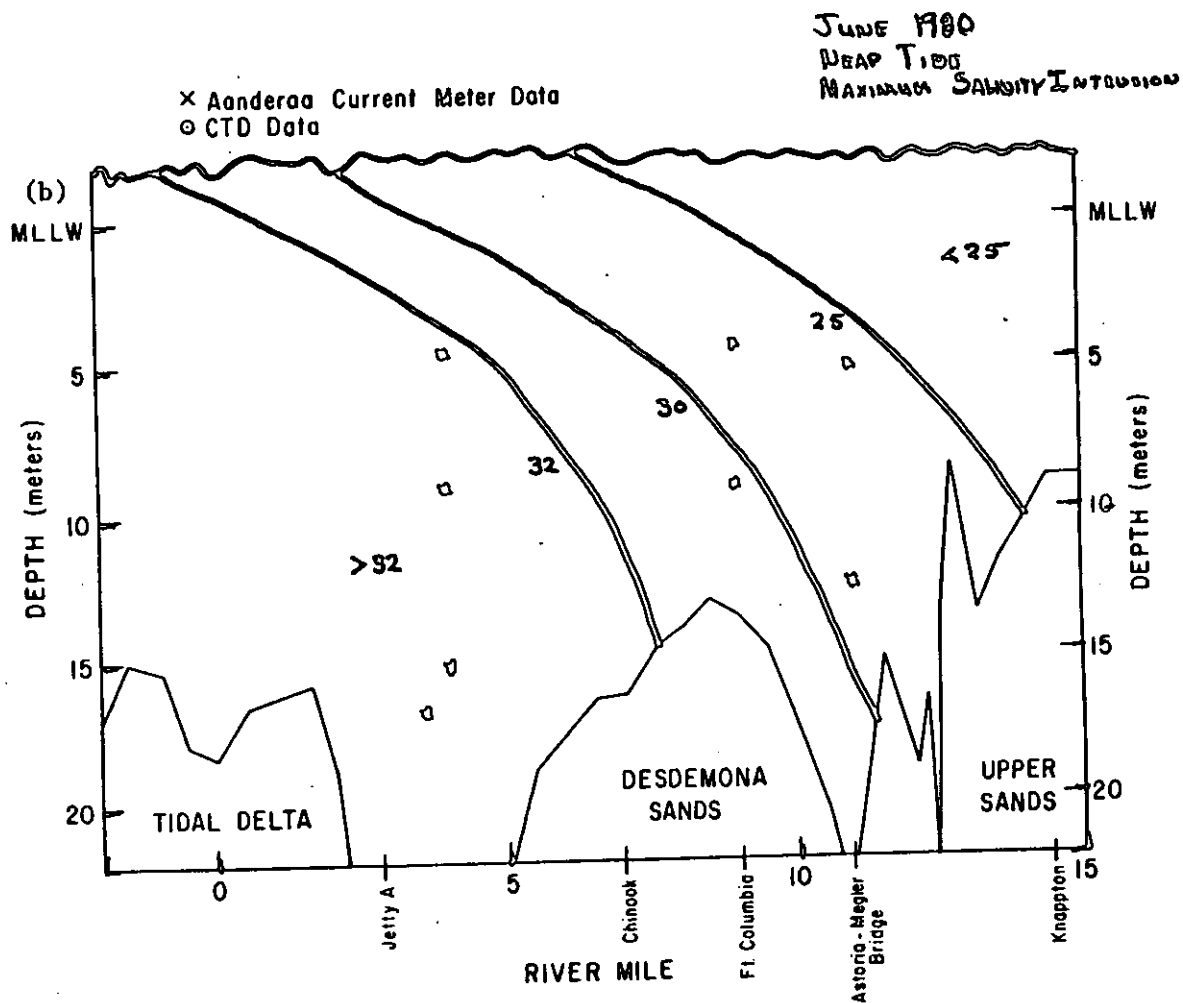


Figure 66. (continued).



E-10



Figure 66. (continued).

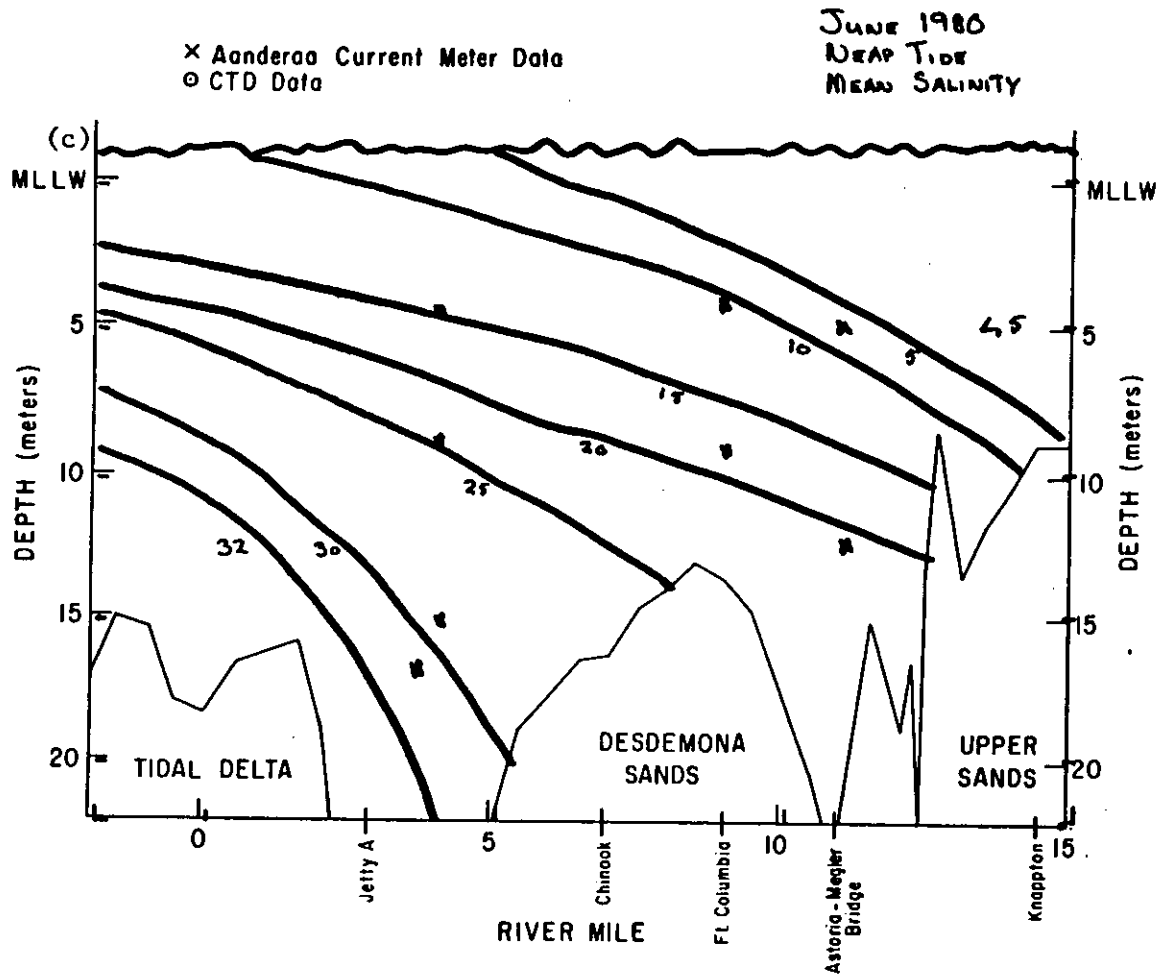


Figure 66. (continued).

JUNE 1980  
NEAP TIDE  
SALINITY RANGE

X Aanderaa Current Meter Data  
O CTD Data

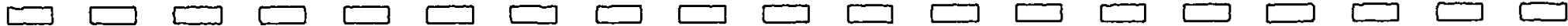
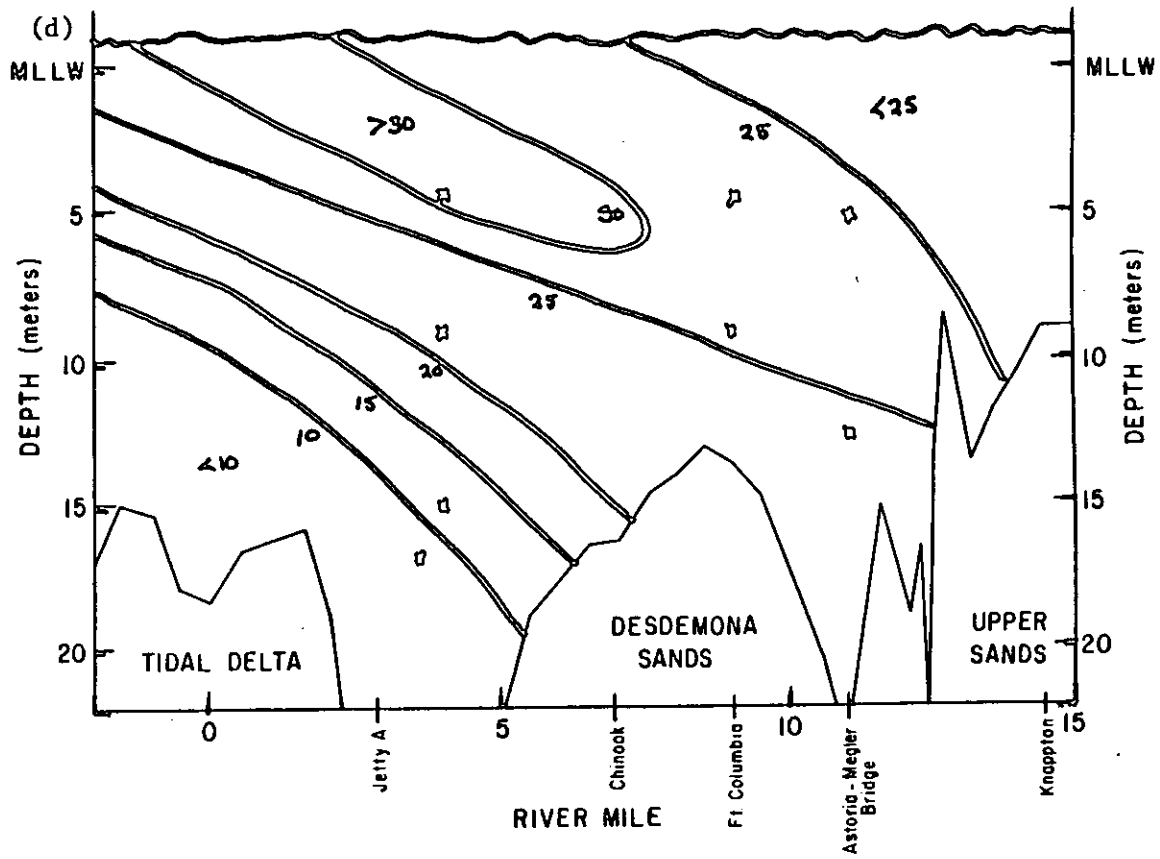




Figure 67. June 1980 (a) minimum, (b) maximum, (c) mean salinity, and (d) salinity range in the North Channel for spring tide.

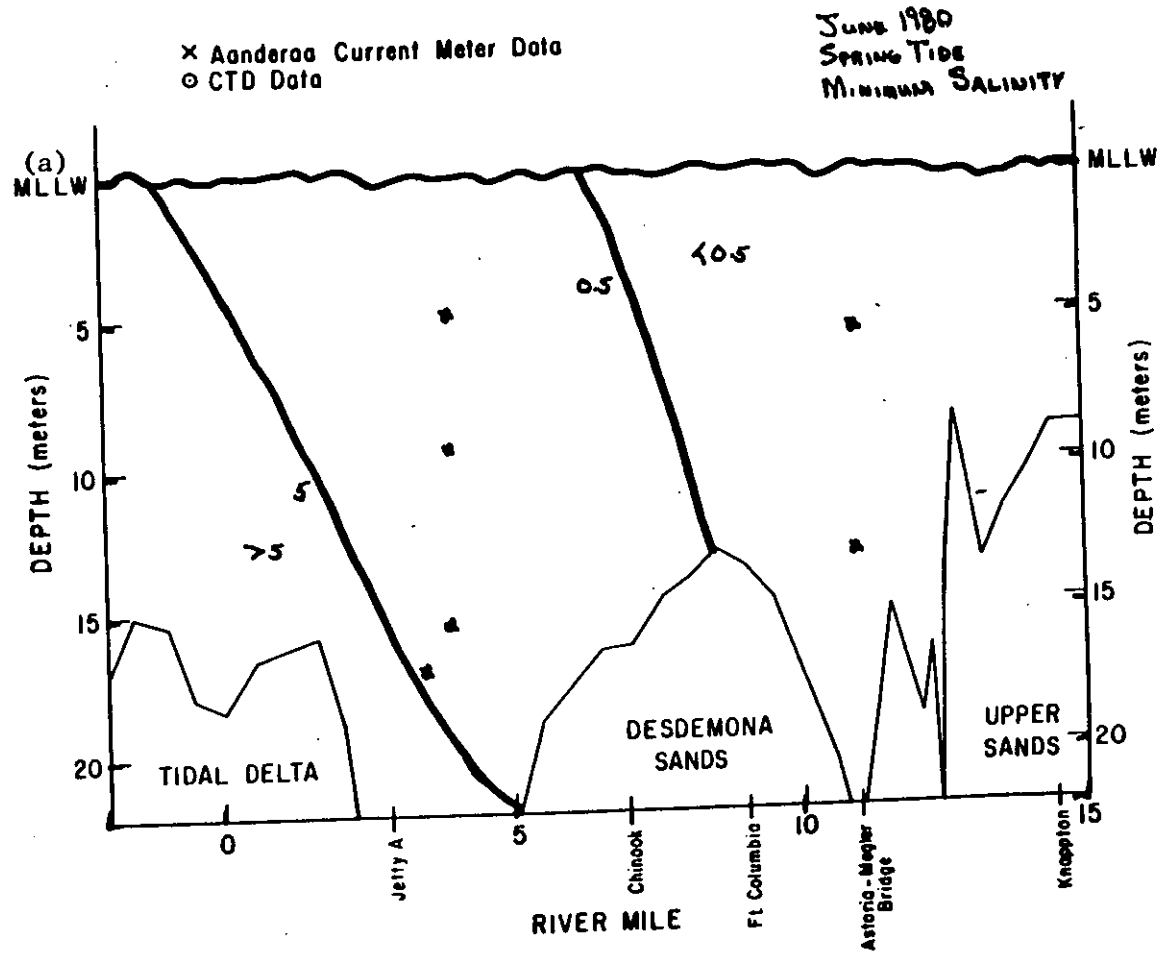


Figure 67. (continued).

JUNE 1988  
SPRING TIDE  
MAXIMUM SALINITY INTRUSION

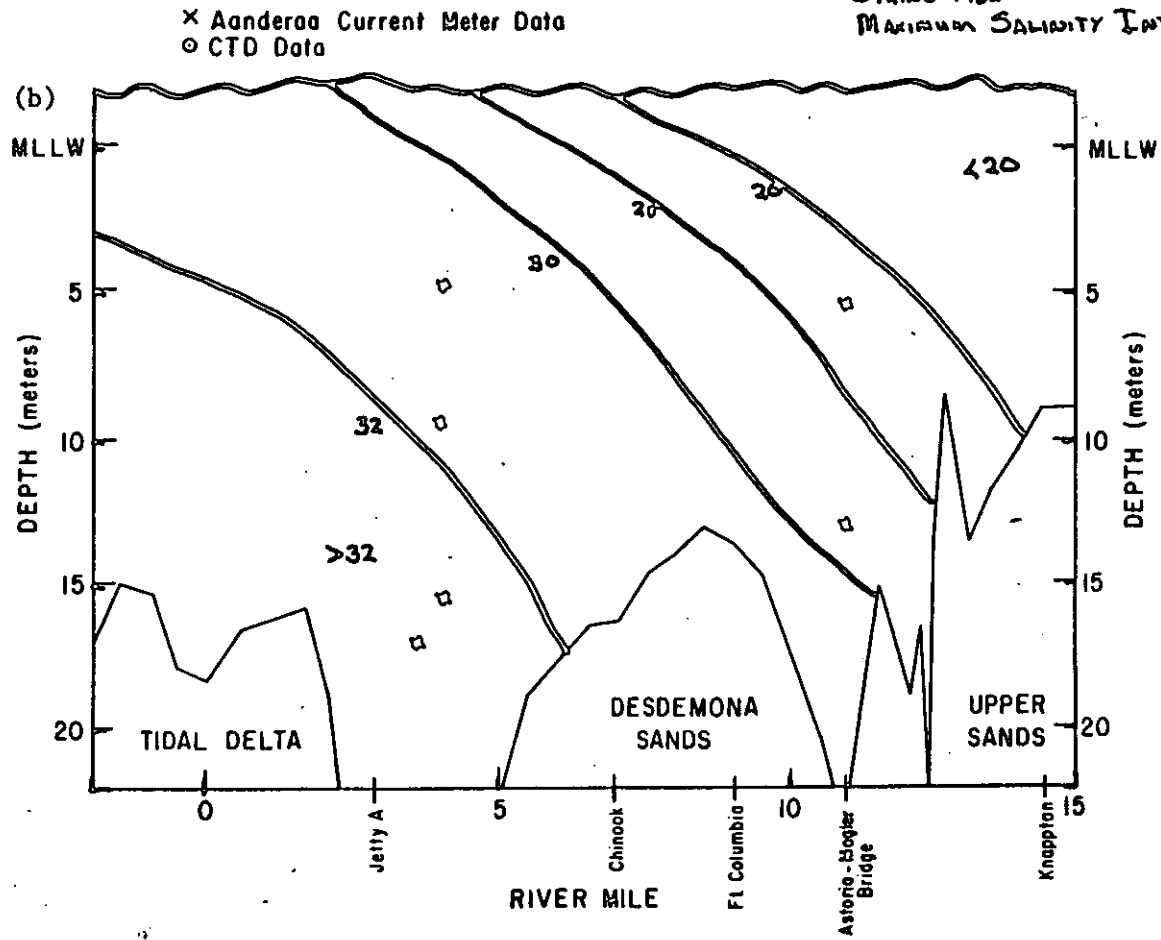


Figure 67. (continued).

JUNE 1980  
SPRING TIDE  
MEAN SALINITY

× Aanderaa Current Meter Data  
○ CTD Data

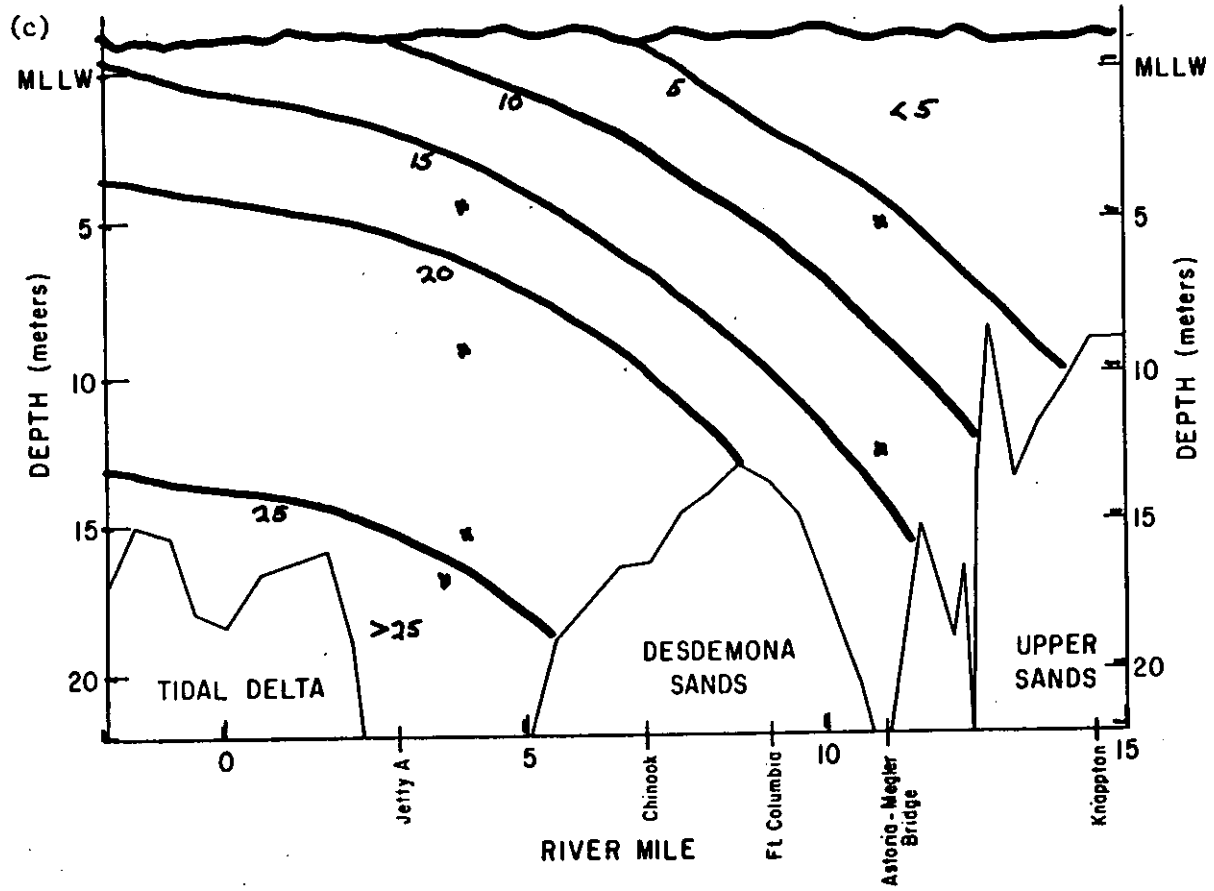


Figure 67. (continued).

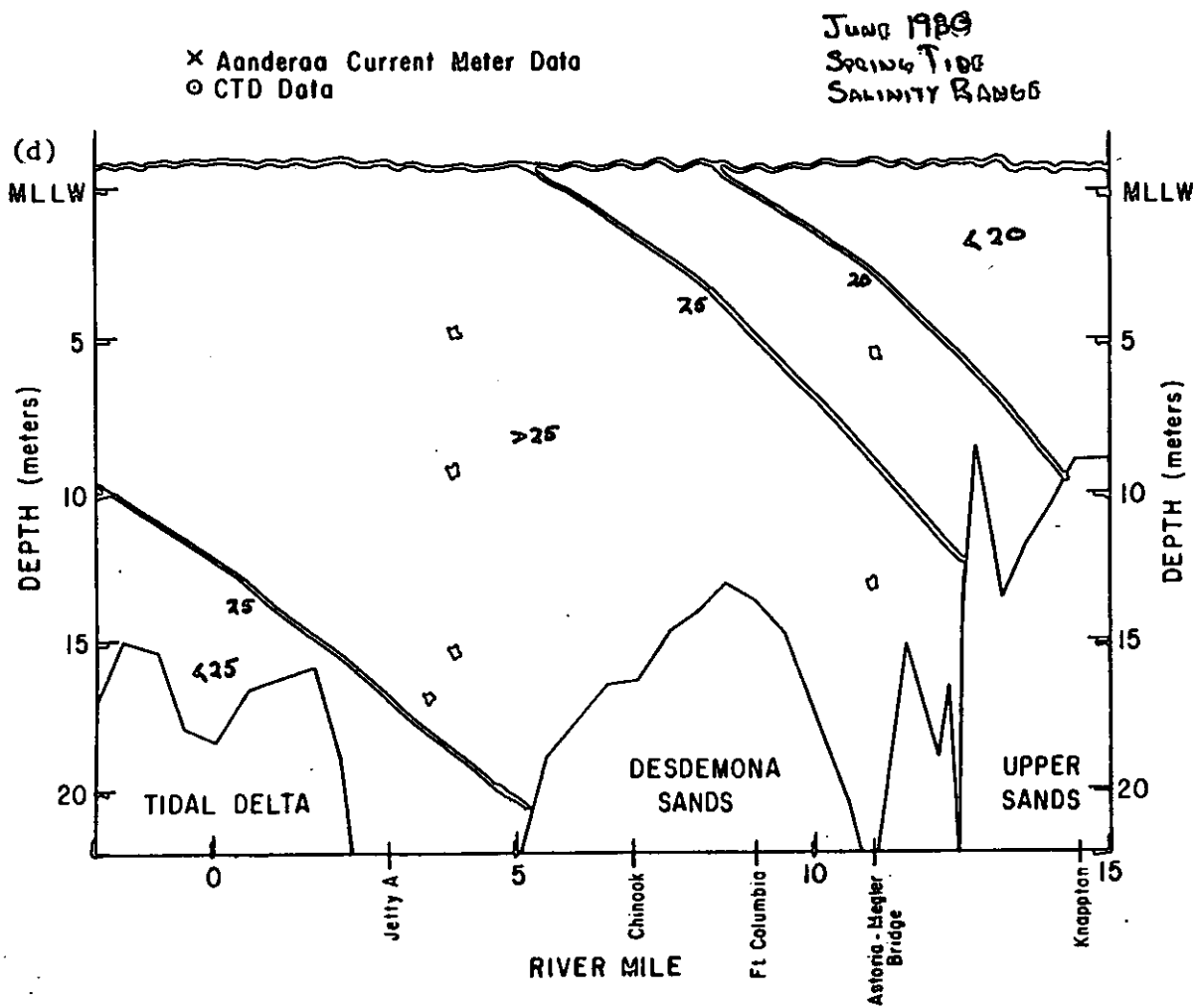
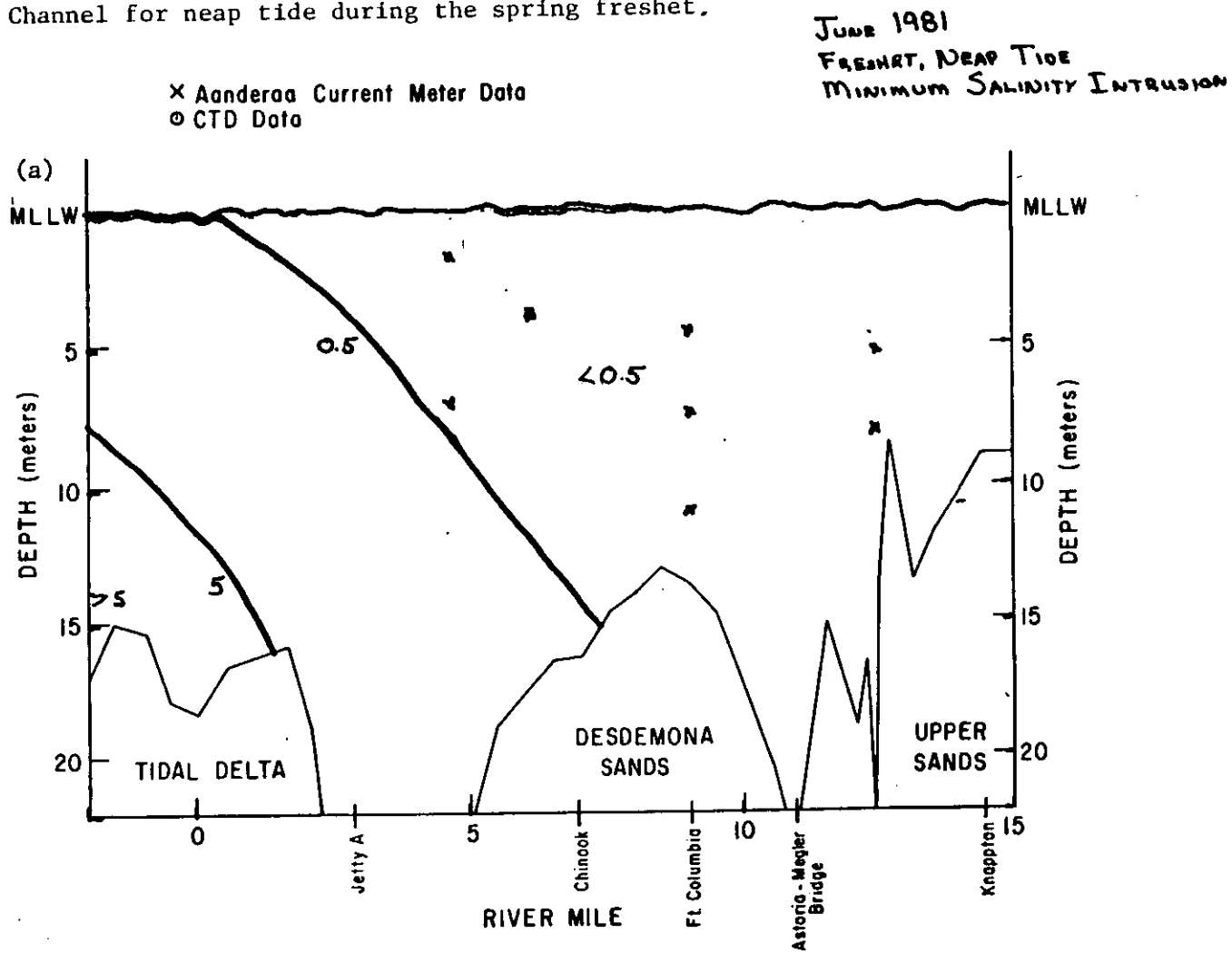


Figure 68. June 1981 (a) minimum, (b) maximum, (c) mean salinity, and (d) salinity range in the North Channel for neap tide during the spring freshet.



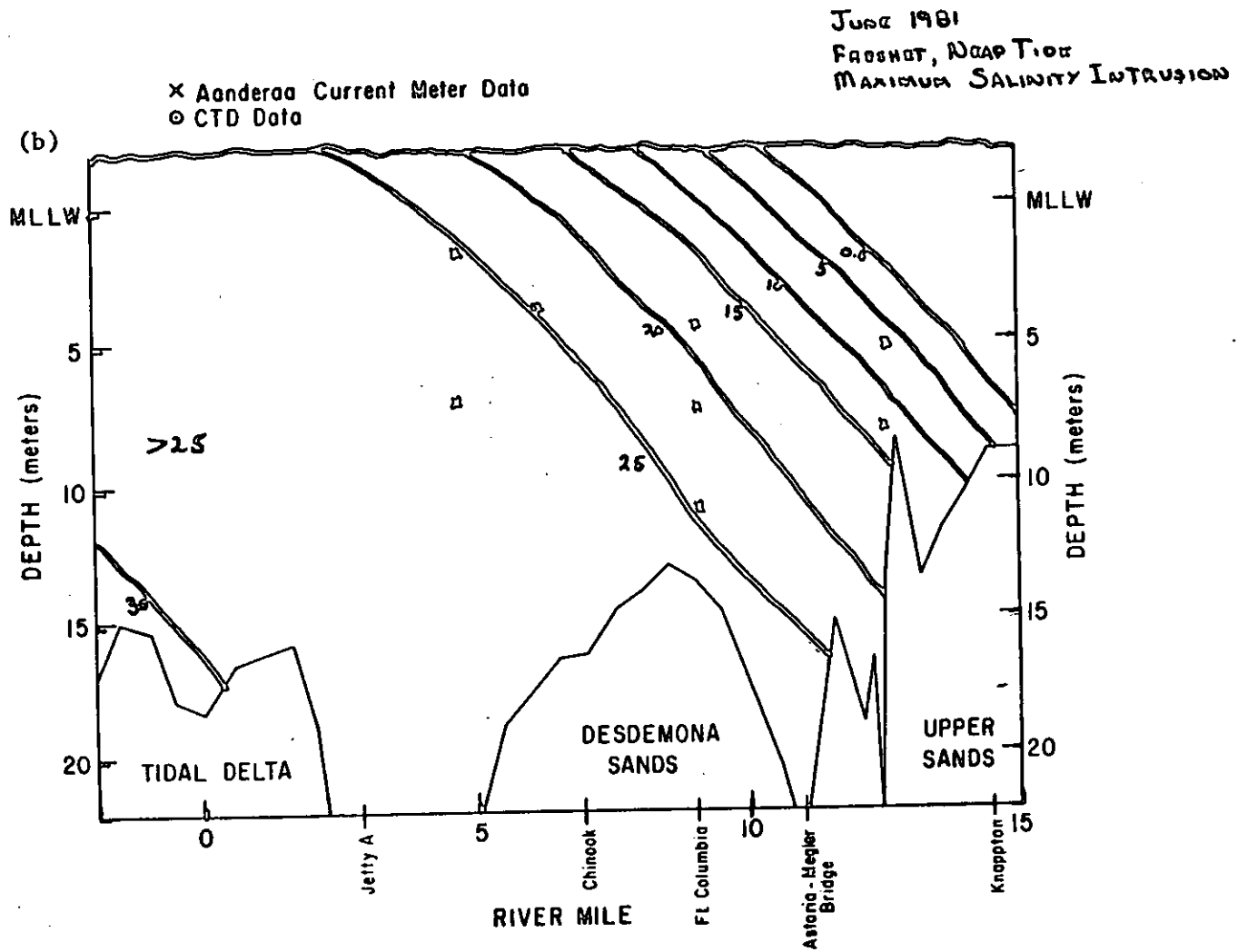


Figure 68. (continued).

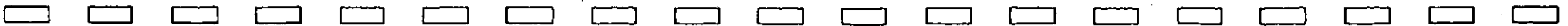


Figure 68. (continued).

JUNE 1981  
FRESHET, NEAP TIDE  
MEAN SALINITY INTRUSION

× Aanderaa Current Meter Data  
○ CTD Data

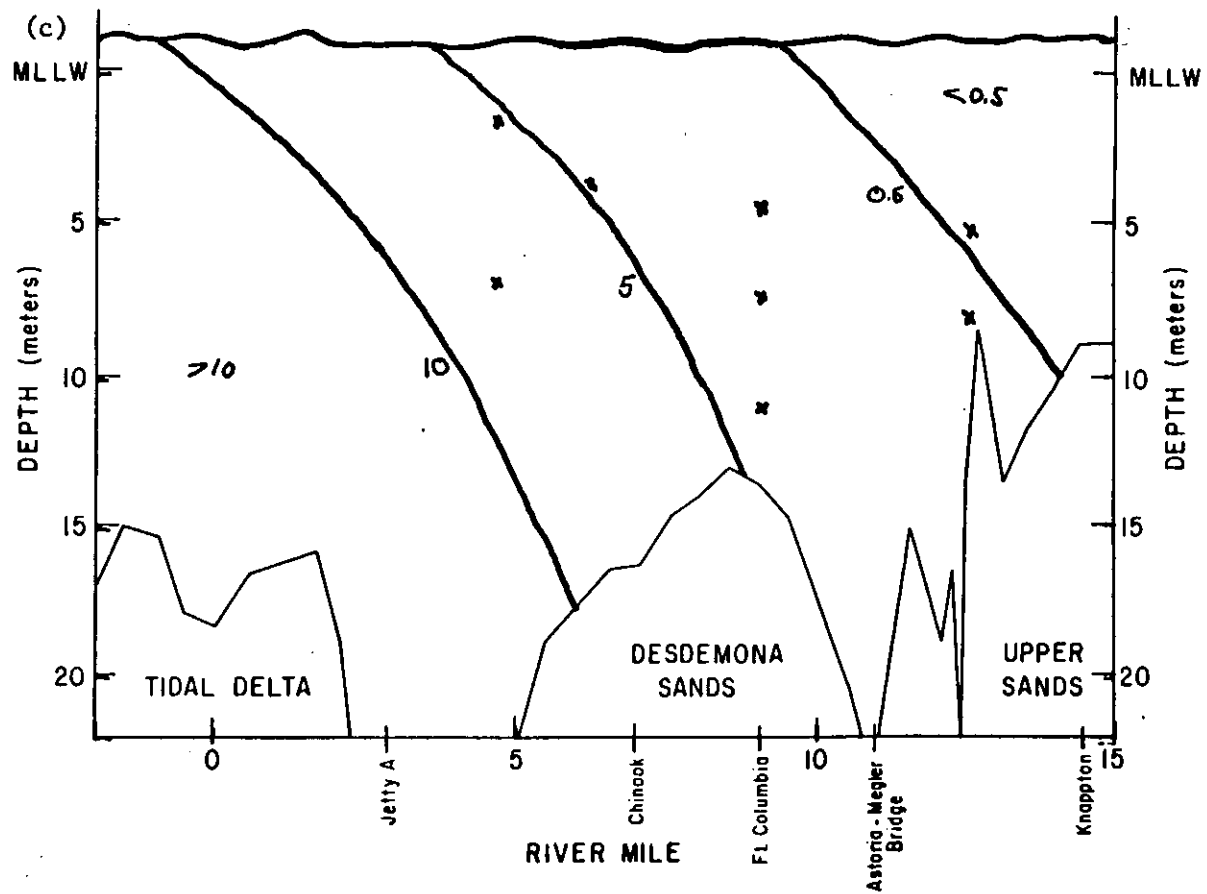
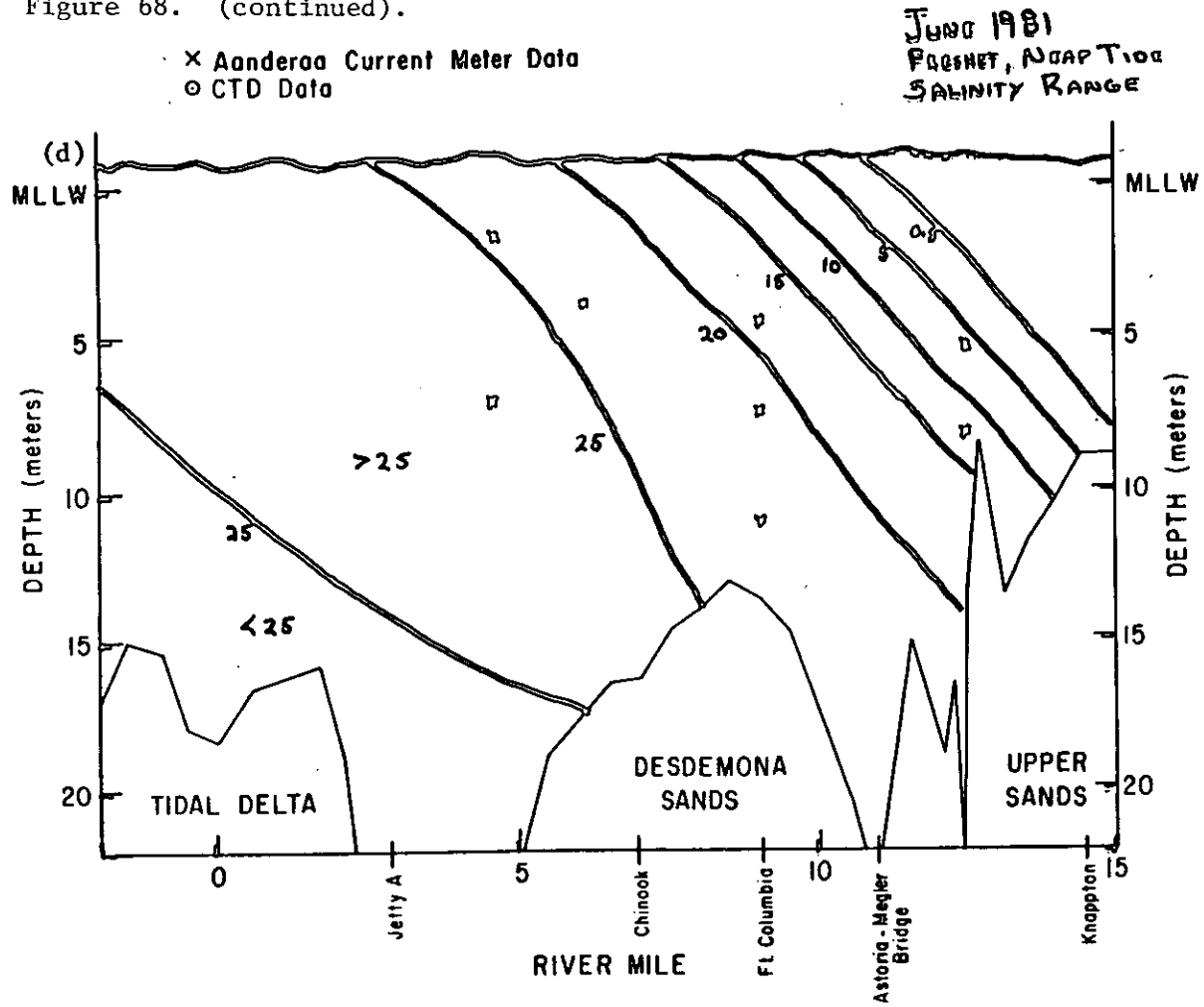


Figure 68. (continued).





APPENDIX F

Daily Estimated Riverflow at Astoria,  
1979 - 81

Table 28. Estimated daily river flow at the mouth of the Columbia River, October 1977 to December 1981.

TIME PERIOD OF TAPE IS FROM: 1(DAY)-10-1977 AT 18: 0: 0 ( PST) TO 30(DAY)-12-1981 AT 18: 0: 0 ( PST)  
 LATITUDE(N)= 46(DEG) 15(MIN) 0.00(SEC) LONGITUDE(W)= 124(DEG) 5(MIN) 0.00(SEC) MAGNETIC DEVIATION= 21.00(DEG )  
 TAPE LOCATION INFORMATION. PROCESSED 9-TRACK TAPE NUMBER IS. 0 FILE NUMBER IS: 1  
 TOTAL NUMBER OF SAMPLES IN FILE IS: 1352  
 HIGH FLOW: F=-10300CFS +1 084\*BUNN DAM FLOW +1 757 WILL RIV AT PORTLAND  
 LOW FLOW: F= 4139CFS+ 1.003\*BONN DAM FLOW +1.632\*WILL RIV AT PORTLAND

					10**5CFS	10**3MCS						10**5CFS	10**3MCS				
1	1977	10	1	18	0	0	1.39	3.93	2	1977	10	2	18	0	0	1.22	3.47
3	1977	10	3	18	0	0	1.57	4.44	4	1977	10	4	18	0	0	1.45	4.11
5	1977	10	5	18	0	0	1.37	3.88	6	1977	10	6	18	0	0	1.59	4.52
7	1977	10	7	18	0	0	1.64	4.63	8	1977	10	8	18	0	0	1.27	3.60
9	1977	10	9	18	0	0	1.25	3.53	10	1977	10	10	18	0	0	1.23	3.49
11	1977	10	11	18	0	0	1.28	3.64	12	1977	10	12	18	0	0	1.34	3.79
13	1977	10	13	18	0	0	1.39	3.94	14	1977	10	14	18	0	0	1.25	3.53
15	1977	10	15	18	0	0	1.09	3.08	16	1977	10	16	18	0	0	1.06	3.01
17	1977	10	17	18	0	0	1.25	3.55	18	1977	10	18	18	0	0	1.38	3.91
19	1977	10	19	18	0	0	1.33	3.77	20	1977	10	20	18	0	0	1.37	3.88
21	1977	10	21	18	0	0	1.22	3.47	22	1977	10	22	18	0	0	1.04	2.96
23	1977	10	23	18	0	0	1.01	2.87	24	1977	10	24	18	0	0	1.11	3.13
25	1977	10	25	18	0	0	1.05	2.97	26	1977	10	26	18	0	0	1.30	3.69
27	1977	10	27	18	0	0	1.58	4.46	28	1977	10	28	18	0	0	1.52	4.31
29	1977	10	29	18	0	0	1.33	3.77	30	1977	10	30	18	0	0	1.28	3.62
31	1977	10	31	18	0	0	1.59	4.50	32	1977	11	1	18	0	0	1.72	4.88
33	1977	11	2	18	0	0	1.97	5.58	34	1977	11	3	18	0	0	1.97	5.58
35	1977	11	4	18	0	0	1.89	5.36	36	1977	11	5	18	0	0	1.71	4.85
37	1977	11	6	18	0	0	1.47	4.17	38	1977	11	7	18	0	0	1.51	4.29
39	1977	11	8	18	0	0	1.72	4.87	40	1977	11	9	18	0	0	1.79	5.07
41	1977	11	10	18	0	0	1.69	4.79	42	1977	11	11	18	0	0	1.39	3.93
43	1977	11	12	18	0	0	1.29	3.64	44	1977	11	13	18	0	0	1.28	3.61
45	1977	11	14	18	0	0	1.49	4.22	46	1977	11	15	18	0	0	1.82	5.16
47	1977	11	16	18	0	0	2.34	6.61	48	1977	11	17	18	0	0	2.39	6.77
49	1977	11	18	18	0	0	2.48	7.01	50	1977	11	19	18	0	0	2.05	5.79
51	1977	11	20	18	0	0	1.96	5.54	52	1977	11	21	18	0	0	2.39	6.77
53	1977	11	22	18	0	0	2.33	6.59	54	1977	11	23	18	0	0	2.26	6.41
55	1977	11	24	18	0	0	2.60	7.35	56	1977	11	25	18	0	0	3.77	10.67
57	1977	11	26	18	0	0	4.44	12.57	58	1977	11	27	18	0	0	3.84	10.86
59	1977	11	28	18	0	0	3.46	9.79	60	1977	11	29	18	0	0	3.28	9.27
61	1977	11	30	18	0	0	3.27	9.25	62	1977	12	1	18	0	0	3.32	9.41
63	1977	12	2	18	0	0	3.87	10.97	64	1977	12	3	18	0	0	4.69	13.28
65	1977	12	4	18	0	0	3.94	11.15	66	1977	12	5	18	0	0	2.13	6.03
67	1977	12	6	18	0	0	4.47	12.65	68	1977	12	7	18	0	0	3.70	10.47
69	1977	12	8	18	0	0	3.85	10.89	70	1977	12	9	18	0	0	3.63	10.28
71	1977	12	10	18	0	0	3.09	8.75	72	1977	12	11	18	0	0	3.09	8.76
73	1977	12	12	18	0	0	4.31	12.20	74	1977	12	13	18	0	0	5.46	15.47
75	1977	12	14	18	0	0	6.63	18.78	76	1977	12	15	18	0	0	6.72	19.03
77	1977	12	16	18	0	0	6.68	18.92	78	1977	12	17	18	0	0	6.44	18.23
79	1977	12	18	18	0	0	5.69	16.12	80	1977	12	19	18	0	0	5.05	14.30
81	1977	12	20	18	0	0	4.56	12.90	82	1977	12	21	18	0	0	3.97	11.25
83	1977	12	22	18	0	0	3.70	10.48	84	1977	12	23	18	0	0	3.54	10.02
85	1977	12	24	18	0	0	3.17	8.97	86	1977	12	25	18	0	0	2.97	8.40
87	1977	12	26	18	0	0	3.02	8.56	88	1977	12	27	18	0	0	3.00	8.51
89	1977	12	28	18	0	0	3.03	8.59	90	1977	12	29	18	0	0	2.90	8.22
91	1977	12	30	18	0	0	2.67	7.56	92	1977	12	31	18	0	0	2.67	7.56
93	1978	1	1	18	0	0	2.46	6.96	94	1978	1	2	18	0	0	2.26	6.40
95	1978	1	3	18	0	0	2.47	7.00	96	1978	1	4	18	0	0	2.93	8.29
97	1978	1	5	18	0	0	2.92	8.27	98	1978	1	6	18	0	0	3.48	9.85
99	1978	1	7	18	0	0	3.74	10.60	100	1978	1	8	18	0	0	3.31	9.37
101	1978	1	9	18	0	0	3.04	8.62	102	1978	1	10	18	0	0	3.24	9.16

Table 28. (continued).

103	1978	1	11	18	0	0	3.18	8.99	104	1978	1	12	18	0	0	3.35	9.49
105	1978	1	13	18	0	0	3.14	8.90	106	1978	1	14	18	0	0	3.07	8.69
107	1978	1	15	18	0	0	2.71	7.68	108	1978	1	16	18	0	0	3.13	8.86
109	1978	1	17	18	0	0	3.02	8.54	110	1978	1	18	18	0	0	3.47	9.82
111	1978	1	19	18	0	0	3.56	10.08	112	1978	1	20	18	0	0	3.02	8.55
113	1978	1	21	18	0	0	2.92	8.25	114	1978	1	22	18	0	0	2.95	8.34
115	1978	1	23	18	0	0	3.38	9.57	116	1978	1	24	18	0	0	3.30	9.33
117	1978	1	25	18	0	0	2.85	8.06	118	1978	1	26	18	0	0	2.77	7.85
119	1978	1	27	18	0	0	3.03	8.57	120	1978	1	28	18	0	0	2.69	7.63
121	1978	1	29	18	0	0	2.34	6.62	122	1978	1	30	18	0	0	2.58	7.32
123	1978	1	31	18	0	0	2.49	7.04	124	1978	2	1	18	0	0	2.48	7.01
125	1978	2	2	18	0	0	2.72	7.70	126	1978	2	3	18	0	0	2.84	8.05
127	1978	2	4	18	0	0	2.70	7.64	128	1978	2	5	18	0	0	2.87	8.12
129	1978	2	6	18	0	0	2.74	7.75	130	1978	2	7	18	0	0	2.87	8.11
131	1978	2	8	18	0	0	3.02	8.56	132	1978	2	9	18	0	0	3.11	8.80
133	1978	2	10	18	0	0	2.98	8.44	134	1978	2	11	18	0	0	2.87	8.13
135	1978	2	12	18	0	0	2.64	7.47	136	1978	2	13	18	0	0	2.41	6.81
137	1978	2	14	18	0	0	2.46	6.96	138	1978	2	15	18	0	0	2.61	7.38
139	1978	2	16	18	0	0	2.67	7.56	140	1978	2	17	18	0	0	2.56	7.25
141	1978	2	18	18	0	0	2.10	5.96	142	1978	2	19	18	0	0	1.99	5.63
143	1978	2	20	18	0	0	2.20	6.23	144	1978	2	21	18	0	0	2.42	6.85
145	1978	2	22	18	0	0	2.27	6.44	146	1978	2	23	18	0	0	2.04	5.77
147	1978	2	24	18	0	0	2.31	6.54	148	1978	2	25	18	0	0	2.20	6.22
149	1978	2	26	18	0	0	2.18	6.17	150	1978	2	27	18	0	0	2.36	6.68
151	1978	2	28	18	0	0	2.44	6.91	152	1978	3	1	18	0	0	2.42	6.86
153	1978	3	2	18	0	0	2.40	6.79	154	1978	3	3	18	0	0	2.62	7.41
155	1978	3	4	18	0	0	1.83	5.17	156	1978	3	5	18	0	0	1.72	4.88
157	1978	3	6	18	0	0	2.21	6.26	158	1978	3	7	18	0	0	2.01	5.69
159	1978	3	8	18	0	0	2.00	5.66	160	1978	3	9	18	0	0	2.09	5.92
161	1978	3	10	18	0	0	2.21	6.26	162	1978	3	11	18	0	0	2.03	5.75
163	1978	3	12	18	0	0	1.90	5.39	164	1978	3	13	18	0	0	1.92	5.44
165	1978	3	14	18	0	0	2.12	6.01	166	1978	3	15	18	0	0	2.31	6.55
167	1978	3	16	18	0	0	2.05	5.81	168	1978	3	17	18	0	0	2.04	5.79
169	1978	3	18	18	0	0	1.93	5.45	170	1978	3	19	18	0	0	1.75	4.95
171	1978	3	20	18	0	0	2.08	5.90	172	1978	3	21	18	0	0	2.02	5.72
173	1978	3	22	18	0	0	2.05	5.81	174	1978	3	23	18	0	0	2.42	6.84
175	1978	3	24	18	0	0	2.60	7.37	176	1978	3	25	18	0	0	2.54	7.19
177	1978	3	26	18	0	0	2.48	7.03	178	1978	3	27	18	0	0	2.45	6.93
179	1978	3	28	18	0	0	2.56	7.26	180	1978	3	29	18	0	0	2.72	7.71
181	1978	3	30	18	0	0	2.76	7.82	182	1978	3	31	18	0	0	3.00	8.51
183	1978	4	1	18	0	0	2.66	7.53	184	1978	4	2	18	0	0	2.92	8.28
185	1978	4	3	18	0	0	3.25	9.21	186	1978	4	4	18	0	0	2.97	8.41
187	1978	4	5	18	0	0	2.84	8.05	188	1978	4	6	18	0	0	3.00	8.50
189	1978	4	7	18	0	0	2.93	8.30	190	1978	4	8	18	0	0	2.68	7.58
191	1978	4	9	18	0	0	2.72	7.69	192	1978	4	10	18	0	0	2.97	8.40
193	1978	4	11	18	0	0	2.89	8.17	194	1978	4	12	18	0	0	2.80	7.93
195	1978	4	13	18	0	0	2.98	8.45	196	1978	4	14	18	0	0	2.97	8.40
197	1978	4	15	18	0	0	2.89	8.19	198	1978	4	16	18	0	0	2.54	7.21
199	1978	4	17	18	0	0	2.66	7.53	200	1978	4	18	18	0	0	2.65	7.50
201	1978	4	19	18	0	0	2.66	7.52	202	1978	4	20	18	0	0	2.96	8.38
203	1978	4	21	18	0	0	2.94	8.33	204	1978	4	22	18	0	0	2.38	6.74
205	1978	4	23	18	0	0	2.67	7.55	206	1978	4	24	18	0	0	2.99	8.47
207	1978	4	25	18	0	0	2.89	8.20	208	1978	4	26	18	0	0	2.94	8.33
209	1978	4	27	18	0	0	3.31	9.38	210	1978	4	28	18	0	0	3.48	9.85
211	1978	4	29	18	0	0	3.38	9.58	212	1978	4	30	18	0	0	3.33	9.43
213	1978	5	1	18	0	0	3.32	9.39	214	1978	5	2	18	0	0	3.14	8.88
215	1978	5	3	18	0	0	3.34	9.45	216	1978	5	4	18	0	0	3.21	9.08
217	1978	5	5	18	0	0	3.37	9.53	218	1978	5	6	18	0	0	3.44	9.74
219	1978	5	7	18	0	0	2.91	8.25	220	1978	5	8	18	0	0	3.25	9.22
221	1978	5	9	18	0	0	2.93	8.29	222	1978	5	10	18	0	0	2.94	8.32
223	1978	5	11	18	0	0	2.92	8.28	224	1978	5	12	18	0	0	3.16	8.95

Table 28. (continued).

225	1978	5	13	18	0	0	3.02	8.54	226	1978	5	14	18	0	0	2.94	8.32
227	1978	5	15	18	0	0	3.67	10.40	228	1978	5	16	18	0	0	3.82	10.83
229	1978	5	17	18	0	0	3.78	10.69	230	1978	5	18	18	0	0	3.72	10.52
231	1978	5	19	18	0	0	3.77	10.68	232	1978	5	20	18	0	0	2.91	8.24
233	1978	5	21	18	0	0	2.71	7.68	234	1978	5	22	18	0	0	3.08	8.73
235	1978	5	23	18	0	0	3.36	9.51	236	1978	5	24	18	0	0	3.57	10.10
237	1978	5	25	18	0	0	3.47	9.82	238	1978	5	26	18	0	0	3.35	9.50
239	1978	5	27	18	0	0	3.30	9.36	240	1978	5	28	18	0	0	2.73	7.73
241	1978	5	29	18	0	0	2.73	7.72	242	1978	5	30	18	0	0	3.19	9.02
243	1978	5	31	18	0	0	2.84	8.04	244	1978	6	1	18	0	0	3.06	8.67
245	1978	6	2	18	0	0	2.82	7.99	246	1978	6	3	18	0	0	2.10	5.95
247	1978	6	4	18	0	0	2.53	7.16	248	1978	6	5	18	0	0	2.62	7.41
249	1978	6	6	18	0	0	2.62	7.41	250	1978	6	7	18	0	0	2.73	7.74
251	1978	6	8	18	0	0	3.00	8.48	252	1978	6	9	18	0	0	3.18	9.00
253	1978	6	10	18	0	0	3.56	10.09	254	1978	6	11	18	0	0	3.25	9.20
255	1978	6	12	18	0	0	3.35	9.49	256	1978	6	13	18	0	0	2.97	8.41
257	1978	6	14	18	0	0	2.94	8.33	258	1978	6	15	18	0	0	2.98	8.45
259	1978	6	16	18	0	0	3.07	8.70	260	1978	6	17	18	0	0	2.74	7.76
261	1978	6	18	18	0	0	2.56	7.26	262	1978	6	19	18	0	0	2.74	7.76
263	1978	6	20	18	0	0	2.75	7.79	264	1978	6	21	18	0	0	2.61	7.39
265	1978	6	22	18	0	0	2.42	6.86	266	1978	6	23	18	0	0	2.41	6.82
267	1978	6	24	18	0	0	2.27	6.43	268	1978	6	25	18	0	0	2.20	6.23
269	1978	6	26	18	0	0	2.68	7.59	270	1978	6	27	18	0	0	2.54	7.18
271	1978	6	28	18	0	0	2.65	7.50	272	1978	6	29	18	0	0	2.57	7.27
273	1978	6	30	18	0	0	2.57	7.28	274	1978	7	1	18	0	0	2.34	6.63
275	1978	7	2	18	0	0	2.15	6.08	276	1978	7	3	18	0	0	2.02	5.73
277	1978	7	4	18	0	0	2.04	5.78	278	1978	7	5	18	0	0	2.44	6.90
279	1978	7	6	18	0	0	2.55	7.23	280	1978	7	7	18	0	0	2.33	6.60
281	1978	7	8	18	0	0	1.97	5.59	282	1978	7	9	18	0	0	2.14	6.05
283	1978	7	10	18	0	0	2.67	7.56	284	1978	7	11	18	0	0	2.45	6.94
285	1978	7	12	18	0	0	2.74	7.77	286	1978	7	13	18	0	0	2.61	7.38
287	1978	7	14	18	0	0	2.66	7.52	288	1978	7	15	18	0	0	2.13	6.04
289	1978	7	16	18	0	0	1.80	5.09	290	1978	7	17	18	0	0	2.18	6.16
291	1978	7	18	18	0	0	2.30	6.50	292	1978	7	19	18	0	0	2.16	6.10
293	1978	7	20	18	0	0	1.98	5.60	294	1978	7	21	18	0	0	2.14	6.05
295	1978	7	22	18	0	0	1.82	5.16	296	1978	7	23	18	0	0	1.61	4.55
297	1978	7	24	18	0	0	2.29	6.48	298	1978	7	25	18	0	0	1.98	5.61
299	1978	7	26	18	0	0	2.00	5.67	300	1978	7	27	18	0	0	1.88	5.32
301	1978	7	28	18	0	0	1.67	4.74	302	1978	7	29	18	0	0	1.45	4.11
303	1978	7	30	18	0	0	1.24	3.51	304	1978	7	31	18	0	0	1.62	4.59
305	1978	8	1	18	0	0	1.89	5.35	306	1978	8	2	18	0	0	1.97	5.59
307	1978	8	3	18	0	0	1.90	5.38	308	1978	8	4	18	0	0	1.62	4.58
309	1978	8	5	18	0	0	1.22	3.46	310	1978	8	6	18	0	0	1.18	3.34
311	1978	8	7	18	0	0	1.42	4.01	312	1978	8	8	18	0	0	1.66	4.70
313	1978	8	9	18	0	0	1.58	4.47	314	1978	8	10	18	0	0	1.56	4.41
315	1978	8	11	18	0	0	1.58	4.47	316	1978	8	12	18	0	0	1.16	3.28
317	1978	8	13	18	0	0	1.17	3.32	318	1978	8	14	18	0	0	1.28	3.64
319	1978	8	15	18	0	0	1.53	4.33	320	1978	8	16	18	0	0	1.59	4.50
321	1978	8	17	18	0	0	1.58	4.49	322	1978	8	18	18	0	0	1.59	4.50
323	1978	8	19	18	0	0	1.34	3.81	324	1978	8	20	18	0	0	1.22	3.45
325	1978	8	21	18	0	0	1.60	4.52	326	1978	8	22	18	0	0	1.50	4.25
327	1978	8	23	18	0	0	1.48	4.18	328	1978	8	24	18	0	0	1.61	4.55
329	1978	8	25	18	0	0	1.46	4.13	330	1978	8	26	18	0	0	1.26	3.58
331	1978	8	27	18	0	0	1.37	3.87	332	1978	8	28	18	0	0	1.46	4.13
333	1978	8	29	18	0	0	1.80	5.09	334	1978	8	30	18	0	0	1.67	4.72
335	1978	8	31	18	0	0	2.00	5.66	336	1978	9	1	18	0	0	1.70	4.82
337	1978	9	2	18	0	0	1.31	3.72	338	1978	9	3	18	0	0	1.22	3.45
339	1978	9	4	18	0	0	1.21	3.43	340	1978	9	5	18	0	0	1.33	3.76
341	1978	9	6	18	0	0	1.80	5.09	342	1978	9	7	18	0	0	2.38	6.74
343	1978	9	8	18	0	0	2.38	6.74	344	1978	9	9	18	0	0	2.10	5.95
345	1978	9	10	18	0	0	1.73	4.90	346	1978	9	11	18	0	0	1.88	5.33

Table 28. (continued).

347	1978	9	12	18	0	0	1.96	5.56	348	1978	9	13	18	0	0	2.10	5.96
349	1978	9	14	18	0	0	2.56	7.24	350	1978	9	15	18	0	0	2.04	5.77
351	1978	9	16	18	0	0	1.81	5.13	352	1978	9	17	18	0	0	1.73	4.91
353	1978	9	18	18	0	0	1.88	5.31	354	1978	9	19	18	0	0	2.29	6.47
355	1978	9	20	18	0	0	2.13	6.04	356	1978	9	21	18	0	0	2.04	5.78
357	1978	9	22	18	0	0	1.95	5.52	358	1978	9	23	18	0	0	1.66	4.71
359	1978	9	24	18	0	0	1.58	4.48	360	1978	9	25	18	0	0	1.82	5.16
361	1978	9	26	18	0	0	1.77	5.00	362	1978	9	27	18	0	0	1.77	5.02
363	1978	9	28	18	0	0	1.67	4.73	364	1978	9	29	18	0	0	1.59	4.50
365	1978	9	30	18	0	0	1.68	4.77	366	1978	10	1	18	0	0	1.57	4.45
367	1978	10	2	18	0	0	1.55	4.40	368	1978	10	3	18	0	0	1.71	4.83
369	1978	10	4	18	0	0	2.02	5.71	370	1978	10	5	18	0	0	1.91	5.41
371	1978	10	6	18	0	0	1.71	4.85	372	1978	10	7	18	0	0	1.55	4.38
373	1978	10	8	18	0	0	1.56	4.41	374	1978	10	9	18	0	0	1.66	4.69
375	1978	10	10	18	0	0	1.58	4.47	376	1978	10	11	18	0	0	1.91	5.40
377	1978	10	12	18	0	0	2.12	6.00	378	1978	10	13	18	0	0	1.72	4.88
379	1978	10	14	18	0	0	1.34	3.78	380	1978	10	15	18	0	0	1.30	3.69
381	1978	10	16	18	0	0	1.41	4.01	382	1978	10	17	18	0	0	1.52	4.30
383	1978	10	18	18	0	0	1.31	4.29	384	1978	10	19	18	0	0	1.57	4.46
385	1978	10	20	18	0	0	1.80	5.09	386	1978	10	21	18	0	0	2.02	5.72
387	1978	10	22	18	0	0	1.56	4.42	388	1978	10	23	18	0	0	1.76	4.98
389	1978	10	24	18	0	0	1.68	4.76	390	1978	10	25	18	0	0	1.67	4.72
391	1978	10	26	18	0	0	1.67	4.73	392	1978	10	27	18	0	0	1.65	4.67
393	1978	10	28	18	0	0	1.66	4.70	394	1978	10	29	18	0	0	1.53	4.32
395	1978	10	30	18	0	0	1.57	4.43	396	1978	10	31	18	0	0	1.64	4.64
397	1978	11	1	18	0	0	1.65	4.66	398	1978	11	2	18	0	0	1.65	4.67
399	1978	11	3	18	0	0	1.65	4.67	400	1978	11	4	18	0	0	1.70	4.82
401	1978	11	5	18	0	0	1.70	4.81	402	1978	11	6	18	0	0	1.69	4.79
403	1978	11	7	18	0	0	1.67	4.74	404	1978	11	8	18	0	0	1.72	4.86
405	1978	11	9	18	0	0	1.65	4.67	406	1978	11	10	18	0	0	2.06	5.83
407	1978	11	11	18	0	0	1.90	5.37	408	1978	11	12	18	0	0	1.45	4.11
409	1978	11	13	18	0	0	1.93	5.47	410	1978	11	14	18	0	0	2.12	6.01
411	1978	11	15	18	0	0	2.20	6.22	412	1978	11	16	18	0	0	1.75	4.96
413	1978	11	17	18	0	0	1.70	4.82	414	1978	11	18	18	0	0	1.47	4.15
415	1978	11	19	18	0	0	1.39	3.95	416	1978	11	20	18	0	0	2.07	5.87
417	1978	11	21	18	0	0	2.34	6.62	418	1978	11	22	18	0	0	2.32	6.57
419	1978	11	23	18	0	0	1.60	4.52	420	1978	11	24	18	0	0	1.55	4.38
421	1978	11	25	18	0	0	1.56	4.43	422	1978	11	26	18	0	0	1.39	3.93
423	1978	11	27	18	0	0	2.14	6.07	424	1978	11	28	18	0	0	1.89	5.37
425	1978	11	29	18	0	0	1.82	5.16	426	1978	11	30	18	0	0	2.04	5.78
427	1978	12	1	18	0	0	2.50	7.09	428	1978	12	2	18	0	0	2.41	6.82
429	1978	12	3	18	0	0	2.30	6.52	430	1978	12	4	18	0	0	2.77	7.85
431	1978	12	5	18	0	0	3.23	9.14	432	1978	12	6	18	0	0	3.08	8.72
433	1978	12	7	18	0	0	3.41	9.64	434	1978	12	8	18	0	0	2.71	7.68
435	1978	12	9	18	0	0	2.00	5.67	436	1978	12	10	18	0	0	1.83	5.19
437	1978	12	11	18	0	0	2.48	7.02	438	1978	12	12	18	0	0	2.85	8.08
439	1978	12	13	18	0	0	3.02	8.55	440	1978	12	14	18	0	0	2.52	7.14
441	1978	12	15	18	0	0	2.66	7.54	442	1978	12	16	18	0	0	2.29	6.50
443	1978	12	17	18	0	0	2.13	6.03	444	1978	12	18	18	0	0	2.31	6.54
445	1978	12	19	18	0	0	2.31	6.53	446	1978	12	20	18	0	0	2.21	6.26
447	1978	12	21	18	0	0	1.93	5.45	448	1978	12	22	18	0	0	1.94	5.48
449	1978	12	23	18	0	0	1.56	4.41	450	1978	12	24	18	0	0	1.58	4.49
451	1978	12	25	18	0	0	1.70	4.81	452	1978	12	26	18	0	0	1.92	5.43
453	1978	12	27	18	0	0	2.32	6.57	454	1978	12	28	18	0	0	2.88	8.16
455	1978	12	29	18	0	0	2.77	7.83	456	1978	12	30	18	0	0	2.65	7.50
457	1978	12	31	18	0	0	1.77	5.02	458	1979	1	1	18	0	0	1.52	4.29
459	1979	1	2	18	0	0	2.40	6.80	460	1979	1	3	18	0	0	2.78	7.89
461	1979	1	4	18	0	0	2.76	7.81	462	1979	1	5	18	0	0	2.57	7.26
463	1979	1	6	18	0	0	1.82	5.15	464	1979	1	7	18	0	0	1.40	3.97
465	1979	1	8	18	0	0	1.91	5.41	466	1979	1	9	18	0	0	1.92	5.45
467	1979	1	10	18	0	0	2.17	6.13	468	1979	1	11	18	0	0	2.13	6.04

Table 28. (continued).

469	1979	1	12	18	0	0	2.42	6.84	470	1979	1	13	18	0	0	2.32	6.57
471	1979	1	14	18	0	0	1.91	5.41	472	1979	1	15	18	0	0	2.41	6.83
473	1979	1	16	18	0	0	2.32	6.58	474	1979	1	17	18	0	0	2.22	6.27
475	1979	1	18	18	0	0	2.38	6.75	476	1979	1	19	18	0	0	2.27	6.43
477	1979	1	20	18	0	0	1.86	5.27	478	1979	1	21	18	0	0	1.85	5.23
479	1979	1	22	18	0	0	2.35	6.66	480	1979	1	23	18	0	0	2.65	7.50
481	1979	1	24	18	0	0	2.61	7.39	482	1979	1	25	18	0	0	2.56	7.25
483	1979	1	26	18	0	0	2.49	7.06	484	1979	1	27	18	0	0	1.52	4.31
485	1979	1	28	18	0	0	1.44	4.07	486	1979	1	29	18	0	0	2.18	6.18
487	1979	1	30	18	0	0	2.13	6.04	488	1979	1	31	18	0	0	2.27	6.44
489	1979	2	1	18	0	0	2.59	7.32	490	1979	2	2	18	0	0	2.67	7.57
491	1979	2	3	18	0	0	2.18	6.18	492	1979	2	4	18	0	0	1.48	4.20
493	1979	2	5	18	0	0	1.84	5.20	494	1979	2	6	18	0	0	2.24	6.34
495	1979	2	7	18	0	0	3.08	8.73	496	1979	2	8	18	0	0	3.66	10.37
497	1979	2	9	18	0	0	3.49	9.89	498	1979	2	10	18	0	0	3.53	10.00
499	1979	2	11	18	0	0	3.37	9.56	500	1979	2	12	18	0	0	4.23	11.98
501	1979	2	13	18	0	0	4.28	12.13	502	1979	2	14	18	0	0	4.26	12.08
503	1979	2	15	18	0	0	4.10	11.61	504	1979	2	16	18	0	0	3.89	11.02
505	1979	2	17	18	0	0	2.76	7.80	506	1979	2	18	18	0	0	2.40	6.80
507	1979	2	19	18	0	0	2.66	7.53	508	1979	2	20	18	0	0	3.26	9.24
509	1979	2	21	18	0	0	3.02	8.55	510	1979	2	22	18	0	0	2.97	8.41
511	1979	2	23	18	0	0	2.99	8.46	512	1979	2	24	18	0	0	2.54	7.19
513	1979	2	25	18	0	0	2.35	6.65	514	1979	2	26	18	0	0	2.65	7.51
515	1979	2	27	18	0	0	2.97	8.41	516	1979	2	28	18	0	0	3.21	9.08
517	1979	3	1	18	0	0	3.39	9.59	518	1979	3	2	18	0	0	3.19	9.03
519	1979	3	3	18	0	0	2.41	6.83	520	1979	3	4	18	0	0	2.51	7.10
521	1979	3	5	18	0	0	2.86	8.11	522	1979	3	6	18	0	0	3.18	9.02
523	1979	3	7	18	0	0	3.26	9.22	524	1979	3	8	18	0	0	3.51	9.94
525	1979	3	9	18	0	0	3.62	10.25	526	1979	3	10	18	0	0	2.69	7.61
527	1979	3	11	18	0	0	2.68	7.60	528	1979	3	12	18	0	0	2.37	6.71
529	1979	3	13	18	0	0	2.57	7.27	530	1979	3	14	18	0	0	2.40	6.79
531	1979	3	15	18	0	0	2.54	7.18	532	1979	3	16	18	0	0	2.60	7.37
533	1979	3	17	18	0	0	2.65	7.51	534	1979	3	18	18	0	0	2.44	6.92
535	1979	3	19	18	0	0	2.79	7.89	536	1979	3	20	18	0	0	2.31	6.55
537	1979	3	21	18	0	0	2.39	6.76	538	1979	3	22	18	0	0	2.60	7.37
539	1979	3	23	18	0	0	2.27	6.44	540	1979	3	24	18	0	0	2.15	6.08
541	1979	3	25	18	0	0	1.91	5.40	542	1979	3	26	18	0	0	2.45	6.93
543	1979	3	27	18	0	0	2.76	7.81	544	1979	3	28	18	0	0	2.82	8.00
545	1979	3	29	18	0	0	2.78	7.86	546	1979	3	30	18	0	0	2.28	6.47
547	1979	3	31	18	0	0	2.11	5.99	548	1979	4	1	18	0	0	2.27	6.41
549	1979	4	2	18	0	0	2.32	6.56	550	1979	4	3	18	0	0	2.57	7.27
551	1979	4	4	18	0	0	2.84	8.04	552	1979	4	5	18	0	0	2.70	7.66
553	1979	4	6	18	0	0	2.24	6.34	554	1979	4	7	18	0	0	2.09	5.91
555	1979	4	8	18	0	0	2.06	5.83	556	1979	4	9	18	0	0	2.69	7.63
557	1979	4	10	18	0	0	3.11	8.82	558	1979	4	11	18	0	0	2.85	8.06
559	1979	4	12	18	0	0	3.08	8.72	560	1979	4	13	18	0	0	2.63	7.45
561	1979	4	14	18	0	0	2.71	7.66	562	1979	4	15	18	0	0	2.87	8.14
563	1979	4	16	18	0	0	2.73	7.73	564	1979	4	17	18	0	0	2.58	7.32
565	1979	4	18	18	0	0	2.73	7.72	566	1979	4	19	18	0	0	2.90	8.21
567	1979	4	20	18	0	0	3.09	8.76	568	1979	4	21	18	0	0	2.67	7.56
569	1979	4	22	18	0	0	2.26	6.40	570	1979	4	23	18	0	0	2.16	6.11
571	1979	4	24	18	0	0	2.50	7.07	572	1979	4	25	18	0	0	2.87	8.14
573	1979	4	26	18	0	0	2.54	7.20	574	1979	4	27	18	0	0	2.44	6.90
575	1979	4	28	18	0	0	2.26	6.39	576	1979	4	29	18	0	0	2.54	7.18
577	1979	4	30	18	0	0	2.90	8.22	578	1979	5	1	18	0	0	2.81	7.97
579	1979	5	2	18	0	0	2.93	8.29	580	1979	5	3	18	0	0	2.42	6.86
581	1979	5	4	18	0	0	2.64	7.48	582	1979	5	5	18	0	0	2.94	8.31
583	1979	5	6	18	0	0	3.29	9.32	584	1979	5	7	18	0	0	3.77	10.68
585	1979	5	8	18	0	0	4.08	11.55	586	1979	5	9	18	0	0	3.99	11.31
587	1979	5	10	18	0	0	4.08	11.56	588	1979	5	11	18	0	0	4.12	11.65
589	1979	5	12	18	0	0	3.92	11.09	590	1979	5	13	18	0	0	3.10	8.79

Table 28. (continued).

591	1979	5	14	18	0	0	3.08	8.73	592	1979	5	15	18	0	0	3.03	8.58
593	1979	5	16	18	0	0	2.92	8.26	594	1979	5	17	18	0	0	3.00	8.49
595	1979	5	18	18	0	0	3.15	8.93	596	1979	5	19	18	0	0	3.16	8.96
597	1979	5	20	18	0	0	3.16	8.94	598	1979	5	21	18	0	0	2.97	8.40
599	1979	5	22	18	0	0	3.05	8.64	600	1979	5	23	18	0	0	3.06	8.65
601	1979	5	24	18	0	0	3.31	9.36	602	1979	5	25	18	0	0	3.49	9.88
603	1979	5	26	18	0	0	3.21	9.09	604	1979	5	27	18	0	0	2.90	8.21
605	1979	5	28	18	0	0	2.99	8.46	606	1979	5	29	18	0	0	3.08	8.71
607	1979	5	30	18	0	0	2.90	8.20	608	1979	5	31	18	0	0	2.85	8.07
609	1979	6	1	18	0	0	2.96	8.40	610	1979	6	2	18	0	0	2.62	7.42
611	1979	6	3	18	0	0	2.21	6.27	612	1979	6	4	18	0	0	2.08	5.88
613	1979	6	5	18	0	0	2.43	6.88	614	1979	6	6	18	0	0	2.76	7.81
615	1979	6	7	18	0	0	2.46	6.98	616	1979	6	8	18	0	0	2.05	5.81
617	1979	6	9	18	0	0	2.00	5.65	618	1979	6	10	18	0	0	1.91	5.42
619	1979	6	11	18	0	0	2.31	6.55	620	1979	6	12	18	0	0	2.17	6.16
621	1979	6	13	18	0	0	2.06	5.84	622	1979	6	14	18	0	0	2.15	6.10
623	1979	6	15	18	0	0	1.95	5.52	624	1979	6	16	18	0	0	1.59	4.51
625	1979	6	17	18	0	0	1.57	4.43	626	1979	6	18	18	0	0	1.90	5.37
627	1979	6	19	18	0	0	1.90	5.37	628	1979	6	20	18	0	0	2.06	5.83
629	1979	6	21	18	0	0	2.11	5.99	630	1979	6	22	18	0	0	1.85	5.25
631	1979	6	23	18	0	0	1.64	4.64	632	1979	6	24	18	0	0	1.60	4.52
633	1979	6	25	18	0	0	1.62	4.58	634	1979	6	26	18	0	0	1.71	4.85
635	1979	6	27	18	0	0	2.00	5.68	636	1979	6	28	18	0	0	1.90	5.39
637	1979	6	29	18	0	0	1.82	5.16	638	1979	6	30	18	0	0	1.60	4.53
639	1979	7	1	18	0	0	1.49	4.21	640	1979	7	2	18	0	0	1.51	4.28
641	1979	7	3	18	0	0	1.70	4.81	642	1979	7	4	18	0	0	1.61	4.55
643	1979	7	5	18	0	0	1.61	4.55	644	1979	7	6	18	0	0	1.58	4.48
645	1979	7	7	18	0	0	1.40	3.95	646	1979	7	8	18	0	0	1.20	3.39
647	1979	7	9	18	0	0	1.42	4.01	648	1979	7	10	18	0	0	1.41	4.00
649	1979	7	11	18	0	0	1.74	4.92	650	1979	7	12	18	0	0	1.70	4.81
651	1979	7	13	18	0	0	1.51	4.26	652	1979	7	14	18	0	0	1.22	3.47
653	1979	7	15	18	0	0	1.23	3.48	654	1979	7	16	18	0	0	1.50	4.24
655	1979	7	17	18	0	0	1.57	4.44	656	1979	7	18	18	0	0	1.66	4.71
657	1979	7	19	18	0	0	1.83	5.17	658	1979	7	20	18	0	0	1.63	4.61
659	1979	7	21	18	0	0	1.21	3.43	660	1979	7	22	18	0	0	1.17	3.34
661	1979	7	23	18	0	0	1.16	3.28	662	1979	7	24	18	0	0	1.46	4.15
663	1979	7	25	18	0	0	1.56	4.41	664	1979	7	26	18	0	0	1.64	4.65
665	1979	7	27	18	0	0	1.54	4.35	666	1979	7	28	18	0	0	1.15	3.25
667	1979	7	29	18	0	0	1.15	3.25	668	1979	7	30	18	0	0	1.42	4.03
669	1979	7	31	18	0	0	1.38	3.91	670	1979	8	1	18	0	0	1.43	4.04
671	1979	8	2	18	0	0	1.39	3.93	672	1979	8	3	18	0	0	1.40	3.96
673	1979	8	4	18	0	0	1.10	3.13	674	1979	8	5	18	0	0	1.14	3.22
675	1979	8	6	18	0	0	1.42	4.02	676	1979	8	7	18	0	0	1.47	4.17
677	1979	8	8	18	0	0	1.47	4.15	678	1979	8	9	18	0	0	1.52	4.31
679	1979	8	10	18	0	0	1.44	4.07	680	1979	8	11	18	0	0	1.14	3.23
681	1979	8	12	18	0	0	1.13	3.21	682	1979	8	13	18	0	0	1.20	3.41
683	1979	8	14	18	0	0	1.15	3.25	684	1979	8	15	18	0	0	1.41	3.99
685	1979	8	16	18	0	0	1.29	3.54	686	1979	8	17	18	0	0	1.20	3.39
687	1979	8	18	18	0	0	1.01	2.87	688	1979	8	19	18	0	0	1.07	3.03
689	1979	8	20	18	0	0	1.20	3.40	690	1979	8	21	18	0	0	1.20	3.40
691	1979	8	22	18	0	0	1.37	3.89	692	1979	8	23	18	0	0	1.51	4.27
693	1979	8	24	18	0	0	1.92	4.31	694	1979	8	25	18	0	0	1.25	3.54
695	1979	8	26	18	0	0	1.16	3.27	696	1979	8	27	18	0	0	1.44	4.07
697	1979	8	28	18	0	0	1.64	4.65	698	1979	8	29	18	0	0	1.46	4.15
699	1979	8	30	18	0	0	1.14	3.23	700	1979	8	31	18	0	0	1.14	3.22
701	1979	9	1	18	0	0	1.11	3.14	702	1979	9	2	18	0	0	1.10	3.12
703	1979	9	3	18	0	0	1.13	3.19	704	1979	9	4	18	0	0	1.19	3.37
705	1979	9	5	18	0	0	1.33	3.77	706	1979	9	6	18	0	0	1.37	3.87
707	1979	9	7	18	0	0	1.57	4.43	708	1979	9	8	18	0	0	1.17	3.30
709	1979	9	9	18	0	0	1.26	3.57	710	1979	9	10	18	0	0	1.44	4.07
711	1979	9	11	18	0	0	1.50	4.25	712	1979	9	12	18	0	0	1.45	4.11

Table 28. (continued).

713	1979	9	13	18	0	0	1.26	3.55	714	1979	9	14	18	0	0	1.23	3.49
715	1979	9	15	18	0	0	1.12	3.17	716	1979	9	16	18	0	0	1.18	3.35
717	1979	9	17	18	0	0	1.33	3.78	718	1979	9	18	18	0	0	1.34	3.80
719	1979	9	19	18	0	0	1.26	3.57	720	1979	9	20	18	0	0	1.34	3.80
721	1979	9	21	18	0	0	1.16	3.30	722	1979	9	22	18	0	0	1.20	3.39
723	1979	9	23	18	0	0	1.26	3.58	724	1979	9	24	18	0	0	1.34	3.78
725	1979	9	25	18	0	0	1.15	3.25	726	1979	9	26	18	0	0	1.21	3.41
727	1979	9	27	18	0	0	1.33	3.77	728	1979	9	28	18	0	0	1.12	3.14
729	1979	9	29	18	0	0	1.05	2.96	730	1979	9	30	18	0	0	1.02	2.89
731	1979	10	1	18	0	0	1.19	3.38	732	1979	10	2	18	0	0	1.27	3.59
733	1979	10	3	18	0	0	1.31	3.70	734	1979	10	4	18	0	0	1.42	4.03
735	1979	10	5	18	0	0	1.42	4.03	736	1979	10	6	18	0	0	1.45	4.09
737	1979	10	7	18	0	0	1.29	3.65	738	1979	10	8	18	0	0	1.42	4.02
739	1979	10	9	18	0	0	1.36	3.86	740	1979	10	10	18	0	0	1.38	3.90
741	1979	10	11	18	0	0	1.47	4.16	742	1979	10	12	18	0	0	1.14	3.23
743	1979	10	13	18	0	0	1.13	3.21	744	1979	10	14	18	0	0	1.26	3.56
745	1979	10	15	18	0	0	1.33	3.76	746	1979	10	16	18	0	0	1.40	3.97
747	1979	10	17	18	0	0	1.23	3.49	748	1979	10	18	18	0	0	1.39	3.94
749	1979	10	19	18	0	0	1.52	4.29	750	1979	10	20	18	0	0	1.65	4.66
751	1979	10	21	18	0	0	1.72	4.86	752	1979	10	22	18	0	0	1.70	4.82
753	1979	10	23	18	0	0	1.67	4.72	754	1979	10	24	18	0	0	1.67	4.72
755	1979	10	25	18	0	0	1.66	4.70	756	1979	10	26	18	0	0	1.68	4.76
757	1979	10	27	18	0	0	1.71	4.85	758	1979	10	28	18	0	0	1.73	4.89
759	1979	10	29	18	0	0	1.73	4.91	760	1979	10	30	18	0	0	1.69	4.78
761	1979	10	31	18	0	0	1.60	4.54	762	1979	11	1	18	0	0	1.70	4.80
763	1979	11	2	18	0	0	1.78	5.04	764	1979	11	3	18	0	0	1.88	5.32
765	1979	11	4	18	0	0	1.87	5.30	766	1979	11	5	18	0	0	1.89	5.34
767	1979	11	6	18	0	0	1.91	5.41	768	1979	11	7	18	0	0	1.91	5.42
769	1979	11	8	18	0	0	1.87	5.30	770	1979	11	9	18	0	0	1.81	5.14
771	1979	11	10	18	0	0	1.81	5.12	772	1979	11	11	18	0	0	1.75	4.96
773	1979	11	12	18	0	0	1.76	5.00	774	1979	11	13	18	0	0	1.70	4.82
775	1979	11	14	18	0	0	1.67	4.72	776	1979	11	15	18	0	0	1.60	4.53
777	1979	11	16	18	0	0	1.66	4.70	778	1979	11	17	18	0	0	1.70	4.81
779	1979	11	18	18	0	0	1.73	4.91	780	1979	11	19	18	0	0	1.75	4.96
781	1979	11	20	18	0	0	1.80	5.11	782	1979	11	21	18	0	0	1.95	5.52
783	1979	11	22	18	0	0	2.05	5.84	784	1979	11	23	18	0	0	1.91	5.40
785	1979	11	24	18	0	0	2.01	5.69	786	1979	11	25	18	0	0	2.22	6.30
787	1979	11	26	18	0	0	2.32	6.57	788	1979	11	27	18	0	0	2.53	7.16
789	1979	11	28	18	0	0	2.44	6.90	790	1979	11	29	18	0	0	2.29	6.48
791	1979	11	30	18	0	0	2.25	6.36	792	1979	12	1	18	0	0	2.18	6.16
793	1979	12	2	18	0	0	2.20	6.22	794	1979	12	3	18	0	0	2.56	7.25
795	1979	12	4	18	0	0	2.93	8.31	796	1979	12	5	18	0	0	3.42	9.68
797	1979	12	6	18	0	0	3.55	10.06	798	1979	12	7	18	0	0	2.89	8.18
799	1979	12	8	18	0	0	2.59	7.33	800	1979	12	9	18	0	0	2.37	6.72
801	1979	12	10	18	0	0	2.29	6.49	802	1979	12	11	18	0	0	2.38	6.75
803	1979	12	12	18	0	0	2.43	6.87	804	1979	12	13	18	0	0	2.44	6.90
805	1979	12	14	18	0	0	2.41	6.83	806	1979	12	15	18	0	0	2.04	5.78
807	1979	12	16	18	0	0	1.93	5.46	808	1979	12	17	18	0	0	1.99	5.65
809	1979	12	18	18	0	0	2.02	5.71	810	1979	12	19	18	0	0	2.31	6.53
811	1979	12	20	18	0	0	2.31	6.55	812	1979	12	21	18	0	0	2.23	6.32
813	1979	12	22	18	0	0	2.28	6.47	814	1979	12	23	18	0	0	2.34	6.63
815	1979	12	24	18	0	0	2.48	7.01	816	1979	12	25	18	0	0	2.40	6.81
817	1979	12	26	18	0	0	2.26	6.39	818	1979	12	27	18	0	0	2.11	5.97
819	1979	12	28	18	0	0	2.01	5.68	820	1979	12	29	18	0	0	1.94	5.48
821	1979	12	30	18	0	0	1.89	5.34	822	1979	12	31	18	0	0	1.87	5.30
823	1980	1	1	18	0	0	1.90	5.38	824	1980	1	2	18	0	0	2.09	5.91
825	1980	1	3	18	0	0	2.13	6.03	826	1980	1	4	18	0	0	2.08	5.89
827	1980	1	5	18	0	0	2.41	6.82	828	1980	1	6	18	0	0	2.51	7.09
829	1980	1	7	18	0	0	3.05	8.63	830	1980	1	8	18	0	0	2.90	8.21
831	1980	1	9	18	0	0	3.68	10.41	832	1980	1	10	18	0	0	3.72	10.53
833	1980	1	11	18	0	0	3.61	10.23	834	1980	1	12	18	0	0	3.67	10.38



Table 28. (continued).

835	1980	1	13	10	0	0	4.38	12.41	836	1980	1	14	18	0	0	5.31	15.03
837	1980	1	15	10	0	0	5.48	15.51	838	1980	1	16	18	0	0	5.25	14.86
839	1980	1	17	10	0	0	4.51	12.77	840	1980	1	18	18	0	0	3.88	10.98
841	1980	1	19	10	0	0	3.85	10.90	842	1980	1	20	18	0	0	3.43	9.72
843	1980	1	21	18	0	0	3.30	9.34	844	1980	1	22	18	0	0	3.35	9.48
845	1980	1	23	18	0	0	3.14	8.91	846	1980	1	24	18	0	0	2.80	7.93
847	1980	1	25	18	0	0	2.48	7.03	848	1980	1	26	18	0	0	2.82	7.99
849	1980	1	27	18	0	0	2.37	6.72	850	1980	1	28	18	0	0	2.58	7.31
851	1980	1	29	18	0	0	3.08	8.72	852	1980	1	30	18	0	0	2.84	8.05
853	1980	1	31	18	0	0	2.53	7.17	854	1980	2	1	18	0	0	2.36	6.69
855	1980	2	2	18	0	0	2.08	5.89	856	1980	2	3	18	0	0	2.20	6.24
857	1980	2	4	18	0	0	2.32	6.29	858	1980	2	5	18	0	0	2.04	5.78
859	1980	2	6	18	0	0	2.02	5.71	860	1980	2	7	18	0	0	2.09	5.92
861	1980	2	8	18	0	0	2.31	6.53	862	1980	2	9	18	0	0	2.22	6.39
863	1980	2	10	18	0	0	1.92	5.45	864	1980	2	11	18	0	0	1.87	5.31
865	1980	2	12	18	0	0	2.08	5.89	866	1980	2	13	18	0	0	2.28	6.46
867	1980	2	14	18	0	0	2.42	6.86	868	1980	2	15	18	0	0	2.71	7.66
869	1980	2	16	18	0	0	1.86	5.26	870	1980	2	17	18	0	0	1.77	5.02
871	1980	2	18	18	0	0	1.79	5.06	872	1980	2	19	18	0	0	1.93	5.47
873	1980	2	20	18	0	0	1.99	5.65	874	1980	2	21	18	0	0	2.33	6.59
875	1980	2	22	18	0	0	2.48	7.03	876	1980	2	23	18	0	0	1.91	5.41
877	1980	2	24	18	0	0	1.87	5.29	878	1980	2	25	18	0	0	1.88	5.34
879	1980	2	26	18	0	0	1.95	5.51	880	1980	2	27	18	0	0	2.54	7.20
881	1980	2	28	18	0	0	2.35	6.66	882	1980	2	29	18	0	0	2.48	7.02
883	1980	3	1	18	0	0	2.25	6.38	884	1980	3	2	18	0	0	2.01	5.69
885	1980	3	3	18	0	0	1.95	5.52	886	1980	3	4	18	0	0	2.38	6.73
887	1980	3	5	18	0	0	2.85	8.06	888	1980	3	6	18	0	0	2.50	7.08
889	1980	3	7	18	0	0	2.49	7.04	890	1980	3	8	18	0	0	2.02	5.73
891	1980	3	9	18	0	0	1.89	5.35	892	1980	3	10	18	0	0	1.85	5.25
893	1980	3	11	18	0	0	2.16	6.11	894	1980	3	12	18	0	0	2.63	7.46
895	1980	3	13	18	0	0	2.87	8.14	896	1980	3	14	18	0	0	2.83	8.02
897	1980	3	15	18	0	0	2.58	7.32	898	1980	3	16	18	0	0	2.65	7.50
899	1980	3	17	18	0	0	2.69	7.61	900	1980	3	18	18	0	0	2.63	7.44
901	1980	3	19	18	0	0	2.39	6.76	902	1980	3	20	18	0	0	2.26	6.39
903	1980	3	21	18	0	0	2.20	6.22	904	1980	3	22	18	0	0	2.12	6.01
905	1980	3	23	18	0	0	2.05	5.81	906	1980	3	24	18	0	0	2.02	5.73
907	1980	3	25	18	0	0	1.89	5.35	908	1980	3	26	18	0	0	1.72	4.87
909	1980	3	27	18	0	0	1.83	5.17	910	1980	3	28	18	0	0	1.78	5.04
911	1980	3	29	18	0	0	1.81	5.13	912	1980	3	30	18	0	0	1.84	5.20
913	1980	3	31	18	0	0	1.80	5.10	914	1980	4	1	18	0	0	1.77	5.02
915	1980	4	2	18	0	0	1.75	4.94	916	1980	4	3	18	0	0	1.72	4.87
917	1980	4	4	18	0	0	1.73	4.91	918	1980	4	5	18	0	0	1.75	4.95
919	1980	4	6	18	0	0	1.73	4.90	920	1980	4	7	18	0	0	1.87	5.30
921	1980	4	8	18	0	0	2.57	7.28	922	1980	4	9	18	0	0	2.33	6.59
923	1980	4	10	18	0	0	2.35	7.21	924	1980	4	11	18	0	0	2.66	7.53
925	1980	4	12	18	0	0	2.06	5.83	926	1980	4	13	18	0	0	1.94	5.49
927	1980	4	14	18	0	0	1.88	5.31	928	1980	4	15	18	0	0	1.99	5.62
929	1980	4	16	18	0	0	2.42	6.86	930	1980	4	17	18	0	0	2.16	6.13
931	1980	4	18	18	0	0	2.40	6.79	932	1980	4	19	18	0	0	2.05	5.81
933	1980	4	20	18	0	0	2.05	5.80	934	1980	4	21	18	0	0	2.61	7.38
935	1980	4	22	18	0	0	2.87	8.13	936	1980	4	23	18	0	0	3.02	8.55
937	1980	4	24	18	0	0	3.17	8.97	938	1980	4	25	18	0	0	2.84	8.05
939	1980	4	26	18	0	0	2.38	6.75	940	1980	4	27	18	0	0	1.99	5.63
941	1980	4	28	18	0	0	2.59	7.34	942	1980	4	29	18	0	0	2.97	8.40
943	1980	4	30	18	0	0	3.51	9.95	944	1980	5	1	18	0	0	3.12	8.83
945	1980	5	2	18	0	0	3.16	8.95	946	1980	5	3	18	0	0	3.07	8.68
947	1980	5	4	18	0	0	2.68	7.60	948	1980	5	5	18	0	0	2.86	8.10
949	1980	5	6	18	0	0	3.10	8.76	950	1980	5	7	18	0	0	3.38	9.57
951	1980	5	8	18	0	0	3.40	9.62	952	1980	5	9	18	0	0	3.29	9.31
953	1980	5	10	18	0	0	3.21	9.08	954	1980	5	11	18	0	0	3.10	8.79
955	1980	5	12	18	0	0	3.12	8.82	956	1980	5	13	18	0	0	2.92	8.28

Table 28. (continued).

957	1980	5	14	18	0	0	2.72	7.71	958	1980	5	15	18	0	0	2.60	7.35
959	1980	5	16	18	0	0	2.77	7.85	960	1980	5	17	18	0	0	2.92	8.27
961	1980	5	18	18	0	0	1.66	4.71	962	1980	5	19	18	0	0	2.72	7.71
963	1980	5	20	18	0	0	2.59	7.33	964	1980	5	21	18	0	0	2.62	7.43
965	1980	5	22	18	0	0	2.90	8.22	966	1980	5	23	18	0	0	3.10	8.77
967	1980	5	24	18	0	0	3.26	9.23	968	1980	5	25	18	0	0	2.75	7.79
969	1980	5	26	18	0	0	2.89	8.19	970	1980	5	27	18	0	0	2.88	8.16
971	1980	5	28	18	0	0	3.17	8.97	972	1980	5	29	18	0	0	3.18	9.01
973	1980	5	30	18	0	0	3.48	9.86	974	1980	5	31	18	0	0	3.49	9.89
975	1980	6	1	18	0	0	3.31	9.37	976	1980	6	2	18	0	0	3.33	9.42
977	1980	6	3	18	0	0	3.30	9.34	978	1980	6	4	18	0	0	3.23	9.15
979	1980	6	5	18	0	0	3.22	9.11	980	1980	6	6	18	0	0	3.29	9.30
981	1980	6	7	18	0	0	3.46	9.79	982	1980	6	8	18	0	0	3.50	9.92
983	1980	6	9	18	0	0	3.41	9.65	984	1980	6	10	18	0	0	3.29	9.33
985	1980	6	11	18	0	0	3.30	9.34	986	1980	6	12	18	0	0	3.34	9.47
987	1980	6	13	18	0	0	3.36	9.52	988	1980	6	14	18	0	0	3.34	9.46
989	1980	6	15	18	0	0	3.37	9.55	990	1980	6	16	18	0	0	3.56	10.08
991	1980	6	17	18	0	0	3.78	10.71	992	1980	6	18	18	0	0	3.74	10.58
993	1980	6	19	18	0	0	3.39	9.59	994	1980	6	20	18	0	0	3.10	8.78
995	1980	6	21	18	0	0	3.14	8.90	996	1980	6	22	18	0	0	3.26	9.22
997	1980	6	23	18	0	0	3.29	9.31	998	1980	6	24	18	0	0	3.28	9.28
999	1980	6	25	18	0	0	3.26	9.24	1000	1980	6	26	18	0	0	2.97	8.42
1001	1980	6	27	18	0	0	2.74	7.76	1002	1980	6	28	18	0	0	2.14	6.07
1003	1980	6	29	18	0	0	2.12	5.99	1004	1980	6	30	18	0	0	2.49	7.04
1005	1980	7	1	18	0	0	2.20	6.23	1006	1980	7	2	18	0	0	1.90	5.38
1007	1980	7	3	18	0	0	1.09	5.35	1008	1980	7	4	18	0	0	1.81	5.13
1009	1980	7	5	18	0	0	2.04	5.78	1010	1980	7	6	18	0	0	2.36	6.68
1011	1980	7	7	18	0	0	2.30	6.51	1012	1980	7	8	18	0	0	2.24	6.36
1013	1980	7	9	18	0	0	2.25	6.37	1014	1980	7	10	18	0	0	2.26	6.40
1015	1980	7	11	18	0	0	1.99	5.63	1016	1980	7	12	18	0	0	1.62	4.58
1017	1980	7	13	18	0	0	1.52	4.29	1018	1980	7	14	18	0	0	1.72	4.86
1019	1980	7	15	18	0	0	1.97	5.57	1020	1980	7	16	18	0	0	1.83	5.17
1021	1980	7	17	18	0	0	1.63	4.61	1022	1980	7	18	18	0	0	1.63	4.61
1023	1980	7	19	18	0	0	1.62	4.59	1024	1980	7	20	18	0	0	1.75	4.96
1025	1980	7	21	18	0	0	1.94	5.50	1026	1980	7	22	18	0	0	1.91	5.41
1027	1980	7	23	18	0	0	1.77	5.01	1028	1980	7	24	18	0	0	1.66	4.70
1029	1980	7	25	18	0	0	1.57	4.45	1030	1980	7	26	18	0	0	1.47	4.16
1031	1980	7	27	18	0	0	1.33	3.76	1032	1980	7	28	18	0	0	1.31	3.71
1033	1980	7	29	18	0	0	1.45	4.10	1034	1980	7	30	18	0	0	1.56	4.42
1035	1980	7	31	18	0	0	1.57	4.45	1036	1980	8	1	18	0	0	1.57	4.45
1037	1980	8	2	18	0	0	1.42	4.02	1038	1980	8	3	18	0	0	1.24	3.51
1039	1980	8	4	18	0	0	1.35	3.81	1040	1980	8	5	18	0	0	1.51	4.28
1041	1980	8	6	18	0	0	1.54	4.36	1042	1980	8	7	18	0	0	1.54	4.36
1043	1980	8	8	18	0	0	1.50	4.25	1044	1980	8	9	18	0	0	1.30	3.68
1045	1980	8	10	18	0	0	1.12	3.17	1046	1980	8	11	18	0	0	1.28	3.62
1047	1980	8	12	18	0	0	1.60	4.53	1048	1980	8	13	18	0	0	1.62	4.59
1049	1980	8	14	18	0	0	1.37	3.88	1050	1980	8	15	18	0	0	1.20	3.39
1051	1980	8	16	18	0	0	1.25	3.53	1052	1980	8	17	18	0	0	1.33	3.75
1053	1980	8	18	18	0	0	1.35	3.81	1054	1980	8	19	18	0	0	1.45	4.09
1055	1980	8	20	18	0	0	1.53	4.32	1056	1980	8	21	18	0	0	1.52	4.29
1057	1980	8	22	18	0	0	1.39	3.92	1058	1980	8	23	18	0	0	1.21	3.41
1059	1980	8	24	18	0	0	1.12	3.19	1060	1980	8	25	18	0	0	1.15	3.27
1061	1980	8	26	18	0	0	1.30	3.67	1062	1980	8	27	18	0	0	1.39	3.92
1063	1980	8	28	18	0	0	1.37	3.87	1064	1980	8	29	18	0	0	1.38	3.90
1065	1980	8	30	18	0	0	1.17	3.33	1066	1980	8	31	18	0	0	1.17	3.33
1067	1980	9	1	18	0	0	1.17	3.33	1068	1980	9	2	18	0	0	1.19	3.37
1069	1980	9	3	18	0	0	1.19	3.37	1070	1980	9	4	18	0	0	1.21	3.42
1071	1980	9	5	18	0	0	1.22	3.47	1072	1980	9	6	18	0	0	1.22	3.47
1073	1980	9	7	18	0	0	1.22	3.47	1074	1980	9	8	18	0	0	1.22	3.47
1075	1980	9	9	18	0	0	1.22	3.47	1076	1980	9	10	18	0	0	1.22	3.47
1077	1980	9	11	18	0	0	1.22	3.47	1078	1980	9	12	18	0	0	1.22	3.47

Table 28. (continued).

1079	1980	9	13	18	0	0	1.22	3.47	1080	1980	9	14	18	0	0	1.22	3.47
1081	1980	9	15	18	0	0	1.20	3.41	1082	1980	9	16	18	0	0	1.35	3.84
1083	1980	9	17	18	0	0	1.40	3.98	1084	1980	9	18	18	0	0	1.40	3.98
1085	1980	9	19	18	0	0	1.35	3.84	1086	1980	9	20	18	0	0	1.29	3.65
1087	1980	9	21	18	0	0	1.27	3.59	1088	1980	9	22	18	0	0	1.28	3.62
1089	1980	9	23	18	0	0	1.28	3.62	1090	1980	9	24	18	0	0	1.26	3.57
1091	1980	9	25	18	0	0	1.34	3.80	1092	1980	9	26	18	0	0	1.40	3.97
1093	1980	9	27	18	0	0	1.41	3.99	1094	1980	9	28	18	0	0	1.39	3.94
1095	1980	9	29	18	0	0	1.35	3.82	1096	1980	9	30	18	0	0	1.36	3.85
1097	1980	10	1	18	0	0	1.40	3.97	1098	1980	10	2	18	0	0	1.44	4.09
1099	1980	10	3	18	0	0	1.37	3.89	1100	1980	10	4	18	0	0	1.18	3.34
1101	1980	10	5	18	0	0	1.10	3.12	1102	1980	10	6	18	0	0	1.14	3.24
1103	1980	10	7	18	0	0	1.12	3.18	1104	1980	10	8	18	0	0	1.15	3.26
1105	1980	10	9	18	0	0	1.21	3.44	1106	1980	10	10	18	0	0	1.17	3.32
1107	1980	10	11	18	0	0	1.14	3.24	1108	1980	10	12	18	0	0	1.10	3.12
1109	1980	10	13	18	0	0	1.11	3.14	1110	1980	10	14	18	0	0	1.33	3.77
1111	1980	10	15	18	0	0	1.48	4.18	1112	1980	10	16	18	0	0	1.46	4.13
1113	1980	10	17	18	0	0	1.50	4.25	1114	1980	10	18	18	0	0	1.45	4.10
1115	1980	10	19	18	0	0	1.34	3.84	1116	1980	10	20	18	0	0	1.38	3.91
1117	1980	10	21	18	0	0	1.32	3.74	1118	1980	10	22	18	0	0	1.29	3.66
1119	1980	10	23	18	0	0	1.36	3.86	1120	1980	10	24	18	0	0	1.28	3.64
1121	1980	10	25	18	0	0	1.22	3.46	1122	1980	10	26	18	0	0	1.30	3.68
1123	1980	10	27	18	0	0	1.41	3.99	1124	1980	10	28	18	0	0	1.43	4.05
1125	1980	10	29	18	0	0	1.41	3.99	1126	1980	10	30	18	0	0	1.40	3.97
1127	1980	10	31	18	0	0	1.43	4.06	1128	1980	11	1	18	0	0	1.44	4.09
1129	1980	11	2	18	0	0	1.48	4.19	1130	1980	11	3	18	0	0	1.52	4.30
1131	1980	11	4	18	0	0	1.51	4.28	1132	1980	11	5	18	0	0	1.43	4.05
1133	1980	11	6	18	0	0	1.40	4.02	1134	1980	11	7	18	0	0	1.59	4.51
1135	1980	11	8	18	0	0	1.25	4.97	1136	1980	11	9	18	0	0	1.84	5.22
1137	1980	11	10	18	0	0	1.90	5.37	1138	1980	11	11	18	0	0	1.86	5.28
1139	1980	11	12	18	0	0	2.14	6.06	1140	1980	11	13	18	0	0	2.36	6.69
1141	1980	11	14	18	0	0	1.97	5.59	1142	1980	11	15	18	0	0	1.59	4.50
1143	1980	11	16	18	0	0	1.53	4.33	1144	1980	11	17	18	0	0	1.55	4.39
1145	1980	11	18	18	0	0	1.63	4.62	1146	1980	11	19	18	0	0	1.70	4.81
1147	1980	11	20	18	0	0	1.73	4.90	1148	1980	11	21	18	0	0	1.85	5.23
1149	1980	11	22	18	0	0	2.09	5.91	1150	1980	11	23	18	0	0	2.04	5.77
1151	1980	11	24	18	0	0	1.94	5.49	1152	1980	11	25	18	0	0	1.96	5.54
1153	1980	11	26	18	0	0	2.00	5.67	1154	1980	11	27	18	0	0	1.91	5.40
1155	1980	11	28	18	0	0	1.84	5.20	1156	1980	11	29	18	0	0	1.84	5.22
1157	1980	11	30	18	0	0	1.87	5.31	1158	1980	12	1	18	0	0	1.88	5.33
1159	1980	12	2	18	0	0	2.26	6.39	1160	1980	12	3	18	0	0	3.66	10.36
1161	1980	12	4	18	0	0	4.25	12.03	1162	1980	12	5	18	0	0	4.24	12.00
1163	1980	12	6	18	0	0	4.05	11.46	1164	1980	12	7	18	0	0	3.74	10.58
1165	1980	12	8	18	0	0	3.52	9.97	1166	1980	12	9	18	0	0	3.18	9.01
1167	1980	12	10	18	0	0	2.90	8.21	1168	1980	12	11	18	0	0	2.77	7.84
1169	1980	12	12	18	0	0	2.67	7.57	1170	1980	12	13	18	0	0	2.46	6.97
1171	1980	12	14	18	0	0	2.33	6.59	1172	1980	12	15	18	0	0	2.33	6.59
1173	1980	12	16	18	0	0	2.37	6.72	1174	1980	12	17	18	0	0	2.40	6.80
1175	1980	12	18	18	0	0	2.42	6.86	1176	1980	12	19	18	0	0	2.24	6.36
1177	1980	12	20	18	0	0	2.07	5.86	1178	1980	12	21	18	0	0	1.99	5.65
1179	1980	12	22	18	0	0	2.36	6.67	1180	1980	12	23	18	0	0	3.06	8.66
1181	1980	12	24	18	0	0	3.46	9.79	1182	1980	12	25	18	0	0	4.60	13.02
1183	1980	12	26	18	0	0	5.66	16.03	1184	1980	12	27	18	0	0	6.33	17.93
1185	1980	12	28	18	0	0	6.07	17.20	1186	1980	12	29	18	0	0	5.56	15.75
1187	1980	12	30	18	0	0	5.12	14.51	1188	1980	12	31	18	0	0	4.86	13.76
1189	1981	1	1	18	0	0	4.44	12.58	1190	1981	1	2	18	0	0	4.40	12.46
1191	1981	1	3	18	0	0	4.14	11.72	1192	1981	1	4	18	0	0	3.75	10.63
1193	1981	1	5	18	0	0	3.18	9.01	1194	1981	1	6	18	0	0	3.25	9.21
1195	1981	1	7	18	0	0	3.06	8.66	1196	1981	1	8	18	0	0	3.03	8.57
1197	1981	1	9	18	0	0	2.95	8.34	1198	1981	1	10	18	0	0	2.87	8.11
1199	1981	1	11	18	0	0	2.52	7.14	1200	1981	1	12	18	0	0	2.47	6.98



Table 28. (continued).

1323	1981	5	15	18	0	0	2.55	7.21	1324	1981	5	16	18	0	0	2.71	7.66
1325	1981	5	17	18	0	0	2.16	6.12	1326	1981	5	18	18	0	0	2.56	7.26
1327	1981	5	19	18	0	0	2.69	7.61	1328	1981	5	20	18	0	0	2.25	6.38
1329	1981	5	21	18	0	0	2.63	7.44	1330	1981	5	22	18	0	0	2.66	7.53
1331	1981	5	23	18	0	0	2.69	7.62	1332	1981	5	24	18	0	0	2.87	8.13
1333	1981	5	25	18	0	0	2.71	7.67	1334	1981	5	26	18	0	0	2.91	8.25
1335	1981	5	27	18	0	0	3.53	9.98	1336	1981	5	28	18	0	0	3.69	10.45
1337	1981	5	29	18	0	0	3.90	11.04	1338	1981	5	30	18	0	0	4.40	12.45
1339	1981	5	31	18	0	0	4.06	11.50	1340	1981	6	1	18	0	0	4.38	12.39
1341	1981	6	2	18	0	0	4.37	12.37	1342	1981	6	3	18	0	0	4.02	11.39
1343	1981	6	4	18	0	0	4.19	11.87	1344	1981	6	5	18	0	0	4.11	11.65
1345	1981	6	6	18	0	0	4.48	12.70	1346	1981	6	7	18	0	0	4.26	12.06
1347	1981	6	8	18	0	0	4.42	12.50	1348	1981	6	9	18	0	0	5.05	14.30
1349	1981	6	10	18	0	0	5.62	15.91	1350	1981	6	11	18	0	0	5.60	15.86
1351	1981	6	12	18	0	0	5.07	14.36	1352	1981	6	13	18	0	0	4.82	13.65
1353	1981	6	14	18	0	0	4.94	14.00	1354	1981	6	15	18	0	0	4.60	13.04
1355	1981	6	16	18	0	0	4.37	12.38	1356	1981	6	17	18	0	0	4.10	11.61
1357	1981	6	18	18	0	0	3.99	11.29	1358	1981	6	19	18	0	0	3.99	11.29
1359	1981	6	20	18	0	0	4.23	11.97	1360	1981	6	21	18	0	0	4.31	12.20
1361	1981	6	22	18	0	0	4.23	11.97	1362	1981	6	23	18	0	0	4.30	12.19
1363	1981	6	24	18	0	0	4.10	11.61	1364	1981	6	25	18	0	0	3.86	10.93
1365	1981	6	26	18	0	0	3.79	10.73	1366	1981	6	27	18	0	0	3.52	9.97
1367	1981	6	28	18	0	0	3.20	9.06	1368	1981	6	29	18	0	0	3.28	9.28
1369	1981	6	30	18	0	0	2.96	8.37	1370	1981	7	1	18	0	0	2.65	7.51
1371	1981	7	2	18	0	0	2.59	7.32	1372	1981	7	3	18	0	0	2.80	7.92
1373	1981	7	4	18	0	0	2.60	7.36	1374	1981	7	5	18	0	0	2.62	7.42
1375	1981	7	6	18	0	0	2.80	7.92	1376	1981	7	7	18	0	0	2.59	7.32
1377	1981	7	8	18	0	0	3.42	9.68	1378	1981	7	9	18	0	0	3.33	9.43
1379	1981	7	10	18	0	0	3.53	9.99	1380	1981	7	11	18	0	0	2.71	7.68
1381	1981	7	12	18	0	0	2.18	6.18	1382	1981	7	13	18	0	0	2.47	6.99
1383	1981	7	14	18	0	0	2.62	7.42	1384	1981	7	15	18	0	0	2.74	7.76
1385	1981	7	16	18	0	0	2.89	8.20	1386	1981	7	17	18	0	0	2.75	7.79
1387	1981	7	18	18	0	0	1.96	5.55	1388	1981	7	19	18	0	0	1.75	4.96
1389	1981	7	20	18	0	0	2.53	7.16	1390	1981	7	21	18	0	0	2.53	7.16
1391	1981	7	22	18	0	0	2.12	6.00	1392	1981	7	23	18	0	0	2.36	6.69
1393	1981	7	24	18	0	0	2.38	6.73	1394	1981	7	25	18	0	0	2.27	6.42
1395	1981	7	26	18	0	0	1.90	5.38	1396	1981	7	27	18	0	0	2.16	6.11
1397	1981	7	28	18	0	0	2.58	7.29	1398	1981	7	29	18	0	0	2.29	6.49
1399	1981	7	30	18	0	0	2.48	7.03	1400	1981	7	31	18	0	0	2.46	6.95
1401	1981	8	1	18	0	0	2.03	5.74	1402	1981	8	2	18	0	0	1.84	5.21
1403	1981	8	3	18	0	0	1.94	5.49	1404	1981	8	4	18	0	0	2.00	5.67
1405	1981	8	5	18	0	0	2.18	6.17	1406	1981	8	6	18	0	0	2.11	5.99
1407	1981	8	7	18	0	0	2.63	7.43	1408	1981	8	8	18	0	0	2.20	6.24
1409	1981	8	9	18	0	0	1.57	4.44	1410	1981	8	10	18	0	0	1.86	5.27
1411	1981	8	11	18	0	0	1.62	4.58	1412	1981	8	12	18	0	0	2.06	5.84
1413	1981	8	13	18	0	0	1.77	5.01	1414	1981	8	14	18	0	0	1.72	4.86
1415	1981	8	15	18	0	0	2.16	6.12	1416	1981	8	16	18	0	0	2.06	5.85
1417	1981	8	17	18	0	0	1.82	5.16	1418	1981	8	18	18	0	0	1.73	4.89
1419	1981	8	19	18	0	0	1.74	4.93	1420	1981	8	20	18	0	0	1.54	4.35
1421	1981	8	21	18	0	0	1.49	4.21	1422	1981	8	22	18	0	0	1.62	4.59
1423	1981	8	23	18	0	0	1.39	3.93	1424	1981	8	24	18	0	0	1.70	4.82
1425	1981	8	25	18	0	0	1.66	4.69	1426	1981	8	26	18	0	0	1.61	4.57
1427	1981	8	27	18	0	0	1.63	4.60	1428	1981	8	28	18	0	0	1.55	4.38
1429	1981	8	29	18	0	0	1.53	4.33	1430	1981	8	30	18	0	0	1.24	3.52
1431	1981	8	31	18	0	0	1.68	4.76	1432	1981	9	1	18	0	0	1.44	4.09
1433	1981	9	2	18	0	0	1.55	4.40	1434	1981	9	3	18	0	0	1.46	4.14
1435	1981	9	4	18	0	0	1.48	4.20	1436	1981	9	5	18	0	0	1.50	4.24
1437	1981	9	6	18	0	0	1.18	3.34	1438	1981	9	7	18	0	0	1.01	2.86
1439	1981	9	8	18	0	0	1.46	4.14	1440	1981	9	9	18	0	0	1.55	4.38
1441	1981	9	10	18	0	0	1.44	4.07	1442	1981	9	11	18	0	0	1.30	3.67
1443	1981	9	12	18	0	0	1.17	3.31	1444	1981	9	13	18	0	0	1.01	2.86

Table 28. (continued).

1445	1981	9	14	18	0	0	1.48	4.19	1446	1981	9	15	18	0	0	1.28	3.62
1447	1981	9	16	18	0	0	1.45	4.11	1448	1981	9	17	18	0	0	1.54	4.36
1449	1981	9	18	18	0	0	1.62	4.60	1450	1981	9	19	18	0	0	1.35	3.82
1451	1981	9	20	18	0	0	1.07	3.03	1452	1981	9	21	18	0	0	1.46	4.13
1453	1981	9	22	18	0	0	1.45	4.12	1454	1981	9	23	18	0	0	1.55	4.38
1455	1981	9	24	18	0	0	1.40	3.98	1456	1981	9	25	18	0	0	1.58	4.48
1457	1981	9	26	18	0	0	1.21	3.42	1458	1981	9	27	18	0	0	1.02	2.87
1459	1981	9	28	18	0	0	1.50	4.25	1460	1981	9	29	18	0	0	1.34	3.79
1461	1981	9	30	18	0	0	1.42	4.01	1462	1981	10	1	18	0	0	1.66	4.69
1463	1981	10	2	18	0	0	1.60	4.54	1464	1981	10	3	18	0	0	1.16	3.30
1465	1981	10	4	18	0	0	0.97	2.76	1466	1981	10	5	18	0	0	1.77	5.01
1467	1981	10	6	18	0	0	1.80	5.11	1468	1981	10	7	18	0	0	1.90	5.39
1469	1981	10	8	18	0	0	1.97	5.57	1470	1981	10	9	18	0	0	1.84	5.21
1471	1981	10	10	18	0	0	1.51	4.28	1472	1981	10	11	18	0	0	1.41	4.00
1473	1981	10	12	18	0	0	1.84	5.22	1474	1981	10	13	18	0	0	1.74	4.94
1475	1981	10	14	18	0	0	1.72	4.88	1476	1981	10	15	18	0	0	1.75	4.97
1477	1981	10	16	18	0	0	1.86	5.25	1478	1981	10	17	18	0	0	1.60	4.54
1479	1981	10	18	18	0	0	1.11	3.15	1480	1981	10	19	18	0	0	1.73	4.90
1481	1981	10	20	18	0	0	1.62	4.59	1482	1981	10	21	18	0	0	1.79	5.06
1483	1981	10	22	18	0	0	1.78	5.04	1484	1981	10	23	18	0	0	1.91	5.42
1485	1981	10	24	18	0	0	1.75	4.97	1486	1981	10	25	18	0	0	1.39	3.92
1487	1981	10	26	18	0	0	1.47	4.15	1488	1981	10	27	18	0	0	1.49	4.23
1489	1981	10	28	18	0	0	1.72	4.86	1490	1981	10	29	18	0	0	1.73	4.89
1491	1981	10	30	18	0	0	1.75	4.95	1492	1981	10	31	18	0	0	1.46	4.13
1493	1981	11	1	18	0	0	1.25	3.54	1494	1981	11	2	18	0	0	1.55	4.40
1495	1981	11	3	18	0	0	1.61	4.55	1496	1981	11	4	18	0	0	1.64	4.64
1497	1981	11	5	18	0	0	1.85	5.23	1498	1981	11	6	18	0	0	1.73	4.89
1499	1981	11	7	18	0	0	1.47	4.15	1500	1981	11	8	18	0	0	1.27	3.59
1501	1981	11	9	18	0	0	1.57	4.45	1502	1981	11	10	18	0	0	1.70	4.82
1503	1981	11	11	18	0	0	1.68	4.76	1504	1981	11	12	18	0	0	1.54	4.35
1505	1981	11	13	18	0	0	1.71	4.84	1506	1981	11	14	18	0	0	1.73	4.89
1507	1981	11	15	18	0	0	1.93	5.45	1508	1981	11	16	18	0	0	2.14	6.06
1509	1981	11	17	18	0	0	2.14	6.05	1510	1981	11	18	18	0	0	2.29	6.49
1511	1981	11	19	18	0	0	2.48	7.03	1512	1981	11	20	18	0	0	2.40	6.78
1513	1981	11	21	18	0	0	2.28	6.45	1514	1981	11	22	18	0	0	2.12	6.00
1515	1981	11	23	18	0	0	2.47	7.00	1516	1981	11	24	18	0	0	2.61	7.38
1517	1981	11	25	18	0	0	2.79	7.89	1518	1981	11	26	18	0	0	2.42	6.84
1519	1981	11	27	18	0	0	2.53	7.16	1520	1981	11	28	18	0	0	2.34	6.61
1521	1981	11	29	18	0	0	1.93	5.48	1522	1981	11	30	18	0	0	2.03	5.75
1523	1981	12	1	18	0	0	2.17	6.15	1524	1981	12	2	18	0	0	2.57	7.28
1525	1981	12	3	18	0	0	3.02	8.55	1526	1981	12	4	18	0	0	3.40	9.62
1527	1981	12	5	18	0	0	3.46	9.81	1528	1981	12	6	18	0	0	4.30	12.18
1529	1981	12	7	18	0	0	4.83	13.67	1530	1981	12	8	18	0	0	5.06	14.33
1531	1981	12	9	18	0	0	4.66	13.19	1532	1981	12	10	18	0	0	3.98	11.28
1533	1981	12	11	18	0	0	3.87	10.95	1534	1981	12	12	18	0	0	3.63	10.29
1535	1981	12	13	18	0	0	3.45	9.78	1536	1981	12	14	18	0	0	3.54	10.01
1537	1981	12	15	18	0	0	3.95	11.19	1538	1981	12	16	18	0	0	4.52	12.79
1539	1981	12	17	18	0	0	4.60	13.04	1540	1981	12	18	18	0	0	4.35	12.31
1541	1981	12	19	18	0	0	4.67	13.22	1542	1981	12	20	18	0	0	4.21	11.92
1543	1981	12	21	18	0	0	4.31	12.20	1544	1981	12	22	18	0	0	4.10	11.61
1545	1981	12	23	18	0	0	4.03	11.42	1546	1981	12	24	18	0	0	3.95	11.19
1547	1981	12	25	18	0	0	3.85	10.91	1548	1981	12	26	18	0	0	3.66	10.36
1549	1981	12	27	18	0	0	3.74	10.59	1550	1981	12	28	18	0	0	3.81	10.80
1551	1981	12	29	18	0	0	3.92	11.09	1552	1981	12	30	18	0	0	3.54	10.03